SEISMIC SENSITIVITY OF TALL GUYED TELECOMMUNICATION TOWERS

by

Gholamreza Ghodrati Amiri

February 1997

Department of Civil Engineering and Applied Mechanics
McGill University
Montreal, Canada

A thesis submitted to
the Faculty of Graduate Studies and Research
in partial fulfilment of the requirements for the degree of
Doctor of Philosophy

0-612-29946-5

Canadä

In the name of God

To My Family

ABSTRACT

In the wireless, microwave, and satellite communications industry, guyed towers are one of the important structural subsystems. They support a variety of antenna broadcasting systems at great heights, or are themselves radiators in order to transmit radio, television, and telephone signals over long distances. Very tall towers are a fundamental component of post-disaster communication systems. Therefore, their protection during a severe earthquake is of high priority, and accordingly the seismic performance of such structures should be properly evaluated.

To the best of the author's knowledge, there have been no simple rules to account for seismic sensitivity of guyed towers, and very limited attention has been paid to the seismic behaviour of such structures to date. Since guyed towers may exhibit significant geometric nonlinearities, their detailed nonlinear seismic analysis is complex and time-consuming. In addition, climatic loads such as wind and ice are likely to govern the design in most cases. As a result, earthquake effects are often ignored or improperly evaluated (based on current procedures) by an equivalent static lateral load proportional to the tower weight, as it is done in most building codes. These effects, however, may yield to a loss of serviceability due to excessive antenna displacements resulting in an unacceptable signal attenuation, and in extreme cases, to permanent deformations. Therefore it is necessary to develop more complete guidelines for seismic design of tall guyed towers.

The main objective of this research is to propose some seismic sensitivity indicators which may be used by tower designers to assess whether a particular tower is sensitive to earthquake effects, and if so, whether a detailed nonlinear modelling study is necessary. A detailed nonlinear numerical modelling study of eight existing tall guyed telecommunication towers (heights varying from 150 to 607 m) has been carried out. Each tower was subjected to three different classical seismic excitations (El Centro, Parkfield and Taft earthquakes) for the seismicity level of the Victoria region, which has one of the highest seismicity levels in Canada. The conclusions drawn from this study are employed to propose some simplified models and develop some guidelines to relate the overall

seismic sensitivity of tall guyed towers to their essential structural properties. The simplified models proposed are used to predict the maximum tower base shear, the distribution of horizontal earthquake forces along the tower height, and the distribution of the maximum dynamic component of mast axial forces along the tower height due to combined vertical and horizontal earthquake motions. The guidelines developed are used to estimate the maximum dynamic component of the mast axial force at the base due to combined vertical and horizontal earthquake motions, the seismic amplification factor of cable tension, and the maximum shear and bending moment in the mast.

SOMMAIRE

Les pylônes haubanés sont des composants importants dans les réseaux de télécommunication sans fil. Ils peuvent supporter une variété de types d'antennes (récepteurs ou émetteurs) à des hauteurs appréciables, ou ils peuvent servir eux-mêmes d'émetteurs sur de longues distances. Les pylônes haubanés très élevés sont considérés comme des infrastructures essentielles des systèmes de communications d'urgence. En conséquence, leur protection est prioritaire durant un séisme majeur, de sorte que leur comportement sismique nécessite une évaluation adéquate.

A notre connaissance, il n'existe pas de règles simples pour évaluer la susceptibilité sismique des pylônes haubanés, et ces structures ont fait l'objet de très peu d'études en ce sens à date. Comme les pylônes haubanés peuvent présenter des non linéarités géométriques importantes, leur analyse sismique détaillée est complexe. Aussi, dans la majorité des cas, il est probable que les charges de verglas et vent gouvernent la conception. Il en résulte que la plupart du temps les effets des séismes sont ignorés, ou incorrectement évalués par les procédures suggérées par les codes du bâtiment (ex. force horizontale équivalente proportionnelle au poids de la structure). Les séismes peuvent cependant avoir des effets très importants: ils peuvent produire des rotations et déplacements excessifs des antennes qui peuvent causer des interruptions du signal. Dans les cas extrêmes, des déformations permanentes peuvent même être induites dans les supports d'antennes ou dans les membrures du pylône comme tel. Il apparaît donc nécessaire et justifié de développer des règles de conception parasismique plus complètes appropriées au pylônes haubanés de grande hauteur.

L'objectif principal de la recherche est de proposer aux concepteurs de pylônes haubanés des indicateurs de susceptibilité sismique qui permettront d'évaluer si un pylône haubané particulier est susceptible aux effets des séismes, et si une analyse dynamique détaillée est nécessaire pour bien quantifier son comportement. Cette thèse est basée sur l'analyse dynamique non linéaire par éléments finis de huit pylônes haubanés réels dont la hauteur varie entre 150 m et 607 m. Chaque pylône a été soumis à trois séismes classiques (ElCentro, Parkfield et Taft) ajustés au niveau de séismicité de la région de

Victoria, qui est l'une des plus sévères au Canada. Les conclusions de l'étude détaillée ont permis de suggérer des modèles simples et des recommandations pratiques basées sur les propriétés structurales de base des pylônes. Les modèles simplifiés qui sont proposés permettent de prédire le cisaillement maximum à la base du pylône, la distribution des forces dynamiques horizontales le long du profil du pylône, ainsi que la distribution des forces dynamiques axiales dans le mât induites par des accélérations horizontales et verticales combinées. D'autres recommandations pratiques permettent d'estimer la composante dynamique maximale de la force axiale à la base du mât sous l'effet combiné d'accélérations horizontales et verticales, ainsi que les facteurs d'amplification dynamique de la tension dans les haubans, et les forces de cisaillement et les moments de flexion extrêmes dans le mât.

ACKNOWLEDGEMENTS

TABLE OF CONTENTS

CHAPTER 1

INTRODUCTION   1

CHAPTER 2

LITERATURE REVIEW   7

CHAPTER 3

DETAILED NUMERICAL MODELLING STUDY

CHAPTER 4

SEISMIC RESPONSE OF GUYED TOWERS

CHAPTER 5

RESULTS AND DISCUSSIONS

CHAPTER 6

CONCLUSIONS 226

LIST OF FIGURES

x

xvi

LIST OF TABLES

LIST OF SYMBOLS

A	=	Cross sectional area of cable
B.A.	=	Dynamic component of mast base axial force
B.S.	=	Total base shear
E	=	Modulus of elasticity
F	=	Scaling factor of ground accelerogram in Schiff's method
F_1	=	First scaling factor of ground accelerogram in Schiff's method
F_2	=	Second scaling factor of ground accelerogram in Schiff's method
g	=	Gravity acceleration
h	=	Sectional elevation of mast
H	=	Tower height
I.T.	=	Cable initial tension
k	=	Lateral stiffness of guy cluster
k_0	=	Lateral stiffness of guy cluster without sag
L	=	Cable length
P_{dyn}	=	Maximum dynamic component of axial force in the mast at a section of given elevation
PGA	=	Peak horizontal ground acceleration
PGV	=	Peak horizontal ground velocity
PS_a	=	Spectral pseudoacceleration
PS_v	=	Spectral pseudovelocity
r	=	Correlation factor
SI_a	=	Spectral intensity in the acceleration range of NBCC
SI_v	=	Spectrum intensity in the velocity range of NBCC
T	=	Period
T_0	=	Cable initial tension

T_{dyn}	=	Dynamic component of cable tension
T_{total}	=	Cable tension
W	=	Total weight of guyed tower
α	=	Angle of guy cable to horizon
β	=	Second parameter of Newmark-β method
γ	=	First parameter of Newmark-β method
δ	=	Logarithmic damping ratio
ζ	=	Structural damping ratio

CHAPTER 1

INTRODUCTION

1.1 GENERALITIES

Recent developments in the telecommunications industry have led to an extensive use of tall guyed towers in these systems. They support radio, television and telephone broadcasting antennas, or are themselves radiators to transmit communication signals. Guyed towers normally provide an economical and efficient solution for tall towers of 150 m and higher, compared to self-supporting ones. The main component of these structures is usually a slender lattice steel mast of triangular cross section, which is pinned at its base. Sets of inclined pretensioned guy cables support the mast laterally at several levels along its height. The various components of a typical tall guyed tower are shown in Fig. 1.1. In some towers, in order to increase the torsional rigidity of the structure, the guy cables are connected to stabilizers or outriggers at some stay levels (e.g. cable Set 4 in Fig. 1.1).

The structural behaviour of guyed towers is complex. This complexity arises from significant geometric nonlinear behaviour due to, in the first order, the sagging tendency of the guy cables and the interaction between the cables and the mast, and in the second order, the slenderness of the mast (beam-column effects). Although geometrically nonlinear effects are negligible in most structures, they may be very important in guyed towers.

1
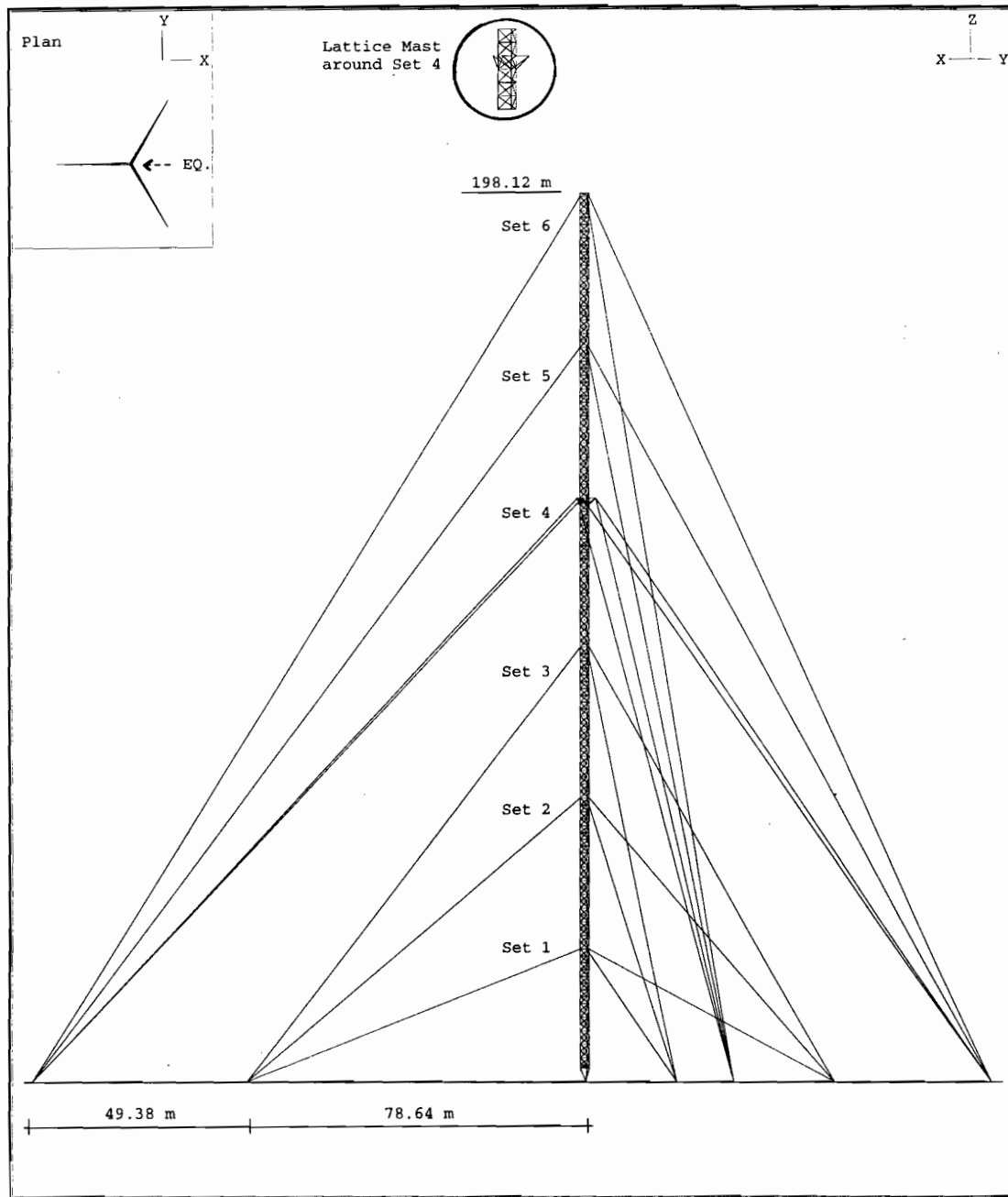
Fig. 1.1. Typical geometry of tall guyed tower

1.2 RESEARCH SIGNIFICANCE

The study of the seismic behaviour of tall guyed towers has received very little attention to date. To the best of the author's knowledge, no simple rules have been

2

proposed which could account for the seismic sensitivity of guyed telecommunication towers. Therefore, researchers in this field have recommended a full nonlinear analysis under seismic load whenever the structure is located in a high-risk seismic zone and is a major installation due to its height or its relative importance in the reliability of the telecommunication network. In practice, because guyed towers exhibit significant geometric nonlinearities, their full nonlinear dynamic analysis is complex and time-consuming. In addition, since climatic loads such as wind and ice are likely to govern the design in most cases, earthquake effects are often ignored in design or improperly evaluated (based on current building code procedures) by an equivalent static lateral load proportional to the tower weight. These effects, however, may yield to a loss of serviceability due to excessive antenna displacements resulting in an unacceptable signal attenuation, and in extreme cases, to permanent deformations.

A common type of damage observed during the 1995 Kobe earthquake (CAEE, 1995), was the tilting of telecommunication towers. The tower oscillations during the earthquake were greater than the serviceability criteria and caused permanent deformation of the structure. These damages resulted in major interruptions in the communications system due to the loss of signal.

The International Association for Shell and Spatial Structures (IASS) presents very general recommendations for the seismic analysis of guyed masts in a special report published by its Working Group 4 on Masts and Towers (IASS, 1981). This report suggests that guyed towers may be analyzed under a static lateral load proportional to their weight to model earthquake effects. This approach is used in most building design codes for base shear distribution. It recommends several simplifying assumptions in order to linearize the analysis and to use modal superposition. However, it recommends caution in its use for very tall guyed masts or for unusual towers, which may exhibit significant geometric nonlinearities.

According to the Canadian Standards Association, CAN/CSA S-37 Antennas, Towers, and Antenna-Supporting Structures, (CAN/CSA, 1994) *"earthquake effects should be considered for susceptible towers of critical importance (e.g. post-disaster communication systems) in high-risk earthquake zones"*. Referring to McClure et al.

3

(1993) "*very tall guyed towers are usually strategic points in a telecommunication network, and their preservation in the event of a severe seismic excitation is of high priority. They may or may not be required to be serviceable during a major earthquake, but they should suffer only minor damages in order to resume normal operations shortly after the event*", and be protected from local permanent deformations at the antenna attachment locations. Therefore, a proper evaluation of the seismic response of such structures is necessary and, in order to develop more complete guidelines, a comprehensive study of the behaviour of these structures under seismic excitation is required.

1.3 OBJECTIVES

The two main goals of this thesis are:

1)   To provide an improved understanding of the seismic behaviour of tall guyed telecommunication towers;

2)   To propose some simple seismic sensitivity indicators which may be used by tower designers to assess whether a particular tower is sensitive to earthquake effects, and if so, whether a detailed nonlinear dynamic analysis is necessary.

The development of tower seismic sensitivity indicators is based on the following five specific research objectives:

1)   To propose a simplified model for predicting the maximum tower base shear;

2)   To estimate the maximum dynamic component of the mast axial force at the base due to combined vertical and horizontal earthquake motions;

4

3)   To propose a simplified model for the distribution of horizontal earthquake forces along the tower height;

4)   To propose a simplified model for the distribution of the maximum dynamic component of mast axial forces along the tower height due to combined vertical and horizontal earthquake motions;

5)   To propose some simple design guidelines to estimate the seismic amplification factor of the cable tension , and the maximum shear and bending moment of the mast.

1.4 THESIS ORGANIZATION

This thesis is comprised of six chapters as follows:

Chapter 1, "Introduction" presents the general aspects of this research and its importance. It also lists the objectives of the research, and outlines the organization of the thesis.

Chapter 2, "Literature Review" begins with a general review of the previous research on static analysis of guyed towers. Dynamic analysis is then presented in more detail, and finally, because of the importance of recent research, a separate section deals with "Survey of Recent Studies". In all sections of this chapter, the references are introduced in chronological order.

Chapter 3, "Detailed Nonlinear Modelling Study" describes the numerical finite element modelling of guyed towers subjected to base motion. It begins with an outline of the methodology of the research and then summarizes the properties of the eight existing towers studied. The input ground accelerograms, the scaling method used, and the procedure for combining vertical and horizontal earthquake motions are presented

next. The modelling of the mast and the guy cables, along with a special section on damping, are then discussed in more detail. The computer programs used in this research, namely the dynamic nonlinear finite element software ADINA and a special in-house post-processor program developed by the author, are briefly presented at the end.

Chapter 4, "Seismic Response of the Towers" explains in detail the seismic behaviour of each tower studied. It begins with the results of the frequency analyses and then presents the most important response indicators. Results of the detailed seismic nonlinear analysis of each tower are summarized in the next section. The sections "Typical Behaviour" and "Serviceability Considerations" highlight the seismic features of the towers response.

Chapter 5, "Results and Discussions" presents the important results of this study. In the first section, the essential characteristics of the eight guyed towers are outlined, grouped under six sections: 1) contribution of mast and cables to the total weight of the guyed towers, 2) mass distribution of mast, 3) initial sag of guy clusters due to self weight and initial prestress, 4) equivalent lateral stiffness of guy clusters, 5) sensitive region in the mast, and 6) anticipated predominant mode shape of mast. The fundamental parameters of seismic response of the towers are explained next in the four sub-sections entitled 1) base shear, 2) seismic component of mast base axial force, 3) seismic amplification factor of cable tension, and 4) maximum shear and bending moment of mast. A presentation of simplified models for maximum base shear, distribution of earthquake forces, and distribution of maximum dynamic component of mast axial forces along tower elevation follows. Finally some seismic sensitivity indicators are proposed as important results of this research.

Chapter 6, "Conclusions" summarizes the results of the thesis and highlights its key conclusions. It also makes some recommendations for future work.

6

CHAPTER 2

LITERATURE REVIEW

2.1 STATIC ANALYSIS

Most of the early investigations on guyed towers (Cohen and Perrin 1957, Hull 1962, Poskitt and Livesley 1963, and Goldberg and Meyers 1965) studied their static analysis by considering the tower as a continuous beam-column resting on nonlinear elastic supports where the spring constants are provided by the lateral stiffness of the guys attached to the shaft. They used solution techniques based on linearized slope-deflection equations.

Shears and Clough (1968) considered a finite element idealisation for an integrated guyed tower analysis in which parabolic cable elements were used for the guys and beam-column elements for the mast. An iterative procedure was used to obtain the nonlinear static response. Aspects regarding the stability of guyed towers were not considered.

Later, Goldberg and Gaunt (1973) studied stability of guyed towers using linearized slope-deflection equations to analyze a multi-level guyed tower. They considered the secondary effects due to bending and changes in the axial thrust in the mast based on the small deflection theory. Their results confirmed that instability in guyed towers is not of the bifurcation type, but happens as a relatively large increase in lateral deformation for a small increase in applied loads.

Chajes and Chen (1979) and Chajes and Ling (1981) investigated mainly the

7

behaviour of short guyed towers. Schrefler, Odorizzi and Wood (1983) proposed a method of analysis for combined beam and cable structures. They used a unified formulation for the geometrically nonlinear analysis of two-dimensional beam and line elements using a total Lagrangian approach. The geometrically nonlinear behaviour was considered especially when the cables become slack due to the loss of prestress.

Also, various approaches for static analysis have been presented by Fiesenheiser (1957), Odley (1966), Williamson and Margolin (1966), Reichelt, Brown and Melin (1971), Rosenthal and Skop (1980, 1982), and McClure (1984).

Raman et al. (1988) considered static analysis using substructuring and finite element techniques for large displacement analysis of guyed towers. Two-node (12 degrees of freedom) 3-D beam-column elements and two-node (six d.o.f.'s) 3-D truss elements are employed in the finite element model to discretize the mast and the cables respectively. The equilibrium of the guys and mast is resolved separately and alternately the compatibility of displacements at the guy support points is applied until the final equilibrium configuration is obtained. The nonlinear effects due to axial load and bowing of the mast, pretension of the cables, and eccentric moments due to the cable reactions were considered in the formulation. A linear elastic material behaviour was considered for the mast, and trilinear elasto-plastic behaviour for the guy cables. The study used both small and large displacement theories (but small strains) for the mast.

Ekhande and Madugula (1988) studied modelling aspects concerning geometrical nonlinear effects. They presented a three-dimensional nonlinear static analysis of guyed towers consisting of cable, truss and beam member combinations. A linear isoparametric formulation for the elements within an updated Lagrangian coordinate framework was employed. Straight line elements with an equivalent reduced modulus of elasticity were used instead of the continuous catenary. Reduced-order integration and a modified elastic shear modulus in the mast were considered to avoid shear locking in the elements. In addition to the cables, the mast was also considered as a geometrically nonlinear element.

Issa and Avent (1991) used a discrete field analysis approach to develop a solution procedure for the analysis of guyed towers. The assumptions of small kinematics and linear elastic behaviour were used for modelling of the tower. The effects of nonlinear

8

cable/tower interaction were also included. The discrete field analysis approach is an alternative to either approximating a space truss as an equivalent continuous beam or for repetitive space truss analysis. This procedure is used to obtain closed-form or field solutions for the space truss by discrete field mechanics. This technique was applied to determine the bending stiffness matrix of a truss rather than using equivalent beam properties.

Ben Kahla (1993 and 1995) has recently proposed a method for static analysis of guyed towers under wind. An assembly of truss and catenary cable elements was considered in the modelling, and the equivalent beam-column model of the mast was also used.

2.2 DYNAMIC ANALYSIS

Many attempts have been made to model the dynamic response of guyed towers. Davenport (1959) developed a linear model to describe the vibration of the guys under wind loads, assuming that the static deflected shape of the guy is parabolic.

McCaffrey and Hartman (1972) also proposed a mathematical model to predict the dynamic response under wind. They analyzed a 302 m (990 ft) tower with fixed base and five guying levels, using truncated modal superposition (the structure was assumed to oscillate linearly about its static equilibrium position). The lowest three transverse modes of the guy wires were considered in the response. The mast was modelled as an equivalent beam-column with a lumped mass idealization. They studied the effects of the following parameters on the free vibration response: (1) assuming a parabolic rather than a catenary static deflected shape for the guys; (2) the number of degrees of freedom of the mast; (3) the ambient temperature; and (4) the higher guy modes, such as, second and third transverse modes. They simplified the analysis by assuming that the mast could vibrate only in one plane and that all the guys attached to the mast at a given level have the same dynamic characteristics. Important results of their study are as follows:
(1) The natural frequencies calculated using a parabolic guy model are essentially the same as those obtained with a catenary guy model;

9

(2) The difference in the two models lies in the calculated mode shapes of the mast corresponding to the various frequencies;

(3) As most of the lower natural frequencies are due to the mass inertia of the guys, it is desirable to consider more than just the first mode for each guy in the dynamic analysis;

(4) The even (asymmetric) guy modes may be important in calculating the dynamic response when the slope of the cable is steep or the cable is very heavy.

Irvine (1981) also investigated the dynamic behaviour of guyed towers, with emphasis on analytical expressions for linearized cable vibrations.

Very general recommendations were made by the International Association for Shell and Spatial Structures (IASS) for the seismic analysis of guyed masts, in a special report published by its Working Group 4 on masts and towers (IASS, 1981). This report suggests that a static lateral load proportional to the weight of the structure may be used to model earthquake effects, as is considered in most building design codes for the base shear distributions. Designers are then advised to use their national standards for more specific guidelines on dynamic amplification factors and force distribution. There are several simplifying assumptions in the IASS report such as considering that the tower oscillates linearly about a given static equilibrium position. This assumption cannot be used when the tension in leeward guys becomes very small and also when the dynamic displacements of the guy attachment points on the mast become large compared to the displacements of the static equilibrium position. Some IASS recommendations are related to modelling considerations applicable to the detailed dynamic analysis for the various loads. Simple linear springs are suggested to represent the guys, and are associated with moving masses that properly model the inertia effects of the cables (Fig. 2.1). The use of a random vibration approach in load modelling and the assumption about neglecting of wave propagation effects at the ground surface (synchronous ground motion at all supports) are particular recommendations for the seismic analysis. Since seismic loads are already extreme events, their combination with dead loads only is suggested, and it is assumed to occur in still air conditions.

Gerstoft and Davenport (1986) established a simplified procedure to analyze

10

a) Guyed Tower   b) Spring-Mass Model   c) Spring-Mass-Damper Model
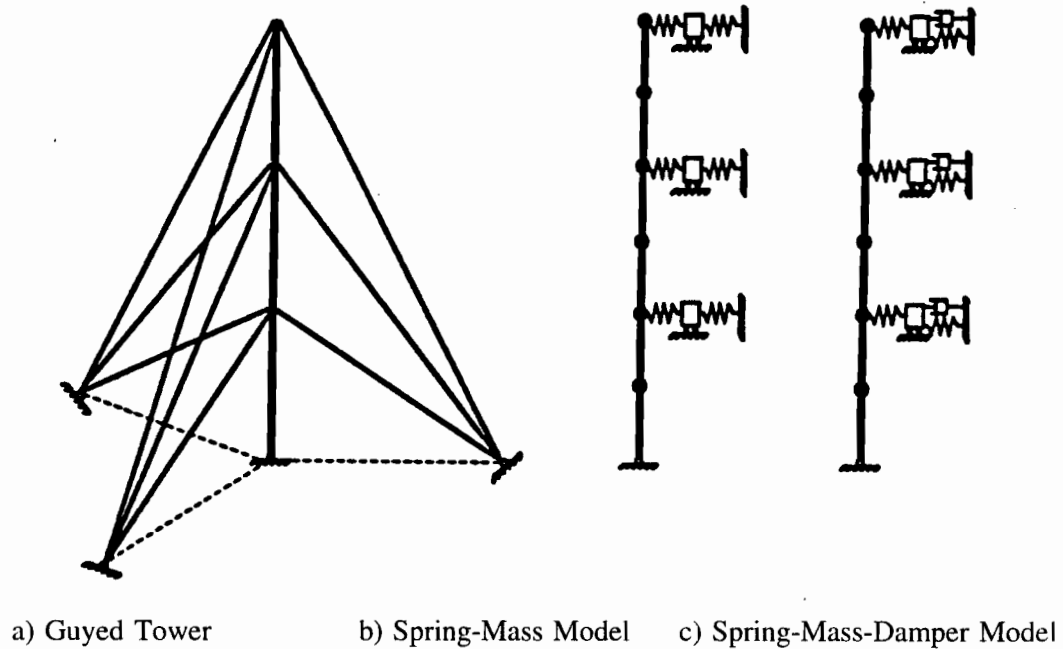
Fig. 2.1. Guy Cable Model (Ben Kahla 1993)

nonlinear guyed towers under wind load. The guyed mast itself was modelled as a beam on elastic supports. These guy supports have nonlinear behaviour for large deflections but linear behaviour was considered for small amplitude dynamic motions. A complicating factor in the treatment of guys is the effect of their mass. This was simplified using the equivalent spring-mass-spring lumped parameter model (Fig. 2.1b), which represents accurately the first transverse mode of a taut cable. As the cable slackens, however, contributions to the response from the higher modes increase and this model is no longer satisfactory. Because the springs are connected on the vertical axis of the mast, the model does not account for the torsional vibrations, nor for the additional forces due to guy attachment eccentricities. Karna (1984) improved this spring-mass-spring model to include a viscous dashpot with each lumped parameter unit (Fig. 2.1c). His model can be employed in a linear three-dimensional dynamic analysis of guyed masts. The frequency response method and a substructuring technique where frequency-dependent springs and dashpots are substituted for the guys were used in this regard. He studied the three-dimensional motion of the guy attachment point on the mast and also the two-dimensional

11

sectional guy motions under the influence of structural and aerodynamic damping.

Augusti et al. (1986) modelled a 200 m guyed mast with three guying levels using equivalent linear elastic springs for the guy cables. The spring stiffness depends on the frequency of oscillation; therefore, successive iterations had been used in the calculation of the response to obtain an appropriate stiffness. However, the inertia effects of the cables were ignored, and the mast was modelled as a space truss with seven lumped masses along its height. The Newmark-β (trapezoidal rule) integration operator was used to calculate the horizontal displacements of the mass points. This formulation is not appropriate for a full dynamic cable-mast interaction.

Buchholdt, Moossavinejad and Iannuzzi (1986) studied time domain methods and compared them with frequency domain methods for structures subjected to wind loads and guy ruptures. They assumed: (a) the structural elements have linear elastic behaviour, (b) the guys can be treated as assemblies of Hookean pin-jointed link elements, (c) structural damping may be expressed as equivalent viscous damping, (d) the dynamic loads may be applied as equivalent concentrated point loads. The mast was assumed to vibrate linearly about the static equilibrium configuration.

Augusti, Borri and Gusella (1990) reported the results detailed geometrically nonlinear analyses of two guyed towers under wind loading. They analyzed a 130 m tall guyed mast with four stay levels, and another one, 275 m tall, with five stay levels. The mast was modelled by tridimensional beam finite elements. The guy cables were represented by a mesh of five to twelve two-node cable elements. Both types of elements may account for the second-order phenomena. Since in the presence of nonlinearities, dynamic analysis cannot be carried out in the frequency domain, direct step-by-step integration in the time domain was used. The implicit Newmark-β integration operator (trapezoidal rule) was used, combined with the classic Newton-Raphson equilibrium iteration procedure at each time step.

Argyris and Mlejnek (1991) analyzed a 152.5 m transmitter tower with two guy stay levels subjected to an idealized sinusoidal earthquake loading (as a rough simulation of an earthquake). The amplitude of the acceleration was 0.5g (half of the gravity acceleration) and the period of loading was one second. Their results indicated that the

computed displacements have large amplitude (about 1.5 m), and therefore serviceability conditions might be exceeded during the earthquake.

2.3 SURVEY OF RECENT STUDIES

The geometrically nonlinear seismic response of antenna-supporting guyed towers has been investigated recently by Guevara and McClure (1993), Guevara (1993), McClure and Guevara (1994) and McClure, Guevara and Lin (1993). They have analyzed three towers: 24 m tall with two stay levels, 107 m tall with six stay levels, and 342 m tall with seven stay levels. A detailed numerical model of both the guy cables and the mast was employed. The S00E 1940 El Centro and N65E 1966 Parkfield accelerograms were used in the simulations. Each earthquake record was scaled down to match the elastic design spectra of the 1990 National Building Code of Canada for the Montreal region. The combination of lateral and vertical ground motions for the tallest (342 m) tower was also studied. In addition, the effects of surface wave propagation were considered for the tallest tower by using asynchronous input motions at the ground anchorage points and at the base of the mast. Guevara and McClure have used ADINA - Automatic Dynamic Incremental Nonlinear Analysis - (ADINA R&D, 1992), a nonlinear dynamic analysis finite element software with direct integration in the time domain to solve the equations of motion. A lumped mass model was employed. The small and intermediate masts were modelled as equivalent Timoshenko beam-columns, whereas a detailed three-dimensional truss model was used for the tallest mast. Three-node tension-only, isoparametric truss elements with initial prestress were used to model the guy cables. In order to account for geometric nonlinearities, a large kinematics (but small strains) formulation was used for the cable model.

Due to the difficulties associated with realistic time-domain modelling of damping (structural and aerodynamic) for nonlinear analysis, Guevara (1993) used artificial numerical damping instead of structural damping. In his study, numerical damping was also employed to filter out numerically generated high frequency components, recognizing that in reality spurious high frequency components would likely be filtered out quickly

by physical damping (structural damping). However, the problem is that numerical damping cannot be calibrated with physical damping in nonlinear multiple-degree-of-freedom systems. Algorithmic damping (numerical damping) can be generated by direct integration operators (e.g. Newmark-β operator). To generate numerical damping with the Newmark-β integration operator, Guevara (1993) tested two sets of values of parameters. The first set was $\gamma=0.6$ and $\beta=0.3025$ which reduced displacement amplitudes by more than 35% with respect to the trapezoidal rule solution. Because this reduction was excessive, a second set of parameters with $\gamma=0.55$ and $\beta=0.3$ was studied. This combination proved to be sufficient to eliminate the spurious high frequency components. However, artificial damping is not an ideal substitute for the cables and mast damping. Especially in very tall towers for which the natural frequencies are relatively small, algorithmic damping may not be sufficient to filter out the response peaks.

Their results indicated that the high frequency components of the excitation affect only the shortest tower. However, the magnitude of the peak response was not considerable because of the low seismicity level of the Montreal region. They found more important dynamic amplifications in the extreme guy clusters (top and bottom) for the response of the two other towers. Asynchronous base motion was found to have significant effects only in the guy wire tensions of the bottom cluster. From the point of view of reducing the required total analysis time, the use of the equivalent model formulation for the tall mast was not effective due to the large number of different member properties along the height of the mast. Furthermore, the detailed structure exhibits a warping torsional behaviour that cannot be reproduced in the equivalent beam-column formulation. Therefore, detailed modelling of tall masts is recommended instead of equivalent beam-columns. Also, their results indicated that cable-mast interactions are significant in the frequency range of the lower axial modes of the mast. They found some important dynamic interactions between the mast and the guy wires where combined vertical and horizontal ground accelerations were used as input.

A numerical study of the transient dynamic response of guyed telecommunication towers subjected to sudden ice shedding from the guy wires has been carried out by Lin

(1993) and reported by McClure and Lin (1994) and McClure, Guevara and Lin (1993). Guevara used the ADINA commercial software for detailed nonlinear dynamic analyses. They analyzed three towers with heights of 24.4 m, 60.7 m and 213.4 m, with two, four and seven stay levels respectively. In one case, artificial numerical damping was employed to compare the response with the undamped results. Since only relatively short towers were studied, beam-column elements were used to model the mast with stiffness properties equivalent to those of the three-dimensional truss model. As in Guevara's work, the guy wires were modelled by tension-only three-node isoparametric truss elements with initial prestress and large kinematics (but small strains).

Since there is only very little guidance for considering the earthquake effects of guyed towers in the Canadian Standard CAN/CSA-S37-94 for structural design of antenna-supporting structures, its recommendations are quoted below:

"**4.11 Earthquake Effects (E)**

The effects of earthquake are not covered by this Standard. In most cases earthquake effects on towers are less than the effects due to wind, but they should be considered for susceptible towers of critical importance (eg, post-disaster communication systems) in high earthquake zones (See Appendix M).

[.....]

Appendix M - Seismic Analysis of Towers

Note: *This Appendix is not a mandatory part of this Standard.*

[.....]

M4. Seismic Analysis of Guyed Towers

Recent numerical studies reported by Guevara (1993) and Guevara and McClure (1993) have indicated that if one wishes to perform a detailed dynamic analysis of a guyed tower, modelling of the structure must allow for geometric nonlinearities and potential interactions between the mast and the guy wires. These interactions can be properly assessed only if inertia properties of both the mast and the guy wires are correctly modelled. The simplified model of a continuous beam on elastic supports,

15

which is still used by some designers to carry out static analyses, is therefore not appropriate. The mast itself is relatively lightweight (wind forces will be greater than gravity forces) and since its mass is more or less linearly distributed over its height, the lateral inertia forces generated by seismic excitations of this distributed mass are not going to be as significant as the wind forces. The most important seismic effect appears to be induced by cable-mast interactions, as transverse cable vibrations induce a vertical dynamic force in the mast that may excite its lowest axial modes and, as a result, may create significant vertical forces. These effects are amplified when vertical input accelerations are combined with the usual horizontal accelerations; the vertical effects induced in the mast also propagate into the guy wires and generate additional amplifications in the cable tensions. Numerical studies have shown that dynamic amplifications in the guy wire tensions are more likely to be significant in the top and bottom clusters of multi-level guyed towers.

Detailed nonlinear seismic analyses are far more complex than response spectrum analyses, and not always necessary. A frequency analysis, as suggested in Section M3, for the initial configuration can help to identify the sensitive frequency range of the tower and potential interaction effects due to clustered frequencies. This information will help the designer decide whether it is necessary to proceed with a more detailed nonlinear dynamic analysis."

Dynamic analysis of guyed towers under wind loading has been studied recently by Ben Kahla (1993, 1994). An equivalent beam-column model with lumped mass has been used for the guyed tower. Cable elements were assumed to be perfectly flexible and of uniform cross-section between their attachment points. The exact mathematical model of an elastic catenary was employed for the formulation of these cable elements. The towers studied were subjected to arbitrary combinations of wind, ice and dead weight. A fictitious linear viscous damper with 5% critical damping was applied parallel to each cable element. The energy dissipation in the material and the friction due to the inner-strand rubbing can be modelled with these discrete damping elements, and so can the aerodynamic damping. Because in moderate and high winds, aerodynamic damping is significantly greater than structural damping, aerodynamic damping was modelled and structural damping was neglected. Two towers were analyzed using a two-dimensional model, both are 146.3 m (480 ft) tall towers with one and three stay levels, respectively.

Ben Kahla's results have shown that large amplitude oscillations of guy cables are

16

possible. These large oscillations are accompanied by large guy tensions that would likely result in the failure and collapse of the structure. These failures could be by breakage of one or several guy cables or by local buckling of some of the mast members. Also, the lowest cable modes of vibration proved not to be the critical frequencies. This observation suggests that the spring-mass model could be invalid to represent guy cables in transient analysis, since only the fundamental mode of vibration can be represented by the model. Because of the potentially severe consequences of the large amplitude oscillations of guy cables, Ben Kahla recommended detailed dynamic analysis for guyed structures under wind loads. It is noted that the Australian code (AS3995(Int)-1991, 1991) for the design of steel lattice towers and masts suggests full dynamic analysis under wind loads for those towers and masts with a fundamental frequency less than 1 Hz.

The modelling of tall guyed towers has also been recently studied by Gantes et al. (1993), in relation to an investigation on the collapse of a 579 m (1900 ft) tall guyed tower under ice and wind loads. Based on their investigation, some structural analysis recommendations relating to the loading and modelling concerns were proposed. Their results have shown that an equivalent beam model would be a simple and acceptable solution for the mast, while equivalent springs are satisfactory for cable modelling for preliminary analysis. A nonlinear truss representation in the sagged configuration was suggested for a more exact finite element analysis when cable elements are not available.

Moossavi Nejad (1996) just published a study of the nonlinear dynamic response of guyed masts due to strong ground motion. In this work, a 327-m guyed radio tower with triangular cross-section and five stay levels has been analyzed. Three ground accelerograms (two orthogonal horizontal components and one vertical) were generated which have a 30 second duration with intensities of 0.3g in the horizontal and 0.2g in the vertical directions. Step-by-step integration in the time domain has been used in this study. The mast was modelled as an equivalent beam-column, and a mesh of five to nine two-node elements is used for guy cable modelling. Two values of logarithmic damping, $\delta=4\%$ and $\delta=8\%$ equivalent to the structural damping ratios of $\zeta=0.006$ and $\zeta=0.012$ were employed in the model. The results of this study have indicated that the strong ground motion produces a large tension in the guy cables. The results of the seismic analysis

17

were compared to those of static wind analysis. It was found that the maximum base axial force and the maximum moment in the mast due to the earthquake load were much larger than the corresponding results of the wind load analysis (30% and 170%, respectively). However, the maximum tensions in the guy cables due to the earthquake load were smaller than those of the wind load analysis (but in the same range).

CHAPTER 3

DETAILED NUMERICAL MODELLING STUDY

3.1 METHODOLOGY

In order to develop more complete seismic analysis and design guidelines, a comprehensive study of the behaviour of guyed towers under seismic excitation is required. It was decided to rely on numerical experiments (i.e. detailed full scale simulations using the finite element method) in this research, for the following reasons:

1)   Experimental results relating to the overall seismic behaviour of guyed telecommunication towers are very rare (not to say that they are inexistent);

2)   Since tall guyed towers exhibit significant geometric nonlinearities, experimental studies of scaled-down physical models of such structures are very complex. Also, experimental work on full scale tall guyed towers is not feasible at present.

In this regard, a detailed numerical modelling study of existing guyed telecommunication towers subjected to different seismic excitations has been carried out. The models include geometric nonlinearities and allow for potential dynamic interaction

19

between the mast and guy wires. The results will be used to develop a simplified method to characterize the overall seismic sensitivity of the towers in terms of their essential structural properties and the input ground motion, and finally, to propose seismic sensitivity indicators.

3.2 DESCRIPTION OF TOWERS

In this study, eight existing guyed telecommunication towers were selected for detailed modelling. These towers represent different heights, different number of guying levels and different geographic locations, as listed in Table 3.1. In practice, guyed towers taller than 150 m usually provide economical solutions compared to the self-supporting towers. Therefore, the lower height limitation for tall towers could be 150 m, which is a common criterion to classify towers with respect to their heights. In this regard, available guyed towers taller than 150 m were selected for the simulations. The geometry of each tower is illustrated in Figs. 3.1 to 3.8. All the towers are located on level ground. It should be mentioned that the 607-m tower is located in Sacramento, California, and is one of the tallest guyed telecommunication towers in North America.

3.3 INPUT GROUND MOTIONS

3.3.1 Earthquake Accelerograms

In this research, three classical earthquake accelerograms have been selected for use in the numerical simulations. They represent different types of earthquake loading. The first is the S00E 1940 El Centro earthquake containing a wide range of frequencies and several episodes of strong ground motion; the second is the N65E 1966 Parkfield earthquake representing a single pulse loading with dominant lower frequencies; finally the third is the S69E 1952 Taft earthquake with high frequency content and strong shaking with long duration. These earthquakes were selected to reflect realistic frequency contents as exhibited by real ground motions. The three earthquake accelerograms

20

Table 3.1. Guyed towers used in numerical simulations

Tower Height (m)	Number of Guying Stay Levels	Number of Anchor Groups	Number of Outriggers	Panel Width (m)	Panel Height (m)	Location (Source)
607.1	9	3	0	3	2.250	U.S.A., California, Sacramento (LeBLANC & Royle Telcom Inc.)
342.2	7	2	1	2	1.524	Canada (Wahba et al. 1992)
313.9	5	2	0	2.140	1.524	Canada (Wahba et al. 1992)
213.4	7	2	0	1.524	1.524	Canada (Wahba et al. 1992)
200	8	3	0	1.800	1	Argentina, Buenos Aires (Estudio Ing. M. Oberlander)
198.1	6	2	1	2.134	1.524	Canada, Prince Edward Island, Charlottetown (Trylon Manufacturing Co. Ltd.)
152.4	8	2	2	0.838	0.610	Canada, Alberta, Elk River (AGT, LeBLANC & Royle Telcom Inc.)
150	7	2	3	1.300	1	Canada, Alberta, Little Buffalo (LeBLANC & Royle Telcom Inc., AGT)

Note: All the towers have a triangular cross section of mast, except that of the 200-m tower which is square.

21
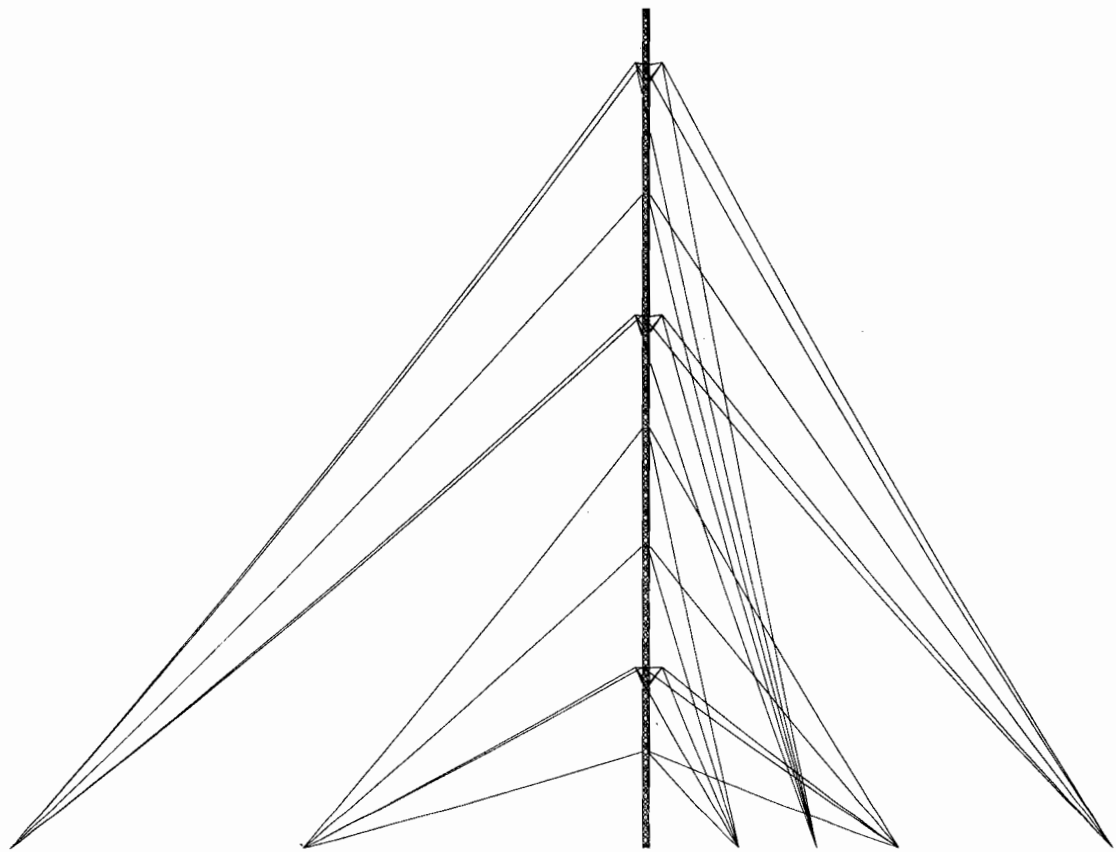
Fig. 3.1. Geometry of 150-m tower
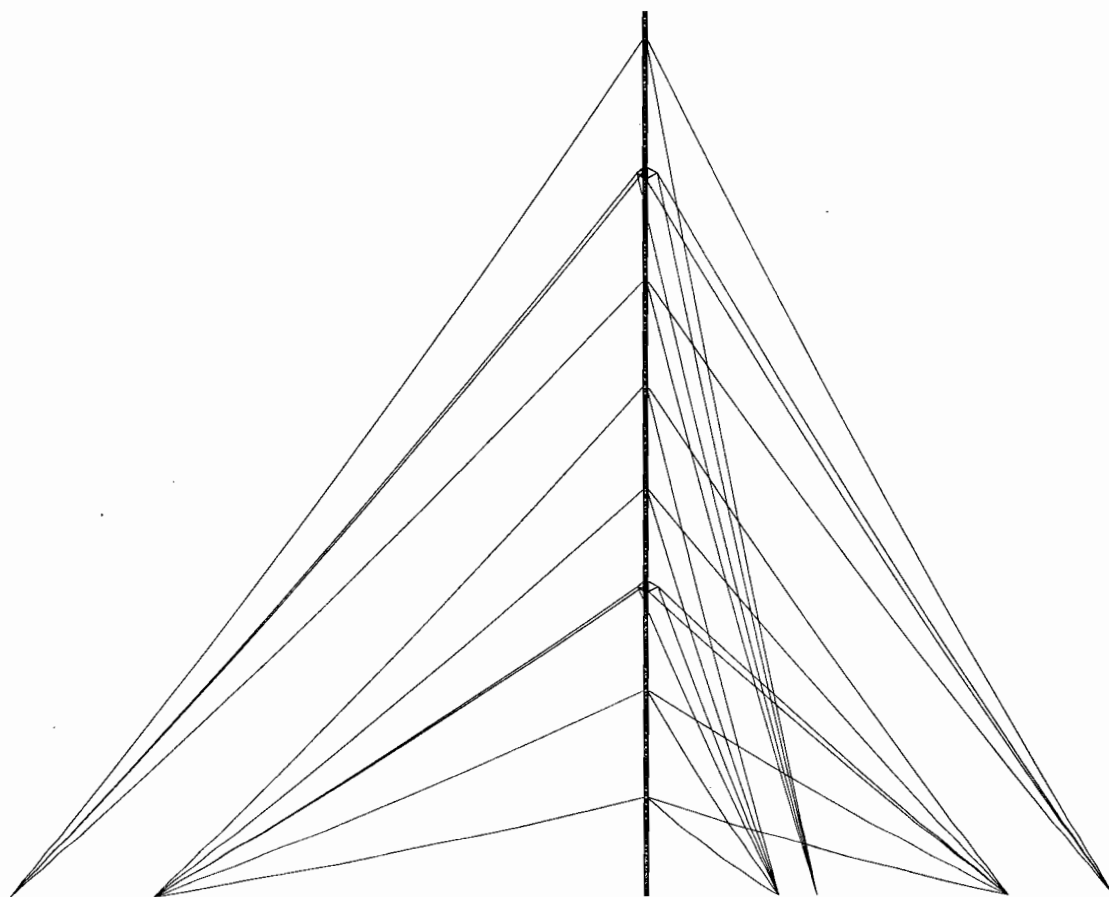
Fig. 3.2. Geometry of 152-m tower
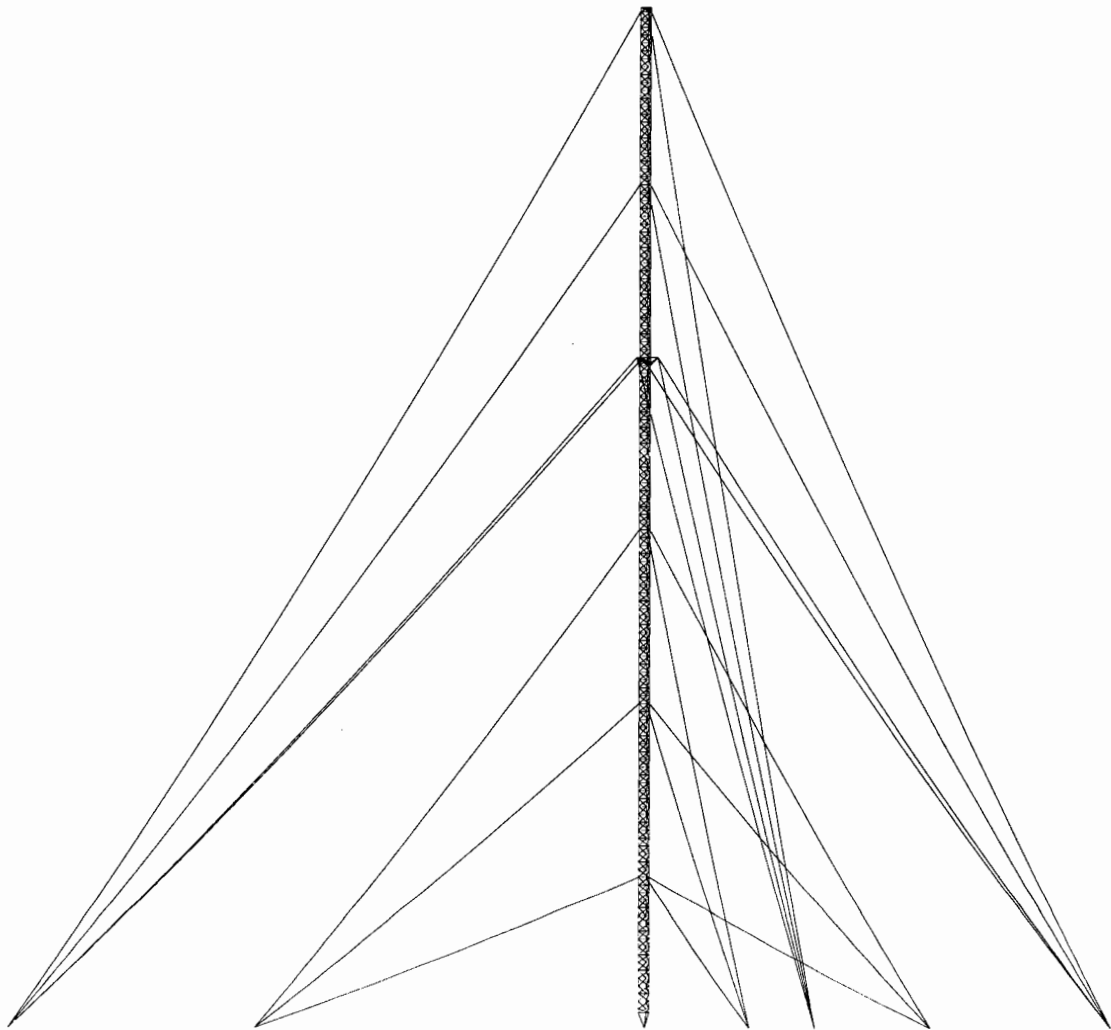
Fig. 3.3. Geometry of 198-m tower
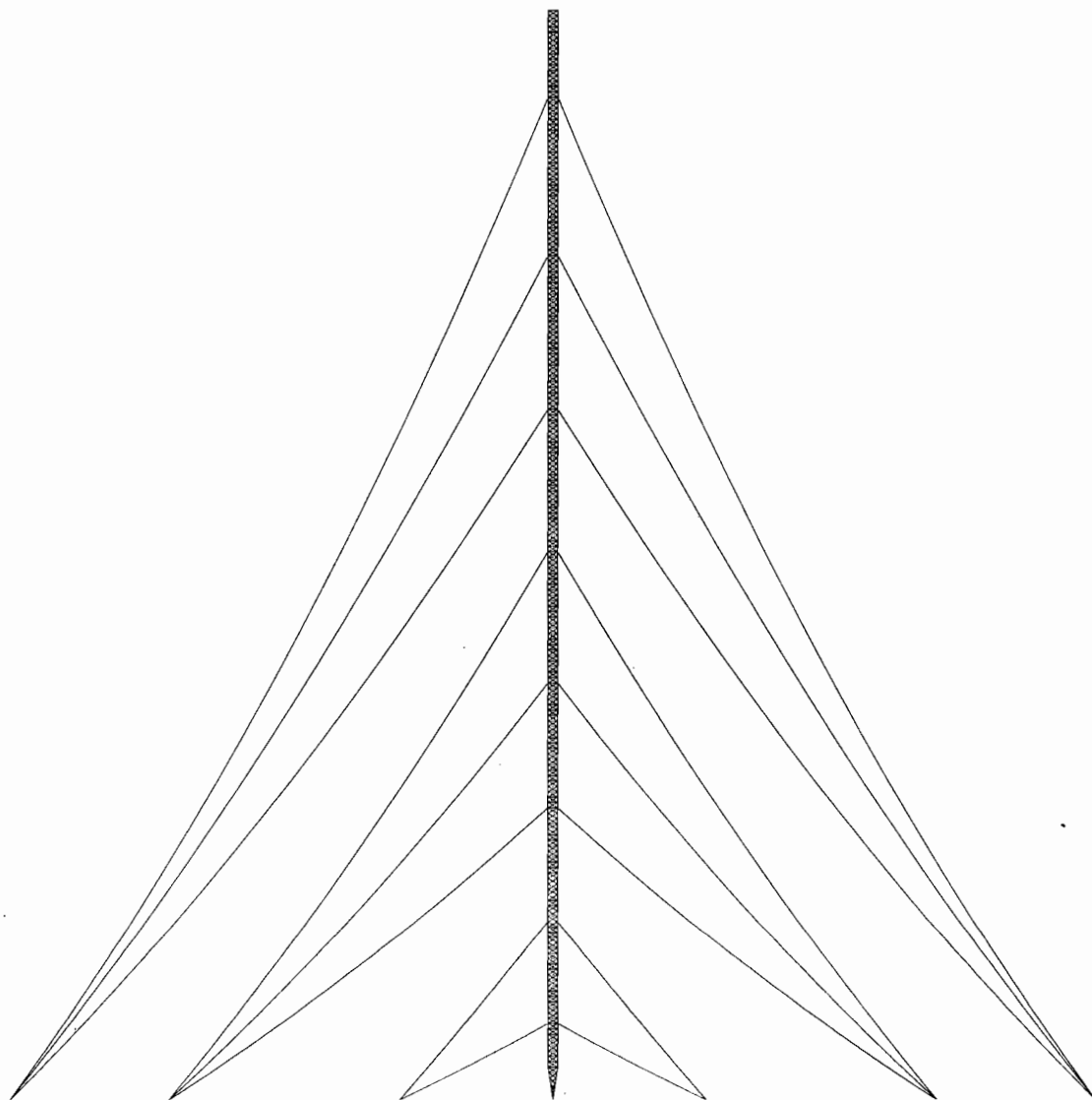
Fig. 3.4. Geometry of 200-m tower
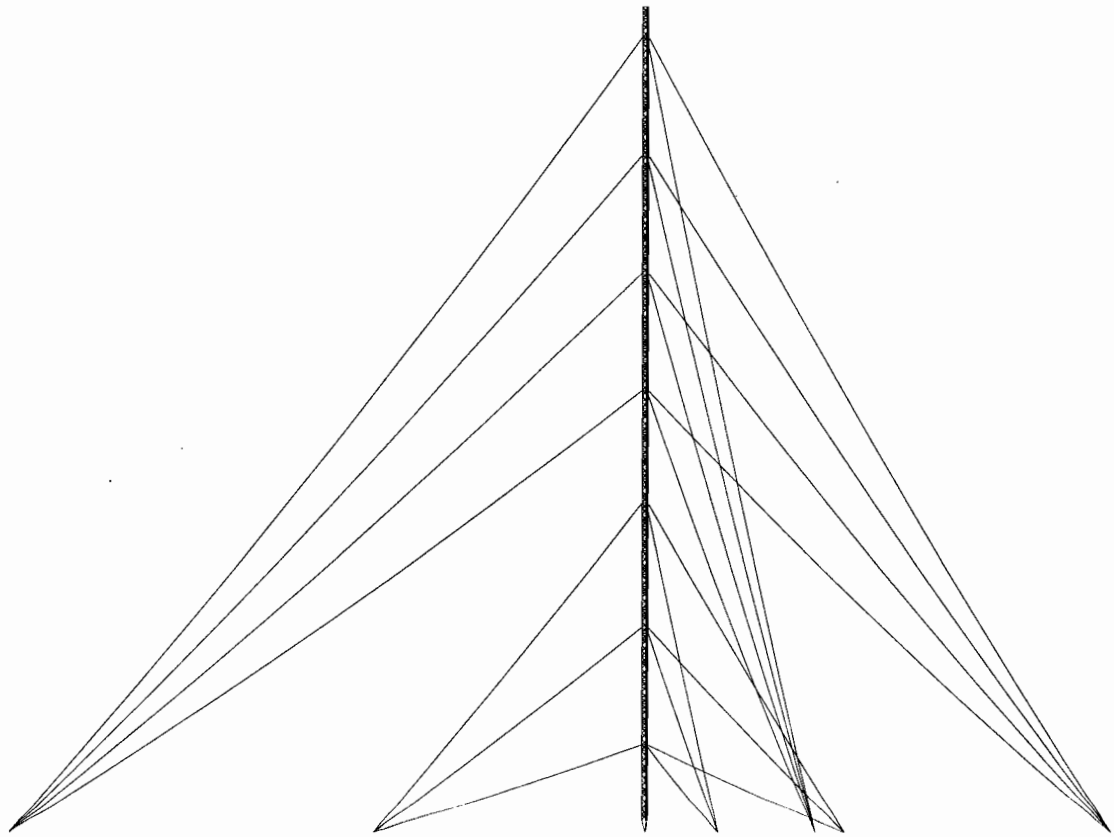
Fig. 3.5. Geometry of 213-m tower

26
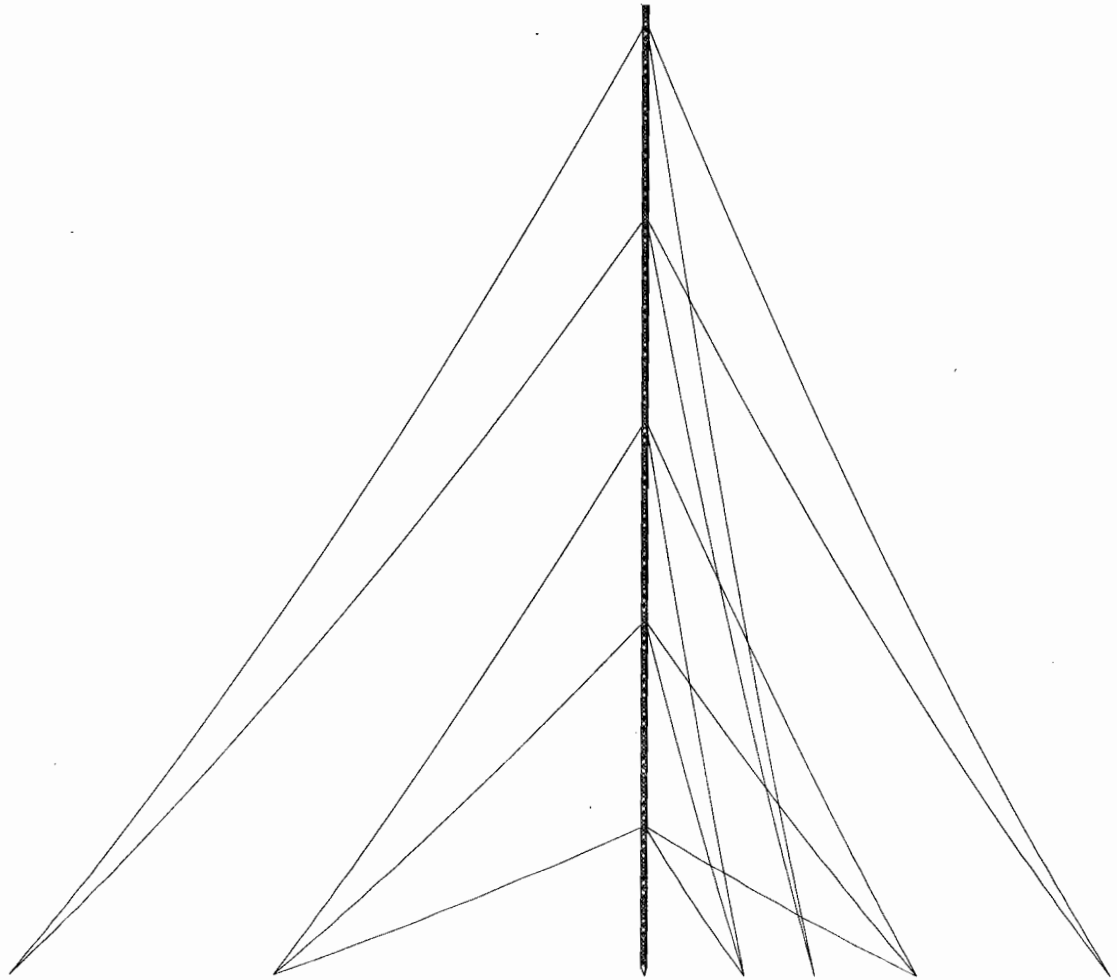
Fig. 3.6. Geometry of 313-m tower
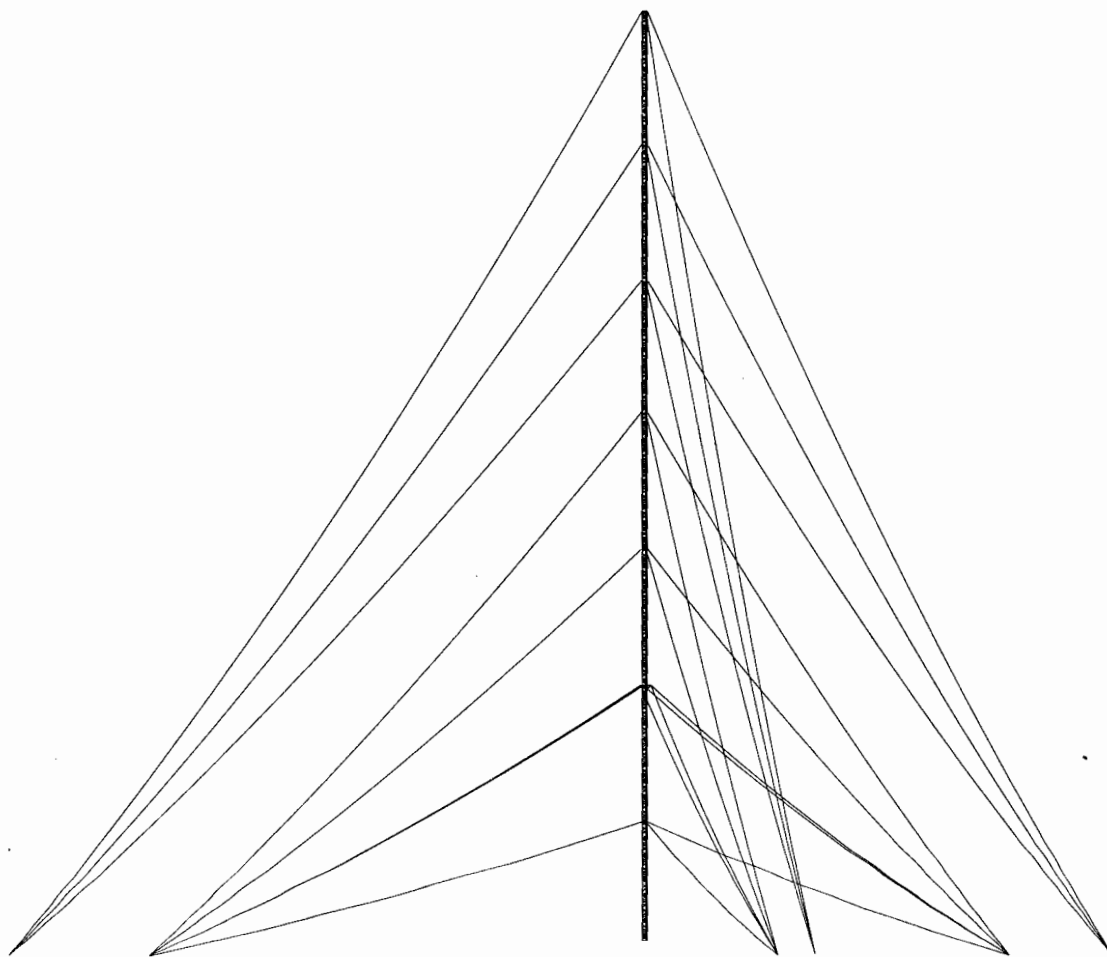
Fig. 3.7. Geometry of 342-m tower
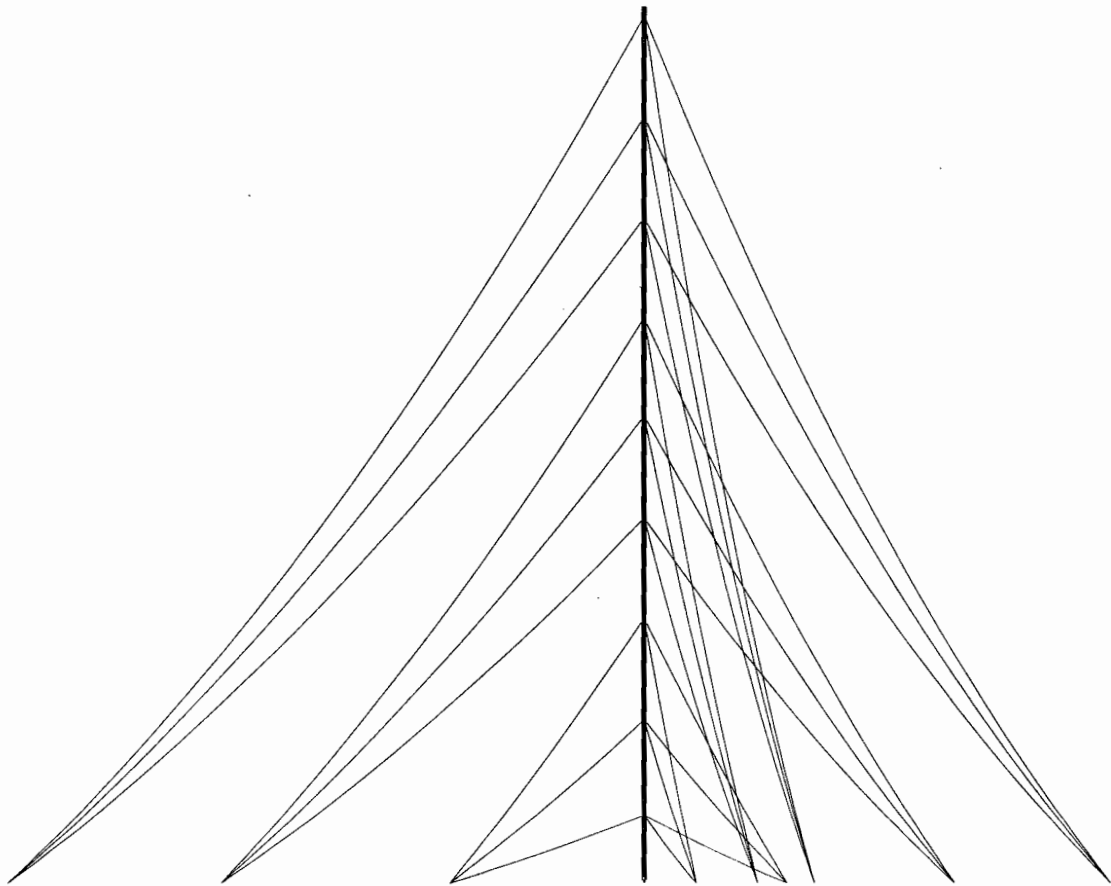
Fig. 3.8. Geometry of 607-m tower

29

are shown in Fig. 3.9. Since most of the strong ground motion occurs within the first twenty seconds of excitation in these three earthquakes, only the first twenty seconds of ground excitation for each record were used for scaling procedure. It should be noted that the earthquake direction was selected to coincide with the principal direction of the mast cross-section to create maximum seismic effects in bending. This was indicated in Fig. 1.1 on the plan view of the tower.
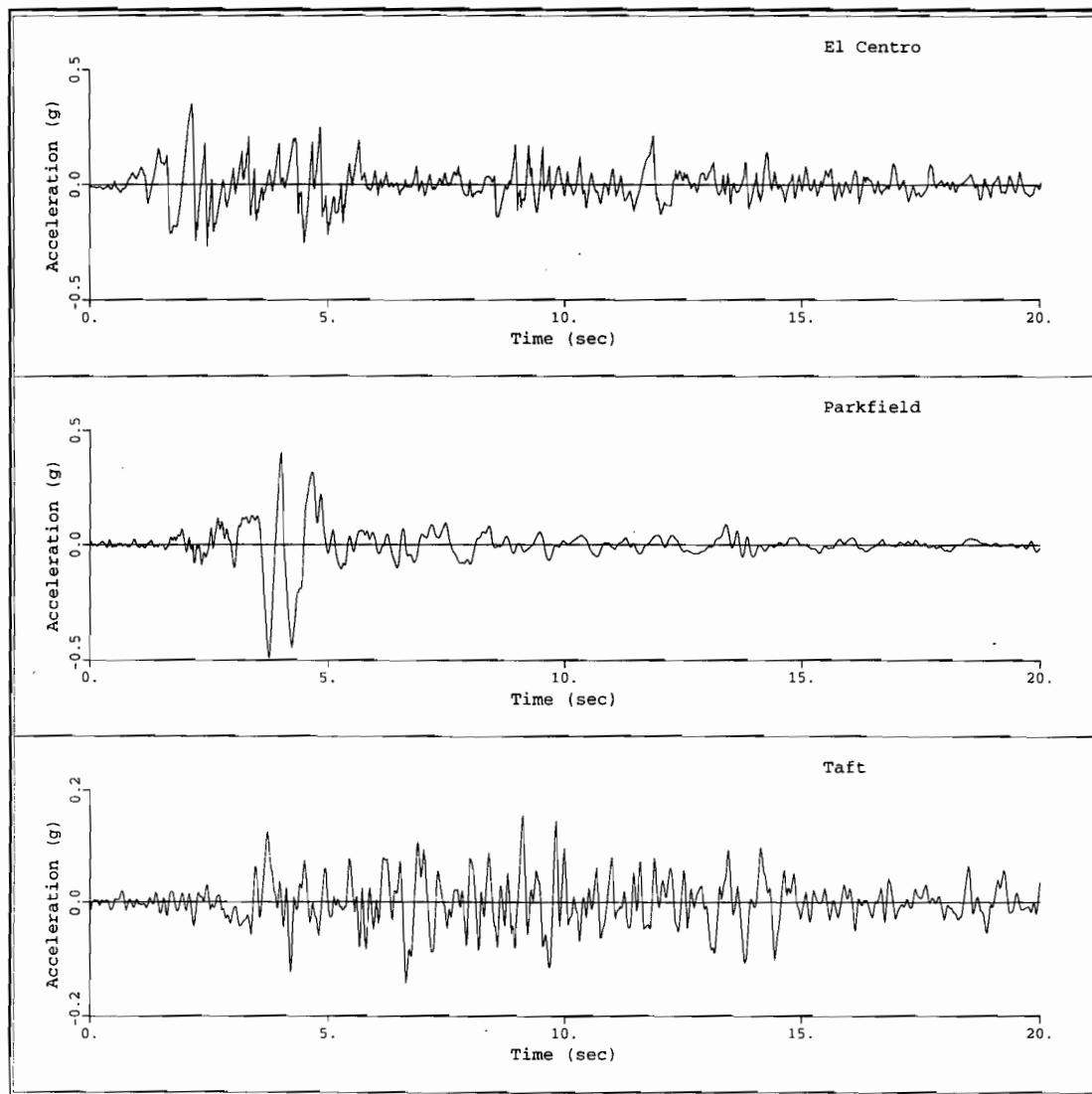
Fig. 3.9. Earthquake accelerograms

3.3.2 Scaling Method

The earthquake records were scaled to fit as much as possible the elastic design spectra of the 1995 National Building Code of Canada (NBCC) for the Victoria region (Peak Horizontal Ground Acceleration = 0.34g and Peak Horizontal Ground Velocity = 0.29 m/s) which has one of the highest seismicity levels in Canada. The scaling allows comparison of the response of the towers for different accelerograms with the same intensity. Schiff's scaling procedure (Schiff, 1988) is used. According to Schiff, a scaling method based on structural response with respect to peak ground motions, gives less dispersion in the response from several earthquake records. Also, for classifying the intensity of a ground motion, peak ground motions cannot be an accurate parameter.

Figure 3.10 illustrates the elastic response spectra for a 5% damped single-degree-of-freedom system for the first twenty seconds of each earthquake excitation.
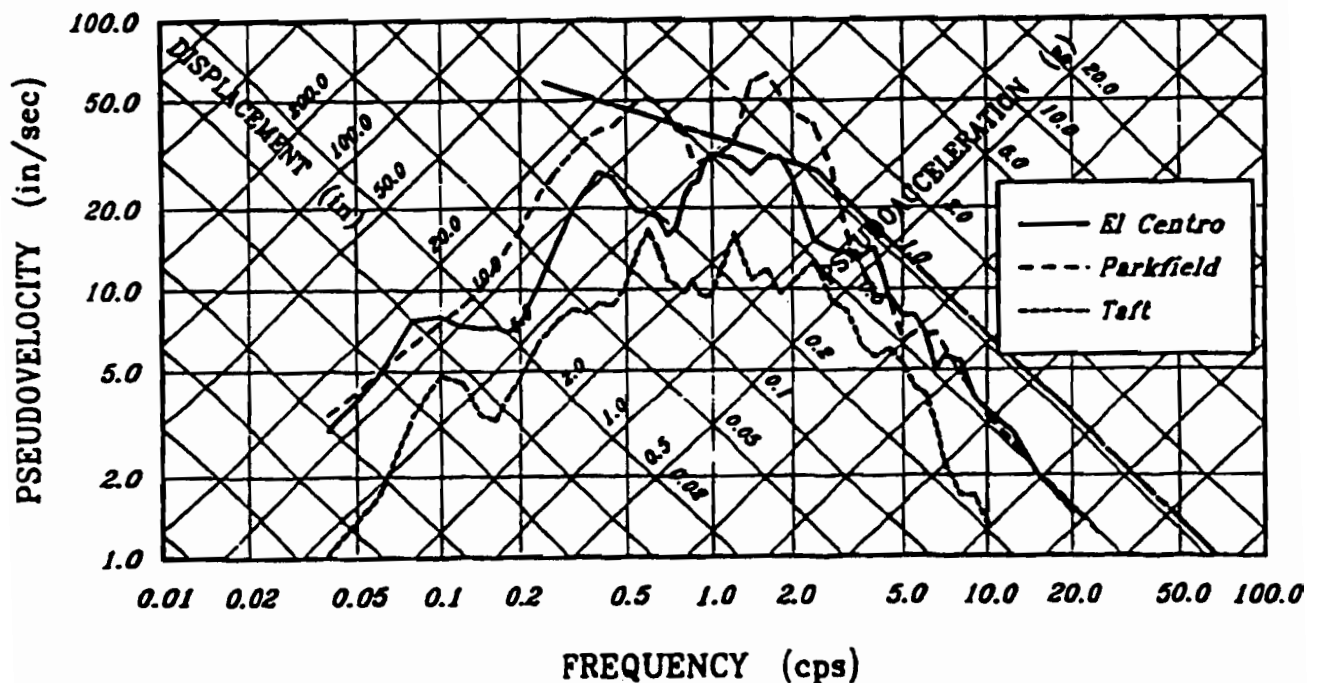
Fig. 3.10. Unscaled elastic response spectra for five percent damping (Schiff, 1988)

31

The calculation of the scaling factors for the acceleration values of each record is done in two steps. The first step is to normalize the earthquake accelerograms so that they have the same spectrum intensity (SI_v) in the velocity range. SI_v is the area under the elastic spectrum curve normalized over the specified frequency range. From Dussault's thesis (Dussault, 1991):

$$SI_v = \frac{1}{3.0 - 0.5} \int_{T=0.5}^{T=3.0} PS_v(T) \cdot dT \qquad (3.1)$$

where PS_v is the spectral pseudovelocity and T is the period in seconds. The first scaling factor (F_1) can be calculated by normalizing SI_v for these earthquake records. They are adopted from Dussault's thesis and shown in Table 3.2. These factors tend to group the elastic response spectra together.

Table 3.2. Scaling factors for earthquake accelerograms

Records	SI_v	F_1	SI_a (g)	F_2	$F = F_1 * F_2$
El Centro	0.613	1.73	1.246		1.19
Parkfield	1.059	1.00	1.216	0.69	0.69
Taft	0.273	3.88	1.676		2.68
NBCC 1995			0.945		

The second step positions the earthquake records around the NBCC elastic spectra by a unique scaling factor of F_2. For calculating F_2, the spectral intensity in the acceleration range (SI_a) of NBCC should be divided by the average of SI_a for the three records already scaled by F_1, given by:

$$SI_a = \frac{1}{0.5 - 0.25} \int_{T=0.25}^{T=0.5} PS_a(T) \cdot dT \qquad (3.2)$$

where PS_a is the spectral pseudoacceleration. The values of F_2 for the three accelerograms are also shown in Table 3.2.

The final scaling factor is the product of F_1 and F_2.

3.3.3 Combination of Vertical and Horizontal Motions

Numerical studies reported by Guevara (1993) and Guevara and McClure (1993) have indicated that combined horizontal and vertical accelerations may cause adverse effects in very tall towers. As reported in Chapter 2, this is now discussed in the most recent edition of the Canadian Standard CAN/CSA-S37-94 for structural design of antenna-supporting structures. To further verify this phenomenon, the combined vertical and horizontal earthquake motions are studied in this research. Referring to the National Building Code of Canada 1995 (Commentary J), and considering that the ratio of vertical-to-horizontal accelerations depends on site conditions and varies widely, an average range of 2/3 to 3/4 was proposed for this ratio. In this study, a ratio of 3/4 is assumed in the absence of real vertical accelerograms. The vertical accelerogram is considered to be synchronous with the horizontal one.

3.4 MODELLING CONSIDERATIONS

3.4.1 Modelling of Mast

The mast is a spatial structure with response in all three dimensions. The elements making up the masts studied are rolled steel sections. A detailed three-dimensional truss model is used for the mast where all elements are pin-ended. This model is more realistic than the beam-column model with equivalent properties (using Timoshenko's beam and St. Venant torsion theories). When there is asymmetry in the pattern of the diagonals for the mast, lateral loading in a principal direction induces coupled bending and torsion in the mast: this phenomenon cannot be replicated in the equivalent 3-D frame model which does not account for warping torsion (McClure and Guevara, 1994).

33

It should be noted that the cross section of the mast is an equilateral triangle (except for the 200-m tower which is square) and its three legs have the same cross-sectional area; therefore, there are two principal axes and the second moments of area in the two principal directions are equal to each other. A lumped mass matrix formulation is used at the element level, and the material properties are assumed to be linear elastic. Treating each element of the mast as a beam element with semi-rigid connections would be the most accurate model; however, the more traditional solution of using truss elements has proven to provide sufficient accuracy (Gantes et al. 1993). As the displacements and rotations of the mast may be large, the large kinematics formulation (with small strains) is also considered for the mast in order to account for potential geometric nonlinearities.

3.4.2 Modelling of Guy Cables

In the author's opinion, the modelling of the guy cables is as important as that of the mast because of the inherent geometric nonlinearities of the guy wires. These nonlinearities increase as the guy cables slacken and the amplitude of their oscillations becomes larger. Proper simulation of mast and cable interactions is achieved by using an appropriate type and number of elements in the cable model, and also the correct modelling of inertia properties of both the mast and the guy wires. The wave propagation effects along the guy wires and the interactions between the guy cables and the mast should be captured by the finite element model. The guy cables are modelled as a linkage of truss elements with prestress. There are three types of truss and cable isoparametric elements in the ADINA program (two-node, three-node, and four-node elements). Guevara and McClure (1993) have conducted a convergence analysis on guy cable meshes that proved the three-node element to be the best compromise in terms of accuracy and numerical efforts. They have also indicated that 10 to 35 tension-only cable elements are required to model the first five transverse modes of a guy cable (since transverse vibrations of the guy wires are likely to dominate the axial high-frequency modes). Also, Gantes et al. (1993) have suggested that ten straight elements per cable can provide satisfactory accuracy.

34

In this research, guy cables are modelled with ten three-node truss elements (tension-only). A large kinematic formulation (with small strains) is used for the cable stiffness to account for full geometric nonlinearities. The stress-strain law is defined only in tension to allow for cable slackening effects to be modelled during the earthquake vibrations. The lumped mass formulation is employed in the analysis, and material properties are assumed to be linear elastic. It should be noted that, because the guy cables are initially pretensioned to approximately 10% of their ultimate strength, the initial stiffness matrix is always nonsingular.

3.4.3 Modelling of Damping

The damping forces in a guyed tower arise mainly from two sources. The first source is structural (material or hysteretic) damping. This damping is partly due to frictional damping within the twisted strands during any flexing action, mostly when it is subjected to transverse vibrations, and partly due to the structural damping in the connections of the mast. The other source of damping is aerodynamic, which is caused by the viscosity of air.

Because of the geometric nonlinearities in the cables, their frictional damping is both frequency dependent and nonlinear with respect to the amplitude of the motion and also varies with the nature of the motion (transverse, axial, or both), which makes it very difficult to model in the time domain. Experiments on somewhat lighter cables [10 mm (0.375 in.) and 8 mm (0.297 in.) diameters, carbon steel cable] used in power transmission, which had been conducted by Yu (1952), indicated that the equivalent viscous damping from this source is not more than 5% of critical equivalent viscous damping in the 8-mm cable and 3% in the 10-mm one.

Damping in the lattice mast depends on the material and the form of construction (welded, riveted, bolted). Bolted structures exhibit more damping than welded ones because of the energy dissipation at the joints, due to friction in the bolted connections. In the case of fully welded structures, the International Association for Shell and Spatial Structures (IASS, 1981) recommends equivalent damping values of 1.2% of the critical

viscous damping for the mast, 2% for high strength friction-bolted steelwork, and 3% for normal bolted and riveted steelwork. Nakamoto and Chiu (1985) have suggested that the critical damping ratios are of approximately 2-5% for frequencies between 0 and 0.5 Hz, and approximately 1-2% for 0.5-5 Hz.

In this study, an equivalent viscous damper with a value of 2% of critical viscous damping is used in parallel with each element to model structural damping. Since the earthquake loads are assumed to occur under still air conditions (IASS, 1981), aerodynamic damping has not been modelled. Nonetheless, this model is an improvement compared to previous studies in the field.

3.4.4 Numerical Methods

The nonlinear dynamic analysis is done by direct step-by-step integration in the time domain. The numerical integration procedure selected is the Newmark-β method (with $\gamma=0.5$ and $\beta=0.25$, i.e. the constant average acceleration method or trapezoidal rule). The BFGS (Broyden-Fletcher-Goldfarb-Shanno) equilibrium iteration procedure is employed in combination with the Newmark-β method to solve the nonlinear equations, which is very effective compared to the other iteration procedures available, and stiffness matrix updates are performed at every time step. Also, the energy convergence criterion is used to bound the iteration process. The subspace-iteration procedure is used in the frequency analysis.

3.5 COMPUTER PROGRAMS

3.5.1 Dynamic Nonlinear Finite Element Program

The nonlinear finite element software ADINA (Automatic Dynamic Incremental Nonlinear Analysis) is used in this research (ADINA, 1992). ADINA is a nonlinear dynamic analysis software to solve the equations of motion with direct step-by-step

integration in the time domain. This program is used for displacement and stress analysis.

3.5.2 Post-Processor Program

The results of the ADINA program are in the form of time-history records for each selected response indicator. Also, the results are given for each element of the mast (e.g. legs, diagonals and horizontal elements), and each cable element. In order to find the maximum values of the response along the tower elevation, a post-processor program (2300 FORTRAN instructions) was developed during the course of this study. This program was created to process detailed results of the following elements of response:

1) Total Base Shear
2) Total Weight
3) Earthquake Force (the resultant lateral force generated by an earthquake
   on the mast at the cable attachment points)
4) Dynamic Component of Cable Tension
5) Mast Shear
6) Dynamic Component of Mast Axial Force
7) Mast Bending Moment
8) Dynamic Component of Cable Oscillation
9) Mast Horizontal Displacement
10) Dynamic Component of Mast Axial Displacement
11) Mast Rotation

This program also calculates the initial values of the above response indicators due to self weight and initial cable tension. Since the initial values of total base shear, earthquake force, mast shear, mast bending moment, mast horizontal displacement, and mast rotation should be zero, they can be used to verify the accuracy of the analysis.

37

CHAPTER 4

SEISMIC RESPONSE OF GUYED TOWERS

4.1 FREQUENCY ANALYSIS

A frequency analysis in the deformed configuration under self weight (tower attachments are not included) and cable prestressing forces has been carried out for each of the eight guyed towers, and the results of the natural periods are summarized in Tables 4.1 and 4.2. The five lowest natural periods of the towers are shown in Table 4.1, and the period of their fundamental flexural mode is identified in Table 4.2. As it can be seen in Table 4.1, there is at least one torsional mode among the five lowest natural modes in most of the towers. It is also noted that the 200-m tower has more torsional modes than the other towers in its lowest five modes. In this study, since the earthquake accelerograms are centric and assumed along a principal direction of the tower, the torsional mode is not excited by seismic motions.

Figure 4.1 represents Table 4.2 graphically. This figure shows an almost linear increase of the first flexural period of the towers with height. The only exception is the 200-m tower,which is very flexible with respect to the other comparable towers. As it will be explained in Chapter 5, Sections 5.1.3 and 5.1.4, the initial tension of the guy cables of the 200-m tower is relatively small compared to that of the other towers (much less than 10% of their ultimate tensile strength). This results in a relatively large initial sag in the cables, which makes the equivalent lateral stiffness of the guy clusters small

38

Table 4.1. Lowest five natural periods (s) of towers
(F = Flexural mode   T = Torsional mode)

Tower Height (m)	Mode No.				
	1	2	3	4	5
607	4.27 (F)	3.59 (T)	3.58 (F)	2.77 (F)	1.85 (F)
342	2.21 (T)	2.10 (F)	1.98 (F)	1.58 (F)	1.21 (F)
313	2.31 T)	2.06 (F)	1.57 (F)	1.24 (T)	1.22 (F)
213	0.88 (T)	0.80 (F)	0.68 (F)	0.58 (F)	0.50 (F)
200	2.36 (F)	1.82 (T)	1.48 (F)	1.25 (T)	0.84 (T)
198	1.22 (T)	0.80 (F)	0.68 (F)	0.56 (T)	0.56 (F)
152	0.58 (F)	0.53 (F)	0.47 (F)	0.45 (F)	0.37 (F)
150	0.69 (F)	0.58 (F)	0.50 (F)	0.40 (F)	0.30 (F)

Table 4.2. First flexural natural periods of towers

Tower Height (m)	First Flexural Natural Period (s)
607	4.27
342	2.10
313	2.06
213	0.80
200	2.36
198	0.80
152	0.58
150	0.69

compared to that of the other towers studied.

To get an estimate of the lowest flexural natural period of guyed towers (whose cable initial tension is about 10% of their ultimate tensile strength), the following formula is suggested:

$$T = 0.0083 \, H - 0.74 \tag{4.1}$$

where T is the lowest flexural natural period in seconds and H is the height of tower in meters. This formula is applicable for guyed towers with height in the range of 150 to 607 m. Figs. 4.2 to 4.9 illustate the four lowest flexural natural mode shapes of all eight towers. The predominant mode shapes excited by seismic loads will be discussed in Chapter 5, Section 5.1.6.

4.2 RESPONSE INDICATORS

The results of the detailed numerical simulations of the towers have been analyzed in terms of amplitude, time at peak response, and frequency content. The response indicators representing the behaviour of the guyed towers are listed below:

1) Earthquake Force
2) Dynamic Component of Cable Tension
3) Mast Shear
4) Dynamic Component of Mast Axial Force
5) Mast Bending Moment
6) Dynamic Component of Cable Oscillation
7) Mast Horizontal Displacement
8) Dynamic Component of Mast Axial Displacement
9) Mast Rotation.

These response indicators have been chosen to study the seismic behaviour in
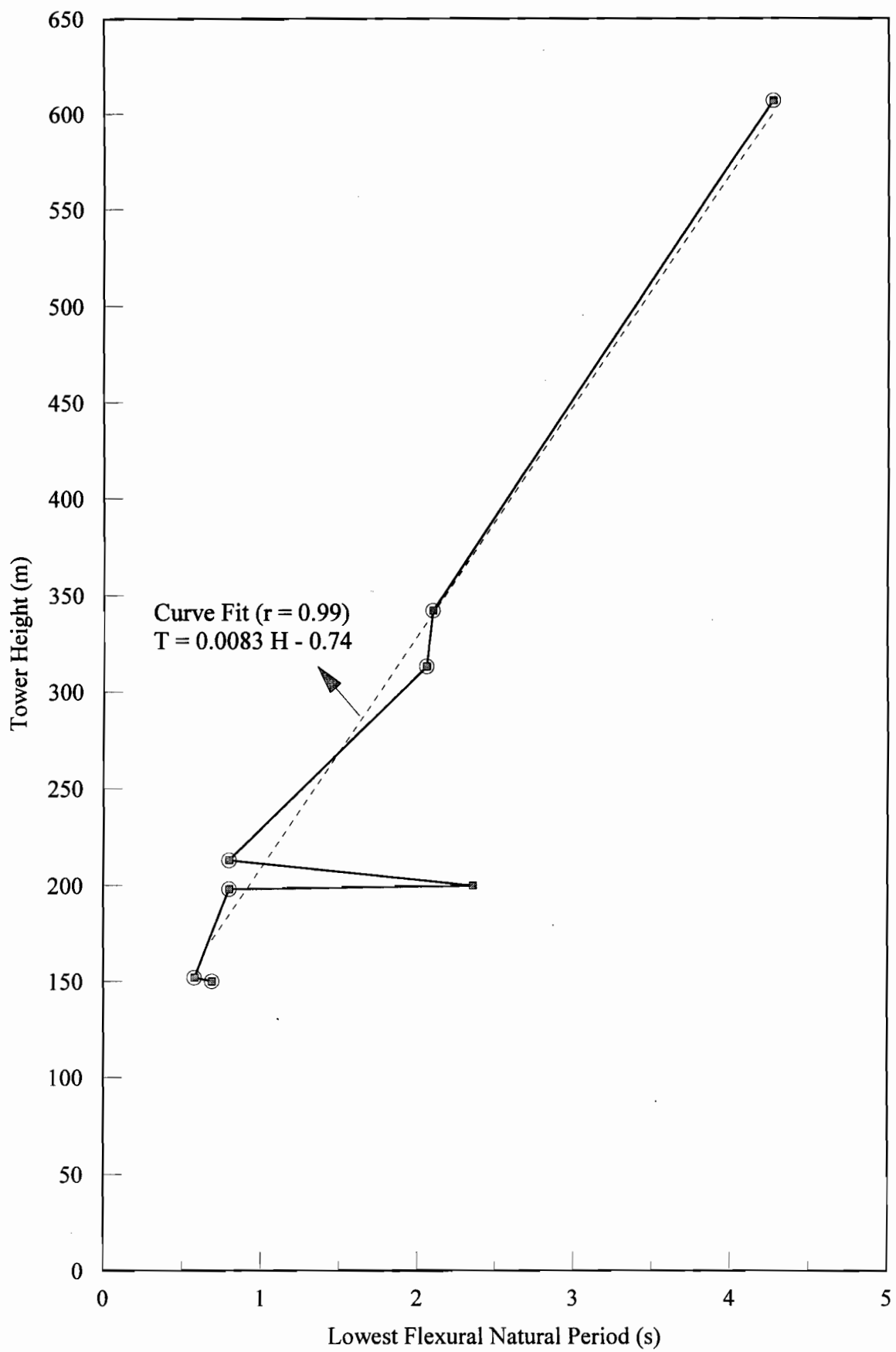
Fig. 4.1. Lowest flexural natural period versus tower height

41

MODE 1
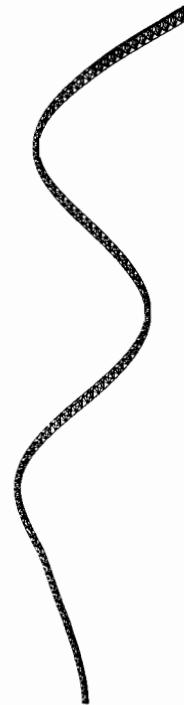
MODE 2

MODE 3

MODE 4

Fig. 4.2. Four lowest flexural mode shapes of the 150-m tower

MODE 1

MODE 2
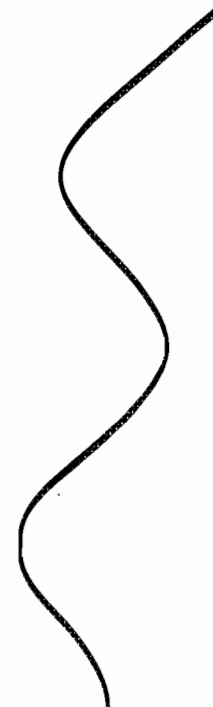
MODE 3

MODE 4

Fig. 4.3. Four lowest flexural mode shapes of the 152-m tower

Fig. 4.4. Four lowest flexural mode shapes of the 198-m tower

44

MODE 1

MODE 2

MODE 3

MODE 4

Fig. 4.5. Four lowest flexural mode shapes of the 200-m tower

MODE 1

MODE 2

MODE 3

MODE 4

Fig. 4.6. Four lowest flexural mode shapes of the 213-m tower

MODE 1

MODE 2
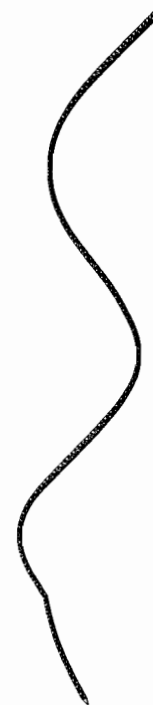
MODE 3

MODE 4

Fig. 4.7. Four lowest flexural mode shapes of the 313-m tower

MODE 1
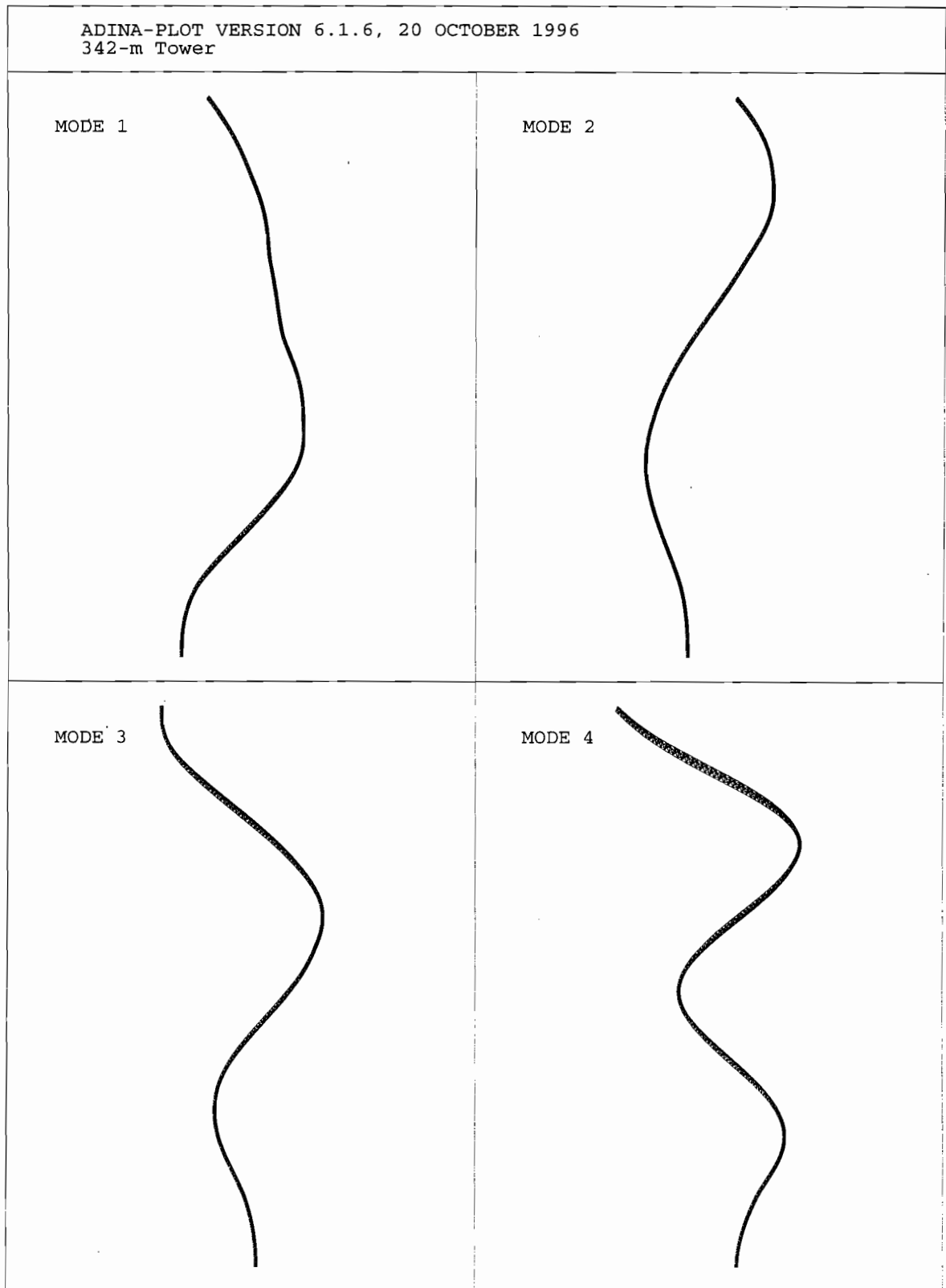
MODE 2

MODE 3

MODE 4

Fig. 4.8. Four lowest flexural mode shapes of the 342-m tower

MODE 1

MODE 2

MODE 3
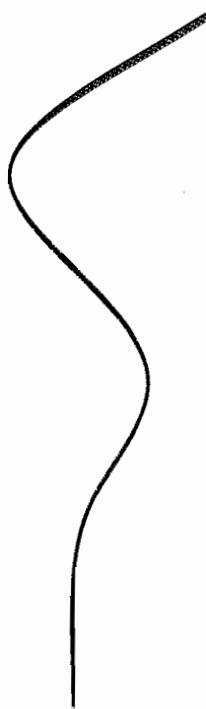
MODE 4
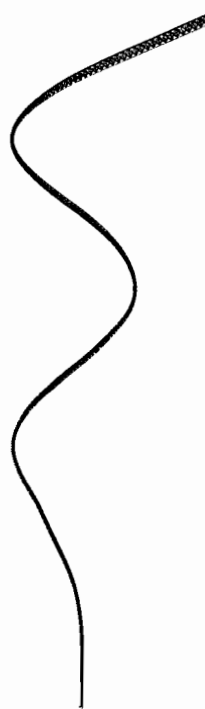
Fig. 4.9. Four lowest flexural mode shapes of the 607-m tower

details, in order to obtain a proper knowledge of the response of the towers. The first five response indicators are the results to use for strength and stability analysis of these structures, whereas the last four are used for serviceability considerations. The followings define these response indicators more precisely:

Earthquake Force: The earthquake force is the resultant horizontal cable reaction force generated by an earthquake on the mast at the cable attachment points. It therefore accounts for inertia effects in both the cables and the mast.

Dynamic Component of Cable Tension: The dynamic component of cable tension is the total cable tension less the initial tension due to self weight and initial prestressing. This is the net cable tension generated by the earthquake.

Mast Shear: The mast shear is the horizontal resultant force at a cross section of the mast due to seismic loading in the earthquake direction. This force is calculated by the vector summation of forces in the mast elements at a cross section (i.e. diagonal elements are included).

Dynamic Component of Mast Axial Force: This force is the vertical resultant force at a cross section of the mast due to the seismic excitation. It is the total force less the initial axial force due to the gravity load and the initial prestressing of the cables. The mast axial force is also calculated by the vector summation of forces of the mast elements (i.e. diagonal and leg elements).

Mast Bending Moment: The mast bending moment is obtained by the vector summation of forces of the mast elements at a cross section. Both diagonal and leg elements are used in this calculation.

Dynamic Component of Cable Oscillation: This variable represents the magnitude of the oscillation of a cable point due to earthquake motion only, and does not include the

initial cable sag due to self weight and initial prestressing. This displacement variable corresponds to the force variable of the dynamic component of cable tension.

Mast Horizontal Displacement: This parameter shows the lateral displacement of the mast due to the earthquake accelerogram. This displacement parameter corresponds to the force parameter of the mast shear.

Dynamic Component of Mast Axial Displacement: This variable represents the total axial displacement minus the initial axial displacement due to self weight and the initial prestressing of cables. This displacement corresponds to the force variable of the dynamic component of mast axial force.

Mast Rotation: This parameter is the rotation (tilting) of the mast due to the earthquake excitation. It corresponds to the mast bending moment.

4.3 DETAILED NONLINEAR DYNAMIC ANALYSES

In this section, 18 figures are presented for each of the eight towers [for example Figs. 4.10, 4.11(a,b,c, and d), 4.12(a,b,c, and d), 4.13, 4.14(a,b,c, and d), and 4.15(a,b,c, and d) for the 150-m tower]. The first nine figures shows the results of analyses due to horizontal earthquake accelerograms only, and the last nine present the results of analyses due to combined horizontal and vertical earthquake motions. All results are due to the three earthquake excitations of El Centro, Parkfield, and Taft. The vertical axis of all figures shows the tower elevation and the locations of guy cluster stay levels. These stay levels are marked with two different signs (diamond and asterisk) representing two different groups of guy clusters, with reference to their ground attachment points. The inner group includes guy clusters which are connected to the inner anchorage points on the ground and the outer group comprises guy clusters which are connected to the outer anchor. For the towers with three groups of ground anchors, the intermediate group is also shown separately (e.g. Fig. 4.28, filled square sign for the 200-m tower). The portion of

51

the mast between two consecutive groups of cables is called the transition zone.

The first figure (e.g. Fig. 4.10) illustrates the variation of the earthquake forces with tower elevation. The next four figures {e.g. Figs. 4.11(a, b, c, and d)} shown depict the variation of the dynamic component of cable tension, mast shear, dynamic component of mast axial force, and mast bending moment along the tower elevation. On a third page, there are four figures of four displacement variables {e.g. Figs. 4.12(a, b, c, and d)} which correspond to the four force variables of the figures on the previous page {e.g. Figs. 4.11(a, b, c, and d)}. These figures illustrate the variation of the dynamic component of cable oscillation, mast horizontal displacement, dynamic component of mast displacement, and mast rotation along the tower elevation.

Since the variables of the earthquake forces, dynamic component of cable tension and dynamic component of cable oscillation are discrete parameters along the tower elevation, their data points are connected by dashed line in order to show the trend of variation. The solid lines in the other figures are not meant to show that the variation of the response indicator between two data points is linear. It only illustrate the trend of that response indicator and its continuous nature.

The parameters of dynamic component of cable tension and dynamic component of cable oscillation are the maximum response among the cables of each set and also along the cables. For this purpose, four points along the cable were monitored: the two end points, the middle point, and the top-quarter point of each guy cable. The other response indicators are measured at guy stay levels and at midspan between two stay levels. It should be mentioned that all of these responses are envelope curves of the maximum amplitudes.

The figures showing results due to the horizontal earthquake and the corresponding figures due to the combined horizontal and vertical earthquake motions, have the same scale on their horizontal axis for ease of comparison (with the exception of the dynamic component of the mast axial force, where a large effect is expected due to the combined horizontal and vertical accelerograms).

It should be mentioned that all the detailed results of the eight guyed towers studied are available in technical reports published by Amiri and McClure (1997, No. 97-

52

1, 97-2, 97-3, 97-4, 97-5, 97-6, 97-7, and 97-8).

4.3.1 150-m Tower

Figures 4.10 to 4.15 show the results of the detailed seismic nonlinear analysis for the 150-m tower. Except for the dynamic component of mast axial force, there is not a significant difference between the results under the horizontal earthquake and the corresponding results for the combined horizontal and vertical earthquake motions.

As illustrated in Figs. 4.10 and 4.13, the earthquake forces at the stay levels of the outer group are larger than those of the inner group. The Parkfield accelerogram has the most effect on the earthquake forces, and the El Centro and Taft accelerograms would be in the second and third order in this regard. The intermediate cable Set 5 (from the base) at the transition zone is the most excited. There is a discontinuity in behaviour around the transition area, between stay levels of Sets 4 and 5.

In Figs. 4.11(a) and 4.14(a), it can be seen that the intermediate cable Set 6 (from the base) close to the transition part is more excited than the other ones. The Parkfield, El Centro and Taft accelerograms are again in the first, second and third order, respectively, in terms of amplitudes of seismic effects. In general, the response increases with the tower elevation, and there is a discontinuity in the behaviour around the transition zone, between stay levels of Sets 4 to 6.

The mast shear and bending moments along the tower elevation are shown in Figs. 4.11(b and d) and 4.14(b and d), respectively. These two response indicators increase with the tower elevation and their maximum value occurs close to the transition area. There is again a discontinuity in behaviour around the transition region, especially in the envelope curve of the bending moment. In general, the maximum shear occurs directly at the stay levels and the minimum shear occurs at midspan between the two stay levels, and vice versa for the mast bending moment (the only exception is stay level #1). The responses are consistent for the three accelerograms.

Figures 4.11(c) and 4.14(c) represent the dynamic component of mast axial force along the tower. As expected, there is no significant axial effect from the load case of

horizontal earthquake motion. However, in the case of combined horizontal and vertical accelerograms, the El Centro and Taft earthquakes cause considerably larger axial effects than the Parkfield earthquake.

The dynamic component of cable oscillations is shown in Figs. 4.12(a) and 4.15(a). It is noted that the behaviour is nonuniform around the transition zone. The oscillations of the cables of the outer group are larger than those of the inner group (except for the Taft accelerogram for which they are about the same). Also, the El Centro and Parkfield accelerograms are considerably more exciting than the Taft accelerogram for the cables of the outer group. The maximum response occurs around the transition area.

The mast horizontal displacement and the mast rotation are summarized in Figs. 4.12(b and d) and 4.15(b and d), respectively. There is also a discontinuity in the behaviour around the transition region for both responses, and the maximum horizontal displacement occurs close to the transition area. The top part of the tower experiences the maximum rotation. The El Centro and Parkfield accelerograms are more exciting than Taft as far as these response indicators are concerned.

As it can be seen from Figs. 4.12(c) and 4.15(c), the dynamic component of mast axial displacement along the tower elevation is negligible in the case of horizontal ground motion, and very small (about 1 cm) in the case of combined horizontal and vertical accelerations.

Fig. 4.10. Response of 150-m tower to three base accelerograms

55

(a) Dynamic Component of Cable Tension (kN)

(b) Mast Shear (kN)

(c) Dynamic Comp. of Mast Axial Force (kN)

(d) Mast Bending Moment (kN-m)

Guy clusters attached to:

Inner Anchor	Outer Anchor
◈	★

Base Accelerograms:

El Centro	Parkfield	Taft
■	⊖	✳
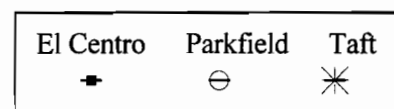
Fig. 4.11. Response of 150-m tower to three base accelerograms

56

(a) Dynamic Component of Cable Oscillation (m)

(b) Mast Horizontal Displacement (m)

(c) Dynamic Component of Mast Axial Displ. (m)

Negligible

(d) Mast Rotation (Degree)

Inner Anchor	Outer Anchor

Guy clusters attached to:

El Centro	Parkfield	Taft
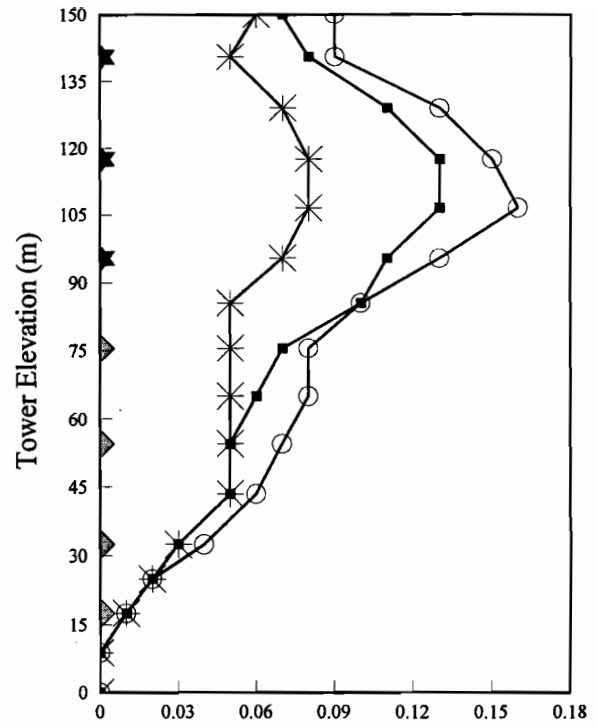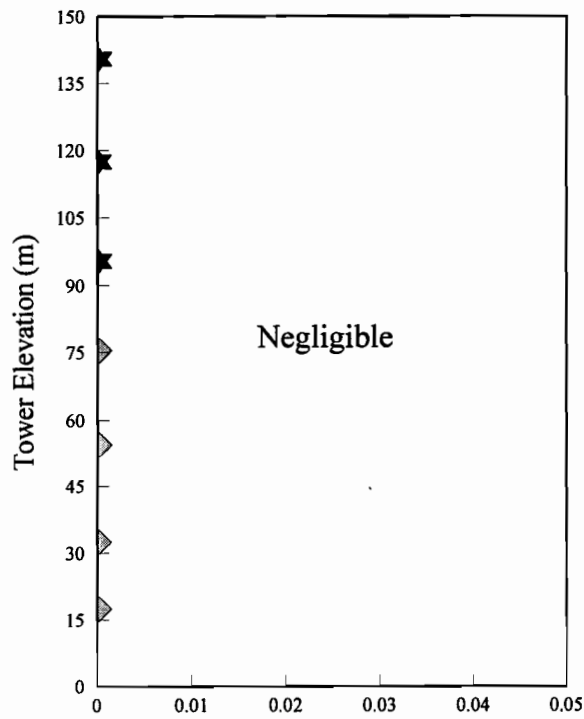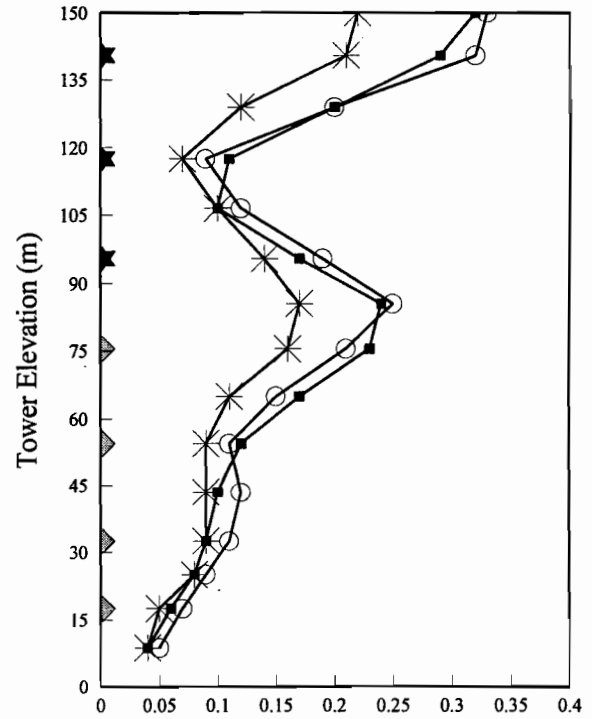
Base Accelerograms:
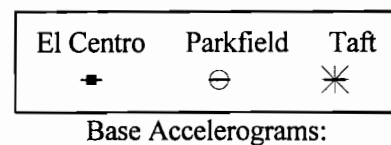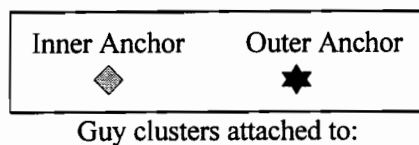
Fig. 4.12. Response of 150-m tower to three base accelerograms

Fig. 4.13. Response of 150-m tower to three base accelerograms (Horizontal + Vertical)

(a) Dynamic Component of Cable Tension (kN)

(b) Mast Shear (kN)

(c) Dynamic Comp. of Mast Axial Force (kN)

(d) Mast Bending Moment (kN-m)

Guy clusters attached to:
Inner Anchor   Outer Anchor

Base Accelerograms:
El Centro   Parkfield   Taft

Fig. 4.14. Response of 150-m tower to three base accelerograms (Horizontal + Vertical)

59

(a) Dynamic Component of Cable Oscillation (m)

(b) Mast Horizontal Displacement (m)

(c) Dynamic Component of Mast Axial Displ. (m)

(d) Mast Rotation (Degree)

Inner Anchor	Outer Anchor
◈	★

Guy clusters attached to:

El Centro	Parkfield	Taft
■	⊖	✳
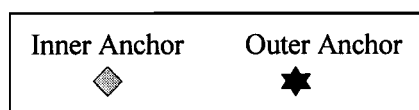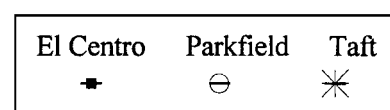
Base Accelerograms:

Fig. 4.15. Response of 150-m tower to three base accelerograms (Horizontal + Vertical)

60

4.3.2 152-m Tower

Figures 4.16 to 4.21 show the results of the detailed seismic nonlinear analysis for the 152-m tower. Except for the dynamic component of mast axial force, there is not a significant difference between the results under the horizontal earthquake and the corresponding results for the combined horizontal and vertical earthquake motions.

As illustrated in Figs. 4.16 and 4.19, the earthquake forces at the stay levels of the outer group are smaller than those of the inner group. The Parkfield and El Centro accelerograms have more effect on the earthquake forces than the Taft accelerogram. The intermediate cable Set 3 (from the base) close to the transition zone is the most excited. There is a nonuniform behaviour around the transition area.

In Figs. 4.17(a) and 4.20(a), it can be seen that the intermediate cable Set 6 (from the base) close to the transition part is more excited than the other ones. The Parkfield and El Centro accelerograms have more effect on the behaviour than the Taft accelerogram. There is again a discontinuity in the behaviour around the transition zone.

The mast shear and bending moments along the tower elevation are shown in Figs. 4.17(b and d) and 4.20(b and d), respectively. The maximum dynamic effect of these two response indicators occurs close to the transition area between stay levels of Sets 3 and 4. There is a definite discontinuity in these figures around the transition region. The maximum shear occurs directly at the stay levels and the minimum shear occurs at the midspan between the two stay levels, and vice versa for the mast bending moment. The responses are consistent for the three accelerograms.

Figures 4.17(c) and 4.20(c) represent the dynamic component of mast axial force along the tower. As expected, there is no significant axial effect from the load case of horizontal earthquake motion. However, in the case of combined horizontal and vertical earthquake accelerograms, the Taft accelerogram has the most effect on the dynamic component of mast axial force and the El Centro and Parkfield accelerograms would be in the second and third order in this regard.

The dynamic component of cable oscillations is shown in Figs. 4.18(a) and 4.21(a). The oscillations of the cables of the outer group are larger those that of the inner

group (except for the Taft accelerogram for which they are almost uniform). Also, the El Centro and Parkfield accelerograms are considerably more exciting than the Taft accelerogram for the cables of the outer group. In general, this variable increases with the stay level elevation (except for the Taft accelerogram).

The mast horizontal displacement and the mast rotation are summarized in Figs. 4.18(b and d) and 4.21(b and d), respectively. There is an obvious discontinuity in the behaviour around the transition region for both responses, and the maximum horizontal displacement occurs close to the transition area. Again the top part of the tower experiences the maximum rotation. The El Centro and Parkfield accelerograms are more exciting than Taft as far as these response indicators are concerned.

As it can be seen from Figs. 4.18(c) and 4.21(c), the dynamic component of mast axial displacement along the tower elevation is negligible in the case of horizontal ground motion, and very small (about 1 cm) in the case of combined horizontal and vertical accelerations.
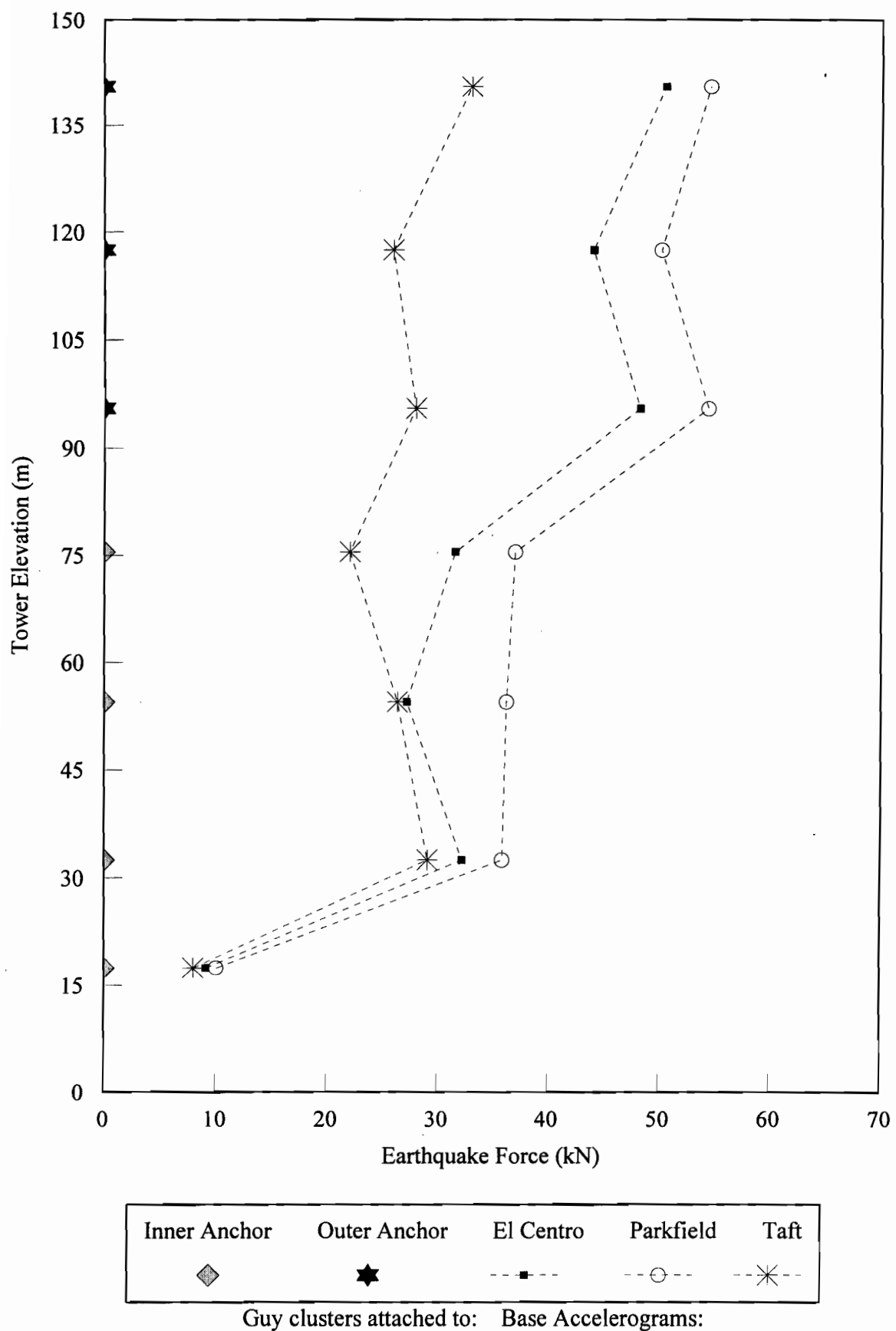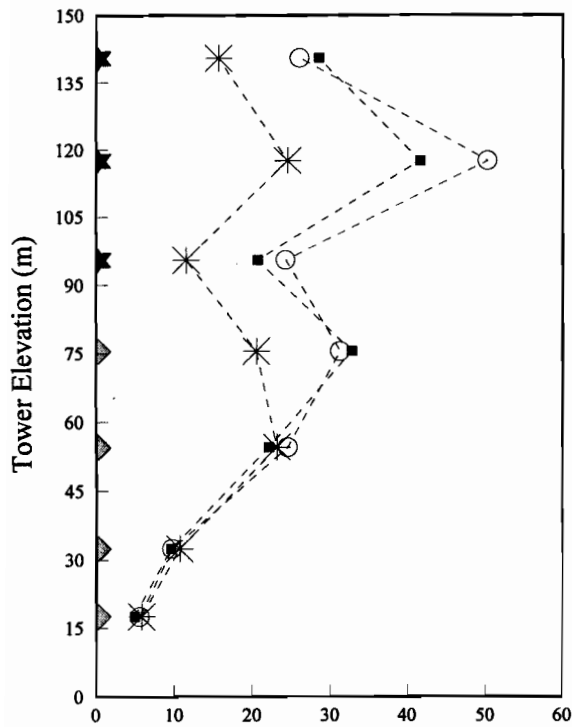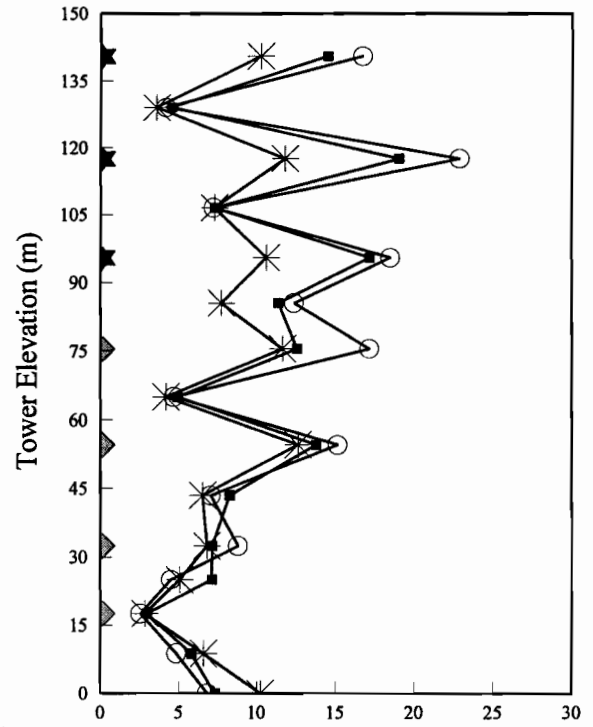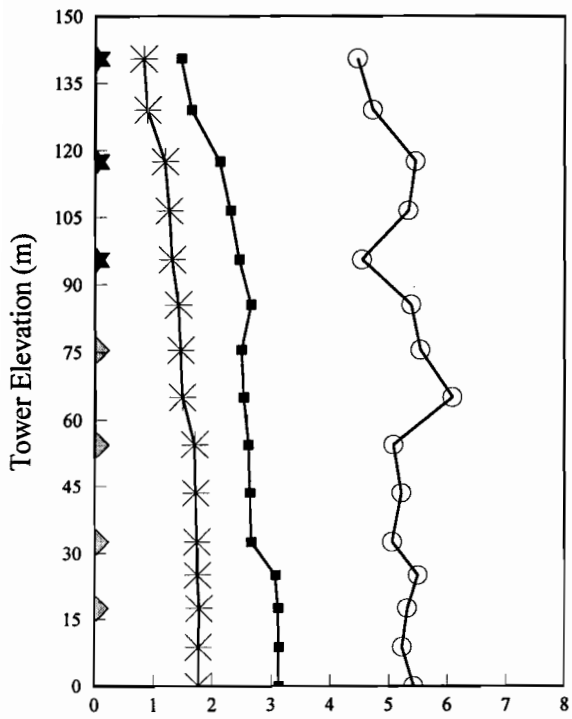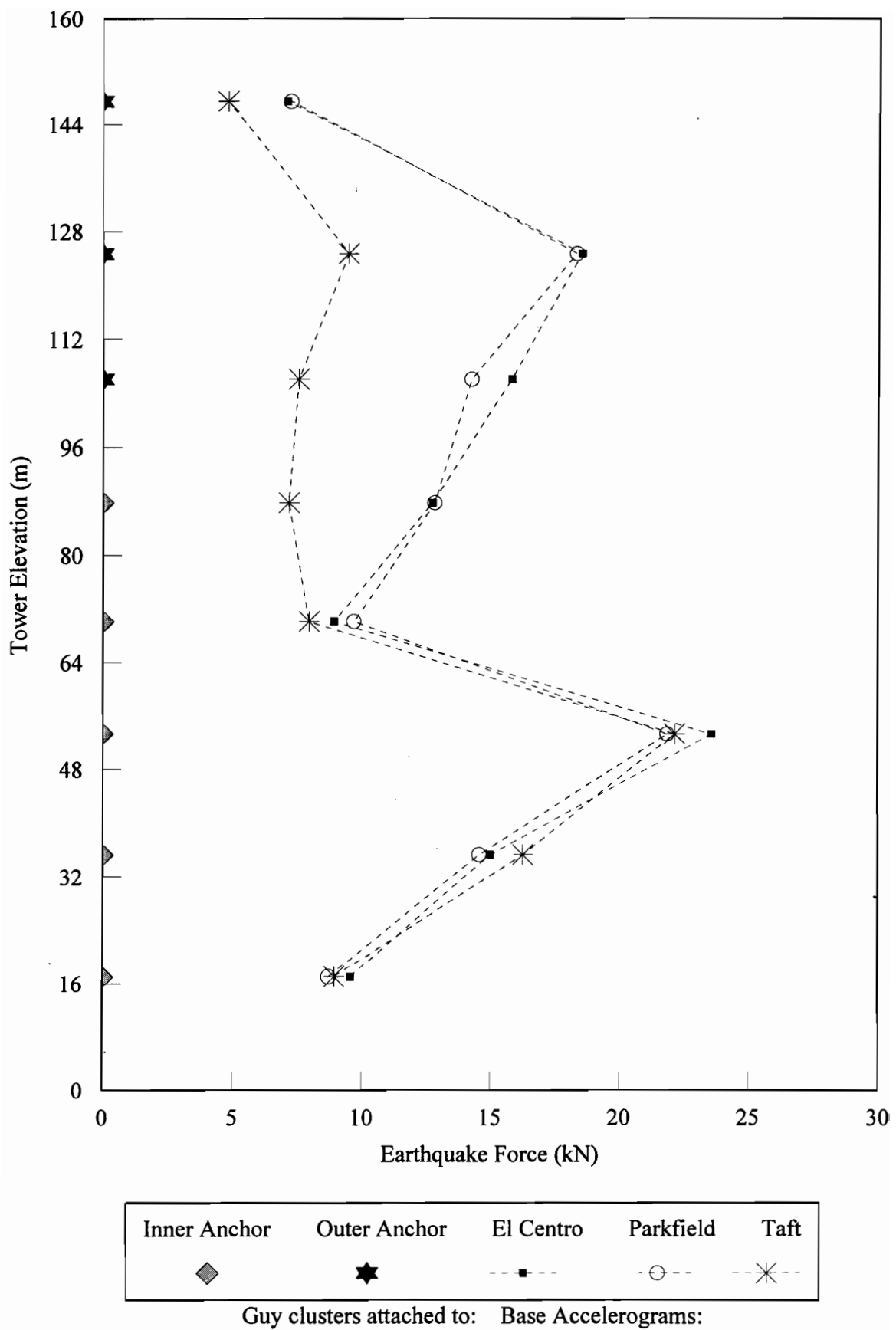
Fig. 4.16. Response of 152-m tower to three base accelerograms
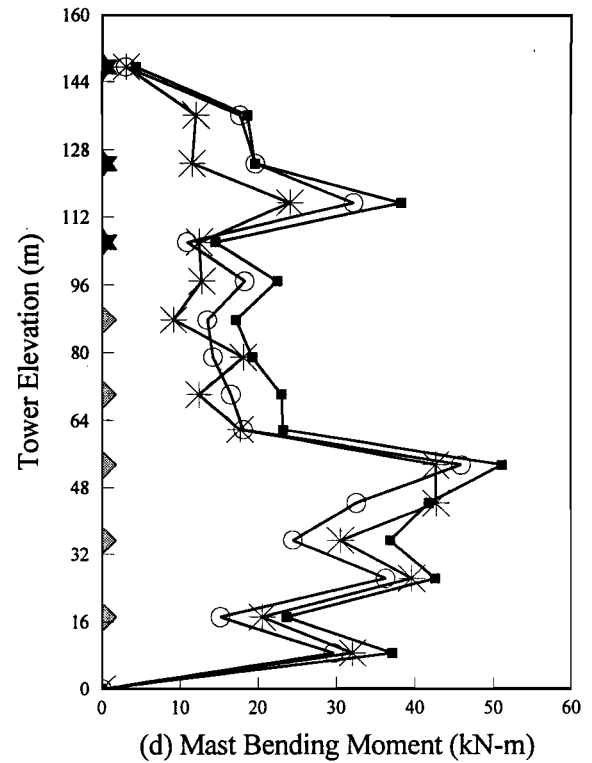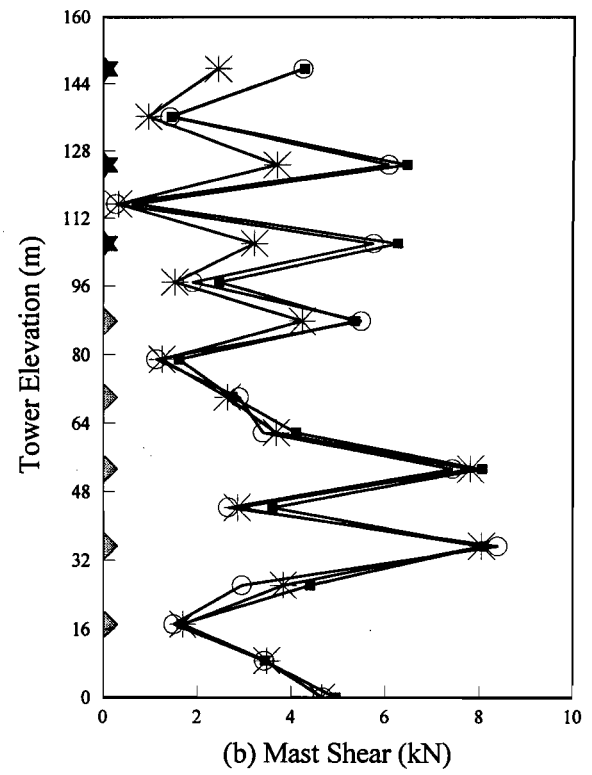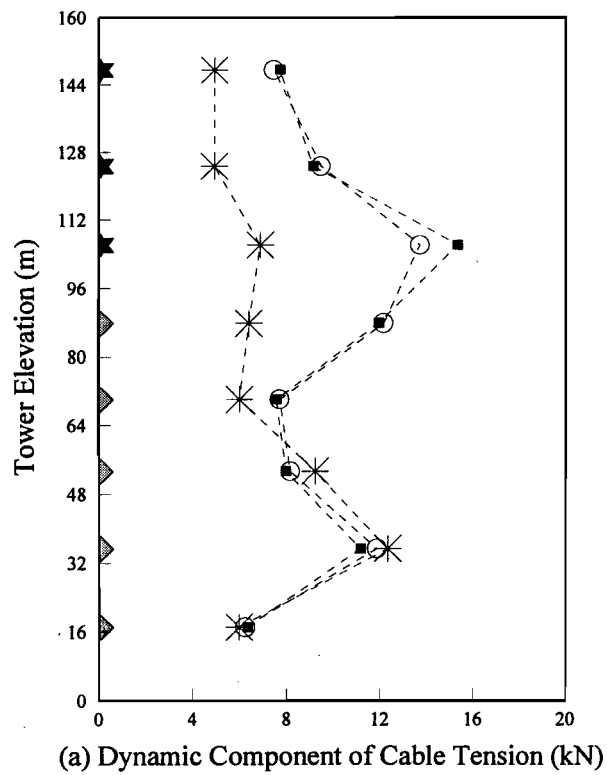
(a) Dynamic Component of Cable Tension (kN)

(b) Mast Shear (kN)

(c) Dynamic Comp. of Mast Axial Force (kN)

(d) Mast Bending Moment (kN-m)

Inner Anchor	Outer Anchor
◈	★

Guy clusters attached to:

El Centro	Parkfield	Taft
■	⊖	✳

Base Accelerograms:

Fig. 4.17. Response of 152-m tower to three base accelerograms
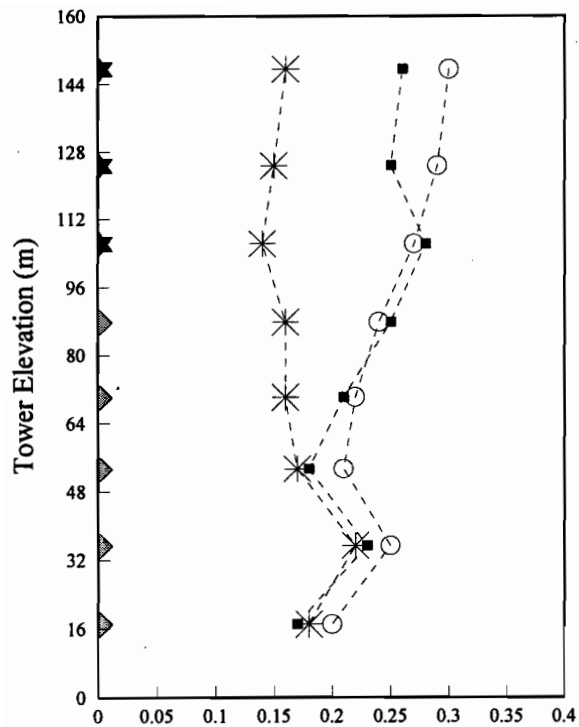
(a) Dynamic Component of Cable Oscillation (m)

(b) Mast Horizontal Displacement (m)

(c) Dynamic Component of Mast Axial Displ. (m)

Negligible

(d) Mast Rotation (Degree)

Inner Anchor	Outer Anchor
◈	★

Guy clusters attached to:

El Centro	Parkfield	Taft
▬	⊖	✳
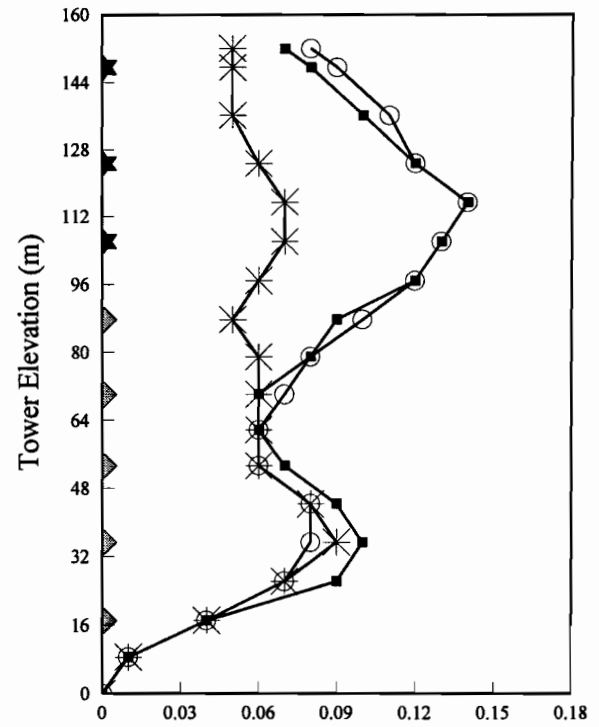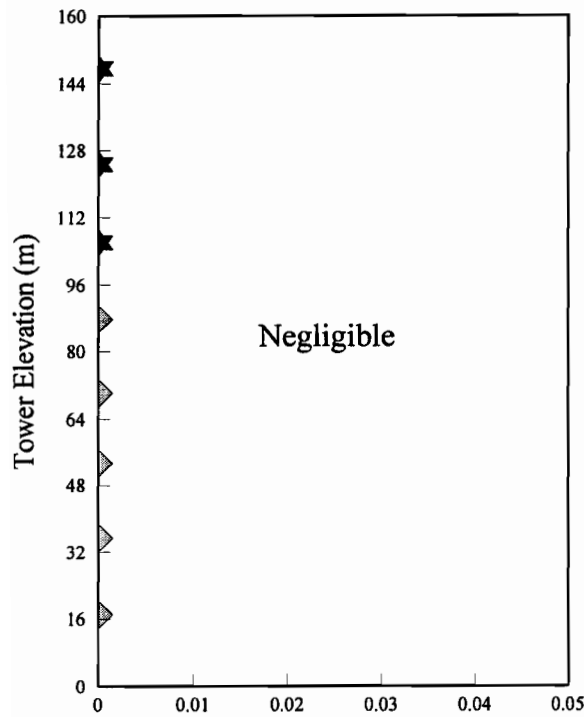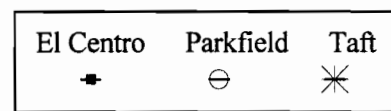
Base Accelerograms:

Fig. 4.18. Response of 152-m tower to three base accelerograms

65
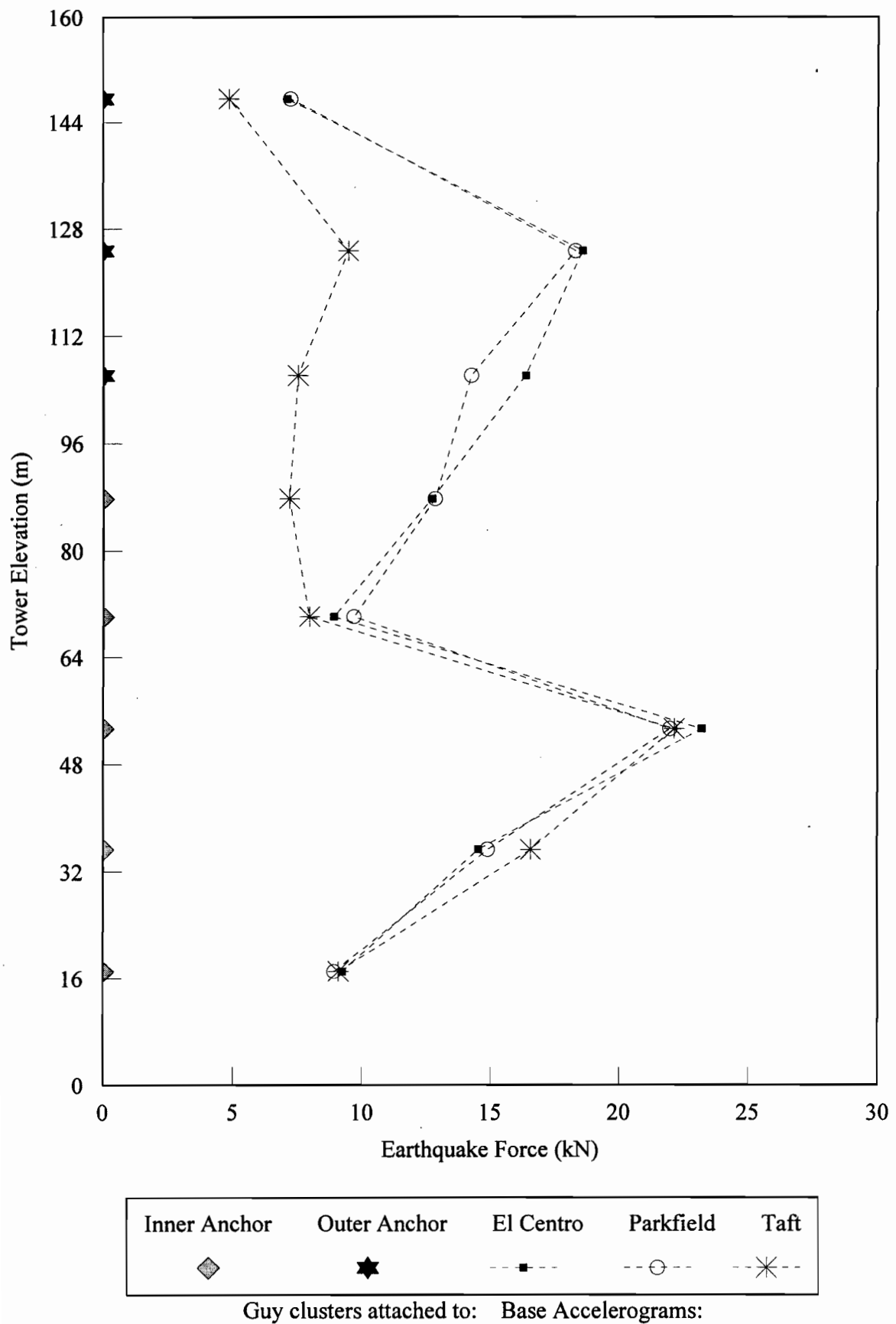
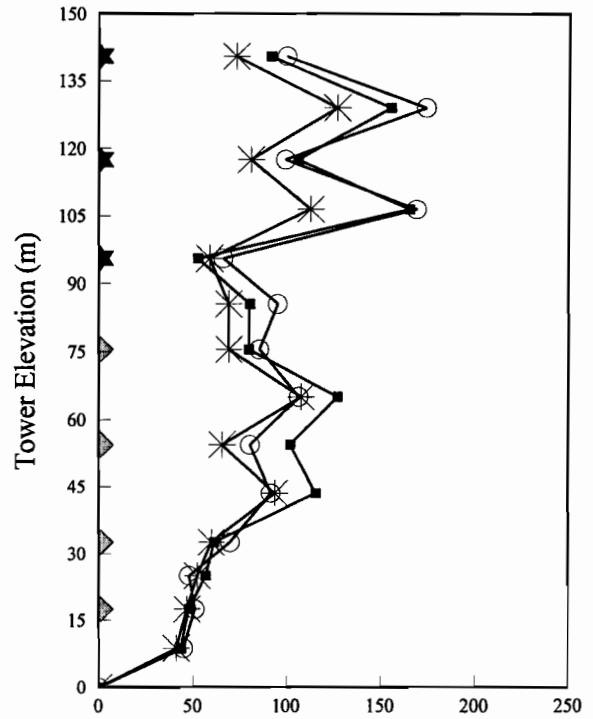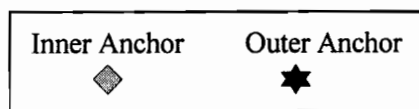Fig. 4.19. Response of 152-m tower to three base accelerograms (Horizontal + Vertical)
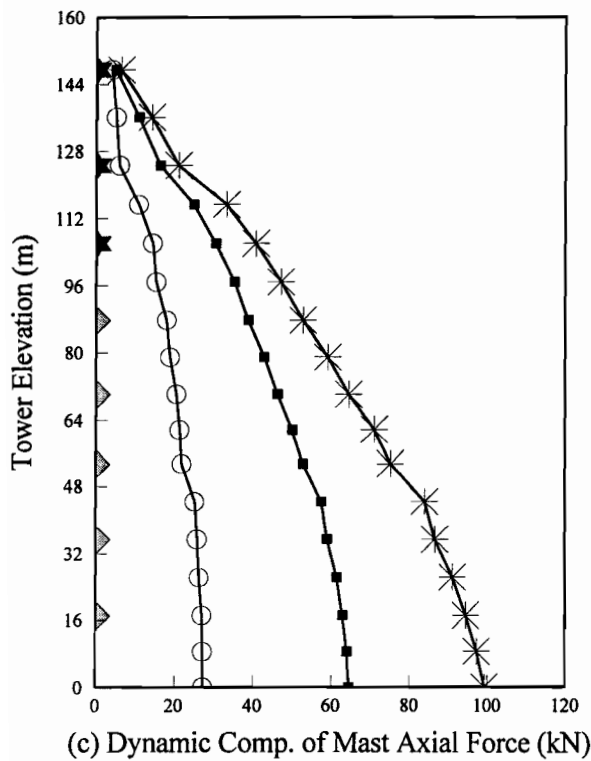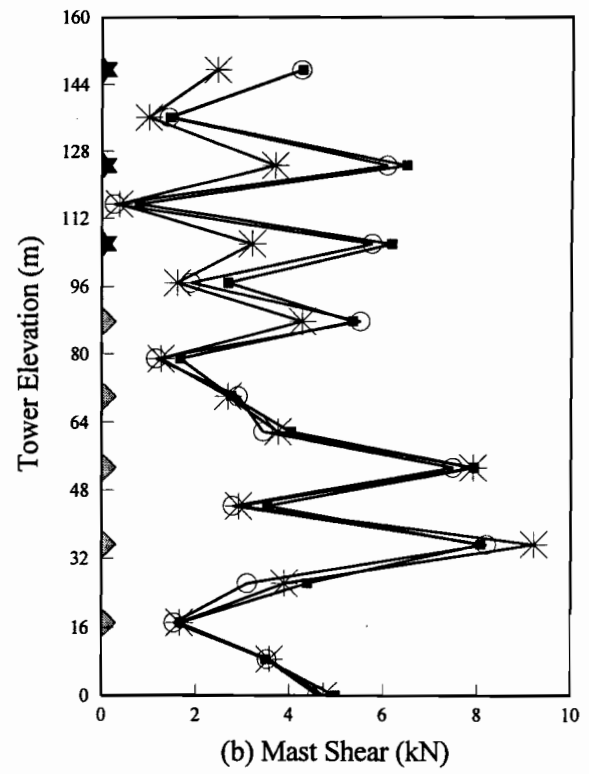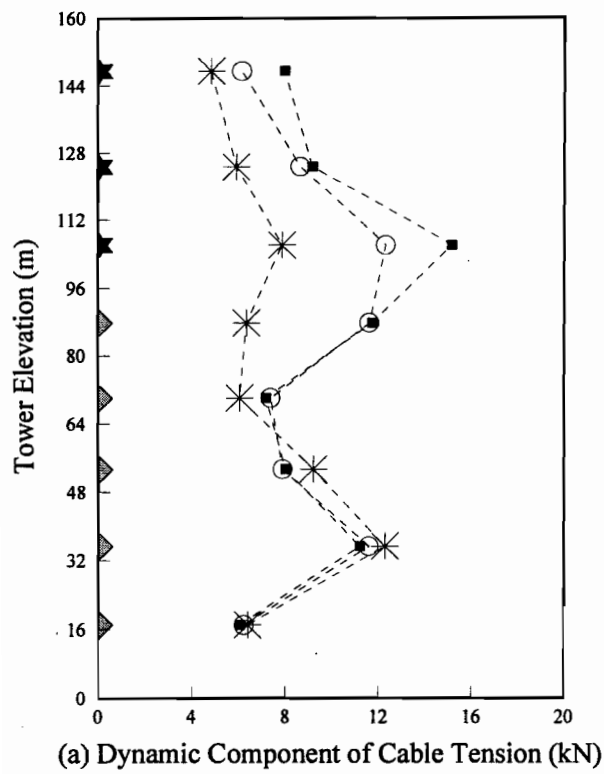
66

(a) Dynamic Component of Cable Tension (kN)

(b) Mast Shear (kN)

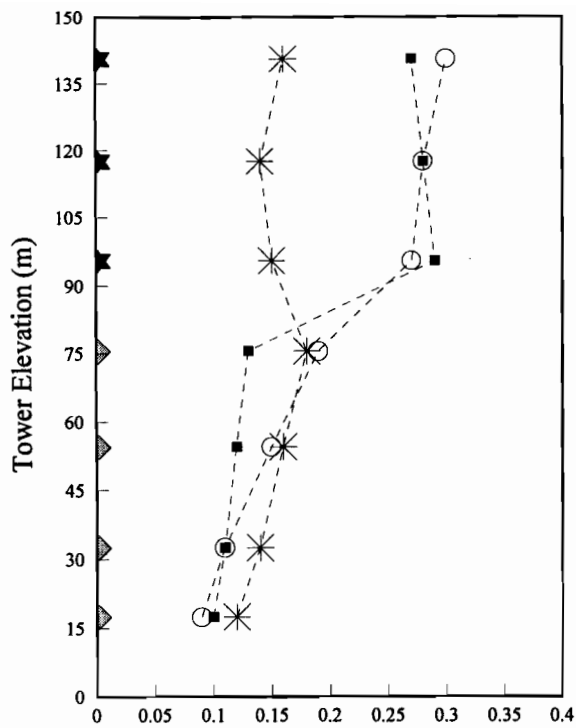(c) Dynamic Comp. of Mast Axial Force (kN)

(d) Mast Bending Moment (kN-m)

Inner Anchor	Outer Anchor
◇	✶

Guy clusters attached to:

El Centro	Parkfield	Taft
▪	⊖	✳

Base Accelerograms:

Fig. 4.20. Response of 152-m tower to three base accelerograms (Horizontal + Vertical)

67
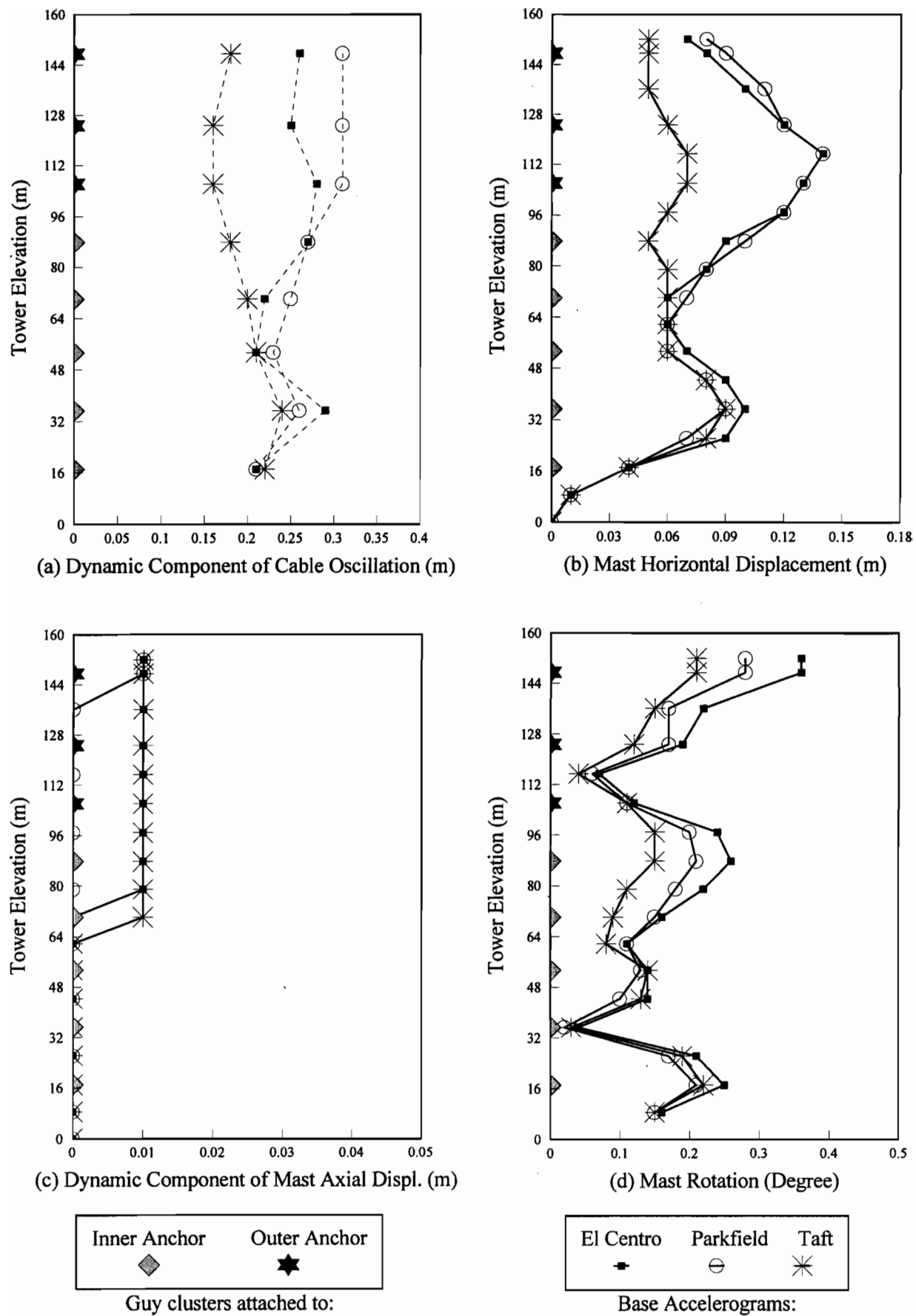
Fig. 4.21. Response of 152-m tower to three base accelerograms (Horizontal + Vertical)

4.3.3 198-m Tower

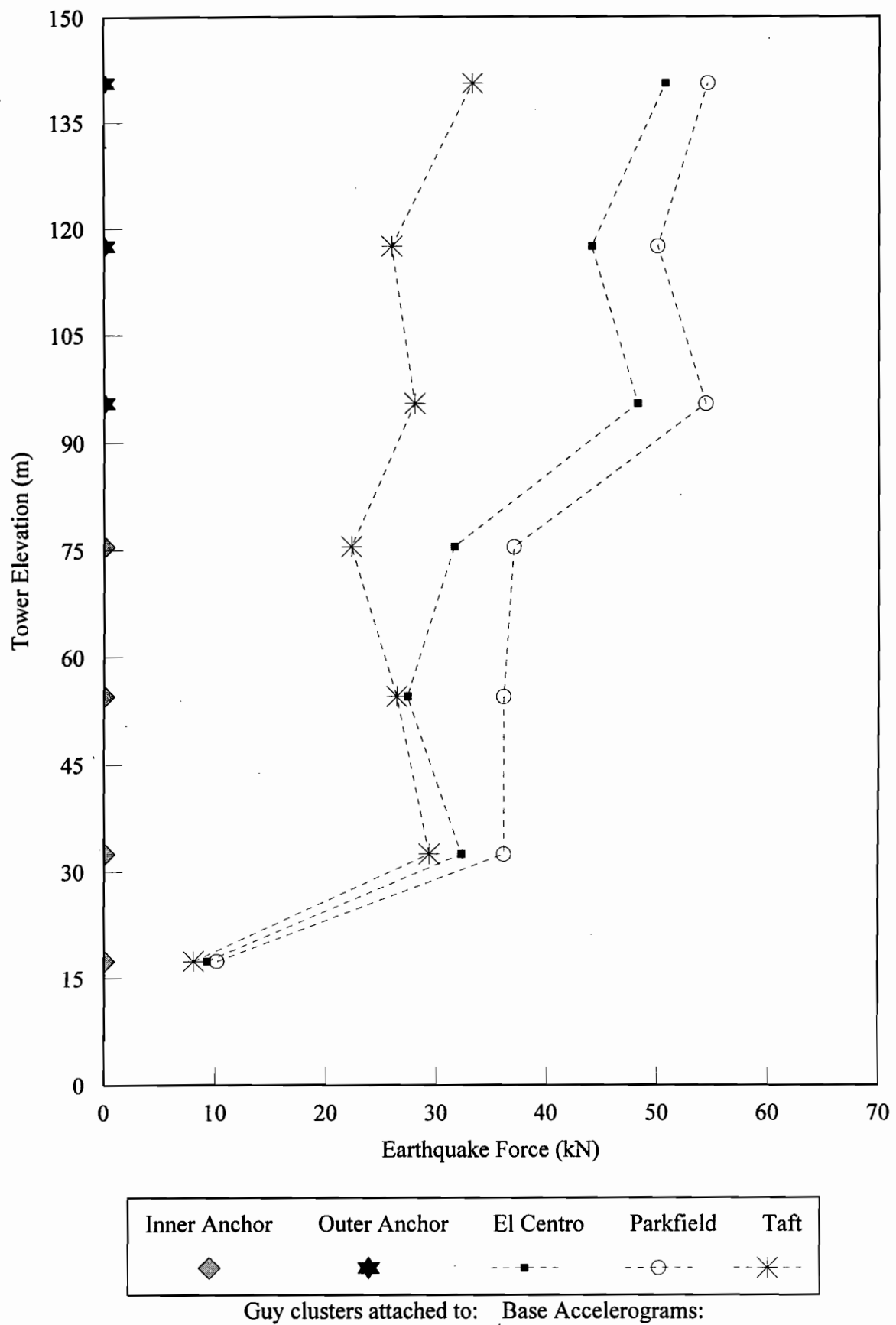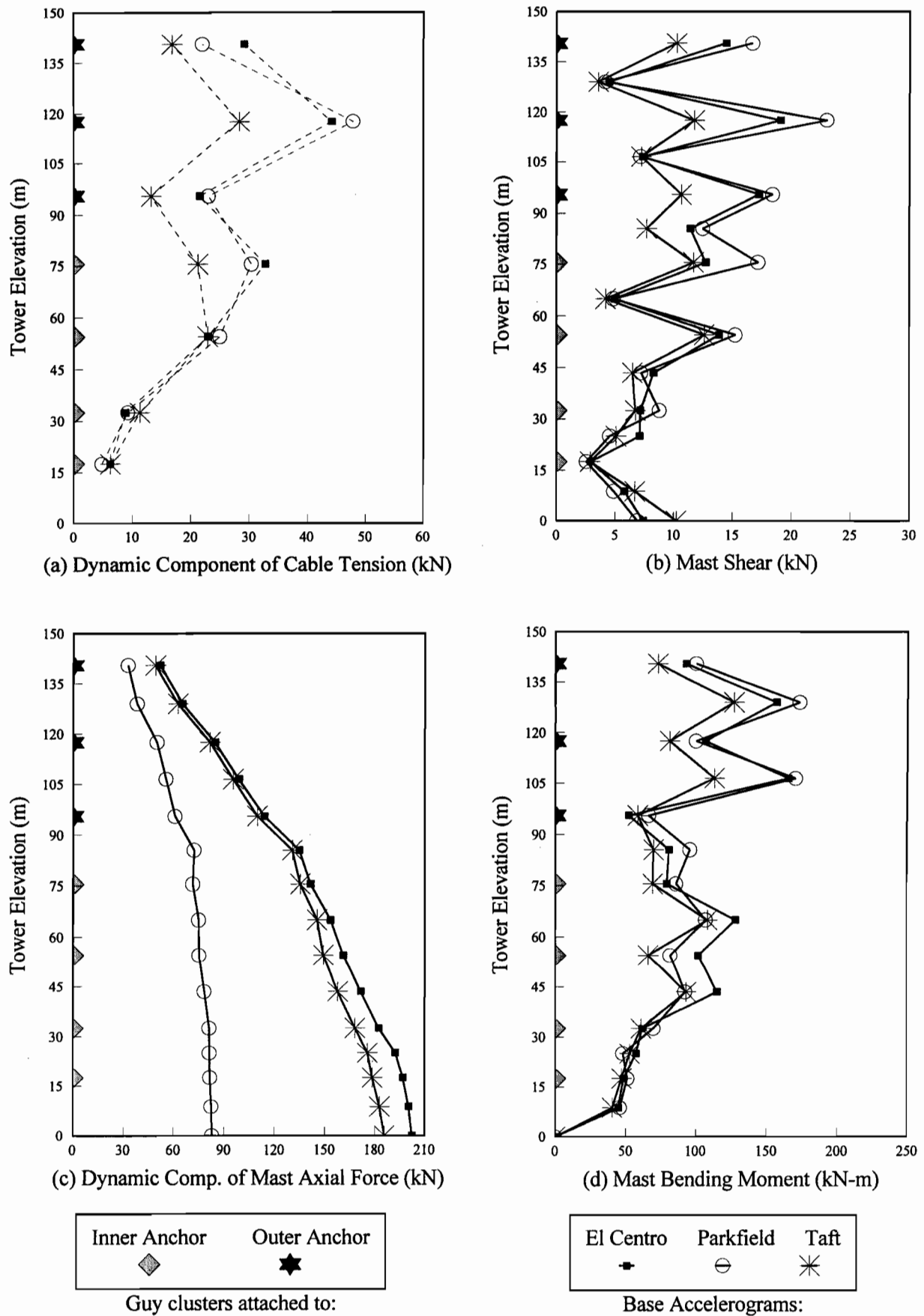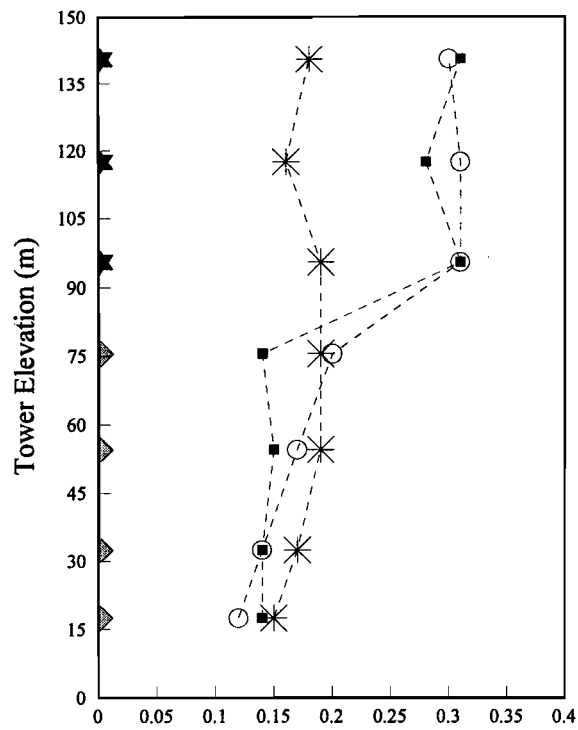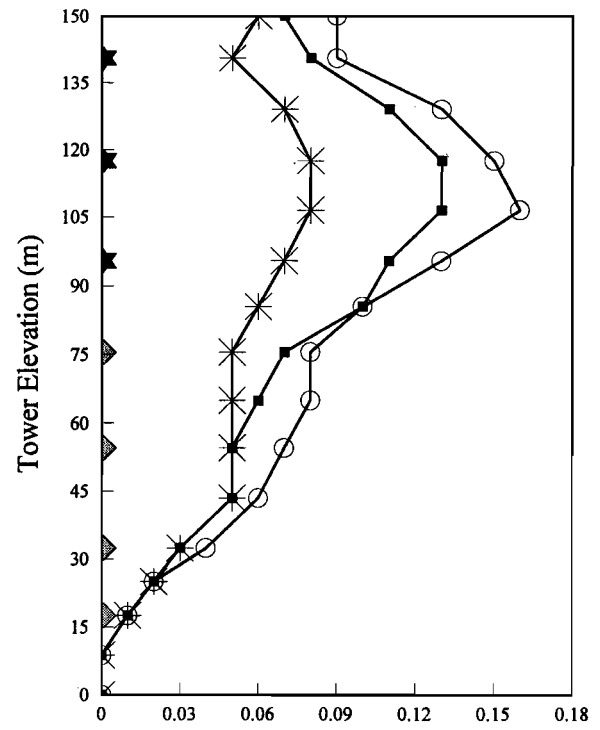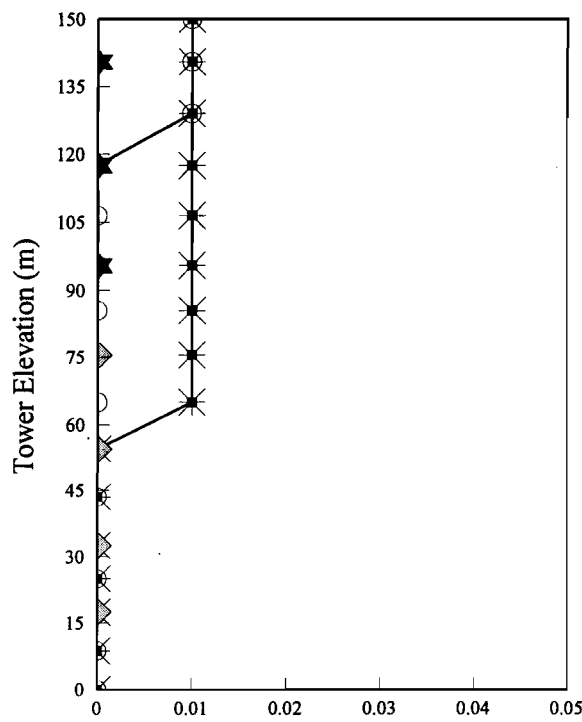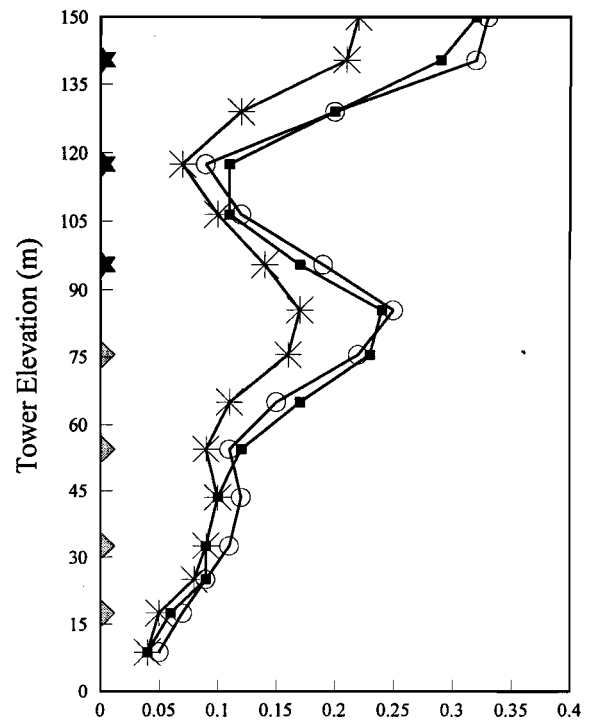Figures 4.22 to 4.27 show the results of the detailed seismic nonlinear analysis for the 198-m tower. Except for the dynamic component of mast axial force, there is not a significant difference between the results under horizontal earthquake and the corresponding results for the combined horizontal and vertical earthquake motions.

As illustrated in Figs. 4.22 and 4.25, the Taft accelerogram has the most effect on the earthquake forces, and the El Centro and Parkfield accelerograms are in the second place. The intermediate cable Set 4 (from the base) at the transition zone is more excited than the others. There is a nonuniform behaviour around the transition area, between cable Sets 3 and 4.

In Figs. 4.23(a) and 4.26(a), it can be seen that the intermediate cable Set 5 (from the base) close to the transition zone is more excited than the other ones. The Taft accelerogram has more effect on the behaviour than the others.

The mast shear and bending moments along the tower elevation are shown in Figs. 4.23(b and d) and 4.26(b and d), respectively. The maximum dynamic effect of these two response indicators occurs close to the transition area. There is also a discontinuity in behaviour around the transition region. In general, the maximum shear occurs directly at the stay levels and the minimum shear occurs at the midspan between the two stay levels, and vice versa for the mast bending moment. The responses are consistent for the three accelerograms.

Figures 4.23(c) and 4.26(c) represent the dynamic component of mast axial force along the tower. As expected, there is no significant axial effect from the load case of horizontal earthquake motion. However, in the case of combined horizontal and vertical earthquake accelerograms, the Taft accelerogram has the most effect on the dynamic component of mast axial force, and the El Centro and Parkfield accelerograms would be in the second and third order in this regard.

The dynamic component of cable oscillations is shown in Figs. 4.24(a) and 4.27(a). It is noted that there is a nonuniform behaviour around the transition zone between stay levels of Sets 2 and 3. The oscillations of cables of the outer group are

69

smaller than those of the inner group for all three accelerograms. The Parkfield accelerogram has the most effect on the dynamic component of cable oscillation and the El Centro and Taft accelerograms would be in the second and third order in this regard. The maximum response occurs around the transition area at the lower stay levels.

The mast horizontal displacement and the mast rotation are summarized in Figs. 4.24(b and d) and 4.27(b and d), respectively. There is a discontinuity in the behaviour around the transition region for both responses, and the maximum horizontal displacement occurs close to the transition area at the upper stay levels. The top part of the tower experiences the maximum rotation. The Taft accelerogram is more exciting than the other ones as far as these response indicators are concerned.

As it can be seen from Figs. 4.24(c) and 4.27(c), the dynamic component of the mast axial displacement along the tower elevation is very small (1 to 2 cm).
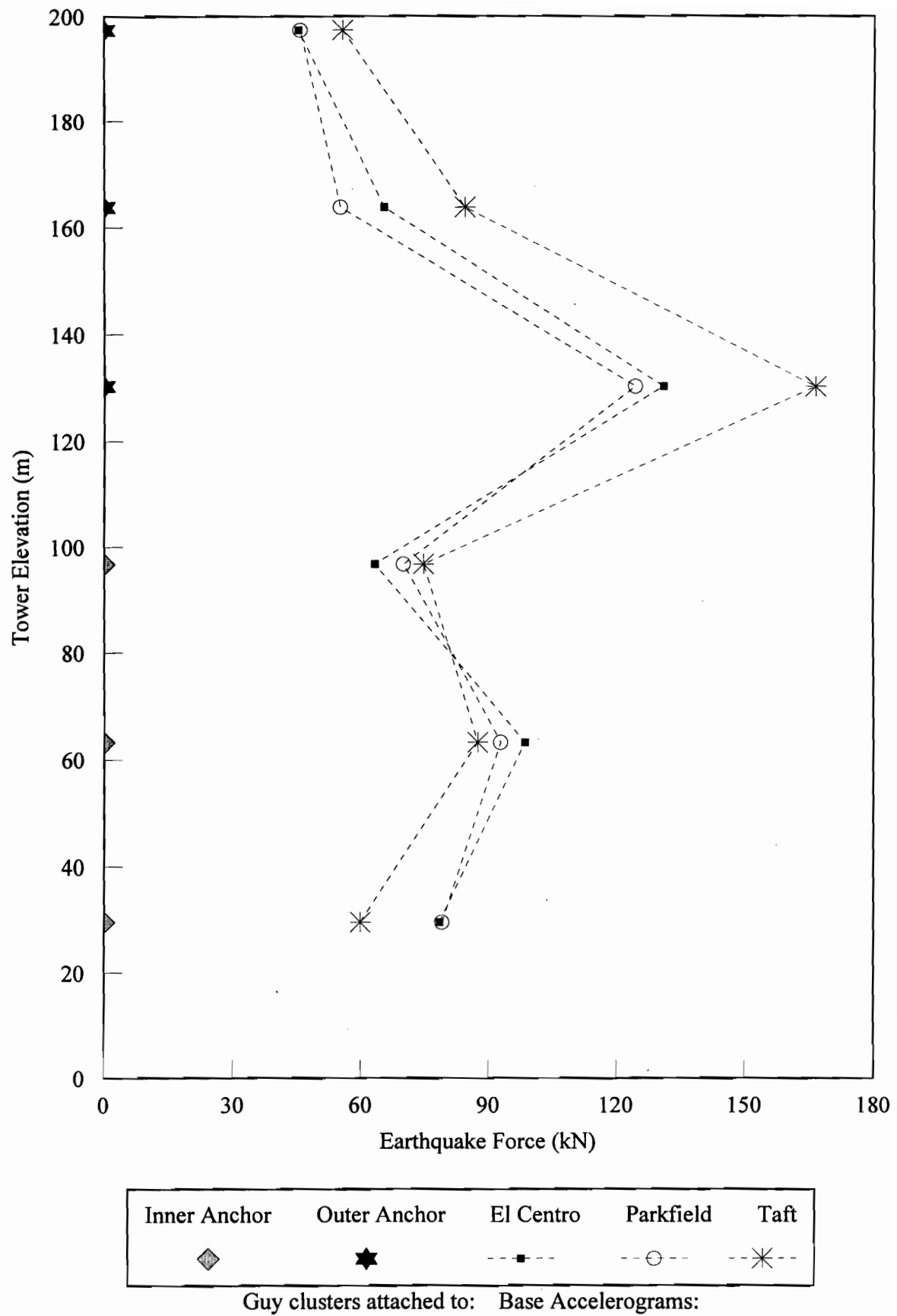
Fig. 4.22. Response of 198-m tower to three base accelerograms
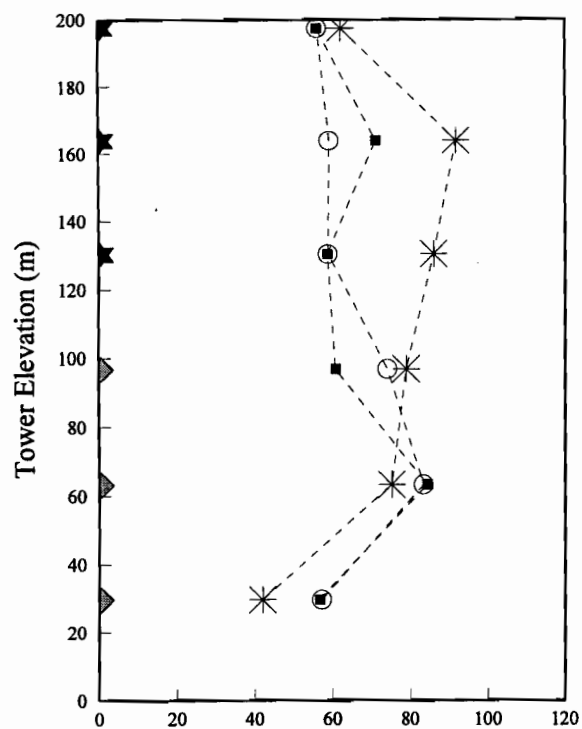
(a) Dynamic Component of Cable Tension (kN)

(b) Mast Shear (kN)

(c) Dynamic Comp. of Mast Axial Force (kN)

(d) Mast Bending Moment (kN-m)

Inner Anchor	Outer Anchor
◈	✶

Guy clusters attached to:

El Centro	Parkfield	Taft
■	⊖	✳
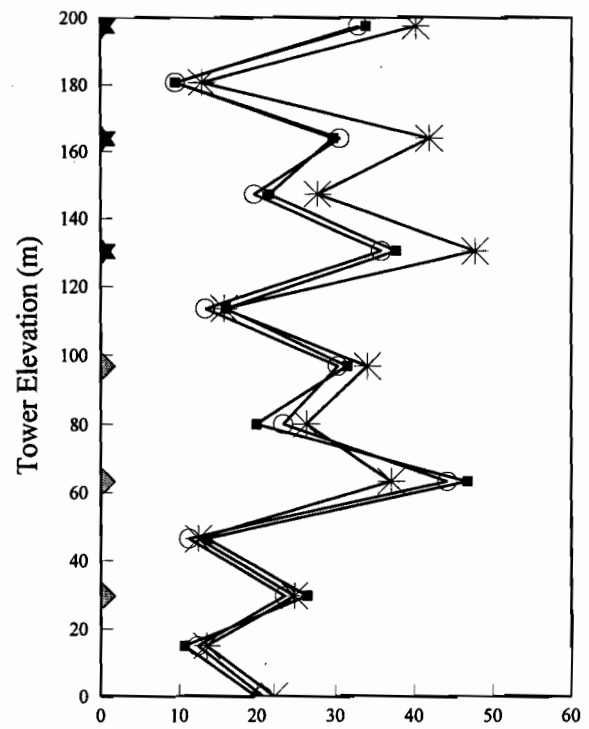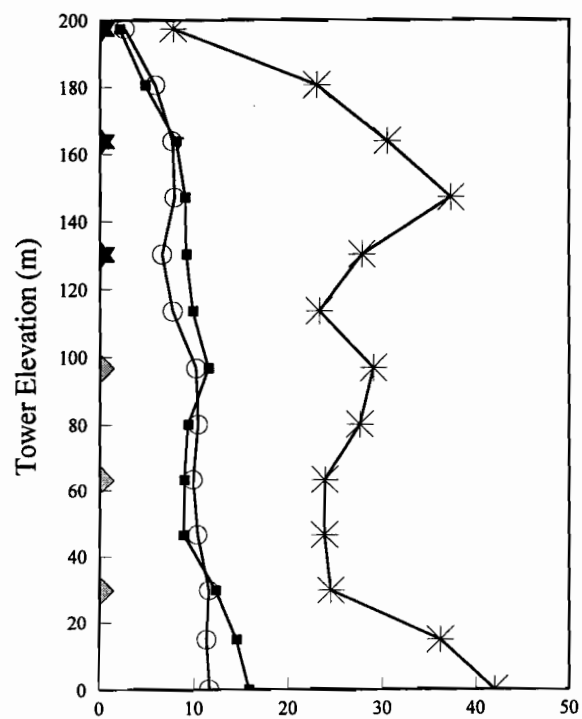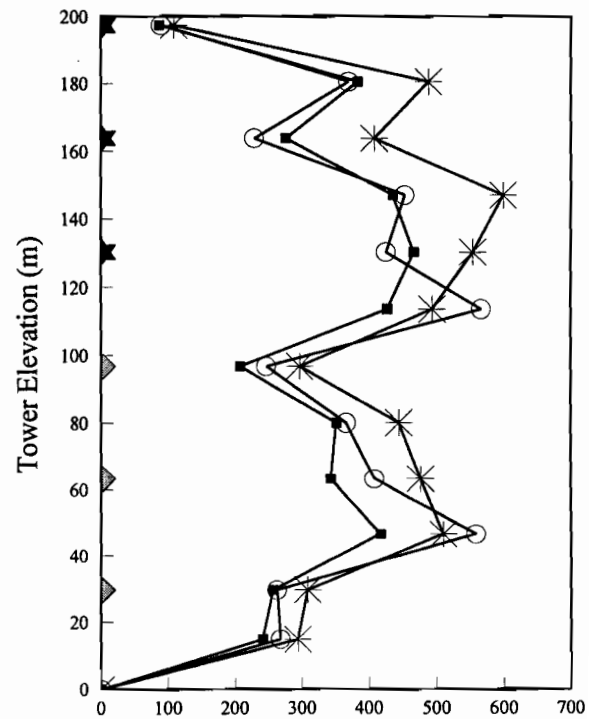
Base Accelerograms:
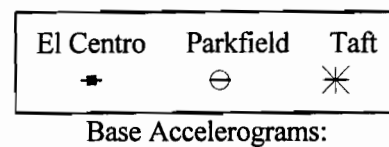
Fig. 4.23. Response of 198-m tower to three base accelerograms
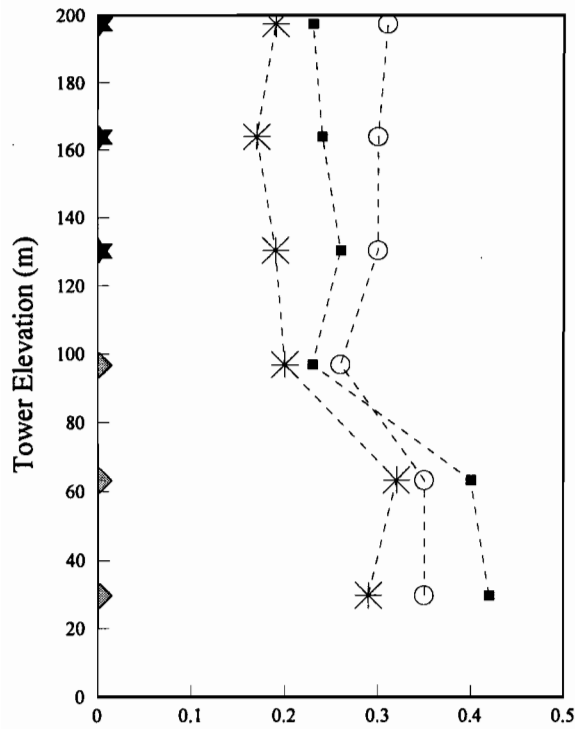
(a) Dynamic Component of Cable Oscillation (m)

(b) Mast Horizontal Displacement (m)

(c) Dynamic Component of Mast Axial Displ. (m)

Negligible

(d) Mast Rotation (Degree)

Inner Anchor	Outer Anchor
◇	✦

Guy clusters attached to:

El Centro	Parkfield	Taft
■	⊖	✳
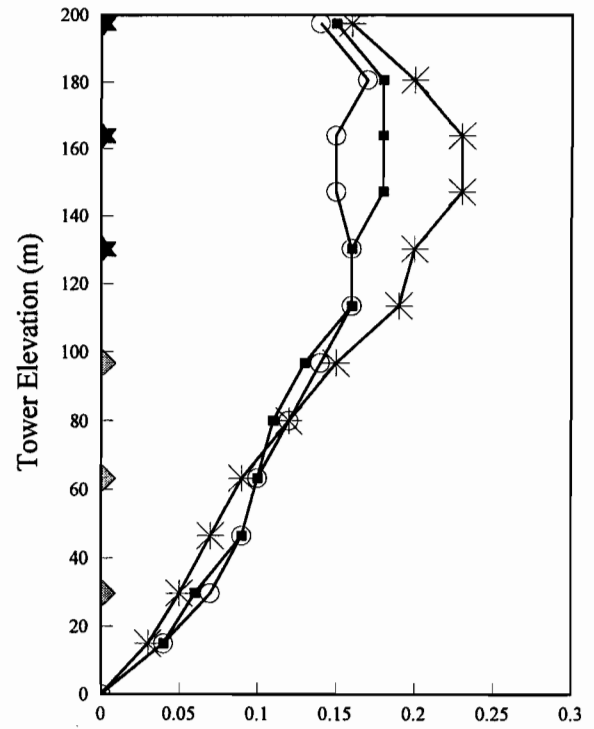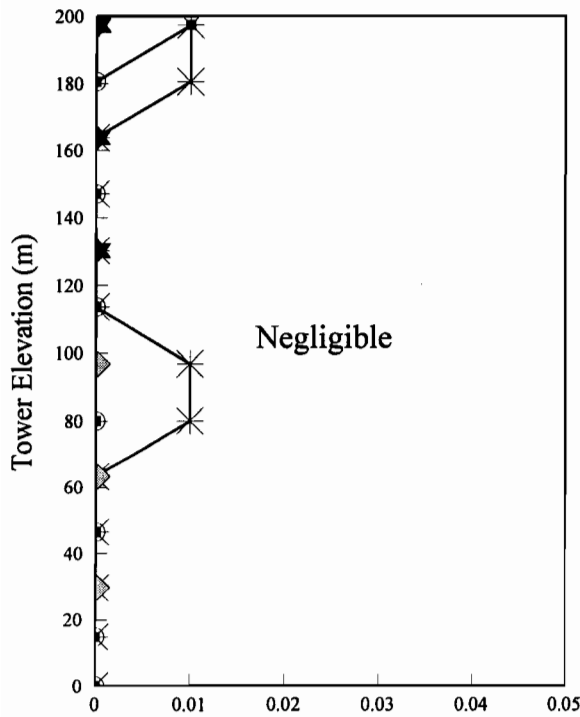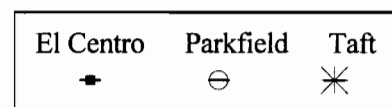
Base Accelerograms:

Fig. 4.24. Response of 198-m tower to three base accelerograms
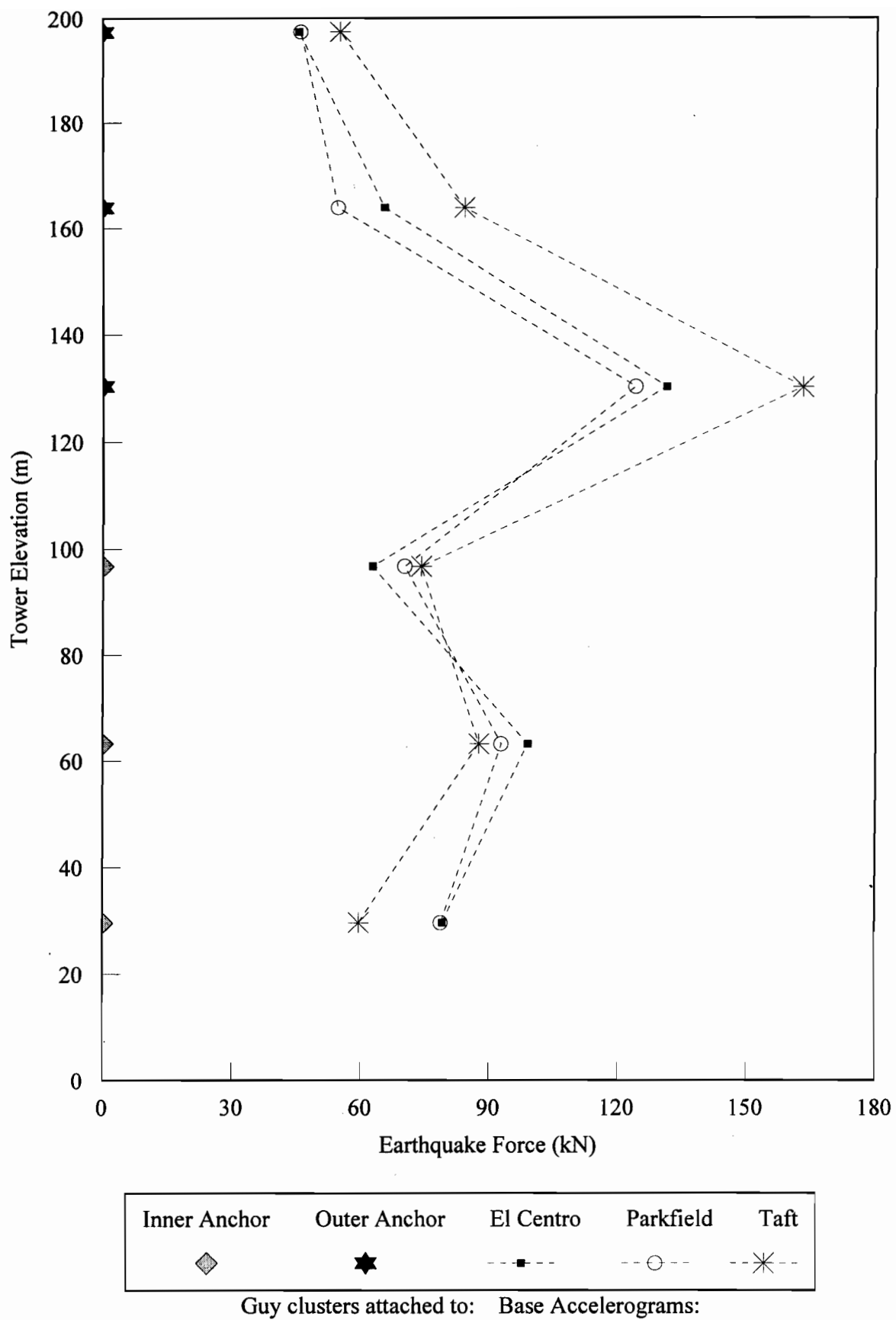
Fig. 4.25. Response of 198-m tower to three base accelerograms (Horizontal + Vertical)
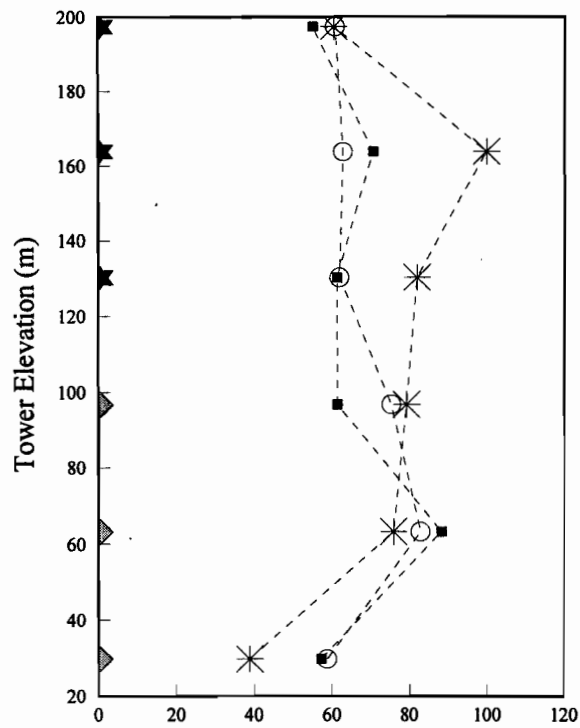
74

(a) Dynamic Component of Cable Tension (kN)

(b) Mast Shear (kN)

(c) Dynamic Comp. of Mast Axial Force (kN)

(d) Mast Bending Moment (kN-m)

Inner Anchor	Outer Anchor
◈	✸

Guy clusters attached to:

El Centro	Parkfield	Taft
▪	⊖	✳

Base Accelerograms:

Fig. 4.26. Response of 198-m tower to three base accelerograms (Horizontal + Vertical)

75

(a) Dynamic Component of Cable Oscillation (m)

(b) Mast Horizontal Displacement (m)

(c) Dynamic Component of Mast Axial Displ. (m)

(d) Mast Rotation (Degree)

Guy clusters attached to:

Inner Anchor   Outer Anchor

Base Accelerograms:

El Centro   Parkfield   Taft
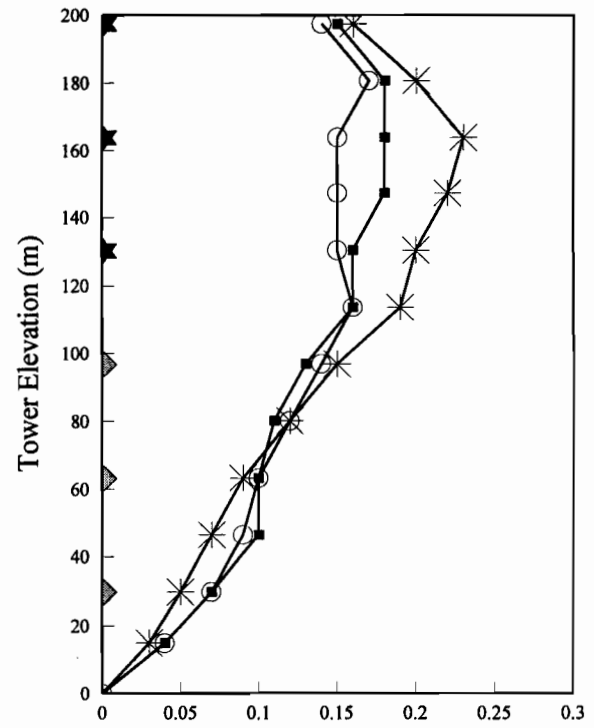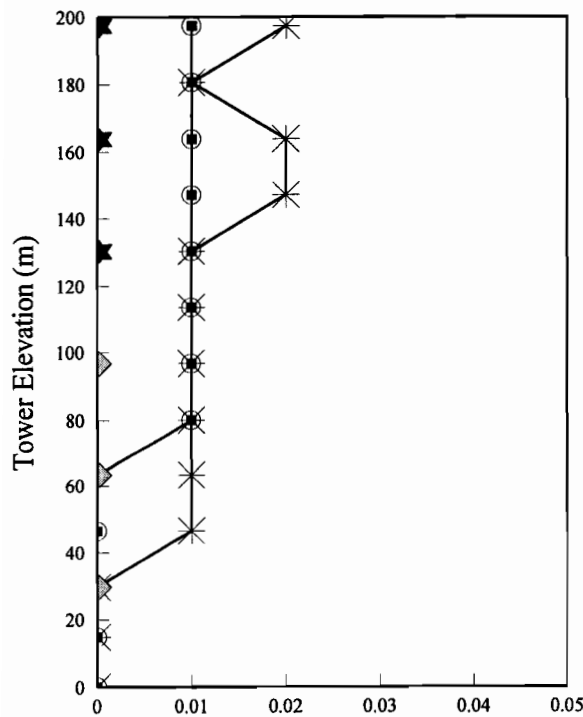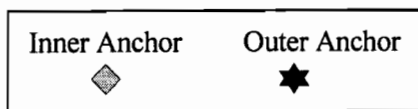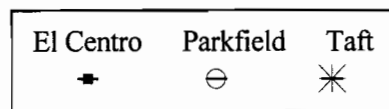
Fig. 4.27. Response of 198-m tower to three base accelerograms (Horizontal + Vertical)

76

4.3.4 200-m Tower

Figures 4.28 to 4.33 show the results of the detailed seismic nonlinear analysis for the 200-m tower. Except for the dynamic component of mast axial force, there is not a significant difference (in terms of maximum response) between the results of dynamic analysis under the horizontal earthquake and the corresponding results for the combined horizontal and vertical earthquake motions. One of the important observations is that the response due to the Taft and Parkfield horizontal accelerograms will be interchanged in the load case of combined horizontal and vertical earthquake motions.

As illustrated in Figs. 4.28 and 4.31, the earthquake forces at the stay levels of the intermediate group are larger than those of the other two groups. The Taft accelerogram has the most effect on the earthquake forces and the El Centro and Parkfield accelerograms come in the second and third order in this regard (in the load case of horizontal earthquake). The intermediate cable Sets 4 to 6 (from the base) at the transition zones are more excited than the others. There is a nonuniform behaviour around the transition areas.

In Figs. 4.29(a) and 4.32(a), it can be seen that the intermediate cable Set 6 (from the base) close to the top transition part is the most excited. This response increases with the tower elevation. There is a discontinuity in the behaviour around the transition zones, and the effect in the top one is more obvious than in the bottom zone.

The mast shear and bending moments along the tower elevation are shown in Figs. 4.29(b and d) and 4.32(b and d), respectively. These two response indicators increase with height and their maximum dynamic effect occurs close to the top transition area. There is also a discontinuity in these figures around the transition regions. In general, the maximum shear occurs directly at the stay levels, and the minimum shear occurs at midspan between the two stay levels, and vice versa for the mast bending moment. The responses are consistent for the three accelerograms.

Figures 4.29(c) and 4.32(c) represent the dynamic component of mast axial force along the tower. As it can be observed, there is no significant axial effect from the load case of horizontal earthquake motion. However, in the case of combined horizontal and

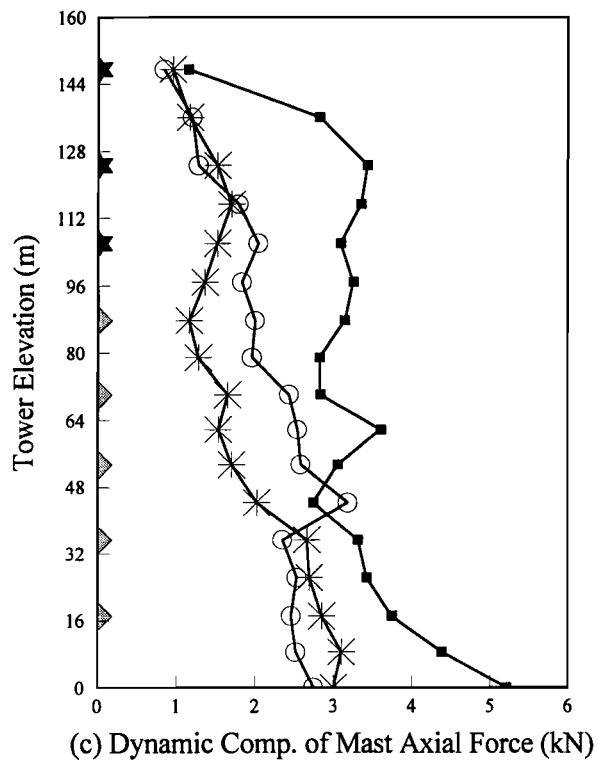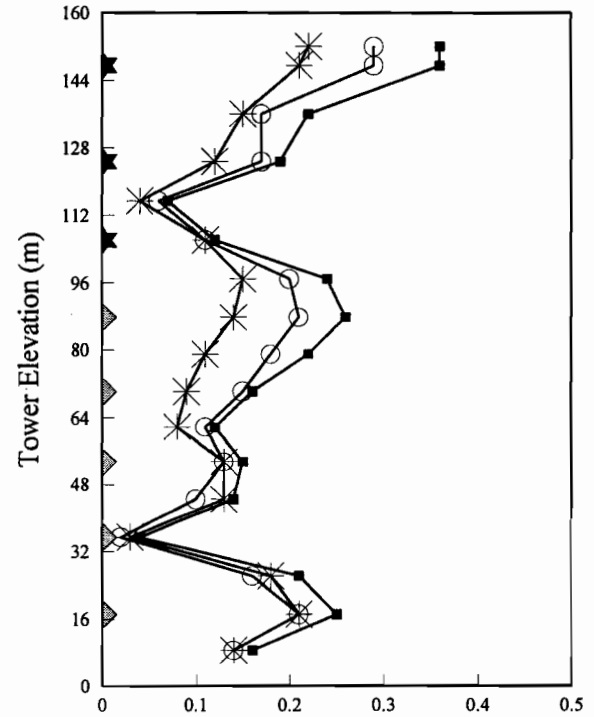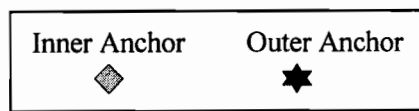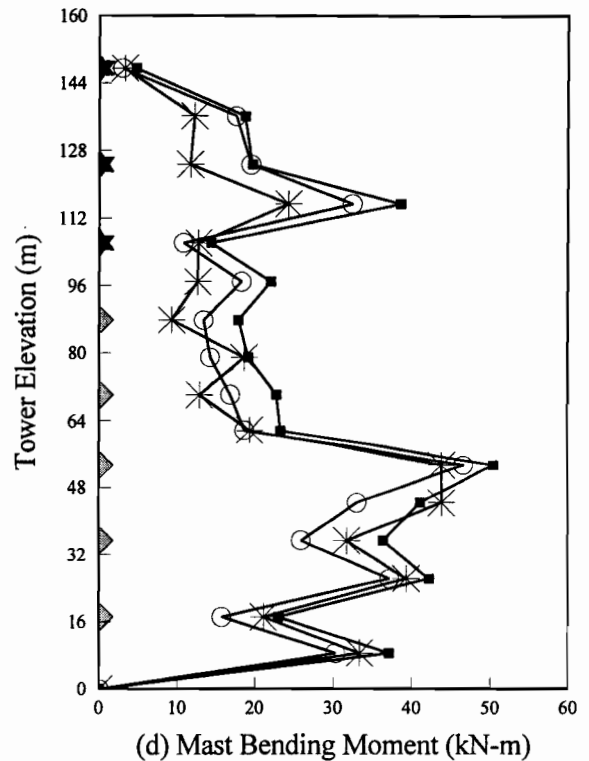vertical accelerograms, the Taft accelerogram has the most effect on the dynamic component of mast axial force, and the El Centro and Parkfield accelerograms come in the second and third order in this regard.

The dynamic component of the cable oscillations is shown in Figs. 4.30(a) and 4.33(a). As shown, there is a nonuniform behaviour around the transition zones, and it is more pronounced in the top region, between stay levels of Sets 5 and 6. The oscillations of the intermediate group are larger than those of the other groups. Also, the El Centro and Taft accelerograms are considerably more exciting than Parkfield for the cables of the intermediate group (in the load case of horizontal earthquake). The maximum response occurs around the top transition area, at the stay level of cable Set 5.

The mast horizontal displacement and rotation are summarized in Figs. 4.30(b and d) and 4.33(b and d), respectively. There is a discontinuity in the behaviour around the top transition region for both responses, and the maximum horizontal displacement occurs close to the top transition area. The top part of the tower experiences the maximum rotation. The Taft accelerogram is the most exciting as far as these response indicators are concerned (in the load case of horizontal earthquake).

As it can be seen from Figs. 4.30(c) and 4.33(c), the dynamic component of mast axial displacement along the tower elevation is negligible to very small (1 cm) in the case of horizontal acceleration, and tends to increase (1 to 3 cm) in the case of combined horizontal and vertical accelerations.

Fig. 4.28. Response of 200-m tower to three base accelerograms

(a) Dynamic Component of Cable Tension (kN)

(b) Mast Shear (kN)

(c) Dynamic Comp. of Mast Axial Force (kN)

(d) Mast Bending Moment (kN-m)

Inner	Intermediate	Outer
◈	■	✦

Guy clusters attached to Anchor:

El Centro	Parkfield	Taft
■	⊖	✳
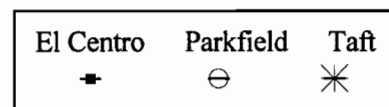
Base Accelerograms:

Fig. 4.29. Response of 200-m tower to three base accelerograms

(a) Dynamic Component of Cable Oscillation (m)

(b) Mast Horizontal Displacement (m)
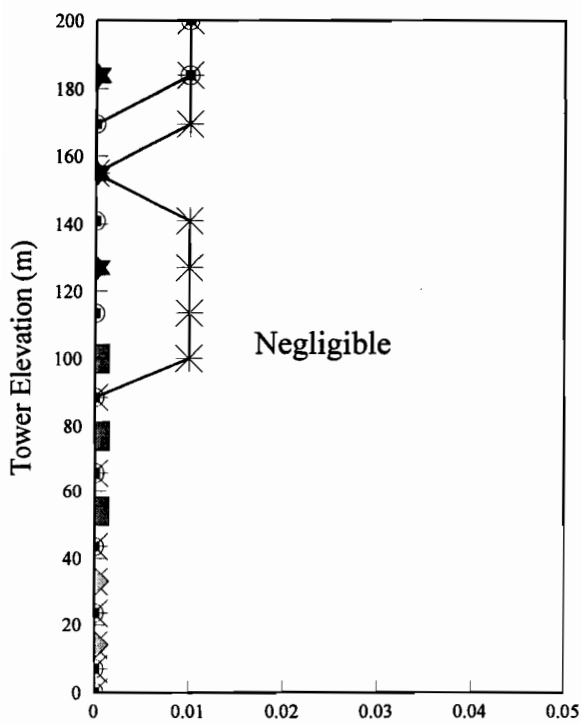
(c) Dynamic Component of Mast Axial Displ. (m)

(d) Mast Rotation (Degree)

Inner	Intermediate	Outer
◇	■	✶

Guy clusters attached to Anchor:

El Centro	Parkfield	Taft
■	⊖	✳

Base Accelerograms:

Fig. 4.30. Response of 200-m tower to three base accelerograms

81

Fig. 4.31. Response of 200-m tower to three base accelerograms (Horizontal + Vertical)

82

(a) Dynamic Component of Cable Tension (kN)

(b) Mast Shear (kN)

(c) Dynamic Comp. of Mast Axial Force (kN)

(d) Mast Bending Moment (kN-m)

Inner	Intermediate	Outer
◇	■	✶

Guy clusters attached to Anchor:

El Centro	Parkfield	Taft
■	⊖	✳
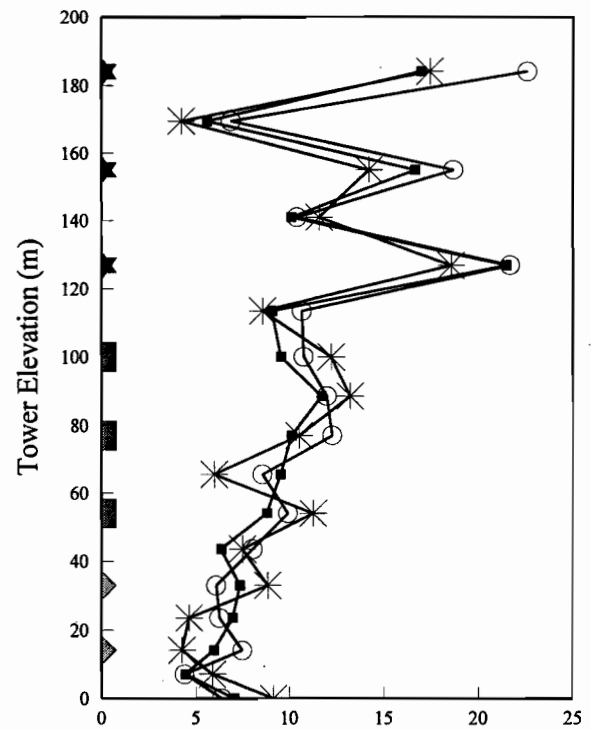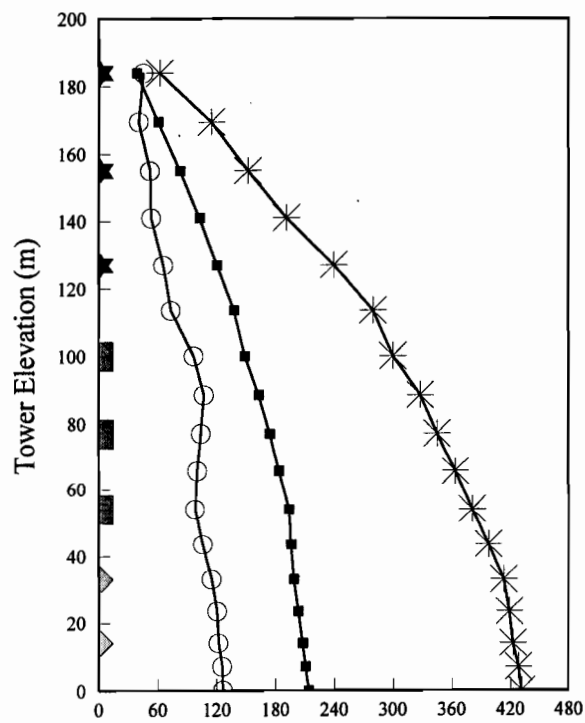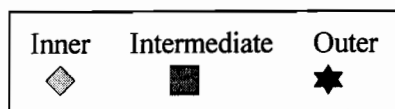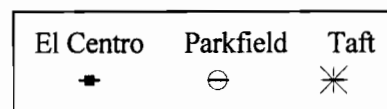
Base Accelerograms:

Fig. 4.32. Response of 200-m tower to three base accelerograms (Horizontal + Vertical)
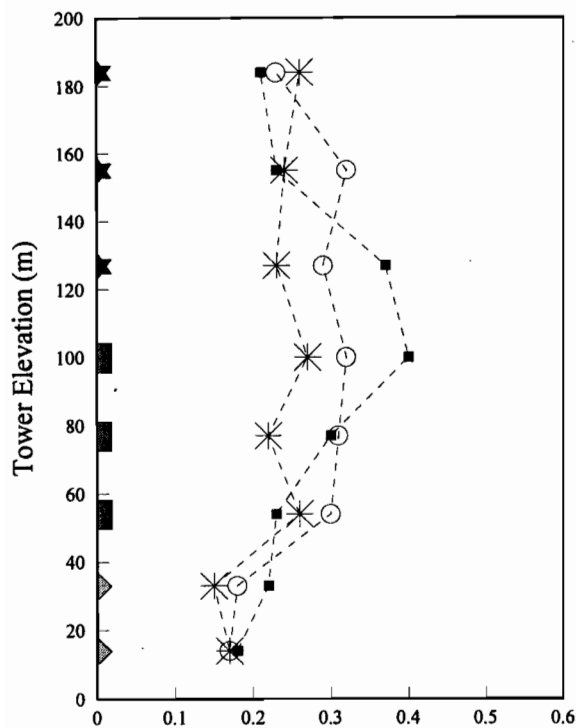
(a) Dynamic Component of Cable Oscillation (m)

(b) Mast Horizontal Displacement (m)

(c) Dynamic Component of Mast Axial Displ. (m)

(d) Mast Rotation (Degree)

Guy clusters attached to Anchor: Inner / Intermediate / Outer

Base Accelerograms: El Centro / Parkfield / Taft
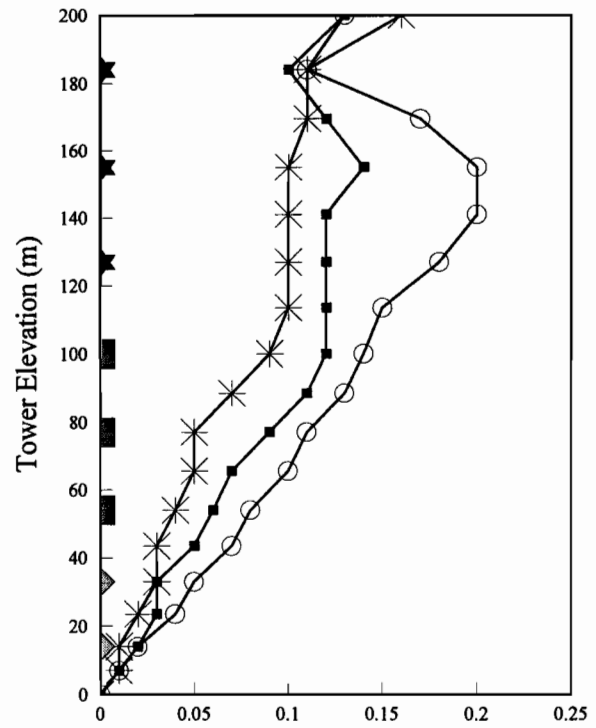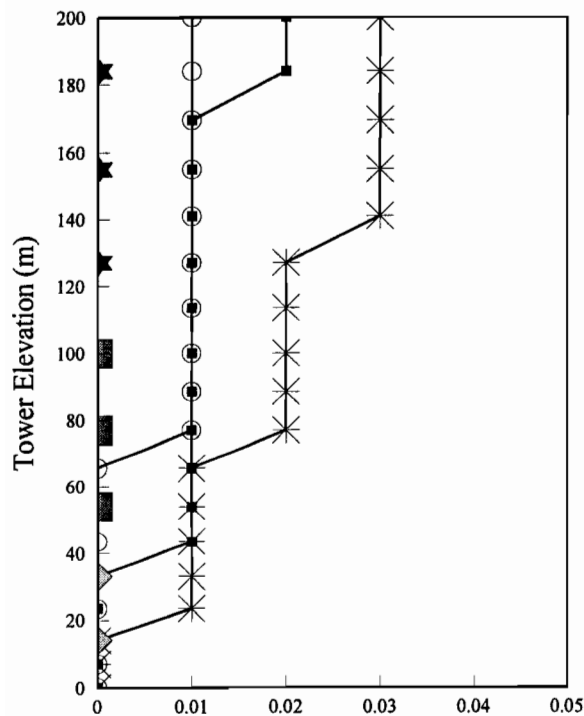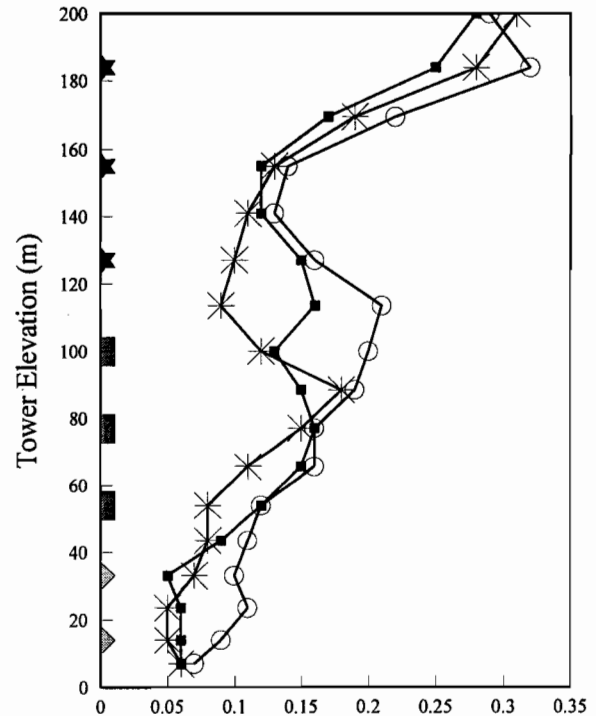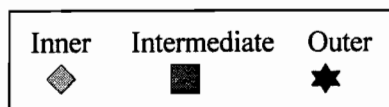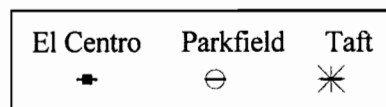
Fig. 4.33. Response of 200-m tower to three base accelerograms (Horizontal + Vertical)

84

4.3.5 213-m Tower

Figures 4.34 to 4.39 show the results of the detailed seismic nonlinear analysis for the 213-m tower. Except for the dynamic component of mast axial force, there is not a significant difference between the results due to the horizontal earthquake and the corresponding results due to the combined horizontal and vertical earthquake motions.

As illustrated in Figs. 4.34 and 4.37, the Taft accelerogram has the most effect on the earthquake forces, and the Parkfield and El Centro accelerograms come in the second and third order in this regard for the cables of the outer group. The intermediate cable Set 5 (from the base) close to the transition zone is more excited than the others. There is a nonuniform behaviour around the transition area, especially for the Taft input.

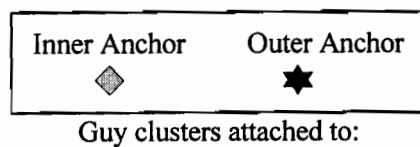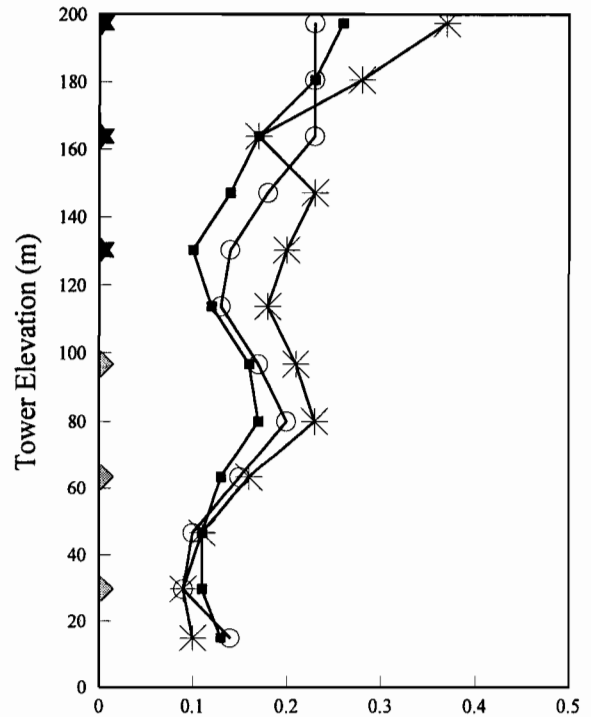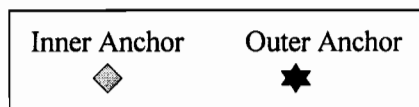In Figs. 4.35(a) and 4.38(a), it can be seen that the intermediate cable set close to the transition part (i.e. Set 3 from the base) is more excited than the other ones. The responses are consistent for the three accelerograms, and there is a discontinuity in the behaviour around the transition zone.

The mast shear and bending moments along the tower elevation are shown in Figs. 4.35(b and d) and 4.38(b and d), respectively. The maximum dynamic effect of these two response indicators occurs close to the transition area. There is a discontinuity in these figures around the transition region, especially in the bending moment envelope. In general, the maximum shear occurs directly at the stay levels and the minimum shear occurs at midspan between the two stay levels, and vice versa for the mast bending moment. The responses are consistent for the three accelerograms.

Figures 4.35(c) and 4.38(c) represent the dynamic component of mast axial force along the tower. As it can be seen, there is no significant axial effect from the load case of horizontal earthquake motion. However, in the case of combined horizontal and vertical earthquake accelerograms, the Taft accelerogram has the most effect on the dynamic component of mast axial force, and the El Centro and Parkfield accelerograms come in second and third order in this regard.

The dynamic component of cable oscillation is shown in Figs. 4.36(a) and 4.39(a). As shown, there is a nonuniform behaviour around the transition zone for the response

of the Taft and El Centro earthquake excitations. This oscillation is larger for the outer group than for the inner group (except for the Taft accelerogram for which it is almost uniform). The Parkfield accelerogram has the most effect on the dynamic component of cable oscillation, and the El Centro and Taft accelerograms would come in second and third order in this regard. The maximum response occurs around the transition area.

The mast horizontal displacement and the mast rotation are summarized in Figs. 4.36(b and d) and 4.39(b and d), respectively. There is a discontinuity in the behaviour around the transition region for both responses. The maximum horizontal displacement occurs close to the transition area, and the top part of the tower experiences the maximum rotation. The Parkfield and Taft accelerograms are more exciting than El Centro as far as these response indicators are concerned.

As it can be seen from Figs. 4.36(c) and 4.39(c), the dynamic component of the mast axial displacement along the tower elevation is negligible to very small (1 to 3 cm).
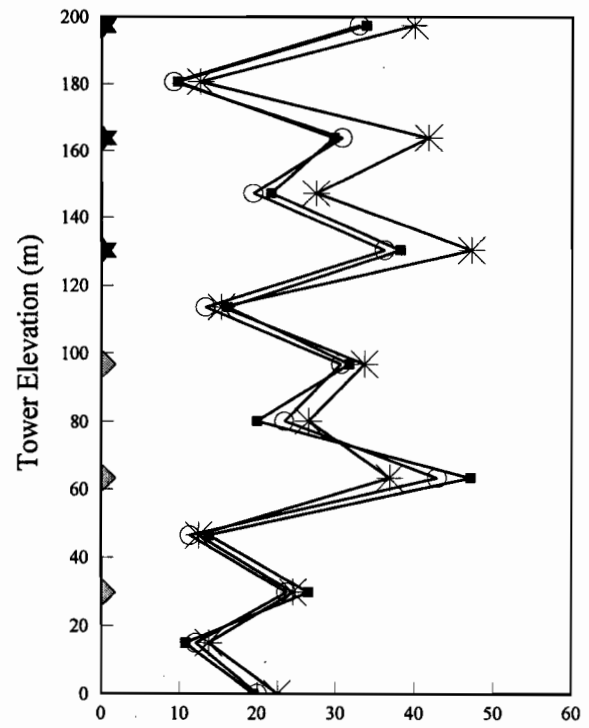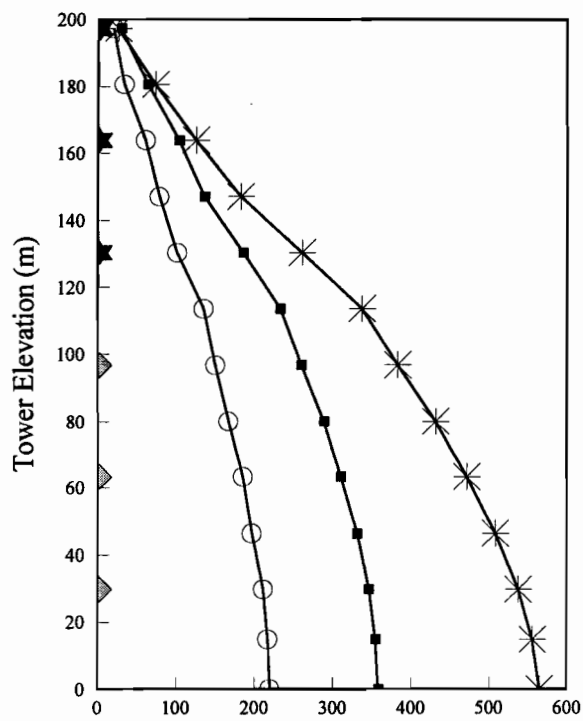
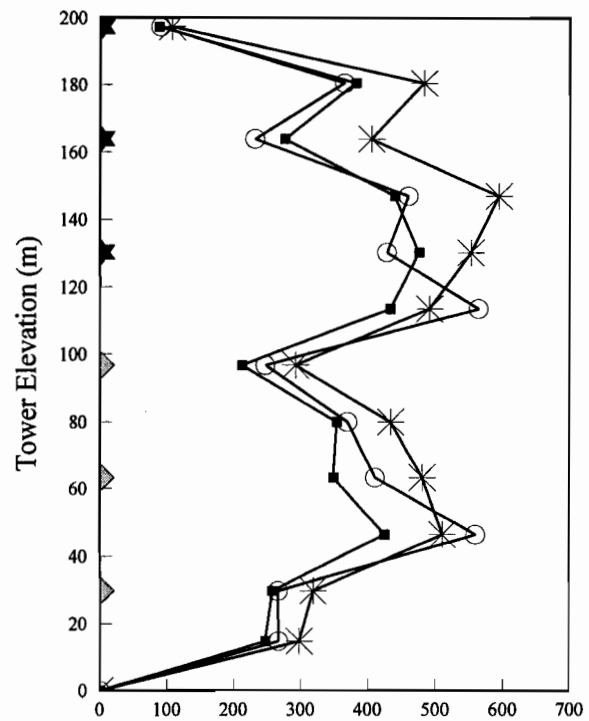Fig. 4.34. Response of 213-m tower to three base accelerograms
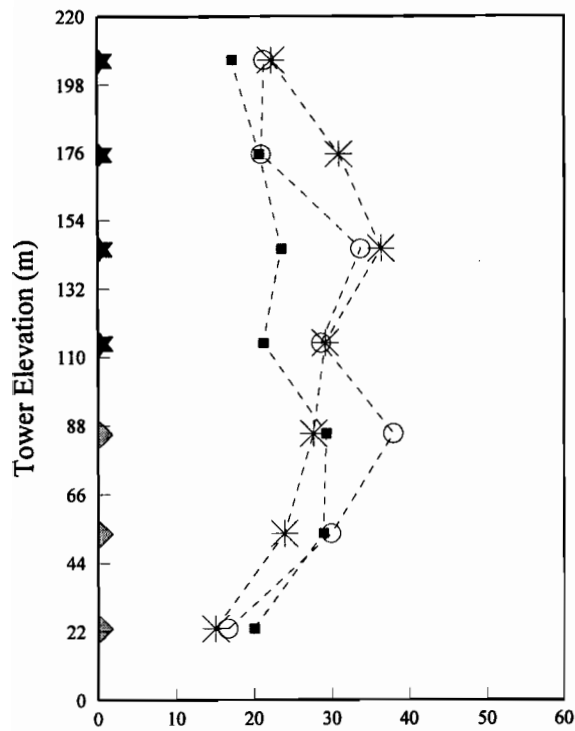
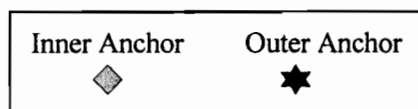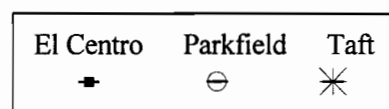(a) Dynamic Component of Cable Tension (kN)
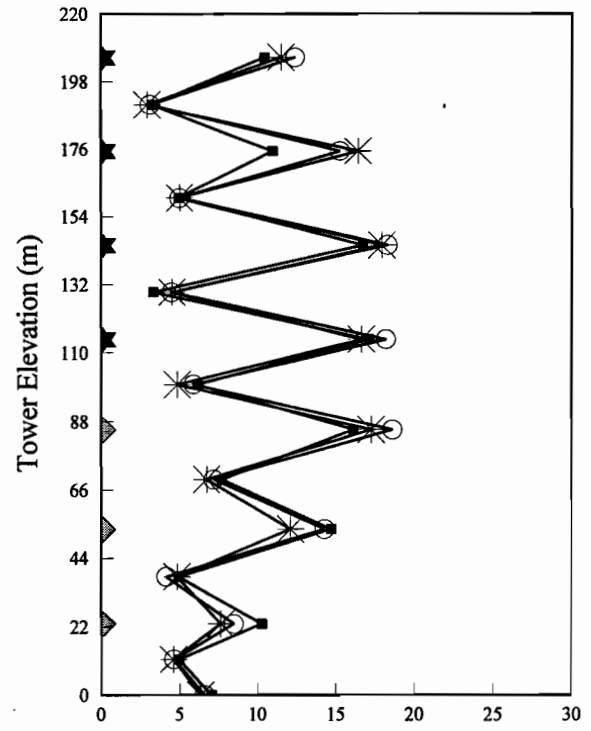
(b) Mast Shear (kN)
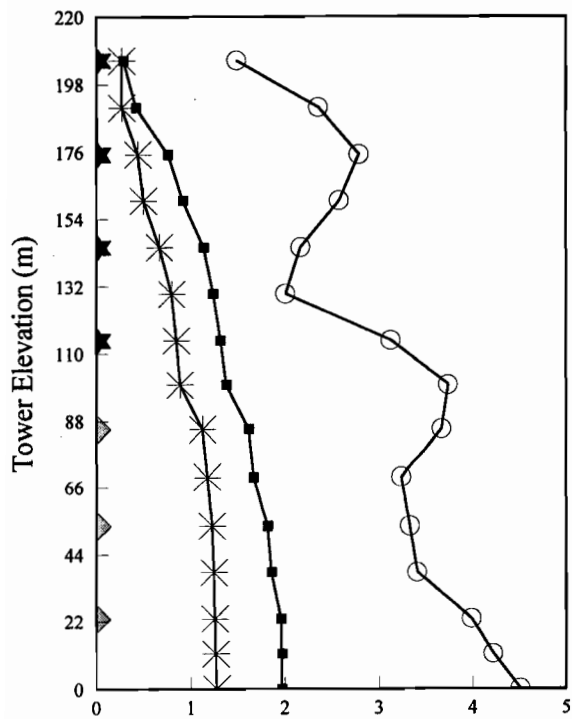
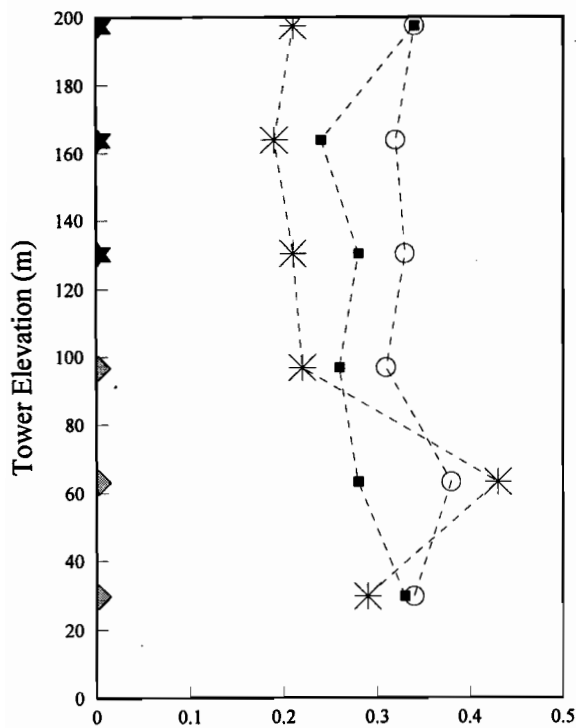(c) Dynamic Comp. of Mast Axial Force (kN)
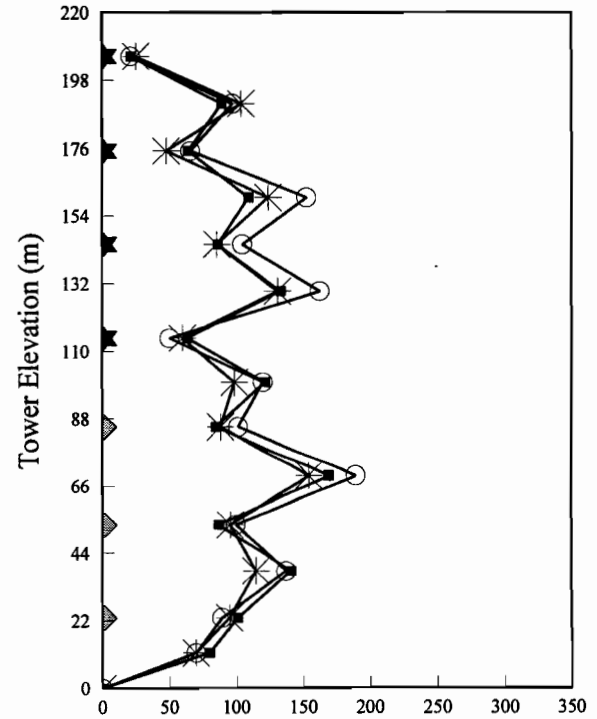
(d) Mast Bending Moment (kN-m)

Guy clusters attached to:

Inner Anchor   Outer Anchor

Base Accelerograms:

El Centro   Parkfield   Taft

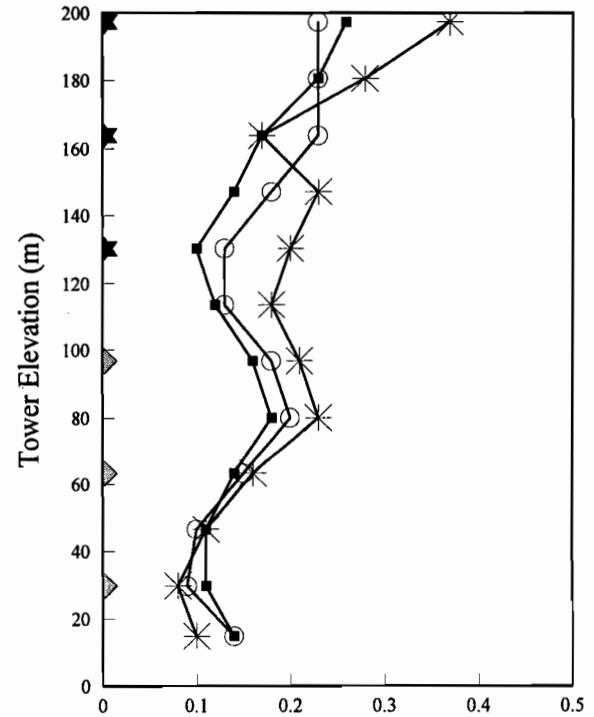Fig. 4.35. Response of 213-m tower to three base accelerograms

88

(a) Dynamic Component of Cable Oscillation (m)

(b) Mast Horizontal Displacement (m)

(c) Dynamic Component of Mast Axial Displ. (m)

Negligible

(d) Mast Rotation (Degree)

Inner Anchor   Outer Anchor

Guy clusters attached to:

El Centro   Parkfield   Taft

Base Accelerograms:

Fig. 4.36. Response of 213-m tower to three base accelerograms

89

Fig. 4.37. Response of 213-m tower to three base accelerograms (Horizontal + Vertical)

90

(a) Dynamic Component of Cable Tension (kN)

(b) Mast Shear (kN)

(c) Dynamic Comp. of Mast Axial Force (kN)

(d) Mast Bending Moment (kN-m)

Guy clusters attached to:

Inner Anchor   Outer Anchor

Base Accelerograms:

El Centro   Parkfield   Taft

Fig. 4.38. Response of 213-m tower to three base accelerograms (Horizontal + Vertical)
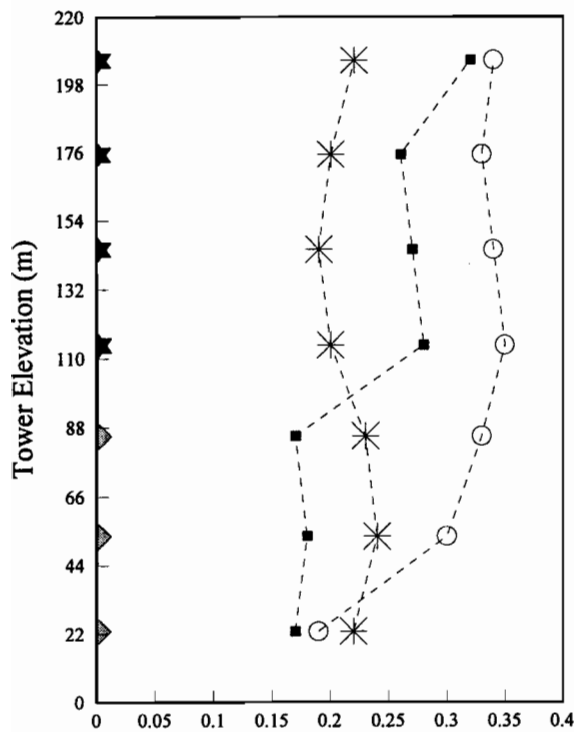
91
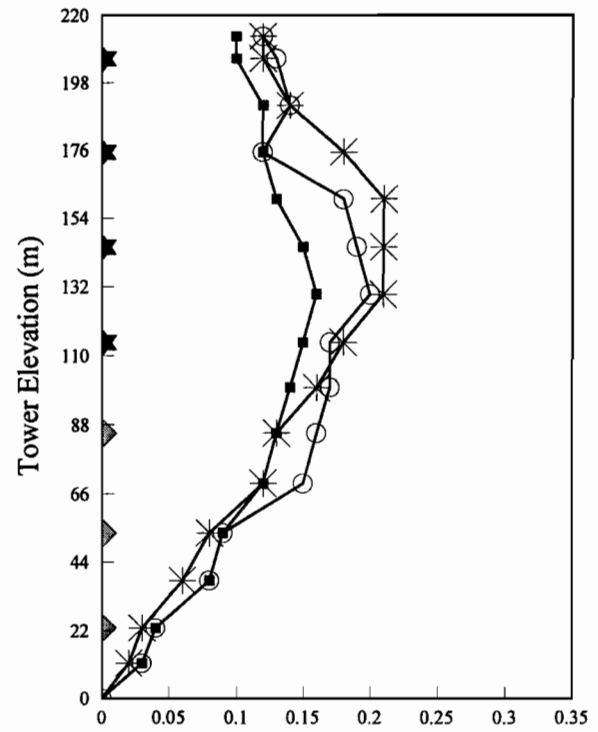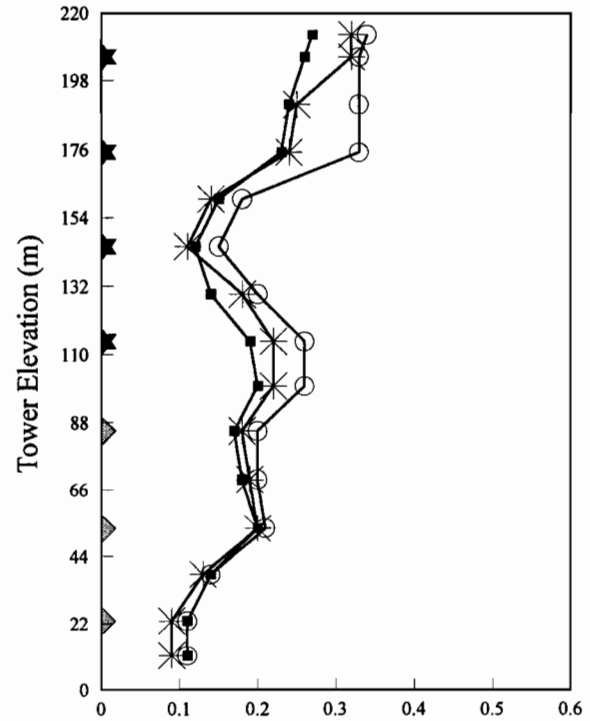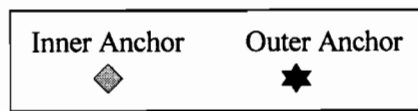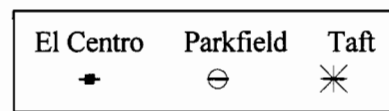
Fig. 4.39. Response of 213-m tower to three base accelerograms (Horizontal + Vertical)

92

4.3.6 313-m Tower

Figures 4.40 to 4.45 show the results of the detailed seismic nonlinear analysis for the 313-m tower. Except for the dynamic component of mast axial force, there is not a significant difference between the results due to the horizontal earthquake and the corresponding results for the combined horizontal and vertical earthquake motions.

As illustrated in Figs. 4.40 and 4.43, the intermediate cable Set 2 (from the base) close to the transition zone is more excited than the others for the earthquake forces. There is a nonuniform behaviour around the transition area. The responses are consistent for the three accelerograms.

In Figs. 4.41(a) and 4.44(a), it can be seen that the intermediate cable Set 4 (from the base) close to the transition part is more excited than the other ones. As described earlier for the earthquake force diagram, there is a discontinuity in the behaviour around the transition zone, and the responses are consistent for the three accelerograms.

The mast shear and bending moments along the tower elevation are shown in Figs. 4.41(b and d) and 4.44(b and d), respectively. The maximum dynamic effect of these two response indicators occurs close to the transition area, in the bottom part of the mast. There is a discontinuity in these figures around the transition region. In general, the maximum shear occurs directly at the stay levels and the minimum shear occurs at midspan between the two stay levels, and vice versa for the mast bending moment. The responses are consistent for the three accelerograms.

Figures 4.41(c) and 4.44(c) represent the dynamic component of mast axial force along the tower. As expected, there is no significant axial effect from the load case of horizontal earthquake motion. However, in the case of combined horizontal and vertical earthquake accelerograms, the El Centro and Taft earthquakes have considerably larger seismic axial effect than the Parkfield earthquake.

The dynamic component of cable oscillation is shown in Figs. 4.42(a) and 4.45(a). As shown, there is a nonuniform behaviour around the transition zone, in the bottom part of the tower. The oscillation of cables of the outer group is smaller than that of the inner group. The responses are consistent for the three accelerograms.

93

The mast horizontal displacement and the mast rotation are summarized in Figs. 4.42(b and d) and 4.45(b and d), respectively. There is a discontinuity in the behaviour around the transition region for both responses. The maximum horizontal displacement and maximum rotation occur close to the transition area. The Parkfield and Taft accelerograms are more exciting than El Centro as far as these response indicators are concerned.

As it can be seen from Figs. 4.42(c) and 4.45(c), the dynamic component of the mast axial displacement along the tower elevation is negligible for the load case of horizontal earthquake. This displacement is 3 cm at the top of the tower for the load case of combined vertical and horizontal earthquake motions.
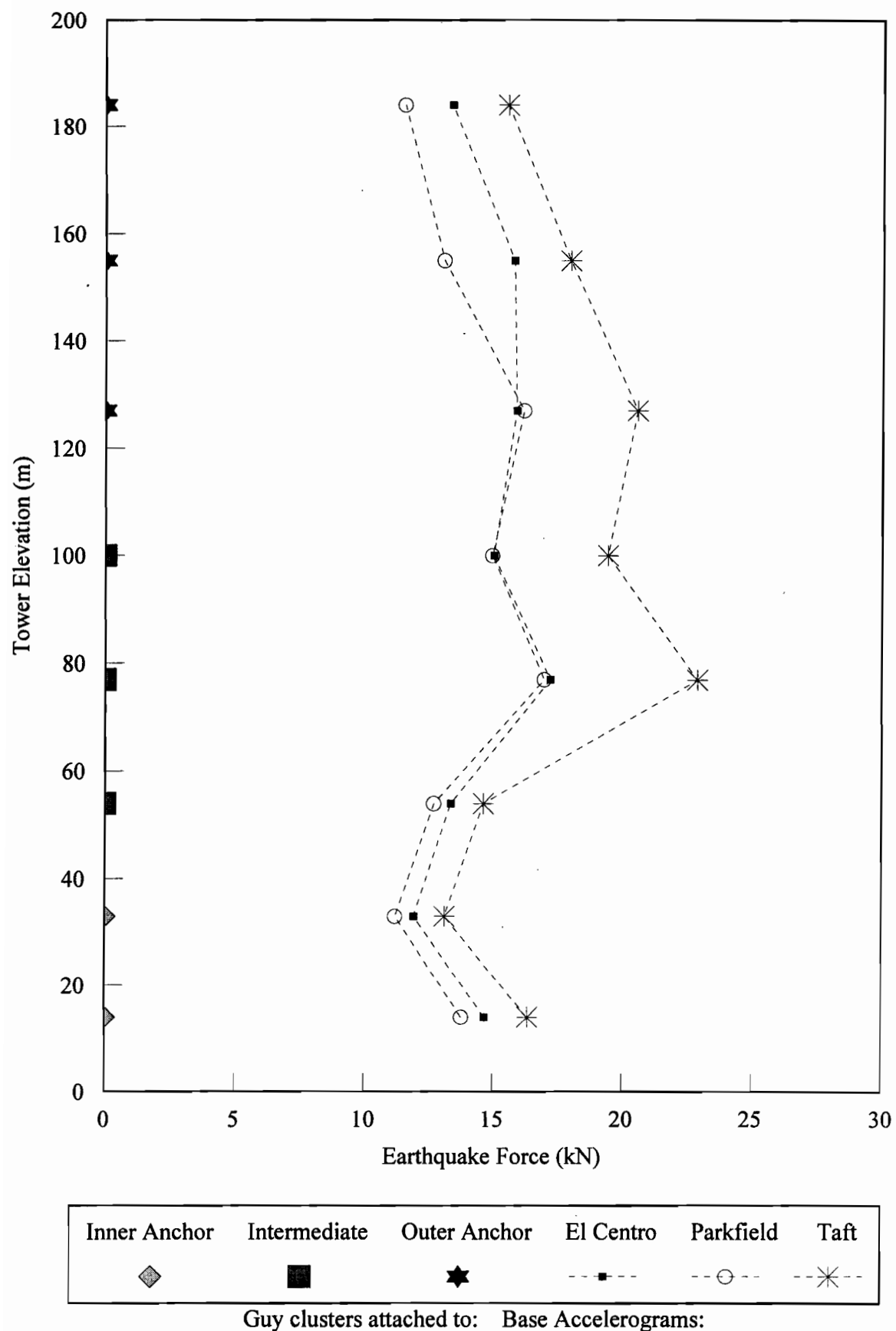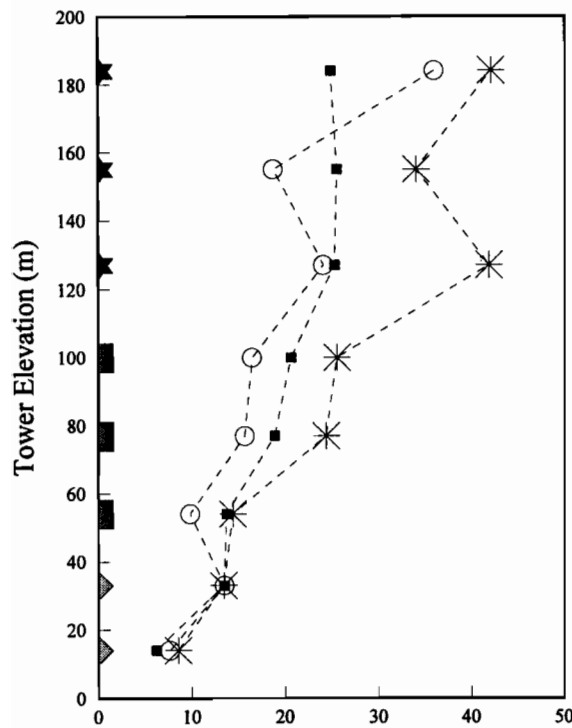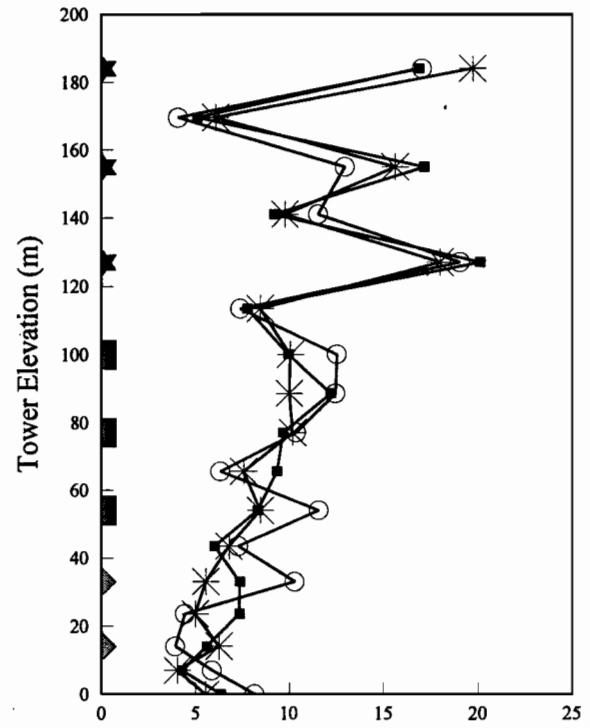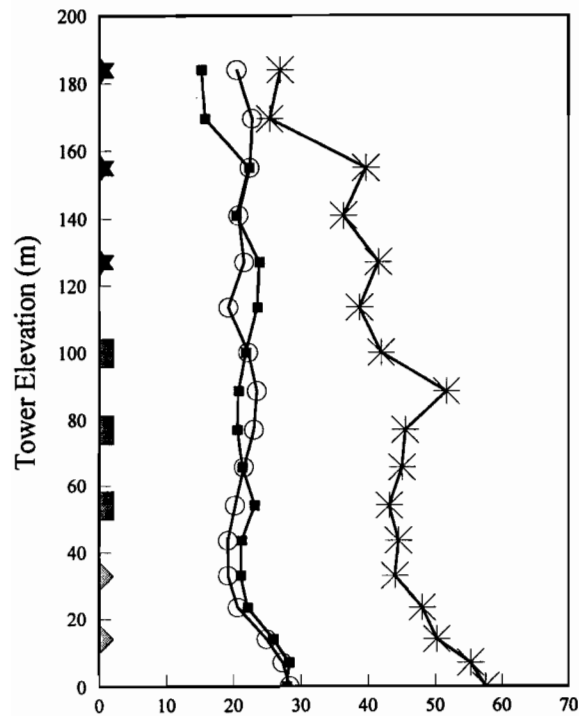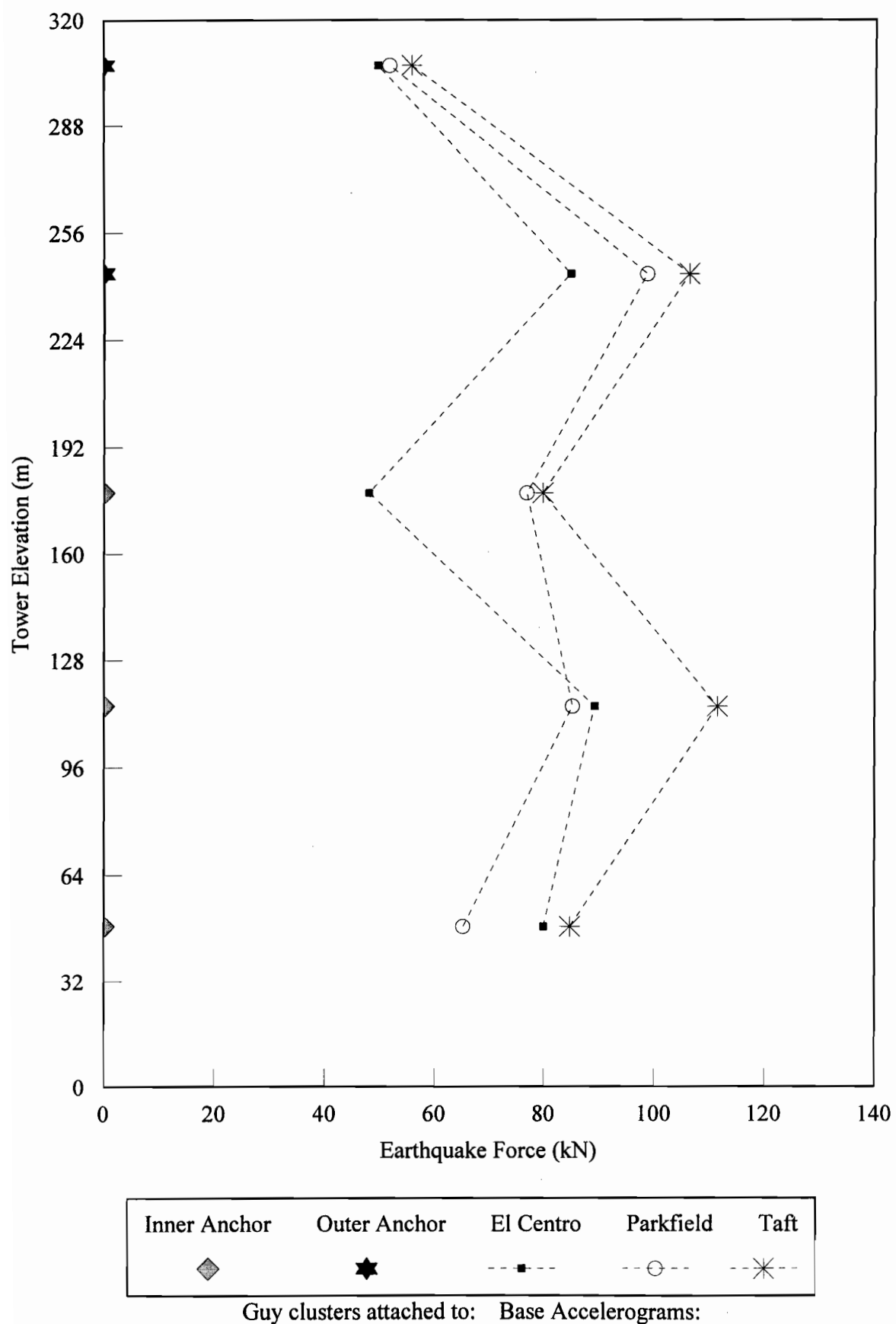
Fig. 4.40. Response of 313-m tower to three base accelerograms

95

(a) Dynamic Component of Cable Tension (kN)

(b) Mast Shear (kN)

(c) Dynamic Comp. of Mast Axial Force (kN)

(d) Mast Bending Moment (kN-m)

Inner Anchor	Outer Anchor

Guy clusters attached to:

El Centro	Parkfield	Taft
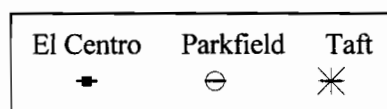
Base Accelerograms:

Fig. 4.41. Response of 313-m tower to three base accelerograms
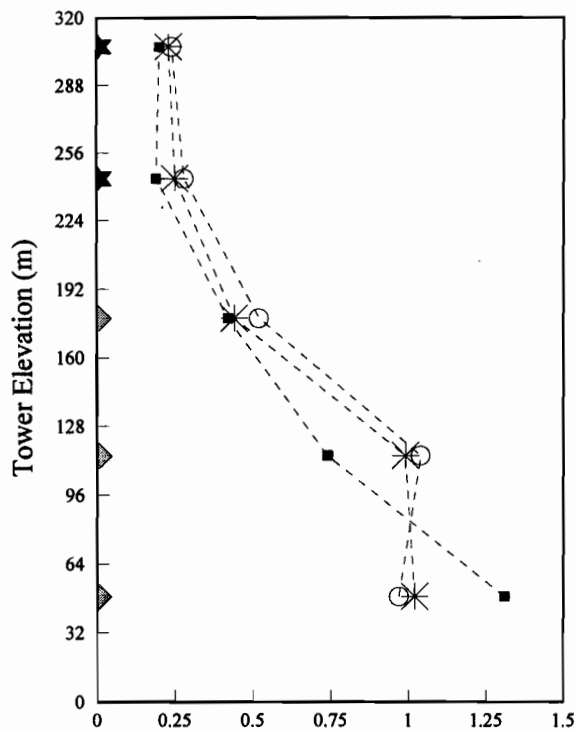
96

(a) Dynamic Component of Cable Oscillation (m)

(b) Mast Horizontal Displacement (m)

(c) Dynamic Component of Mast Axial Displ. (m)

(d) Mast Rotation (Degree)

Negligible

Inner Anchor	Outer Anchor
◈	★

Guy clusters attached to:

El Centro	Parkfield	Taft
■	⊖	✳
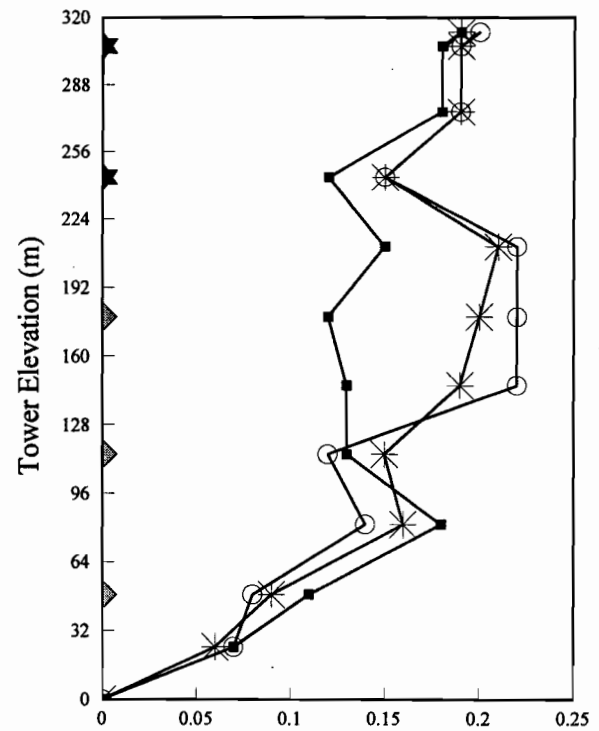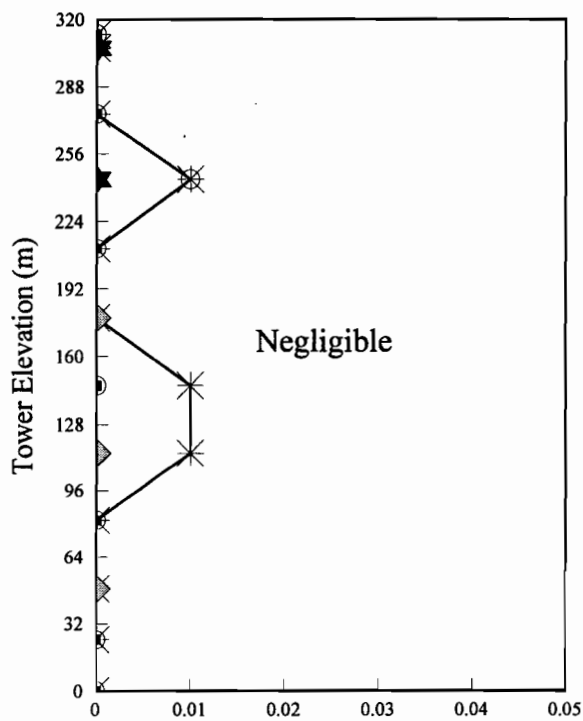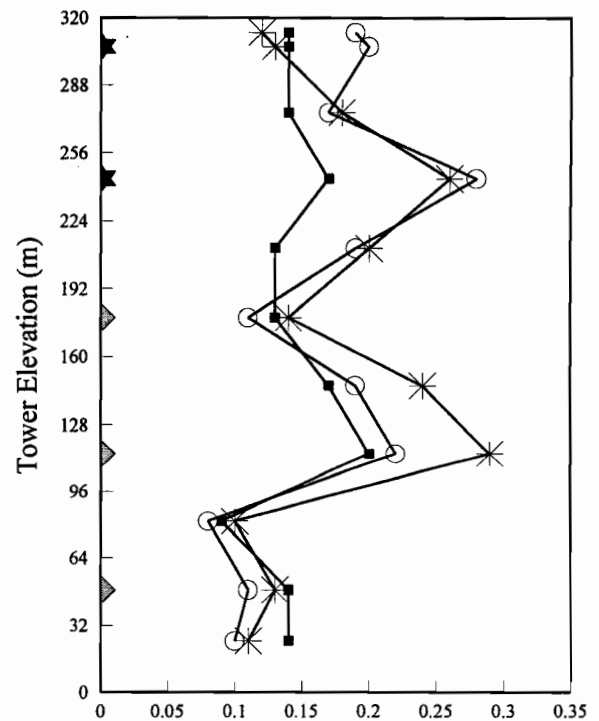
Base Accelerograms:
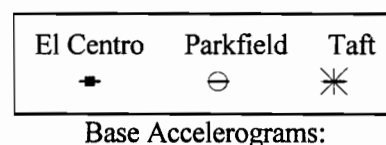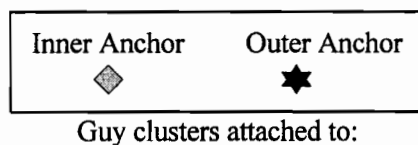
Fig. 4.42. Response of 313-m tower to three base accelerograms

97
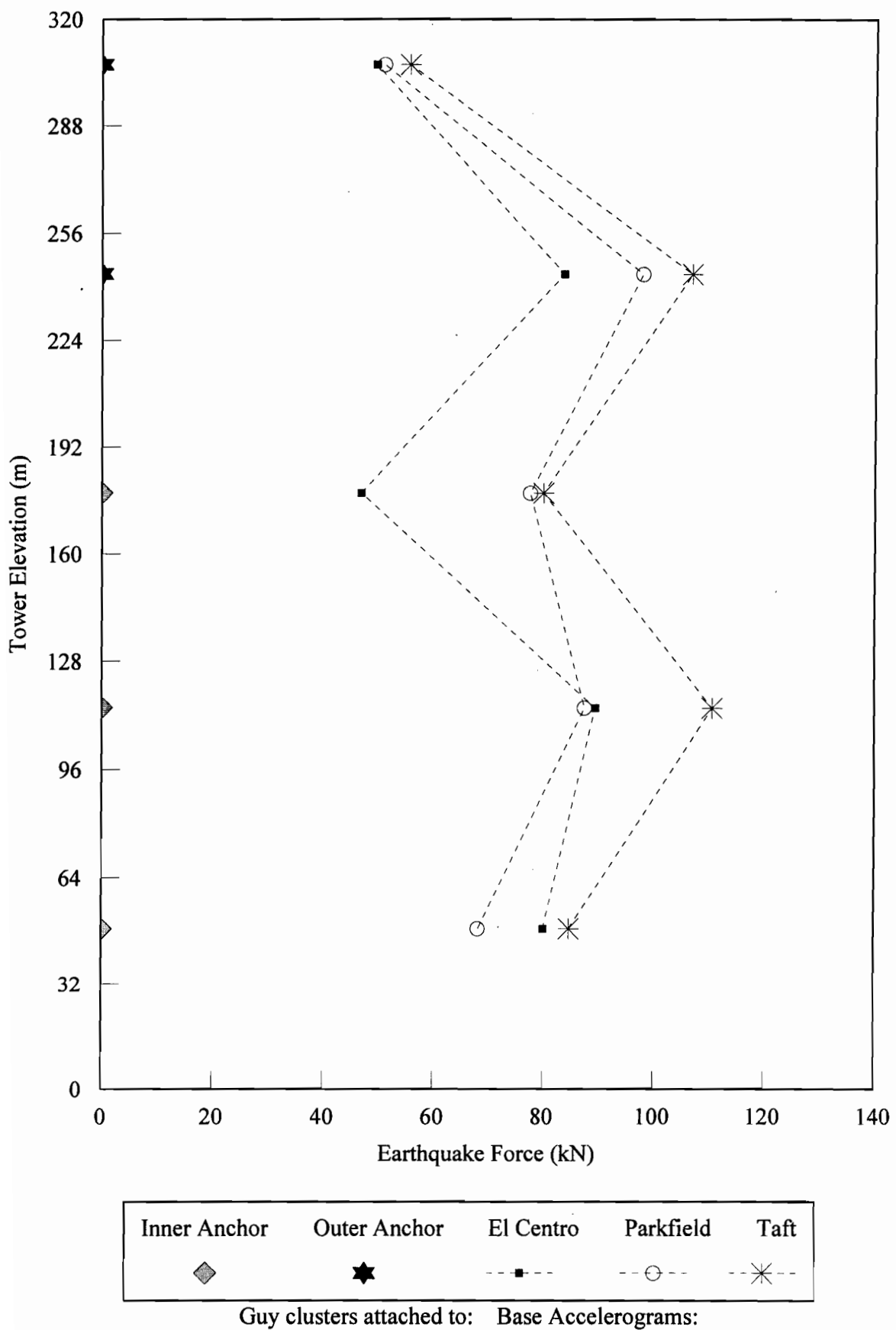
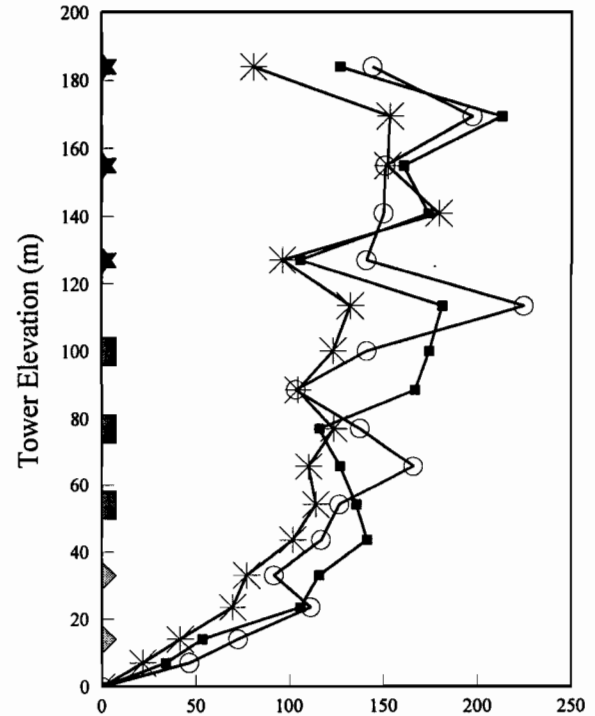Fig. 4.43. Response of 313-m tower to three base accelerograms (Horizontal + Vertical)
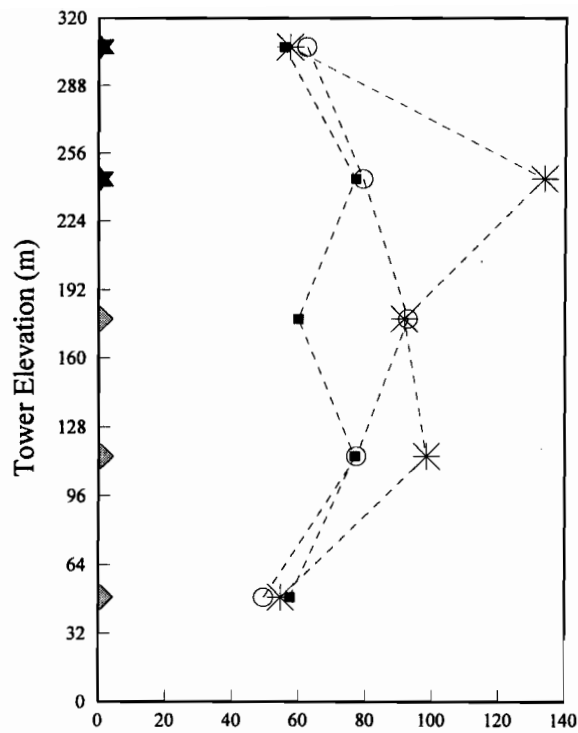
98

(a) Dynamic Component of Cable Tension (kN)

(b) Mast Shear (kN)

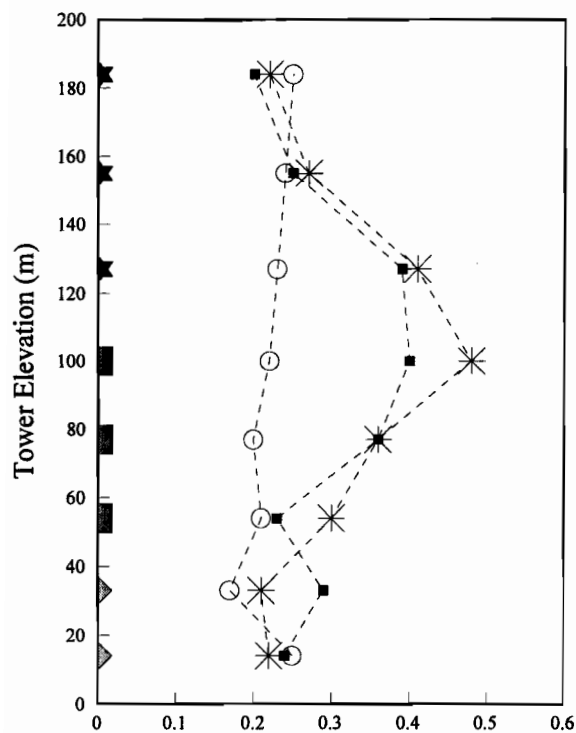(c) Dynamic Comp. of Mast Axial Force (kN)

(d) Mast Bending Moment (kN-m)

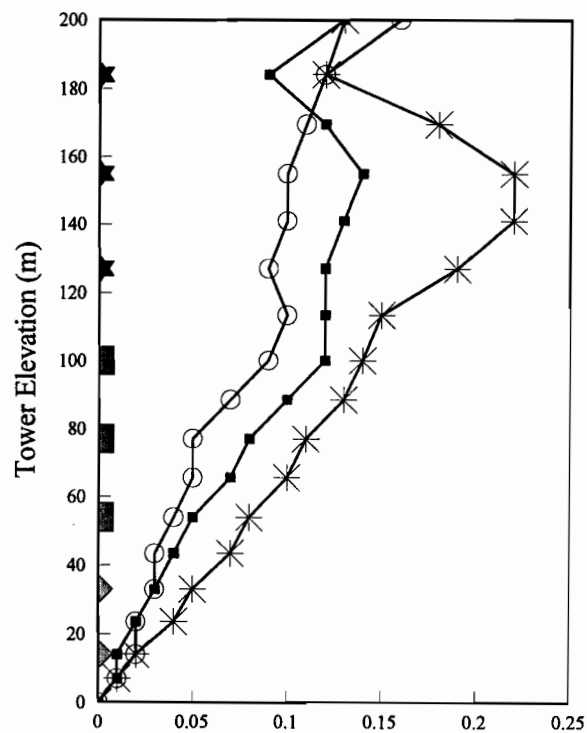| Inner Anchor	Outer Anchor
◈	✶

Guy clusters attached to:

El Centro	Parkfield	Taft
∎	⊖	✳
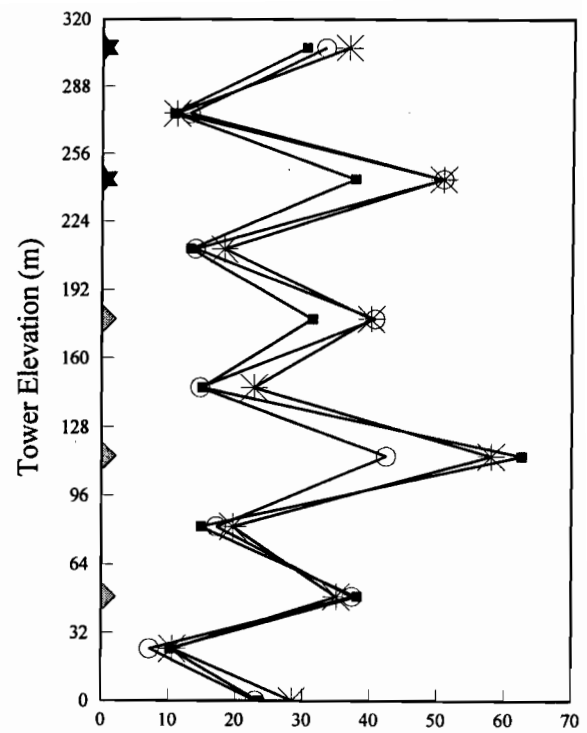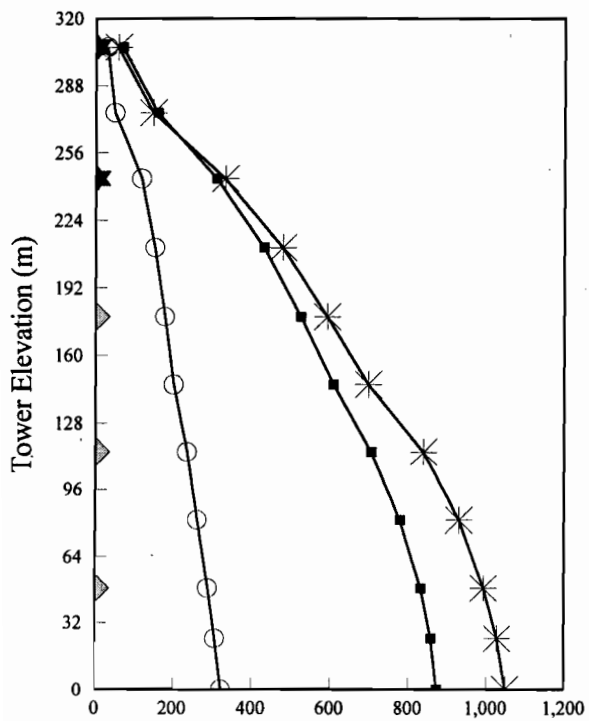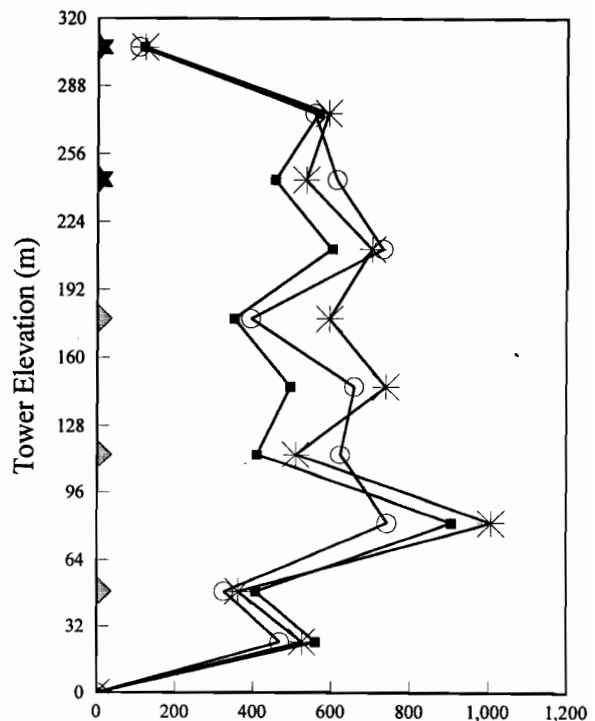
Base Accelerograms:
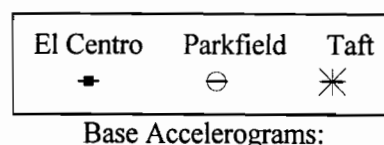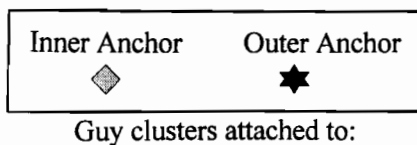
Fig. 4.44. Response of 313-m tower to three base accelerograms (Horizontal + Vertical)
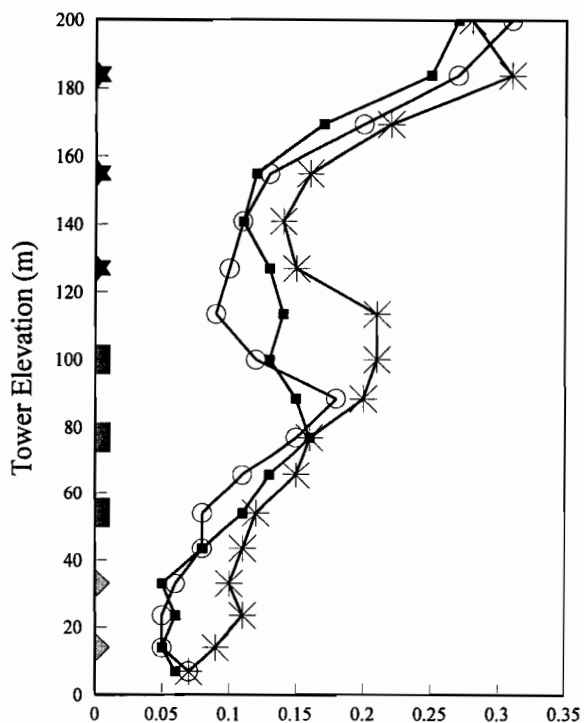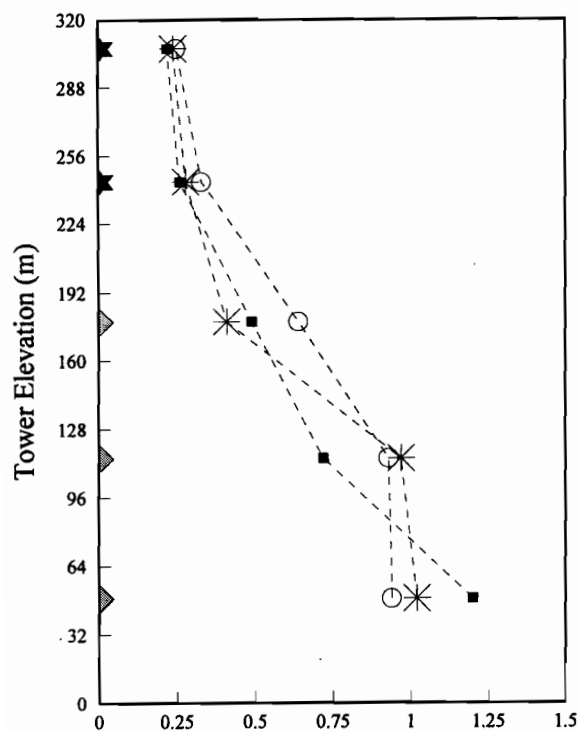
99

(a) Dynamic Component of Cable Oscillation (m)
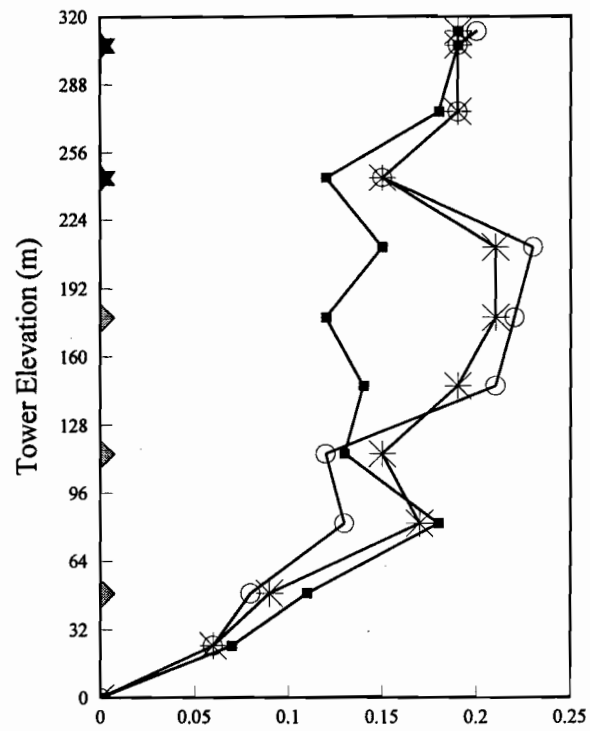
(b) Mast Horizontal Displacement (m)
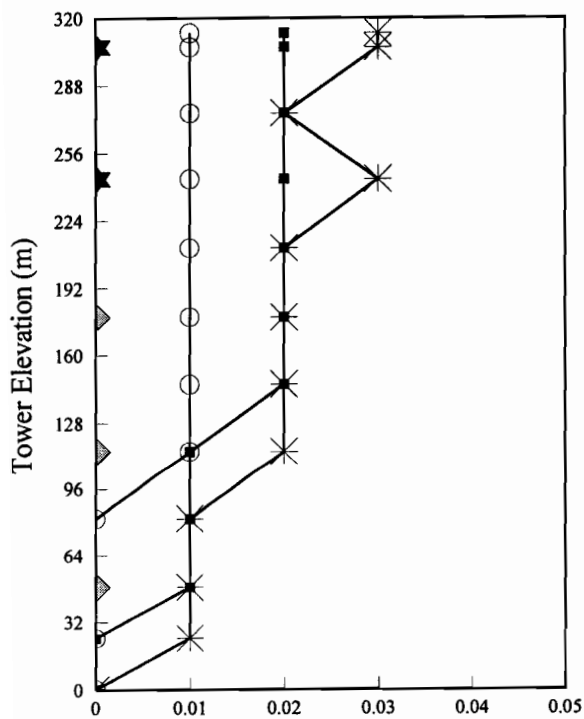
(c) Dynamic Component of Mast Axial Displ. (m)
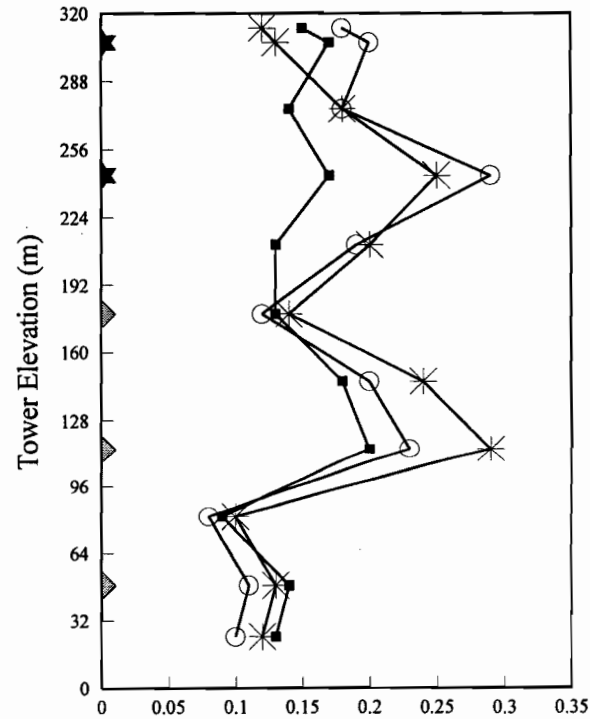
(d) Mast Rotation (Degree)

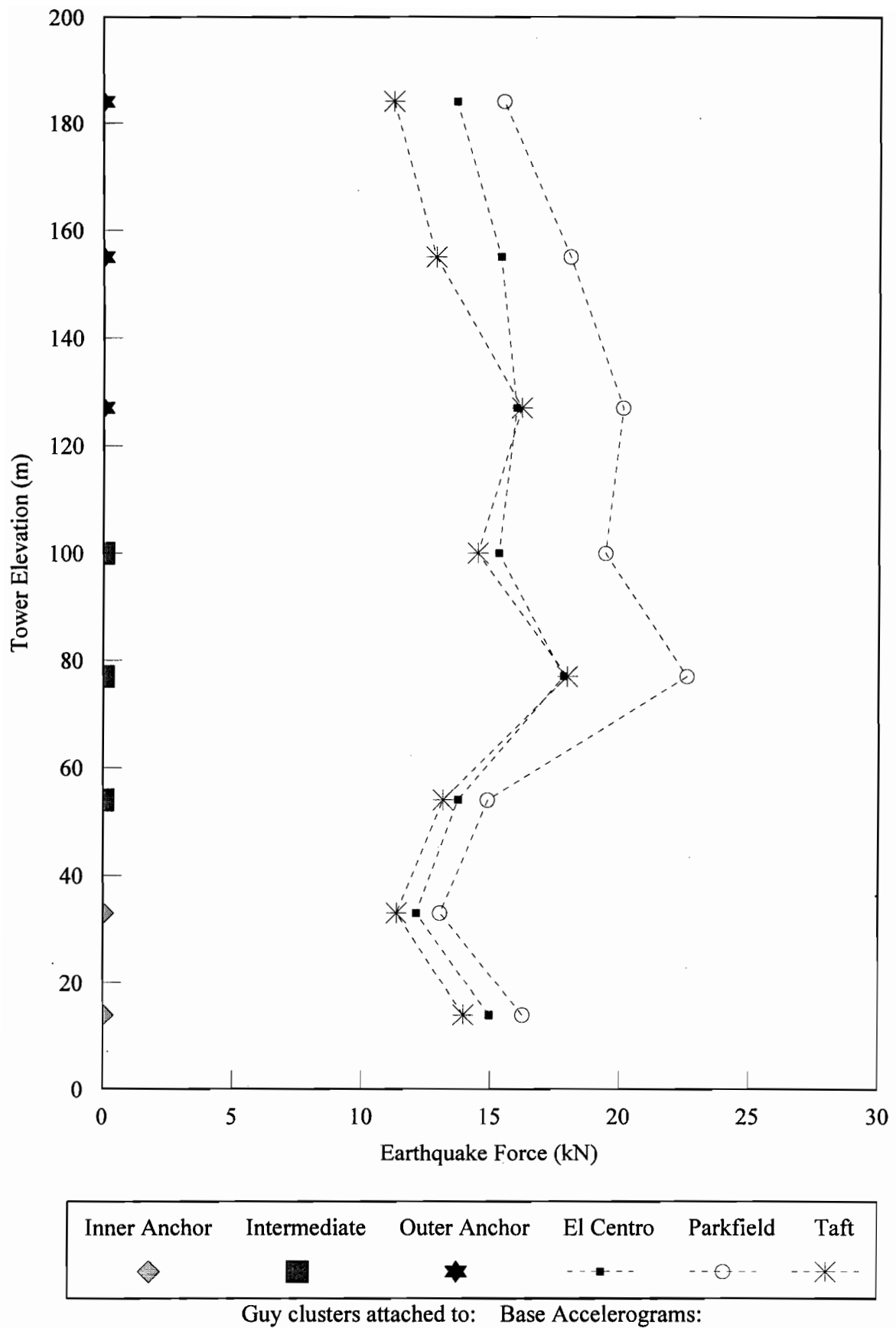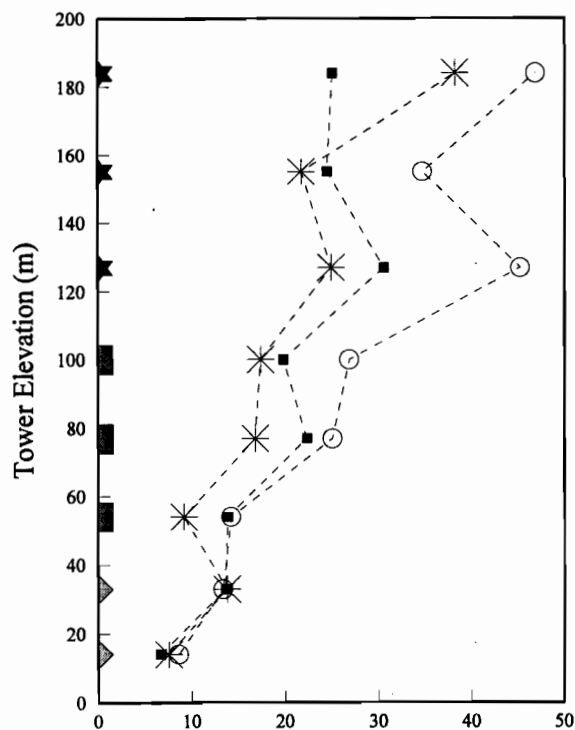| Guy clusters attached to:		Base Accelerograms:		
Inner Anchor	Outer Anchor	El Centro	Parkfield	Taft

Fig. 4.45. Response of 313-m tower to three base accelerograms (Horizontal + Vertical)
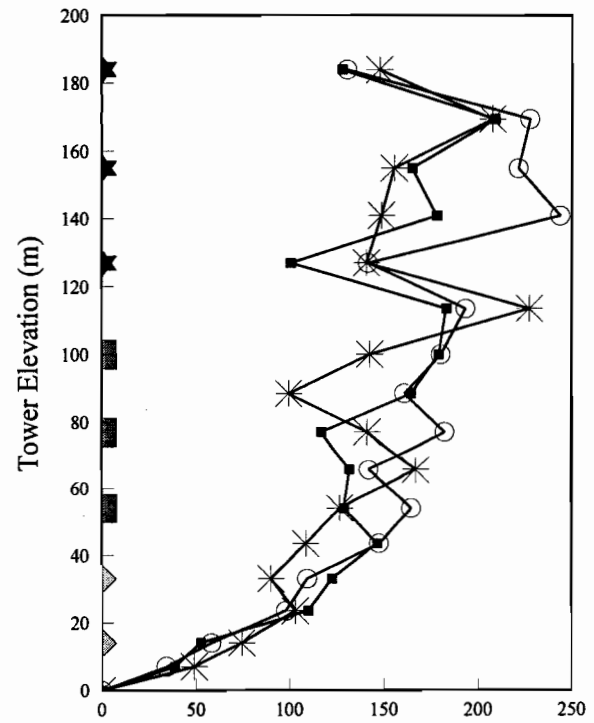
100

4.3.7 342-m Tower

Figures 4.46 to 4.51 show the results of the detailed seismic nonlinear analysis for the 342-m tower. Except for the dynamic component of mast axial force, there is not a significant difference between the results under the horizontal earthquake and its corresponding results for the combined horizontal and vertical earthquake motions.

As illustrated in Figs. 4.46 and 4.49, the earthquake forces of stay levels of the outer group are smaller than those of the inner group. The responses are consistent for the three accelerograms. Cable Set 2 (from the base) is more excited than the others. There is also a nonuniform behaviour close to the transition area.

In Figs. 4.47(a) and 4.50(a), it can be seen that the intermediate cable Set 4 (from the base) close to the transition part is more excited than the other ones. As described earlier for the earthquake force diagram, there is a discontinuity in the behaviour around the transition zone, and the responses are consistent for the three accelerograms.

The mast shear and bending moments along the tower elevation are shown in Figs. 4.47(b and d) and 4.50(b and d), respectively. The maximum dynamic effect of these two response indicators occurs in the bottom part of the tower. There is also a discontinuity in these figures around Set 2. In general, the maximum shear occurs directly at the stay levels and the minimum shear occurs at midspan between the two stay levels, and vice versa for the mast bending moment. The responses are consistent for the three accelerograms.

Figures 4.47(c) and 4.50(c) represent the dynamic component of mast axial force along the tower. As it could be observed, there is no significant axial effect from the load case of horizontal earthquake motion. However, in the case of combined horizontal and vertical earthquake accelerograms, the Taft accelerogram has the most effect on the dynamic component of mast axial force and the El Centro and Parkfield accelerograms come in the second and third order in this regard.

The dynamic component of cable oscillation is shown in Figs. 4.48(a) and 4.51(a). As shown, there is a nonuniform behaviour around Set 2. The oscillation of cables of the outer group is smaller than that of the inner group. The maximum response occurs around

Set 2. The responses are consistent for the three accelerograms.

The mast horizontal displacement and the mast rotation are summarized in Figs. 4.48(b and d) and 4.51(b and d), respectively. There is a discontinuity in the behaviour around the transition region for both responses, and the maximum horizontal displacement occurs close to the transition area. The top part of the tower also experiences the maximum rotation. The responses are consistent for the three accelerograms.

As it can be seen from Figs. 4.48(c) and 4.51(c), the dynamic component of the mast axial displacement along the tower elevation is negligible for the case of the horizontal earthquake. This displacement is up to 4 cm at the top of the tower for the load case of combined vertical and horizontal earthquake motions.
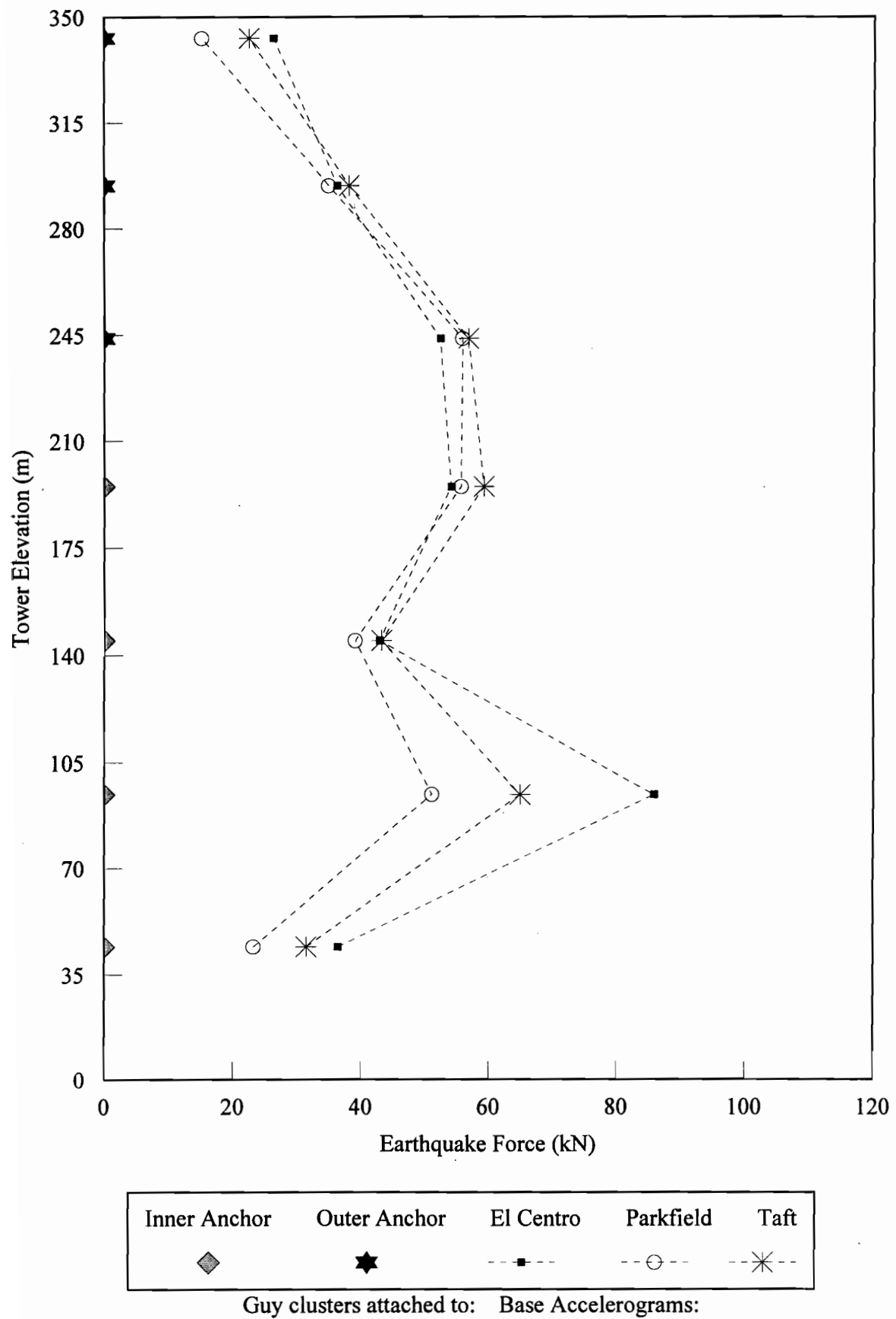
Fig. 4.46. Response of 342-m tower to three base accelerograms

103

(a) Dynamic Component of Cable Tension (kN)

(b) Mast Shear (kN)

(c) Dynamic Comp. of Mast Axial Force (kN)

(d) Mast Bending Moment (kN-m)

Inner Anchor	Outer Anchor
◈	✦

Guy clusters attached to:

El Centro	Parkfield	Taft
▪	⊖	✳

Base Accelerograms:
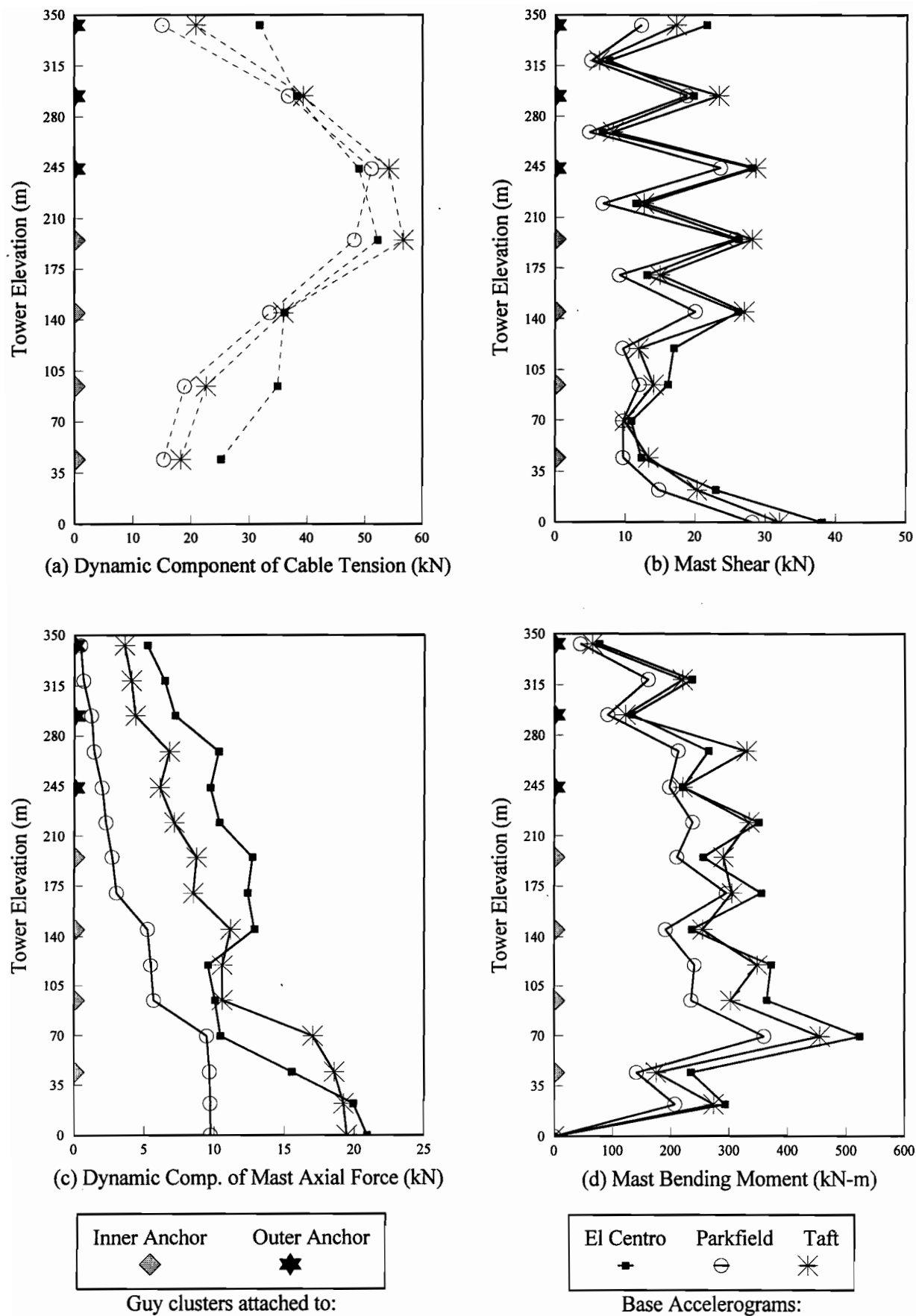
Fig. 4.47. Response of 342-m tower to three base accelerograms
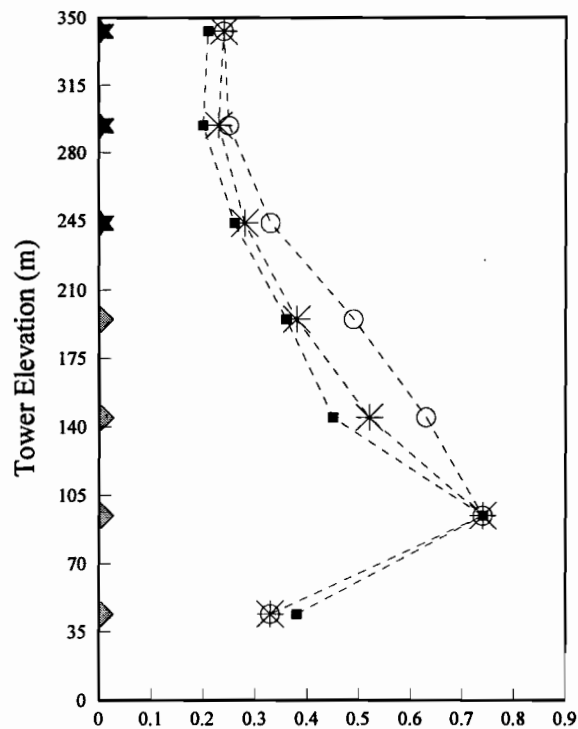
104

(a) Dynamic Component of Cable Oscillation (m)

(b) Mast Horizontal Displacement (m)

(c) Dynamic Component of Mast Axial Displ. (m)

Negligible

(d) Mast Rotation (Degree)

Inner Anchor	Outer Anchor
◈	✶

Guy clusters attached to:

El Centro	Parkfield	Taft
■	⊖	✳
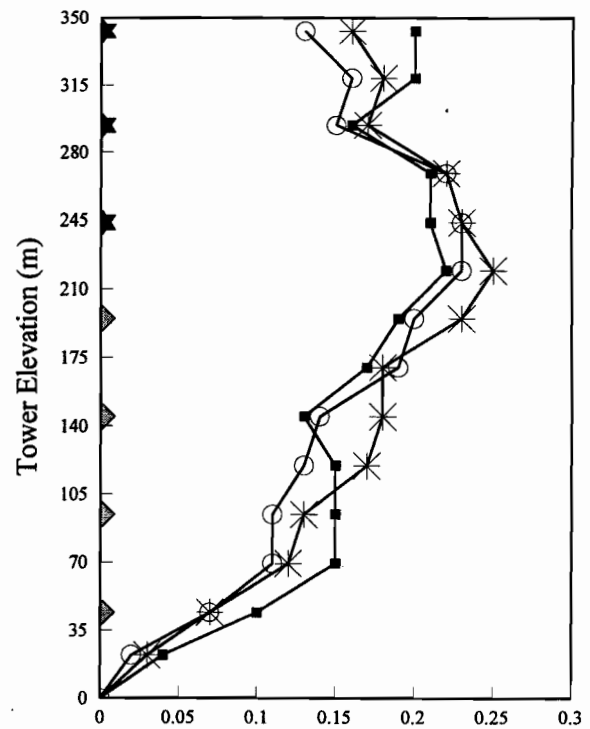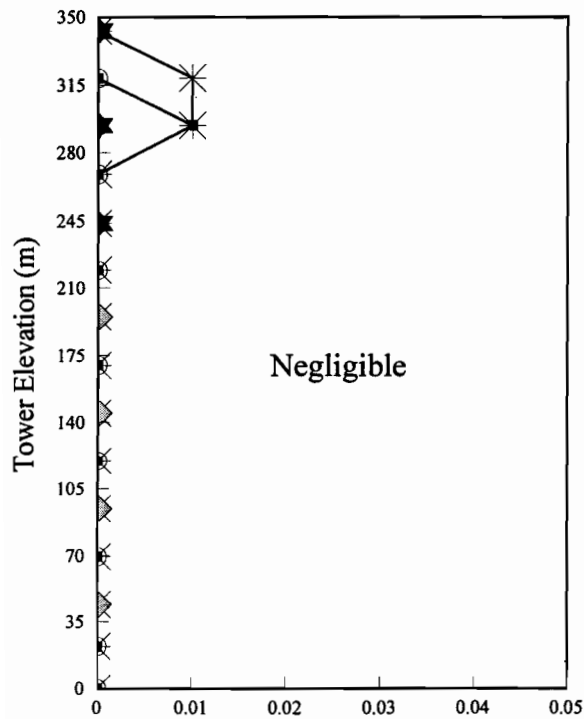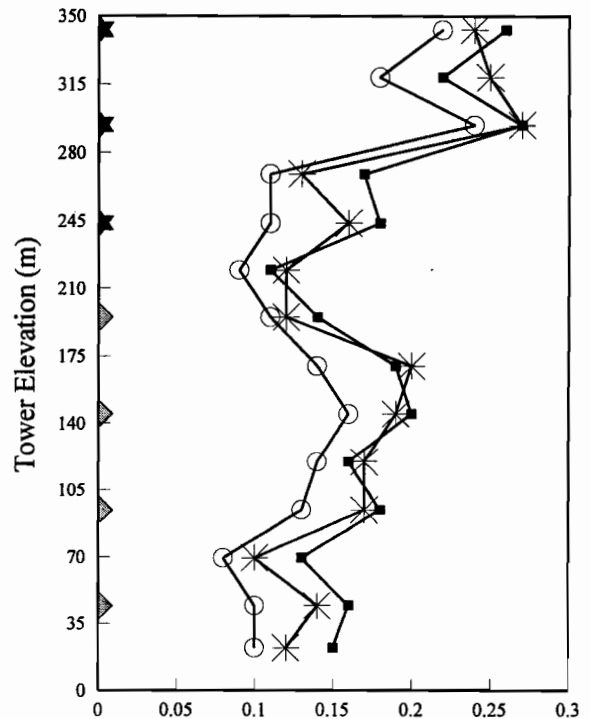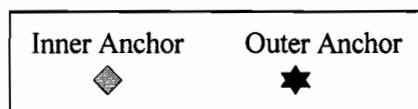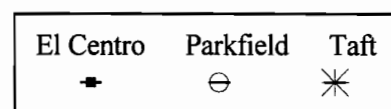
Base Accelerograms:

Fig. 4.48. Response of 342-m tower to three base accelerograms

105
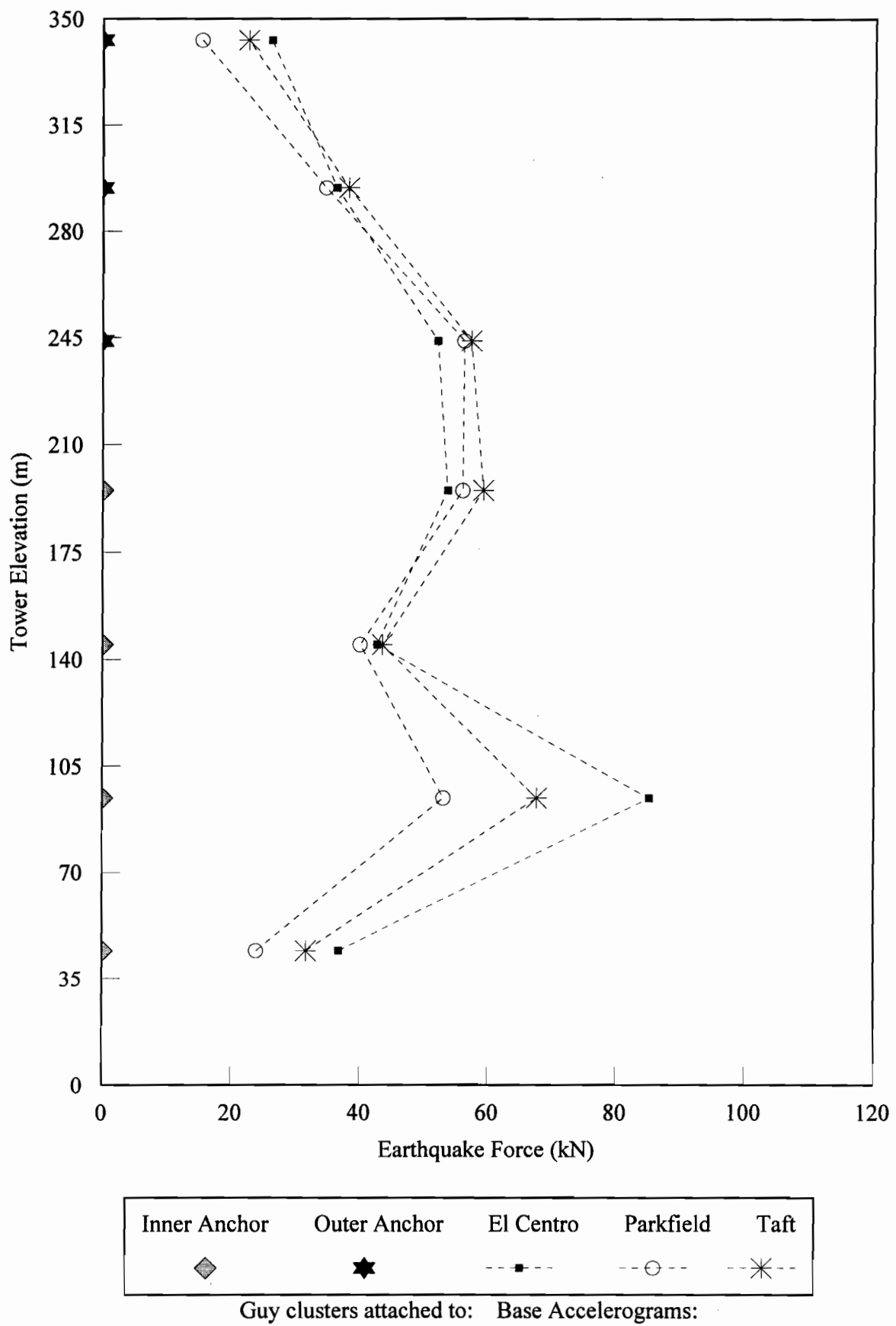
Fig. 4.49. Response of 342-m tower to three base accelerograms (Horizontal + Vertical)
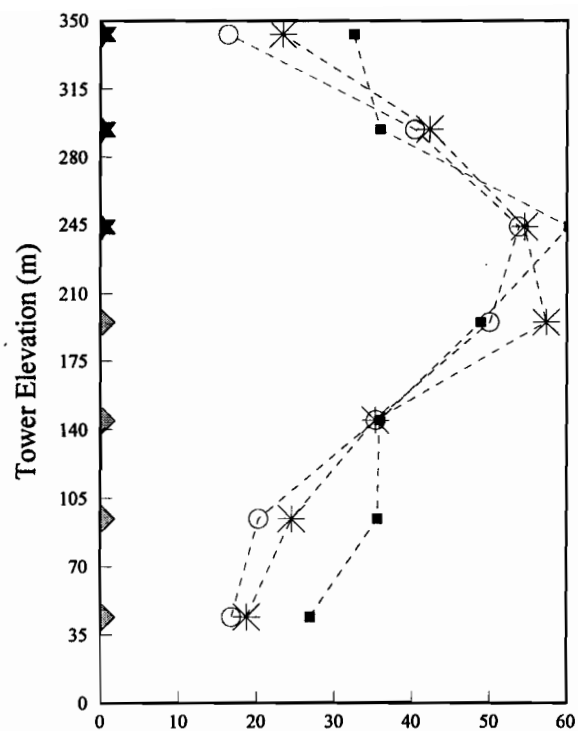
106
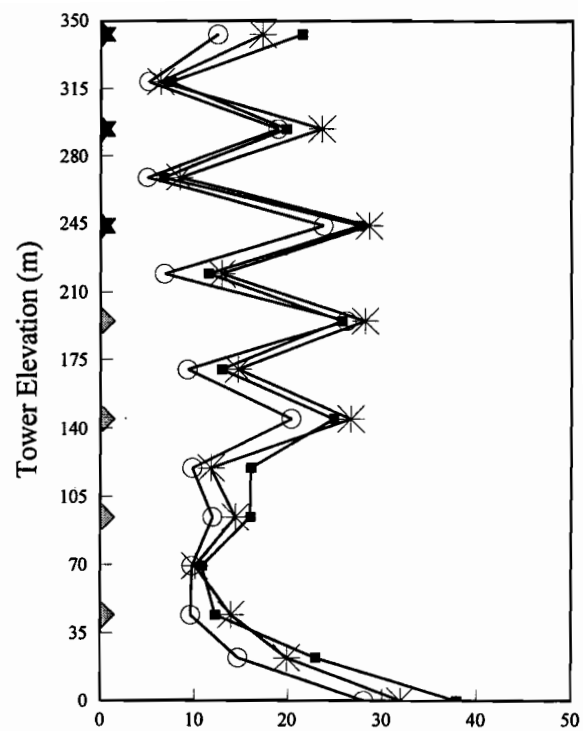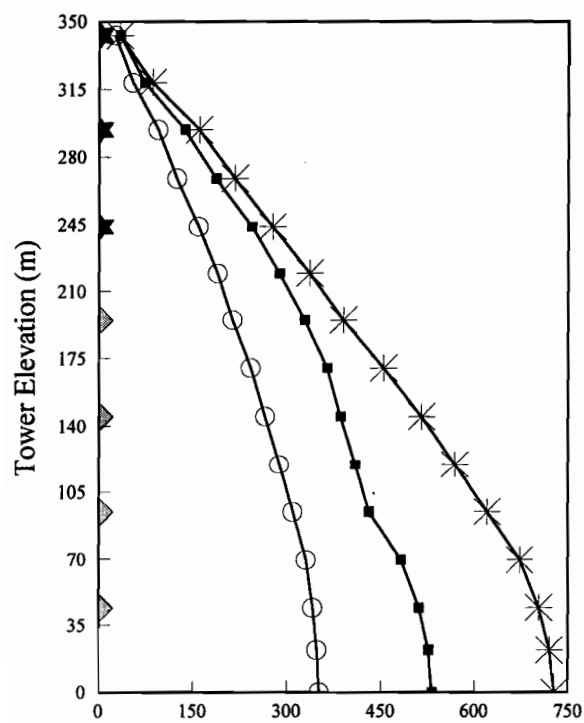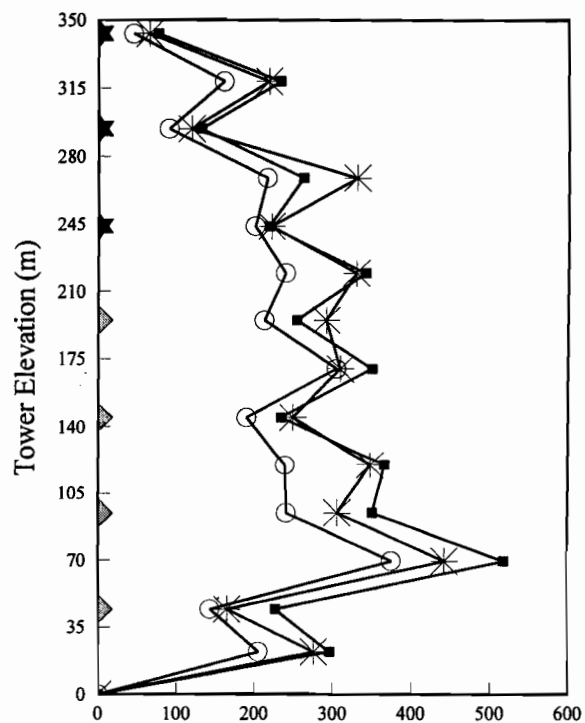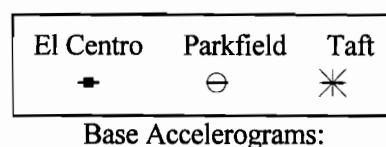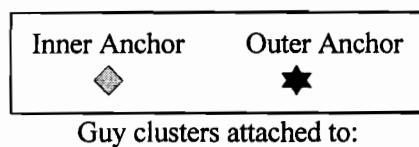
Fig. 4.50. Response of 342-m tower to three base accelerograms (Horizontal + Vertical)
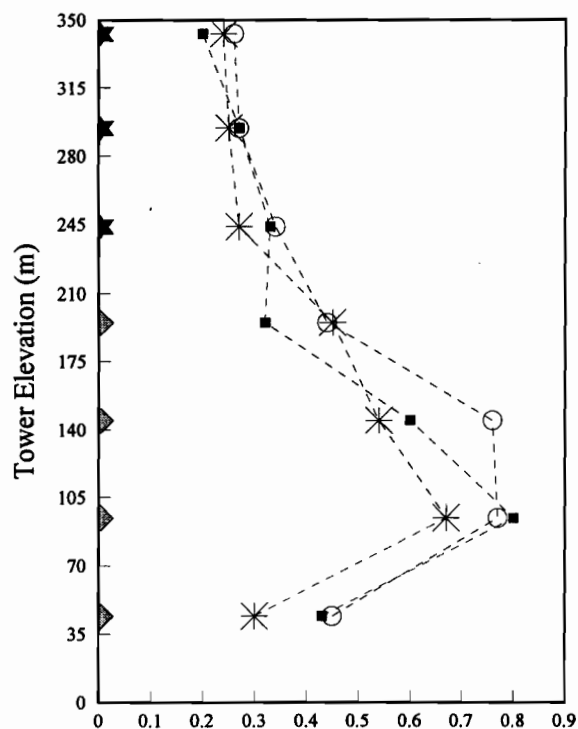
107

(a) Dynamic Component of Cable Oscillation (m)

(b) Mast Horizontal Displacement (m)

(c) Dynamic Component of Mast Axial Displ. (m)

(d) Mast Rotation (Degree)

Inner Anchor	Outer Anchor
◈	★

Guy clusters attached to:

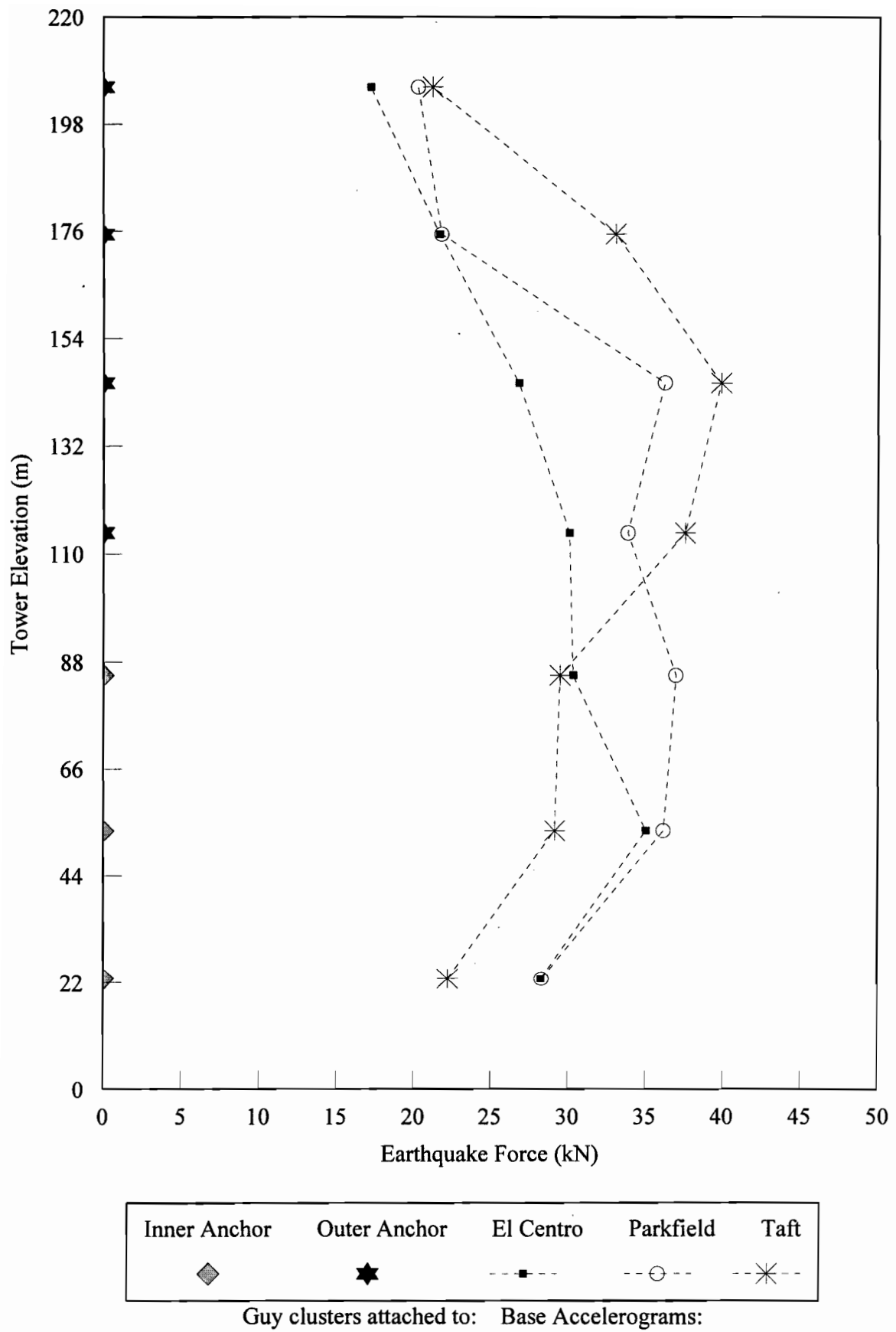| El Centro	Parkfield	Taft
■	⊖	✳
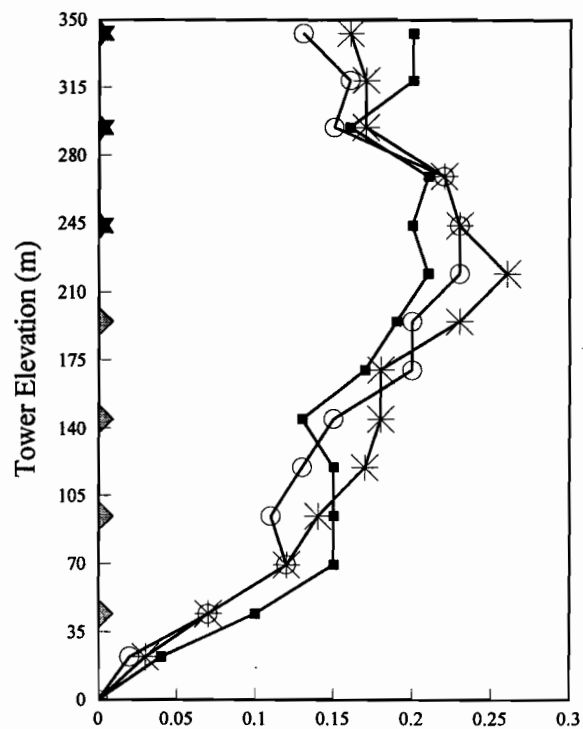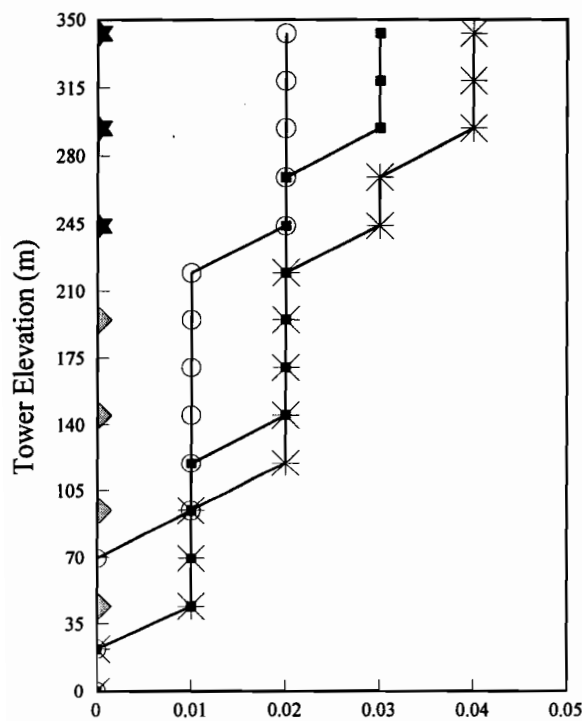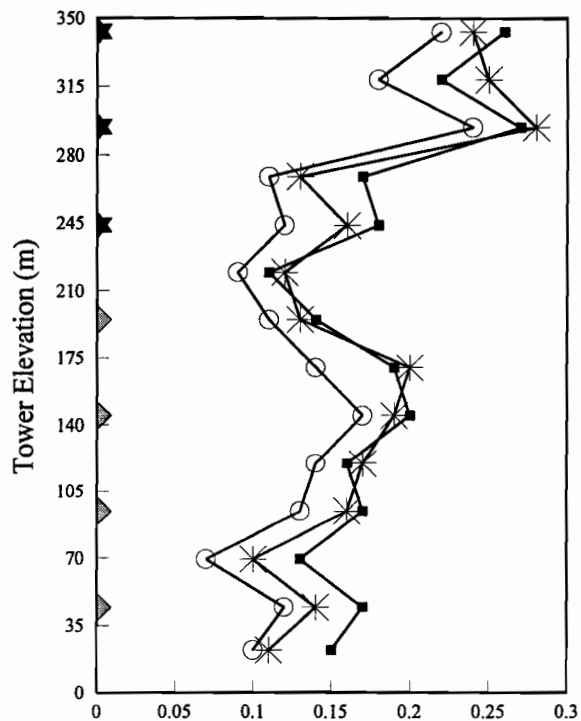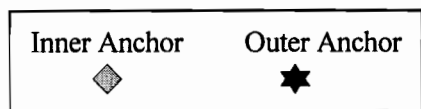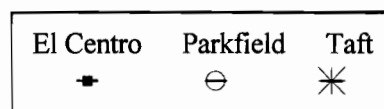
Base Accelerograms:

Fig. 4.51. Response of 342-m tower to three base accelerograms (Horizontal + Vertical)

108

4.3.8 607-m Tower

Figures 4.52 to 4.57 show the results of the detailed seismic nonlinear analysis for the 607-m tower. Except for the dynamic component of mast axial force, there is not a significant difference between the results due to the horizontal earthquake and the corresponding results for the combined horizontal and vertical earthquake motions.

As illustrated in Figs. 4.52 and 4.55, the earthquake forces at stay levels of the intermediate group are larger than those of the other groups. The El Centro and Taft accelerograms have more effect on the earthquake forces than the Parkfield for the guy cables of intermediate and inner groups. However, the response for the El Centro and Parkfield accelerograms are reversed for the guy cables of the outer group. The intermediate cable Set 4 (from the base) at the bottom transition zone is more excited than the others. There is again a nonuniform behaviour around the transition areas.

In Figs. 4.53(a) and 4.56(a), it can be seen that the intermediate cable set close to the bottom transition part (i.e. Set 2 from the base) is more excited than the other ones. There is also a discontinuity in the behaviour around the transition zones.

The mast shear and bending moments along the tower elevation are shown in Figs. 4.53(b and d) and 4.56(b and d), respectively. The maximum dynamic effect of mast shear occurs close to the bottom transition area (i.e. Set 2). The maximum dynamic effect of mast bending moment occurs close to the transition zones (i.e. Sets 2 and 7). There is a discontinuity in these figures around the transition regions. In general, the maximum shear occurs directly at the stay levels and the minimum shear occurs at midspan between the two stay levels, and vice versa for the mast bending moment. The responses are consistent for the three accelerograms.

Figures 4.53(c) and 4.56(c) represent the dynamic component of the mast axial force along the tower. As expected, there is no significant axial effect from the load case of the horizontal earthquake motion. However, in the case of combined horizontal and vertical earthquake accelerograms, the El Centro accelerogram has the most effect on the dynamic component of mast axial force, and the Parkfield and Taft accelerograms come in second order in this regard.

109

The dynamic component of the cable oscillation is shown in Figs. 4.54(a) and 4.57(a). As shown, there is a nonuniform behaviour around the transition zones. The responses are consistent for the three accelerograms.

The mast horizontal displacement and the mast rotation are summarized in Figs. 4.54(b and d) and 4.57(b and d), respectively. There is a discontinuity in the behaviour around the transition regions for both responses. The maximum horizontal displacement occurs close to the top transition area, and the top part of the tower experiences the maximum rotation. The Parkfield accelerogram is the most soliciting accelerogram as far as these response indicators are concerned (in the load case of horizontal earthquake).

As it can be seen from Figs. 4.54(c) and 4.57(c), the dynamic component of the mast axial displacement along the tower elevation is negligible for the load case of horizontal earthquake. This displacement is up to 11 centimetres at the top of the tower for the load case of combined vertical and horizontal earthquake motions.
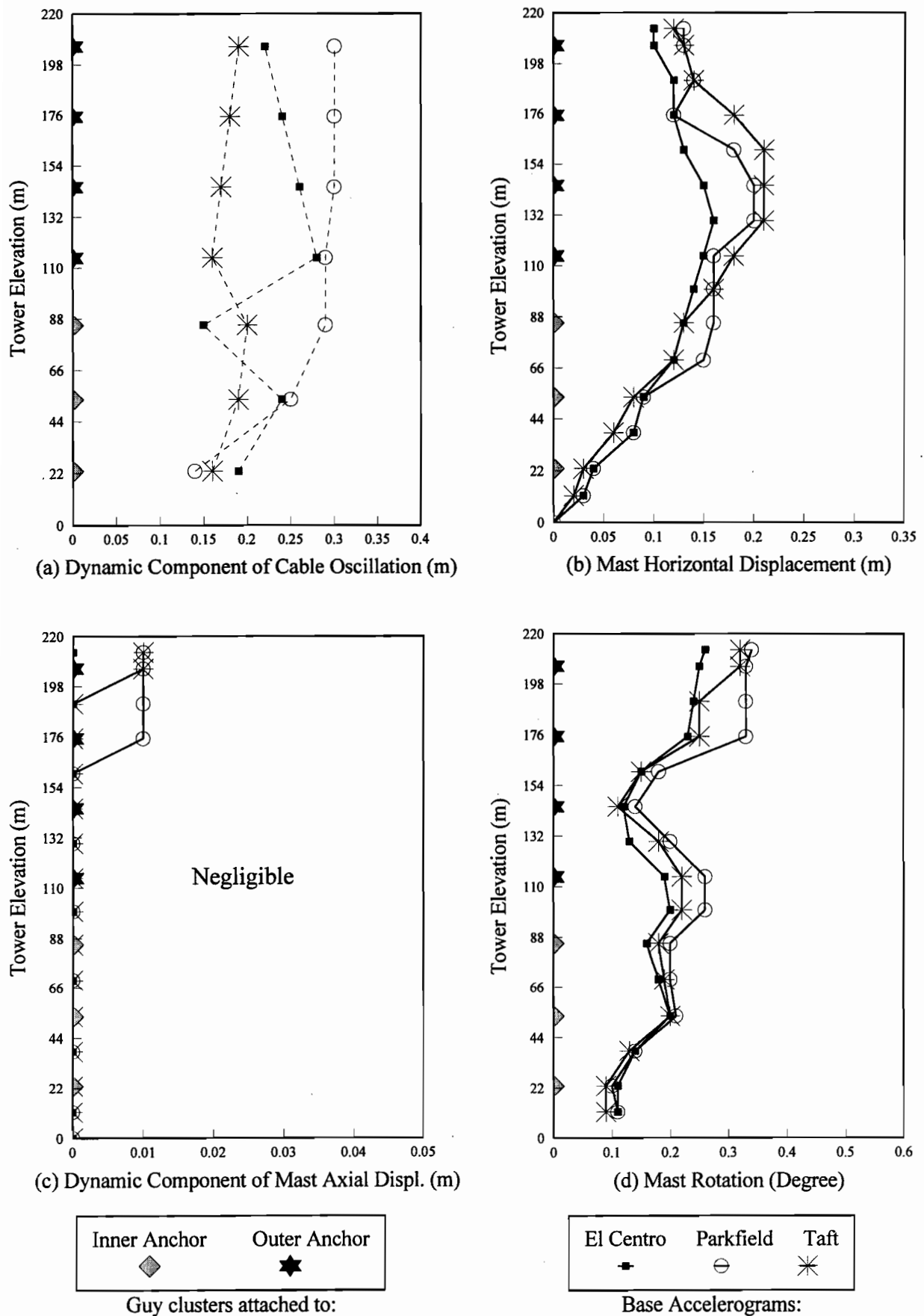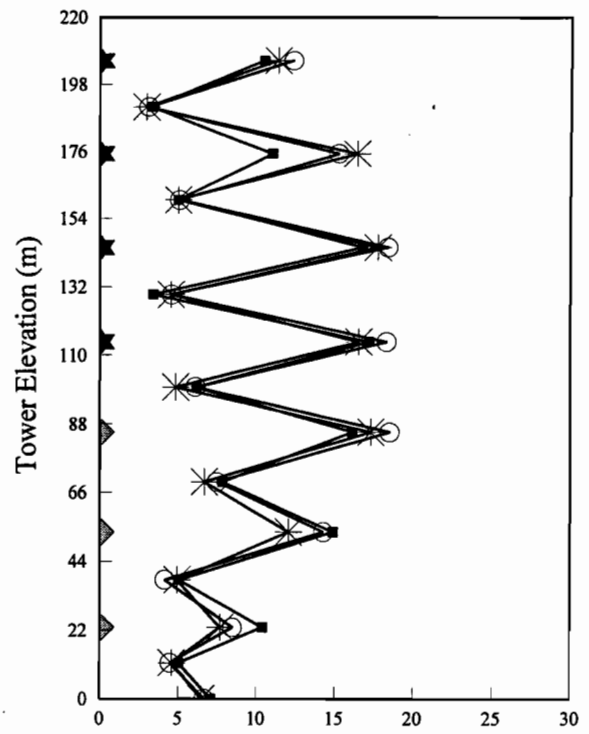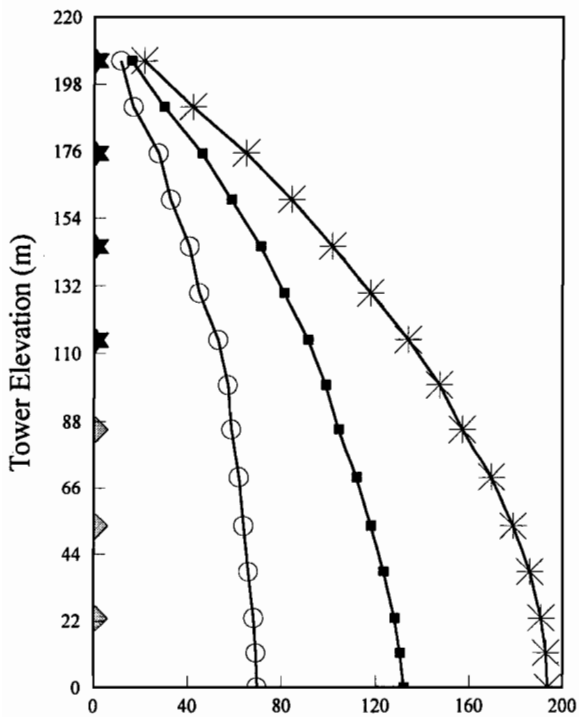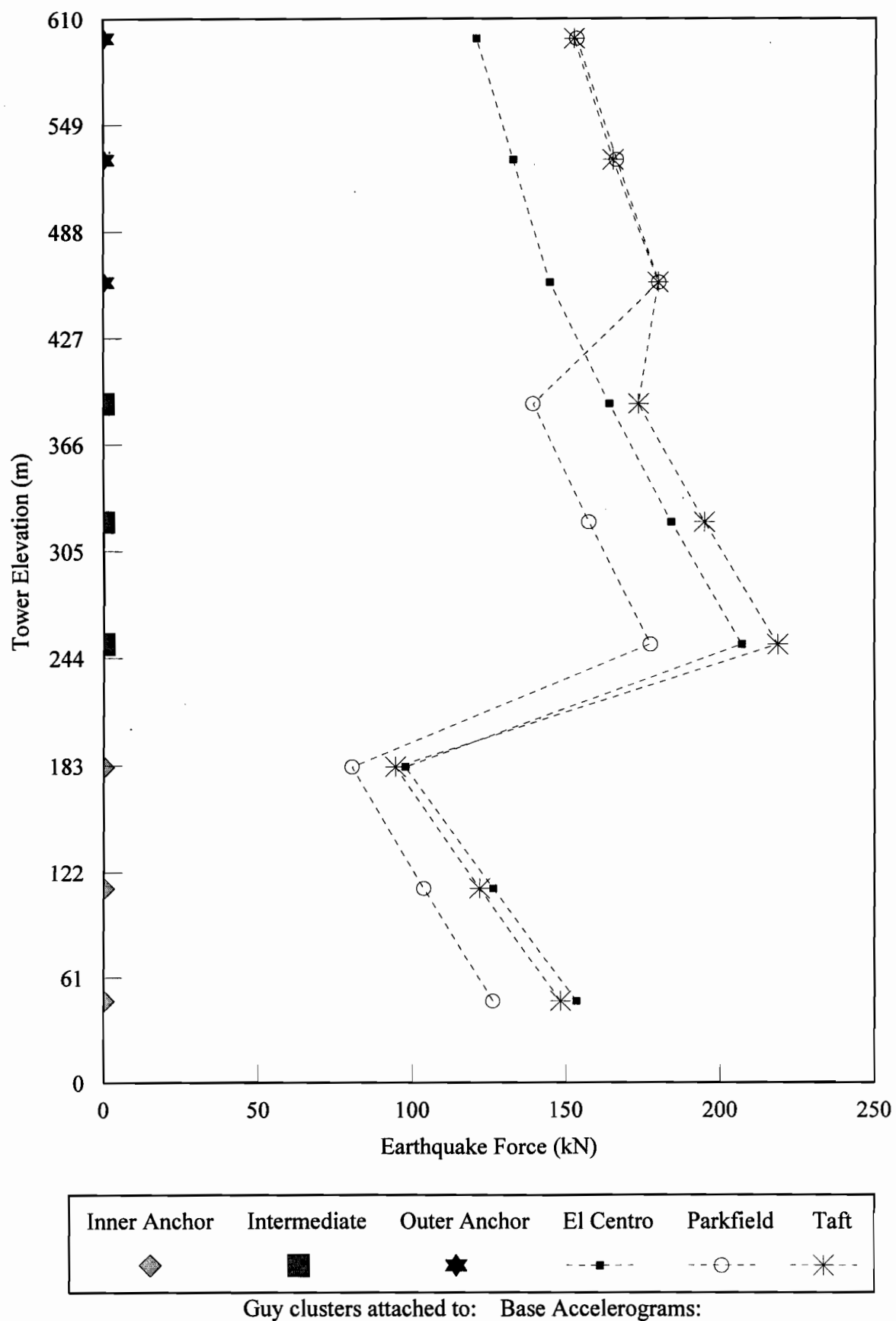
Fig. 4.52. Response of 607-m tower to three base accelerograms
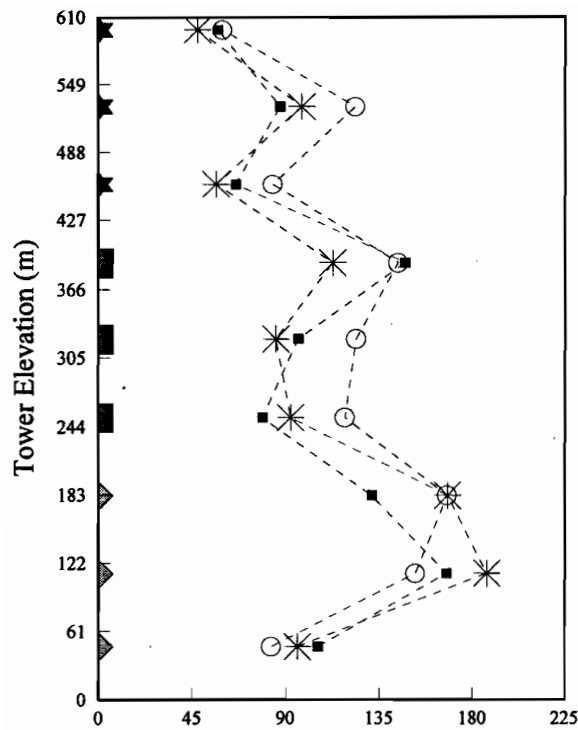
111

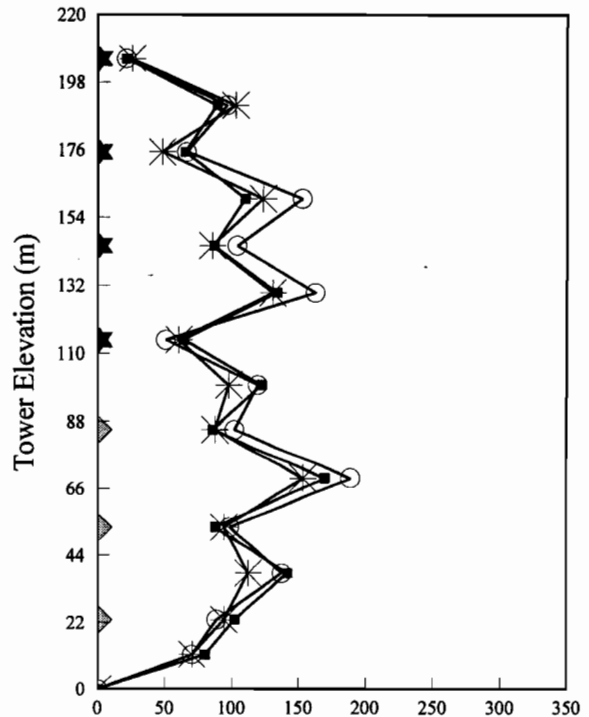(a) Dynamic Component of Cable Tension (kN)

(b) Mast Shear (kN)

(c) Dynamic Comp. of Mast Axial Force (kN)

(d) Mast Bending Moment (kN-m)

Guy clusters attached to Anchor:

Inner	Intermediate	Outer

Base Accelerograms:

El Centro	Parkfield	Taft
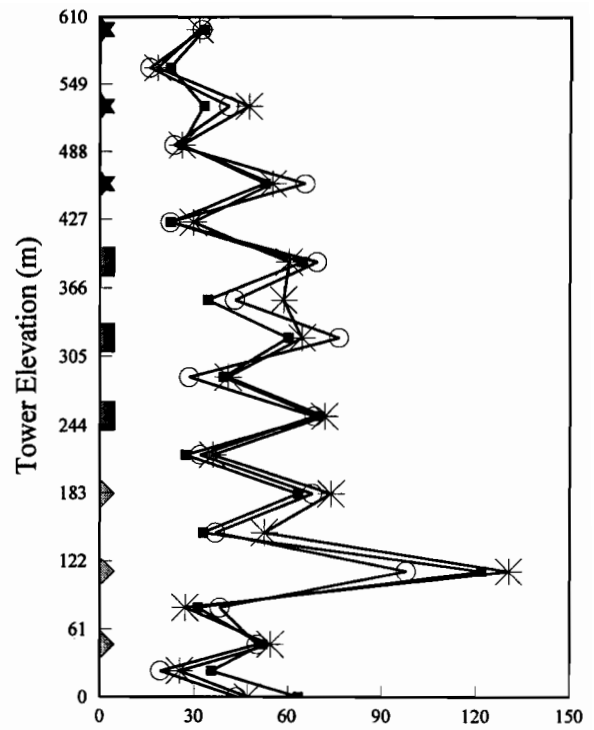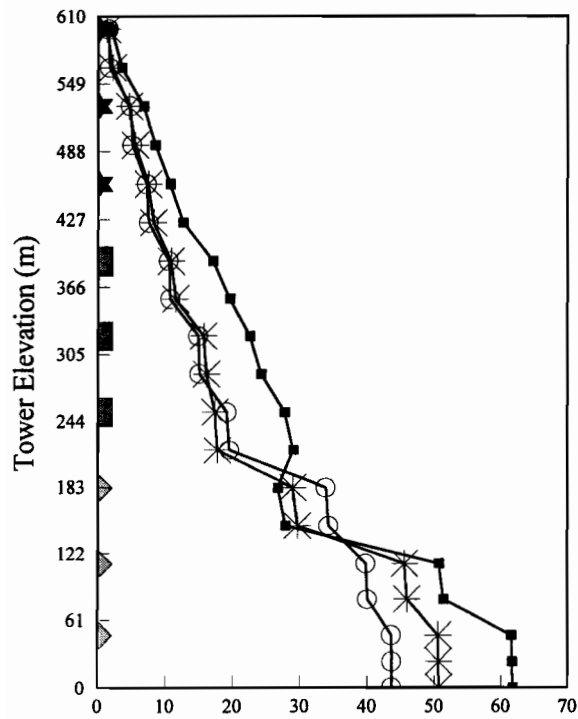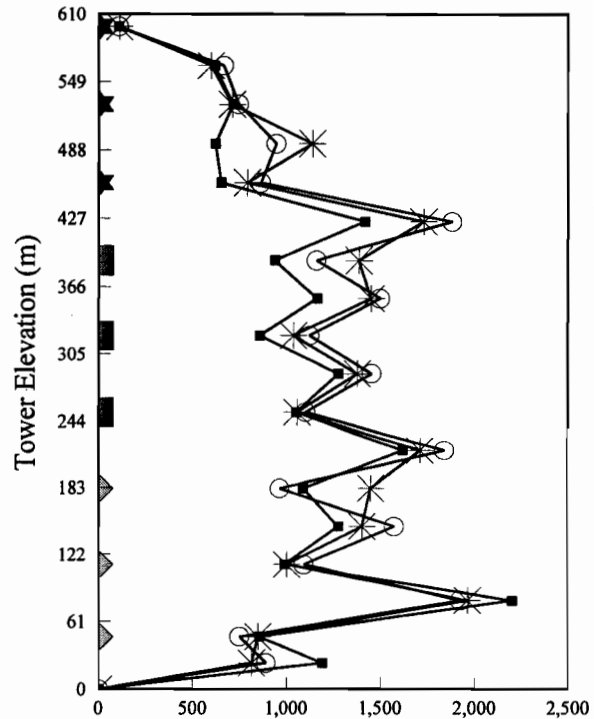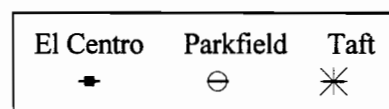
Fig. 4.53. Response of 607-m tower to three base accelerograms
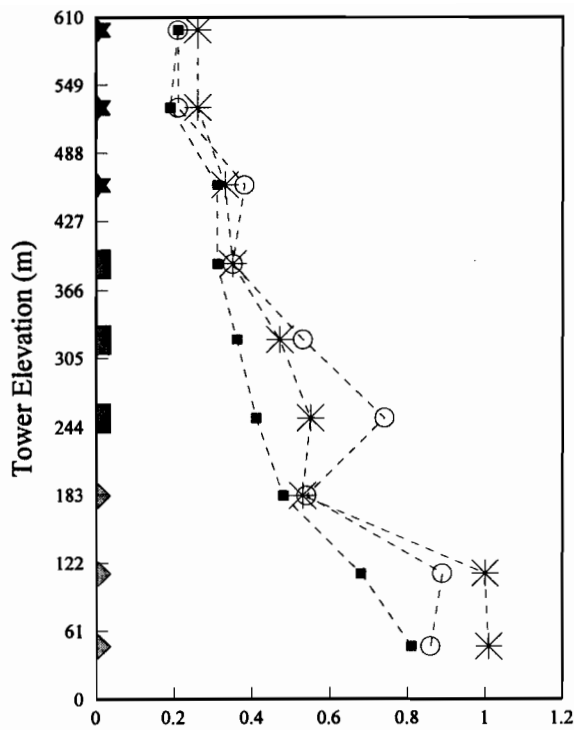
112

(a) Dynamic Component of Cable Oscillation (m)

(b) Mast Horizontal Displacement (m)

(c) Dynamic Component of Mast Axial Displ. (m)

(d) Mast Rotation (Degree)

Inner	Intermediate	Outer
◈	■	✦

Guy clusters attached to Anchor:

El Centro	Parkfield	Taft
■	⊖	✳
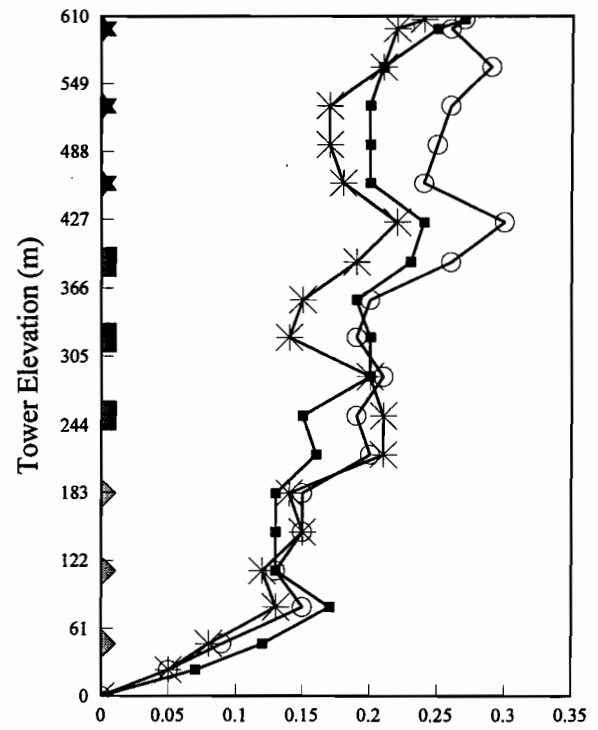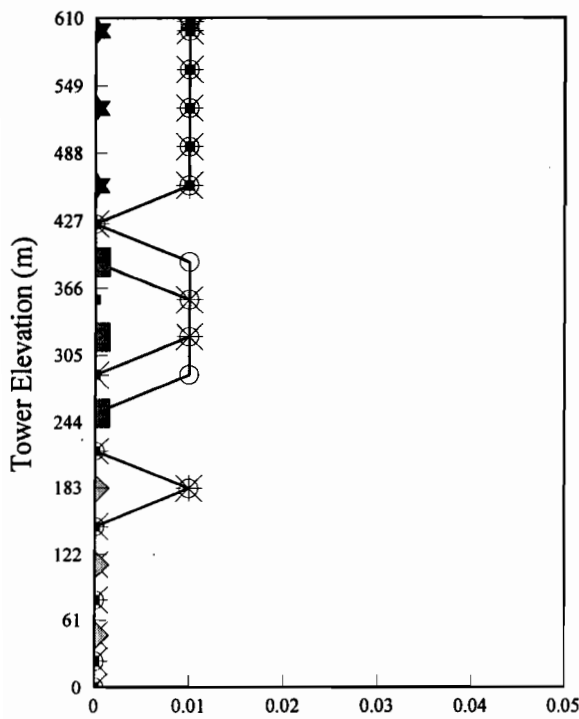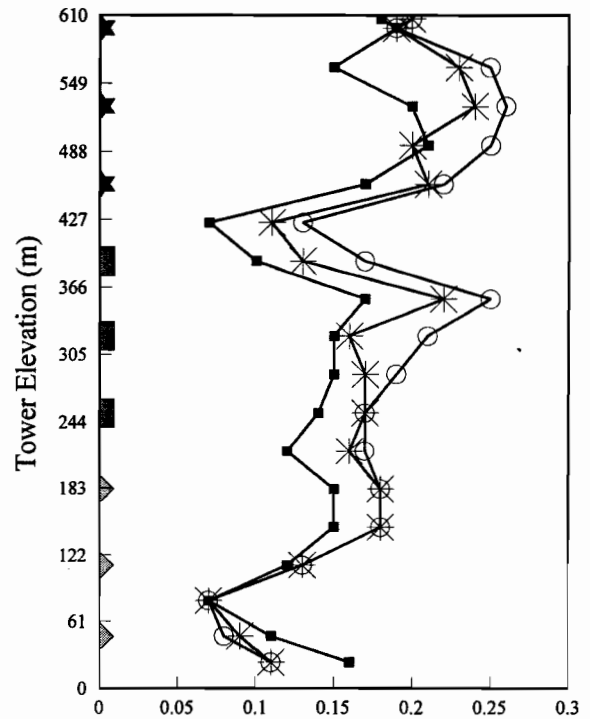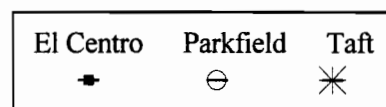
Base Accelerograms:

Fig. 4.54. Response of 607-m tower to three base accelerograms

113
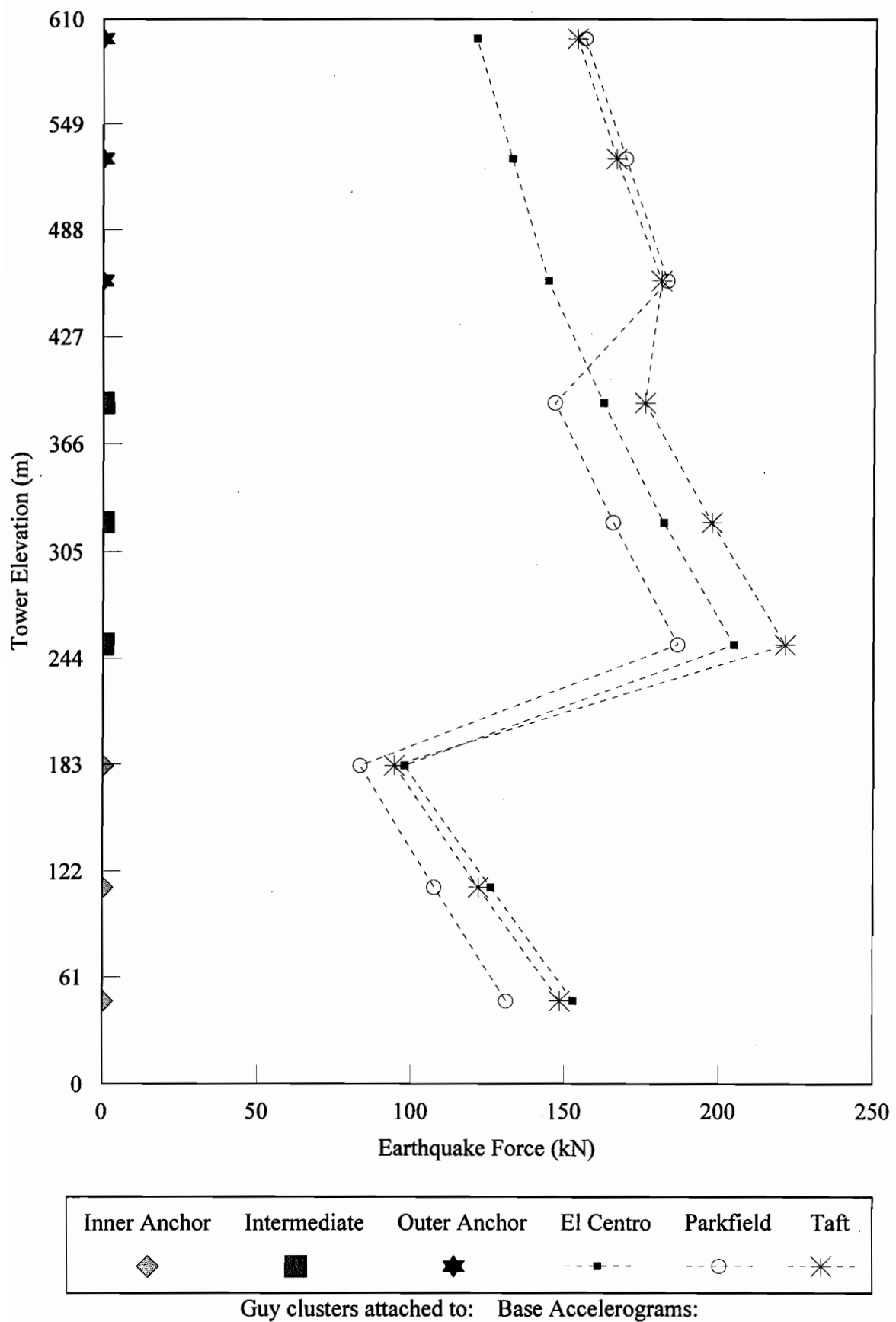
Fig. 4.55. Response of 607-m tower to three base accelerograms (Horizontal + Vertical)
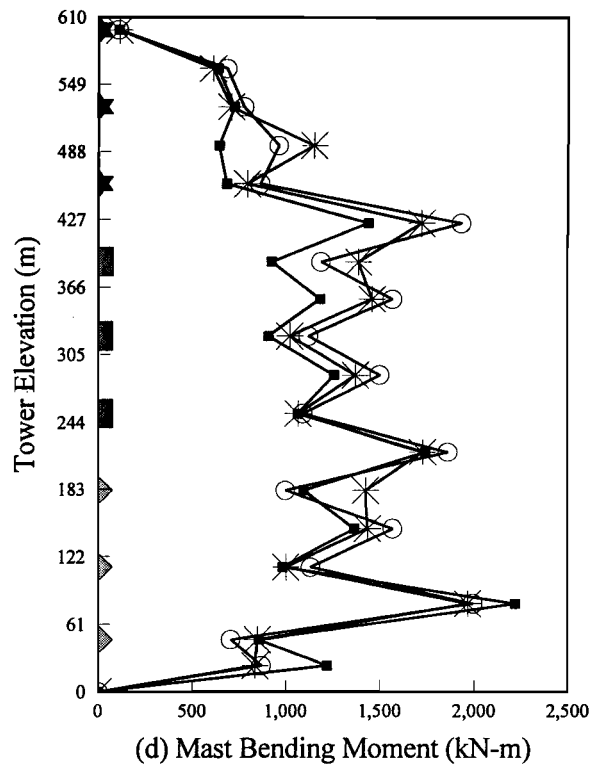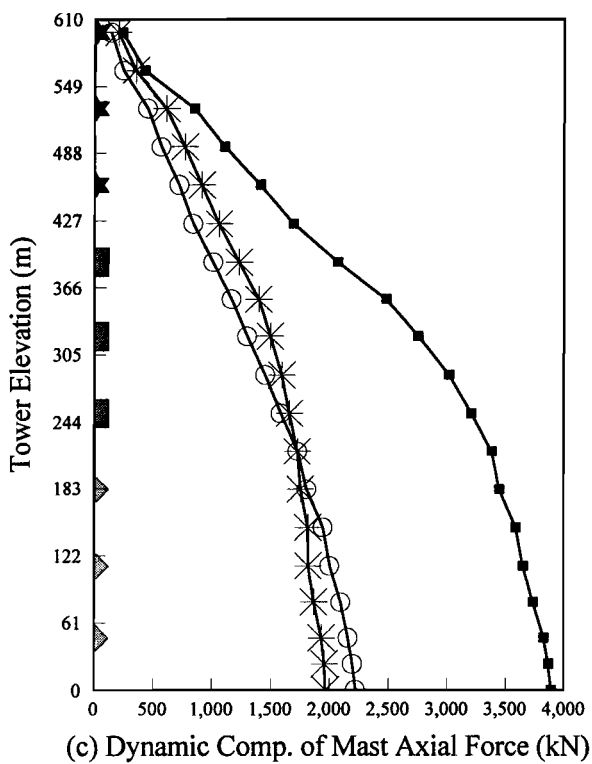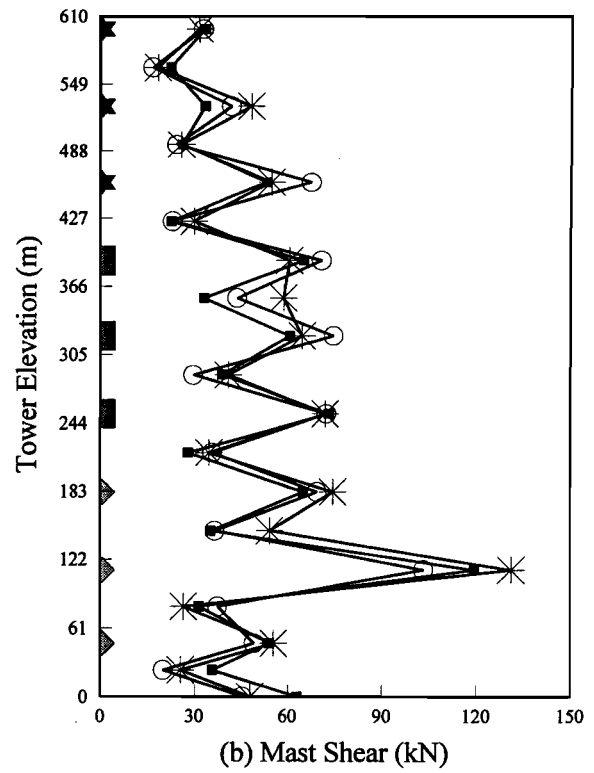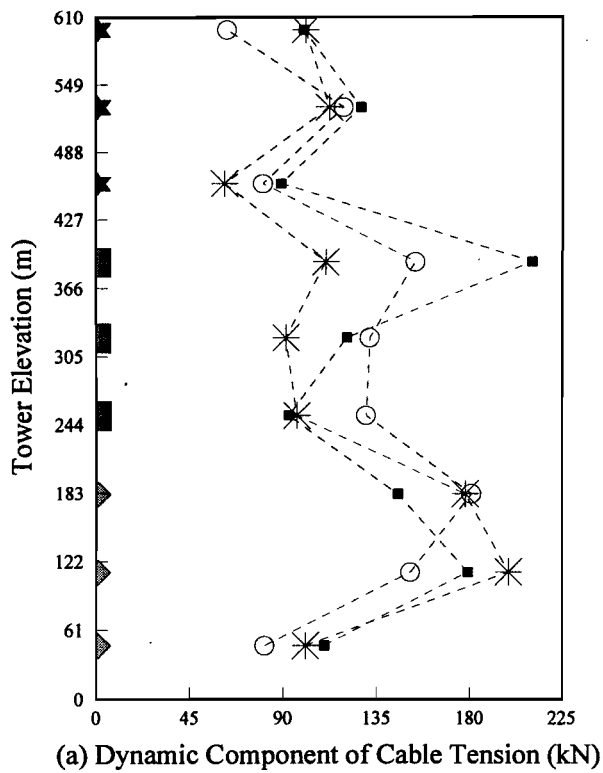
114

(a) Dynamic Component of Cable Tension (kN)

(b) Mast Shear (kN)

(c) Dynamic Comp. of Mast Axial Force (kN)

(d) Mast Bending Moment (kN-m)

Inner	Intermediate	Outer
◈	■	✷

Guy clusters attached to Anchor:

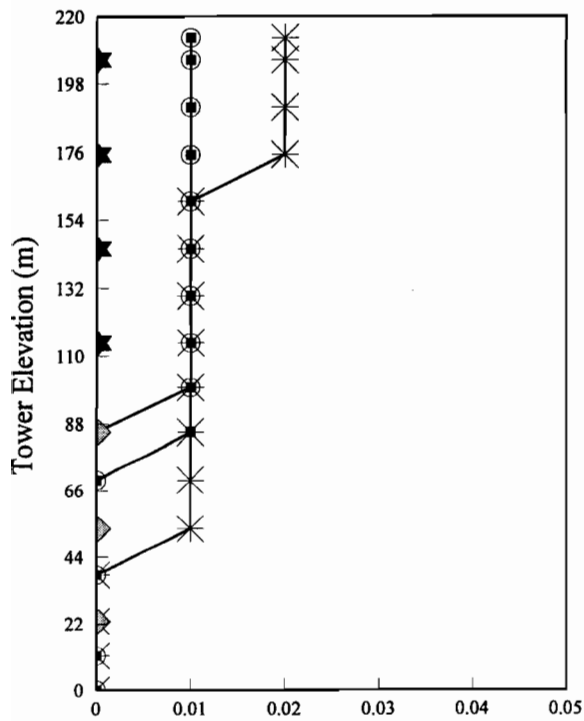| El Centro	Parkfield	Taft
■	⊖	✳

Base Accelerograms:

Fig. 4.56. Response of 607-m tower to three base accelerograms (Horizontal + Vertical)
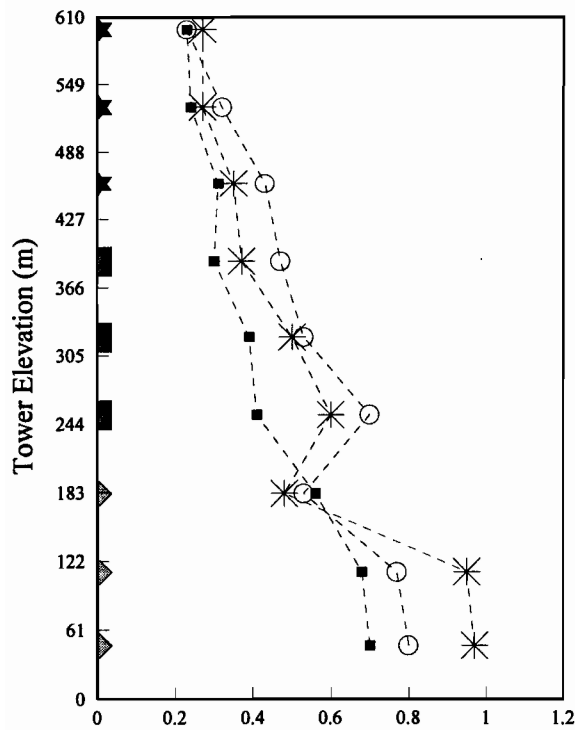
115

(a) Dynamic Component of Cable Oscillation (m)

(b) Mast Horizontal Displacement (m)

(c) Dynamic Component of Mast Axial Displ. (m)

(d) Mast Rotation (Degree)

Inner	Intermediate	Outer
◈	■	✹

Guy clusters attached to Anchor:

El Centro	Parkfield	Taft
▬	⊖	✳
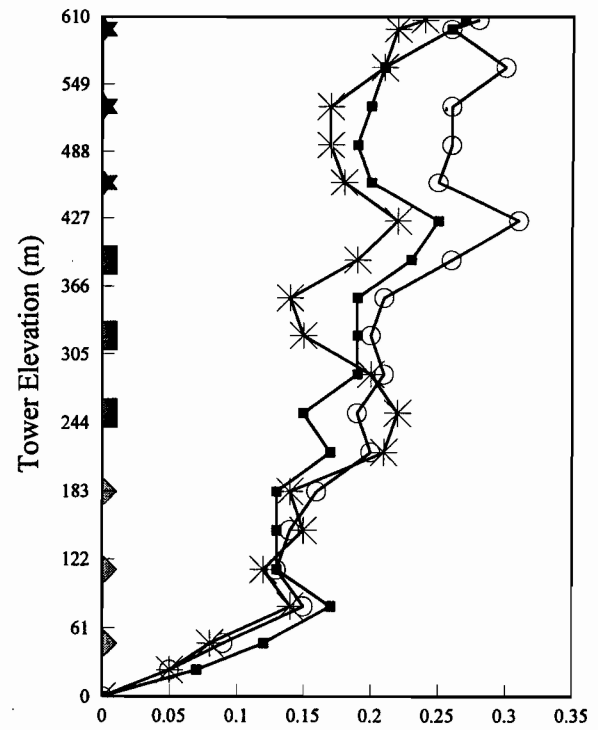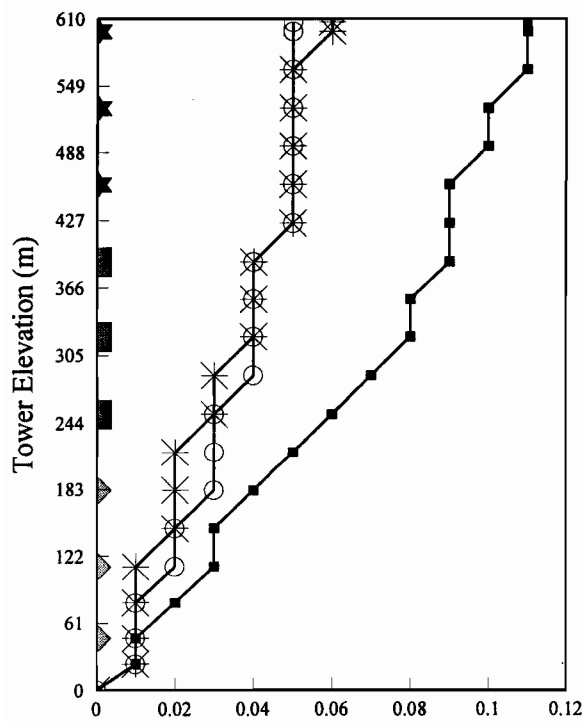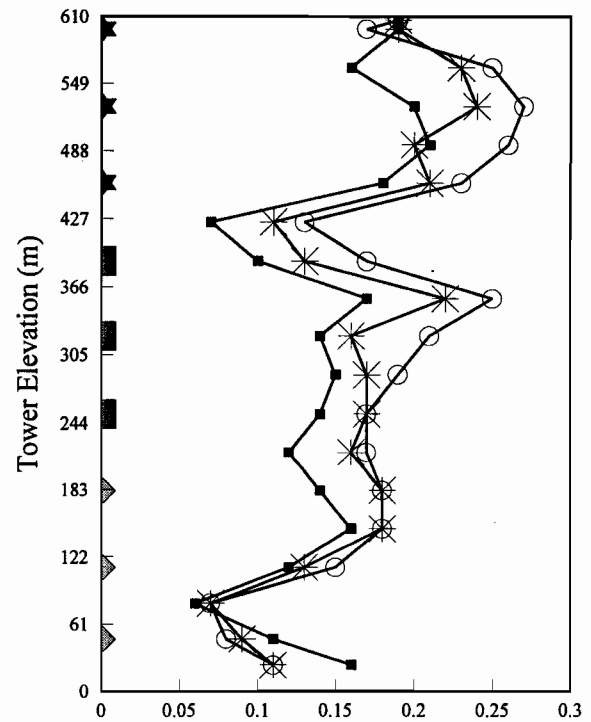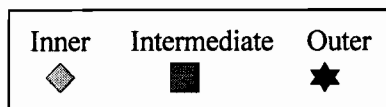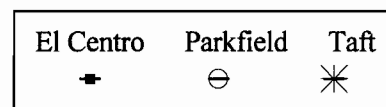
Base Accelerograms:

Fig. 4.57. Response of 607-m tower to three base accelerograms (Horizontal + Vertical)

116

4.4 TYPICAL BEHAVIOUR

For most of the guyed towers studied, there are two groups of cable sets corresponding to the two groups of anchorage points on the ground. For example, for the 198-m tower (Fig. 1.1), Sets 1, 2, and 3 are connected to the inner anchor points and Sets 4, 5, and 6 to the outer ones. In general, there is a nonuniformity in the trend of the tower lateral stiffness in the transition portion from inner to outer anchor points (e.g. between Sets 3 and 4 in the 198-m tower), and this area is a sensitive portion of the tower. For guyed towers with three anchorage points on the ground (e.g. the 200-m and 607-m towers), there are two transition zones along the mast.

From the previous section, the figures of the earthquake force, dynamic component of cable tension, mast shear, mast bending moment, dynamic component of cable oscillation, mast horizontal displacement, and mast rotation show a nonuniform behaviour around the transition area, which reflects the sensitivity of the transition section. Also, with the exception of the dynamic component of mast axial force and the mast rotation, the maximum dynamic response of the other indicators occurs close to the transition area.

Except for the response of the dynamic component of mast axial force, there is not a significant difference between the results for the horizontal earthquake load case and the corresponding results for the load case of the combined horizontal and vertical earthquake motions, for all of the guyed towers (with the exception of the 200-m tower).

Generally, the maximum values of the mast shear occur directly at the stay levels and the minimum shear occurs at midspan between two stay levels, and vice versa for the mast bending moment. Also, there is no significant axial effect from the load case of horizontal earthquake motion.

4.5 SERVICEABILITY CONSIDERATIONS

Antenna-supporting towers must meet strict serviceability criteria that are established by their owners in view of the particular use of the tower. Seismic amplifications of displacements and rotations may affect the top part of the tower where

117

the antennas are attached, but they should not result in any local permanent deformation after the earthquake. Such deformations may result in a loss of serviceability resulting in unacceptable signal attenuation. Table 4.3 summarizes the maximum horizontal displacement along the tower height. Generally, the lateral displacements in the earthquake direction are small, in the range of 0.05% to 0.12% of the tower height. This result confirms that the towers are not very flexible. It should be mentioned that due to serviceability requirements, the mast, in spite of being slender, cannot be very flexible. The displacement of the top (a usual antenna location) is smaller than that of some other locations, which emphasizes the importance of serviceability at this location.

Table 4.3. Maximum horizontal displacement of the towers along mast

Tower Height (m)	Max Horizontal Displacement (m)	Max Horizontal Displacement --- % Tower Height
607	0.31	0.05
342	0.26	0.08
313	0.23	0.07
213	0.21	0.10
200	0.22	0.11
198	0.23	0.12
152	0.14	0.09
150	0.16	0.11

Moossavi Nejad (1996) has recently reported the seismic response of a 327-m tower. From his results, the maximum horizontal displacement along the mast was found to be about 0.10% of the tower height. It should be noted that the intensity of the

118

resultant horizontal ground motions used was 0.42g, whereas the one used in this thesis is 0.34g (Peak Horizontal Ground Acceleration of Victoria). After comparing the two values, it can be concluded that his result for the maximum lateral displacement of the mast is comparable to the one obtained here.

As shown in Table 4.4, the tilting of the top of the mast in each tower is less than 0.5°, which is the usual serviceability criterion for most reflector antennas. It should be mentioned that this part of the tower usually experiences the maximum rotation.

Table 4.4. Maximum rotation of the towers along mast

Tower Height (m)	Maximum Mast Rotation (degree)
607	0.27
342	0.28
313	0.29
213	0.34
200	0.31
198	0.37
152	0.36
150	0.33

The maximum dynamic component of cable oscillation of the eight towers is illustrated in Table 4.5. It is observed that these quantities are small with respect to the tower heights. Therefore, very large oscillations of guy cables would not be expected.

The dynamic component of the mast axial displacement along the tower elevation is very small (inferior to a few centimetres) for most of the guyed towers.

Table 4.5. Maximum dynamic component of cable oscillation for the towers along mast

Tower Height (m)	Maximum Dynamic Component of Cable Oscillation (m)
607	1.01
342	0.80
313	1.31
213	0.35
200	0.48
198	0.43
152	0.31
150	0.31

CHAPTER 5

RESULTS AND DISCUSSIONS

5.1 ESSENTIAL CHARACTERISTICS OF THE TOWERS

5.1.1 Weights of Mast and Cables

The detailed weights of the mast and the cables for the eight guyed towers studied are summarized in Table 5.1 and shown graphically in Fig. 5.1. It is observed that the mast accounts for 69% to 77% of the total tower weight, leaving 23% to 31% to the guy cables. Tower attachments such as antennas and accessories (e.g. ladder, transmision lines, lights for aircraft warning, etc.) are not included in the total weights.

5.1.2 Mass Distribution of Mast

The mass distribution along the mast for the eight towers is illustrated in Table 5.2 and Figs. 5.2 to 5.9. It is seen that the variation of the mass of the mast along the height of the towers is almost uniform for most towers. Exceptions are due to the presence of torsional resistors (or outriggers) in the 150-m (Fig. 5.2) and 152-m (Fig. 5.3) towers. In the 607-m tower (Fig. 5.9), the mast becomes lighter in the top portion around the top three guy stay levels.

Table 5.1. Detailed weights of mast and cables of the eight towers

Tower	Structural Component	Weight (kN)	% of Total Weight
607-m	Cable	1595	31
	Mast	3578	69
	Total	5173	100
342-m	Cable	287	28
	Mast	754	72
	Total	1041	100
313-m	Cable	306	23
	Mast	1033	77
	Total	1339	100
213-m	Cable	91	31
	Mast	205	69
	Total	296	100
200-m	Cable	95	28
	Mast	249	72
	Total	344	100
198-m	Cable	180	25
	Mast	535	75
	Total	715	100
152-m	Cable	36	28
	Mast	91	72
	Total	127	100
150-m	Cable	105	31
	Mast	229	69
	Total	334	100
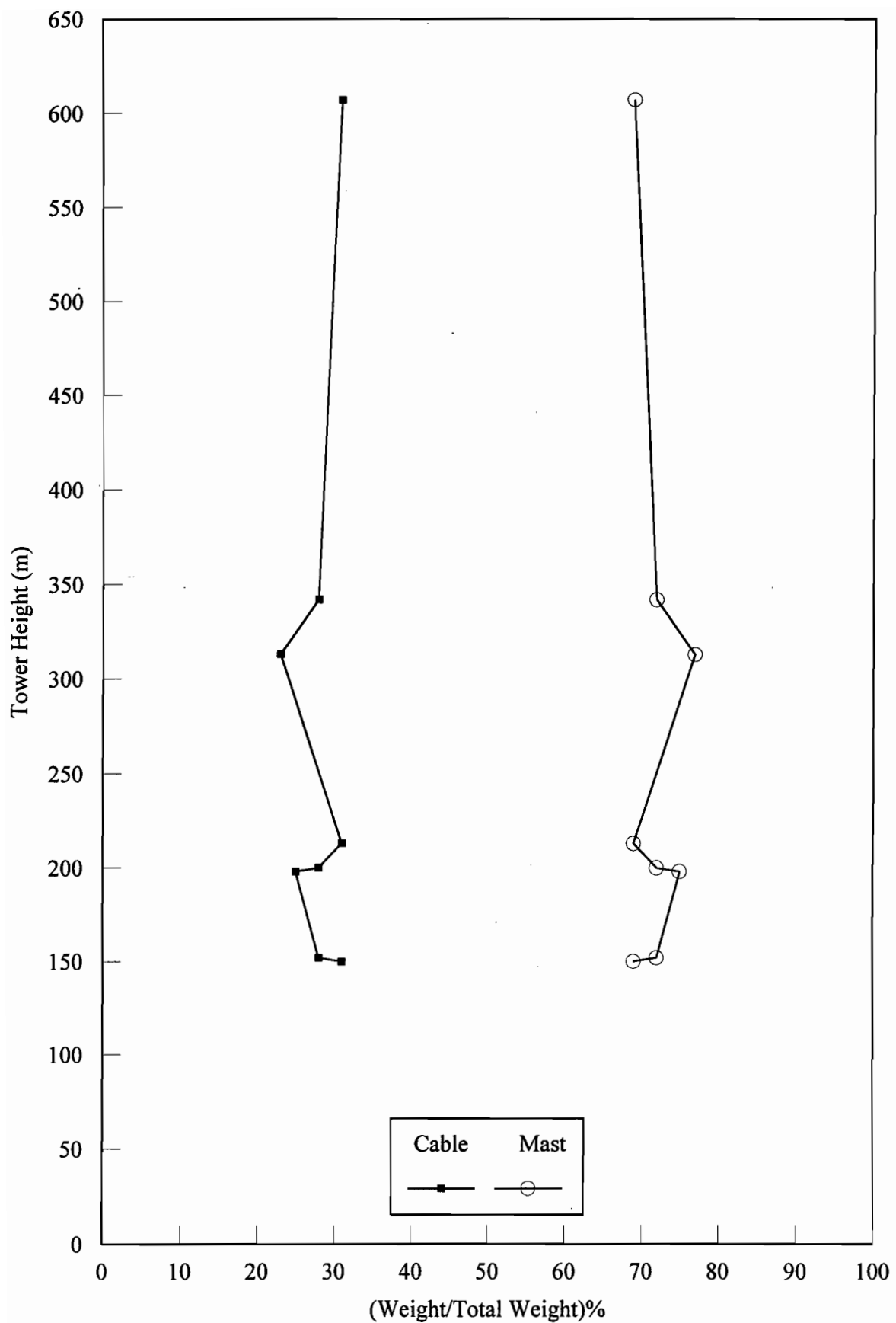
Fig. 5.1. Weight of mast and cable versus tower height

123

Table 5.2. Mass distribution of mast of the guyed towers
(* stabilizer location)

```
================================================================
                    Tower Height (m) = 150
                    ----------------------
Cell No.      Mast Weight (kN)   Mass per unit length (kg/m)
----------------------------------------------------------------
0                    207.93             105.25
9                    198.64             128.48
17.5                 187.93             111.35
25                   179.74             239.28
32.5      *          162.14             170.56
43.5                 143.74             138.12
54.5                 128.84             103.13
65                   118.22             130.91
75.5                 104.74             73.31
85.5                 97.55              188.44
95.5      *          79.07              143.31
106.5                63.61              124.86
117.5                50.14              108.97
129                  37.85              107.38
140.5     *          25.74              276.28
150                  0
----------------------------------------------------------------
Panel Height = 1 m             Average Mass = 141.35 kg/m
================================================================
                    Tower Height (m) = 152
                    ----------------------
Cell No.      Mast Weight (kN)   Mass per unit length (kg/m)
----------------------------------------------------------------
0                    87                 64.76
14                   81.58              69.78
28                   75.74              69.58
43                   69.5               69.81
58                   63.24              56.14
74                   57.87              114.41
89       *           47.61              60.67
100                  43.62              61.00
115                  38.15              53.30
130                  33.37              57.47
144                  28.56              44.94
159                  24.53              48.40
174                  20.19              47.99
190                  15.6               64.71
206      *           9.41               36.06
224                  5.53               40.52
242                  1.17               24.46
250                  0
----------------------------------------------------------------
Panel Height = 0.6096 m        Average Mass = 58.21 kg/m
================================================================
```

Table 5.2. (Continued)

```
================================================================
                    Tower Height (m) = 198
                    ----------------------
Cell No.        Mast Weight (kN)    Mass per unit length (kg/m)
----------------------------------------------------------------
0                   501.28                  248.62
9.5                 465.98                  297.07
19.5                421.58                  306.20
30.5                371.24                  302.79
41.5                321.46                  280.41
52.5                275.36                  269.27
63.5                231.09                  226.27
74.5                193.89                  295.06
85.5     *          145.38                  310.15
96.5                94.39                   228.34
107.5               56.85                   177.49
118.5               27.67                   168.30
129.5               0
----------------------------------------------------------------
Panel Height = 1.524 m              Average Mass = 258.99 kg/m
================================================================
                    Tower Height (m) = 200
                    ----------------------
Cell No.        Mast Weight (kN)    Mass per unit length (kg/m)
----------------------------------------------------------------
0                   244.84                  105.90
7                   237.57                  148.29
14                  227.39                  145.51
24                  213.12                  148.31
33                  200.03                  128.11
44                  186.21                  118.18
54                  174.62                  121.51
66                  160.32                  120.88
77                  147.28                  120.49
89                  133.1                   124.91
101                 118.4                   130.68
114                 101.74                  134.60
127                 84.58                   129.43
141                 66.81                   111.15
155                 51.55                   106.32
170                 35.91                   119.81
184                 19.46                   124.02
200                 0
----------------------------------------------------------------
Panel Height = 1 m                  Average Mass = 124.83 kg/m
================================================================
```

Table 5.2. (Continued)

```
===================================================================
                    Tower Height (m) = 213
                    ---------------------
Cell No.      Mast Weight (kN)   Mass per unit length (kg/m)
-------------------------------------------------------------------
0                  194.4               104.88
8                  181.86              131.52
15                 168.1               120.10
25                 150.15              108.73
35                 133.9               101.27
46                 117.25              108.73
56                 101                 76.81
66                 89.52               96.12
75                 76.59               90.86
85                 63.01               83.10
95                 50.59               75.20
105                39.35               83.10
115                26.93               69.99
125                16.47               83.03
135                4.06                54.33
140                0
-------------------------------------------------------------------
Panel Height = 1.524 m          Average Mass = 92.91 kg/m
===================================================================
                    Tower Height (m) = 313
                    ---------------------
Cell No.      Mast Weight (kN)   Mass per unit length (kg/m)
-------------------------------------------------------------------
0                  1004.13             323.09
17                 922.04              373.61
32                 838.28              359.24
54                 720.16              363.63
75                 606.03              360.50
100                471.33              362.33
117                379.27              265.08
139                292.11              329.19
160                188.79              298.66
184                81.66               251.65
201                17.72               237.12
206                0
-------------------------------------------------------------------
Panel Height = 1.524 m          Average Mass = 326.14 kg/m
===================================================================
```

Table 5.2. (Continued)

```
================================================================
                    Tower Height (m) = 342
                    ----------------------
Cell No.        Mast Weight (kN)   Mass per unit length (kg/m)
----------------------------------------------------------------
0                  740.13               270.18
15                 679.56               286.03
29                 619.71               272.67
46                 550.43               336.63
62      *          469.93               266.02
79                 402.34               239.53
95                 345.06               228.12
112                287.1                229.45
128                232.23               184.21
144                188.18               190.86
160                142.54               162.63
177                101.22               157.32
193                63.6                 133.02
209                31.79                132.94
225                0
----------------------------------------------------------------
Panel Height = 1.524 m             Average Mass = 220.09 kg/m
================================================================
                    Tower Height (m) = 607
                    ----------------------
Cell No.        Mast Weight (kN)   Mass per unit length (kg/m)
----------------------------------------------------------------
0                  3468.88              673.90
11                 3305.31              748.81
21                 3140.08              746.89
36                 2892.87              805.51
50                 2644.03              692.59
66                 2399.51              768.07
81                 2145.29              667.81
97                 1909.52              610.99
112                1707.29              555.90
128                1511.03              599.45
143                1312.62              597.64
158                1114.81              751.24
173                866.16               615.69
189                648.79               479.45
204                490.1                353.15
220                365.42               369.56
235                243.1                341.25
251                122.62               301.83
266                22.72                257.41
270                0
----------------------------------------------------------------
Panel Height = 2.25 m              Average Mass = 582.25 kg/m
================================================================
```
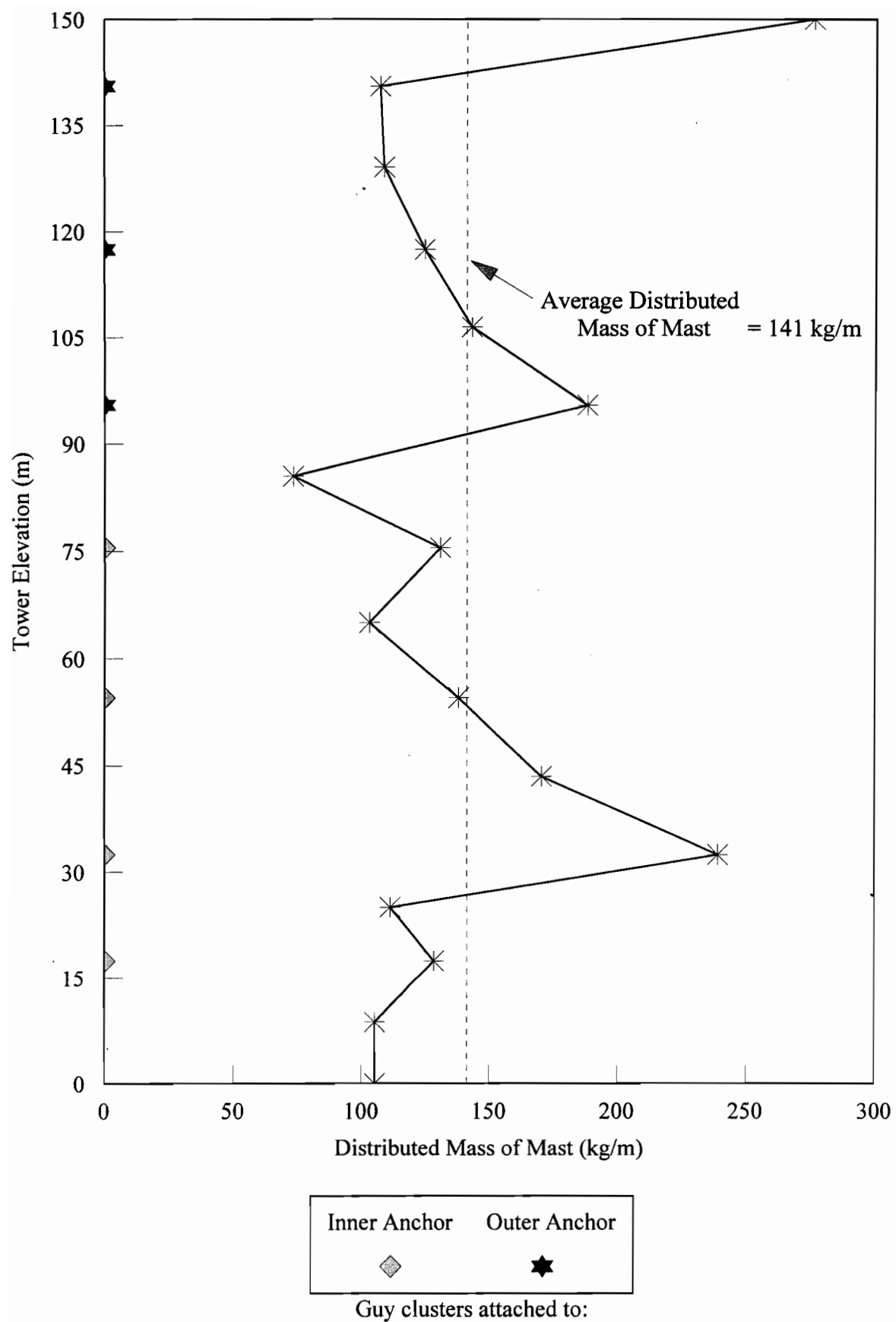
Fig. 5.2. Distributed mass of mast versus tower elevation in 150-m tower

128
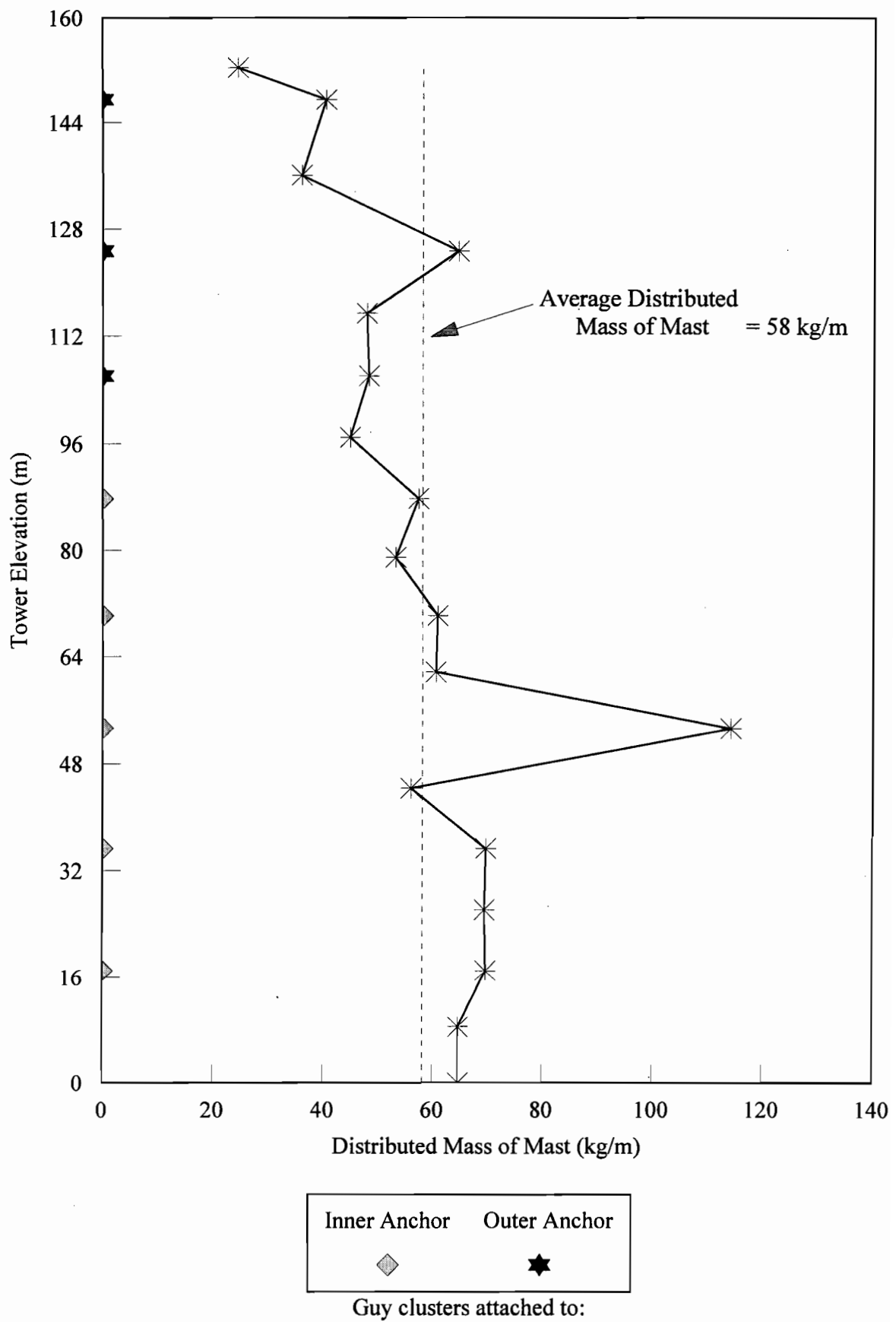
Fig. 5.3. Distributed mass of mast versus tower elevation in 152-m tower

129
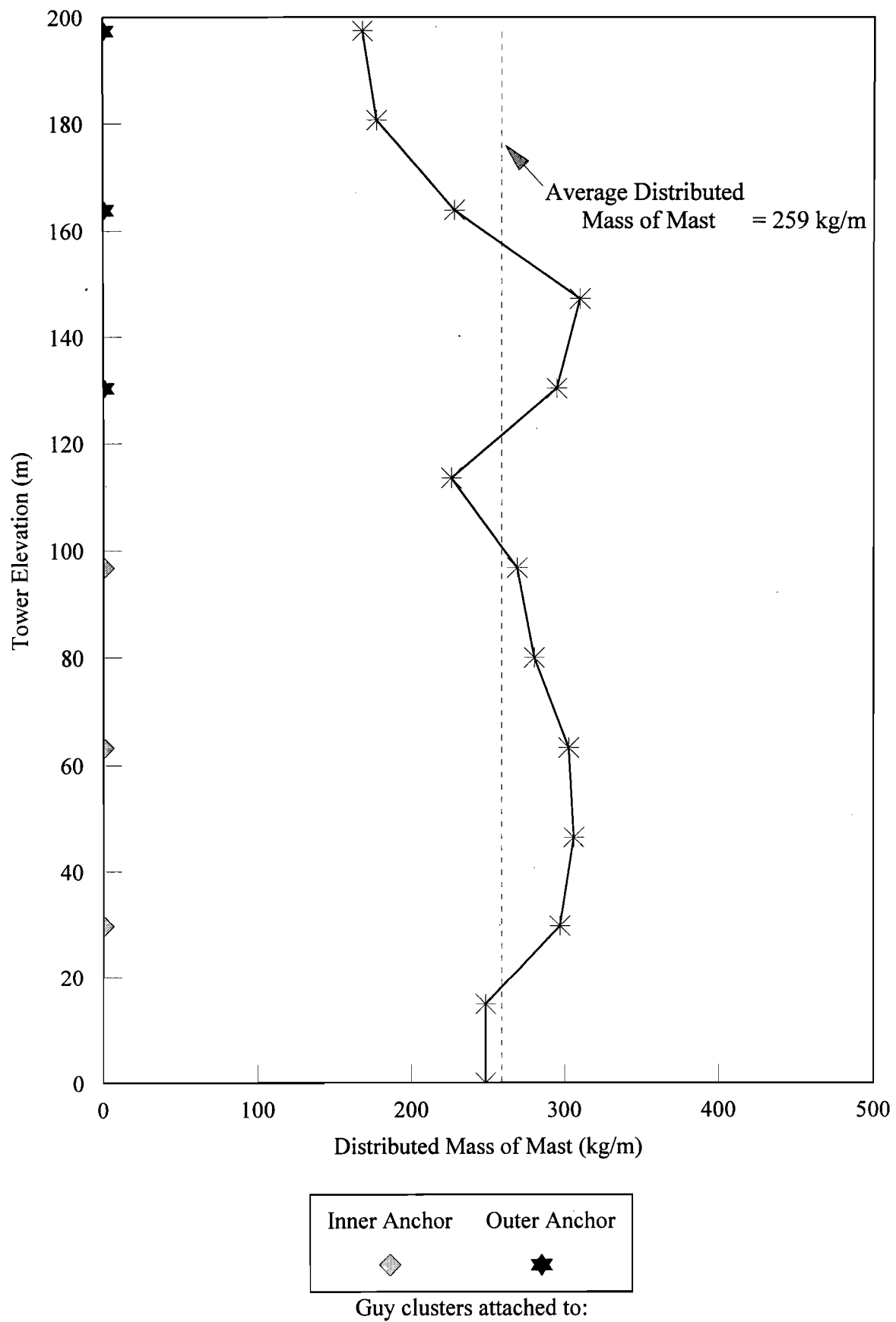
Fig. 5.4. Distributed mass of mast versus tower elevation in 198-m tower
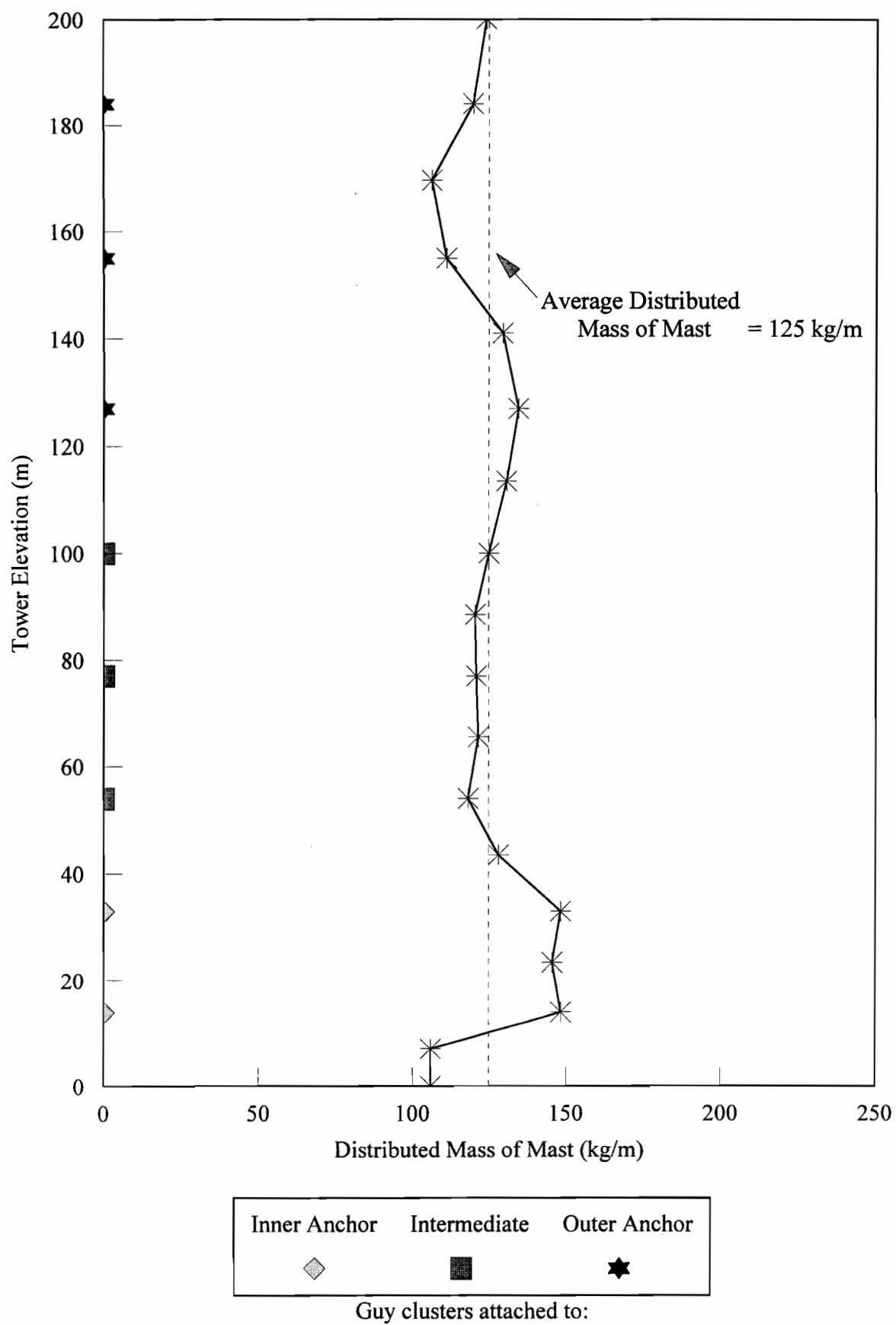
Fig. 5.5. Distributed mass of mast versus tower elevation in 200-m tower

131
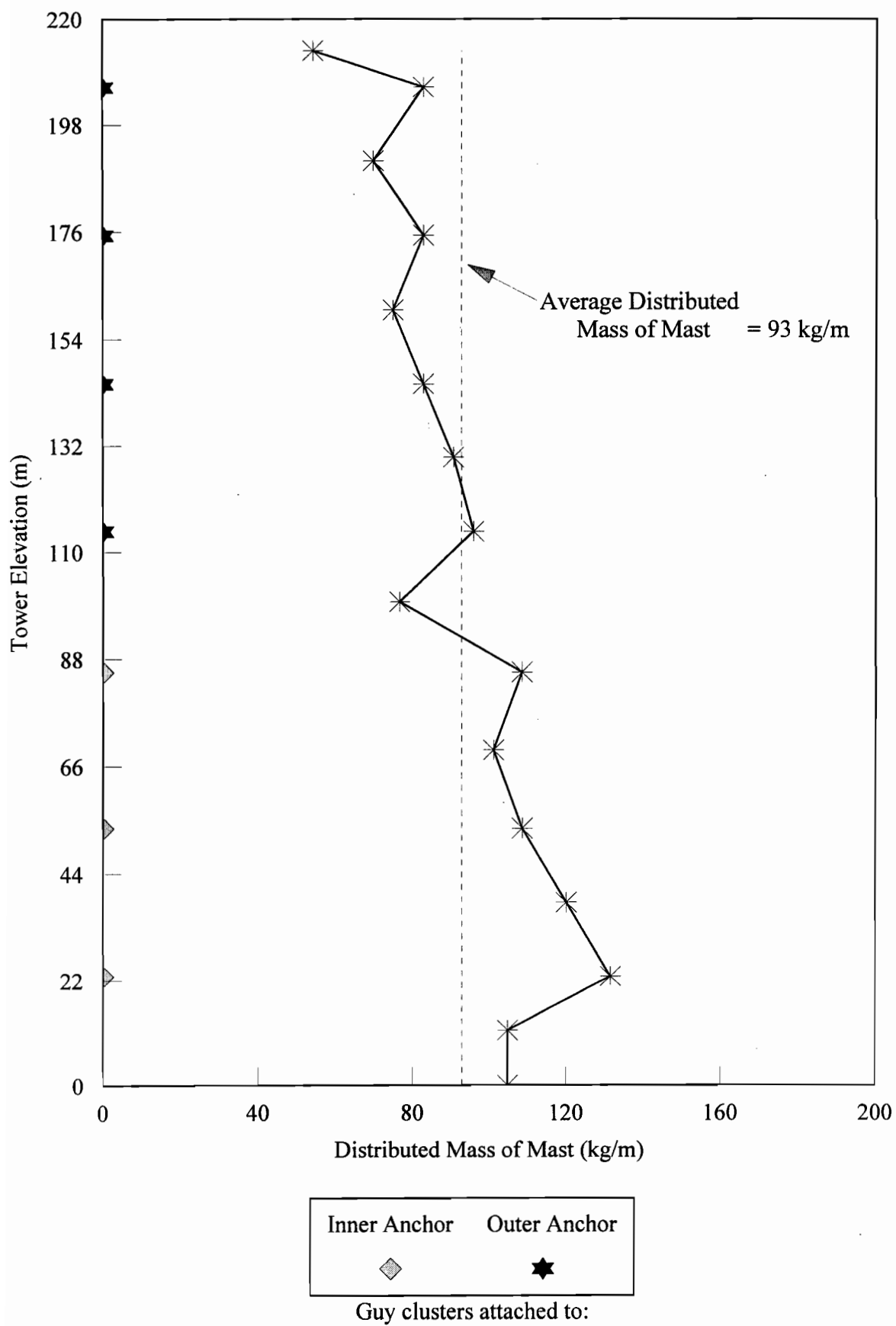
Fig. 5.6. Distributed mass of mast versus tower elevation in 213-m tower

132
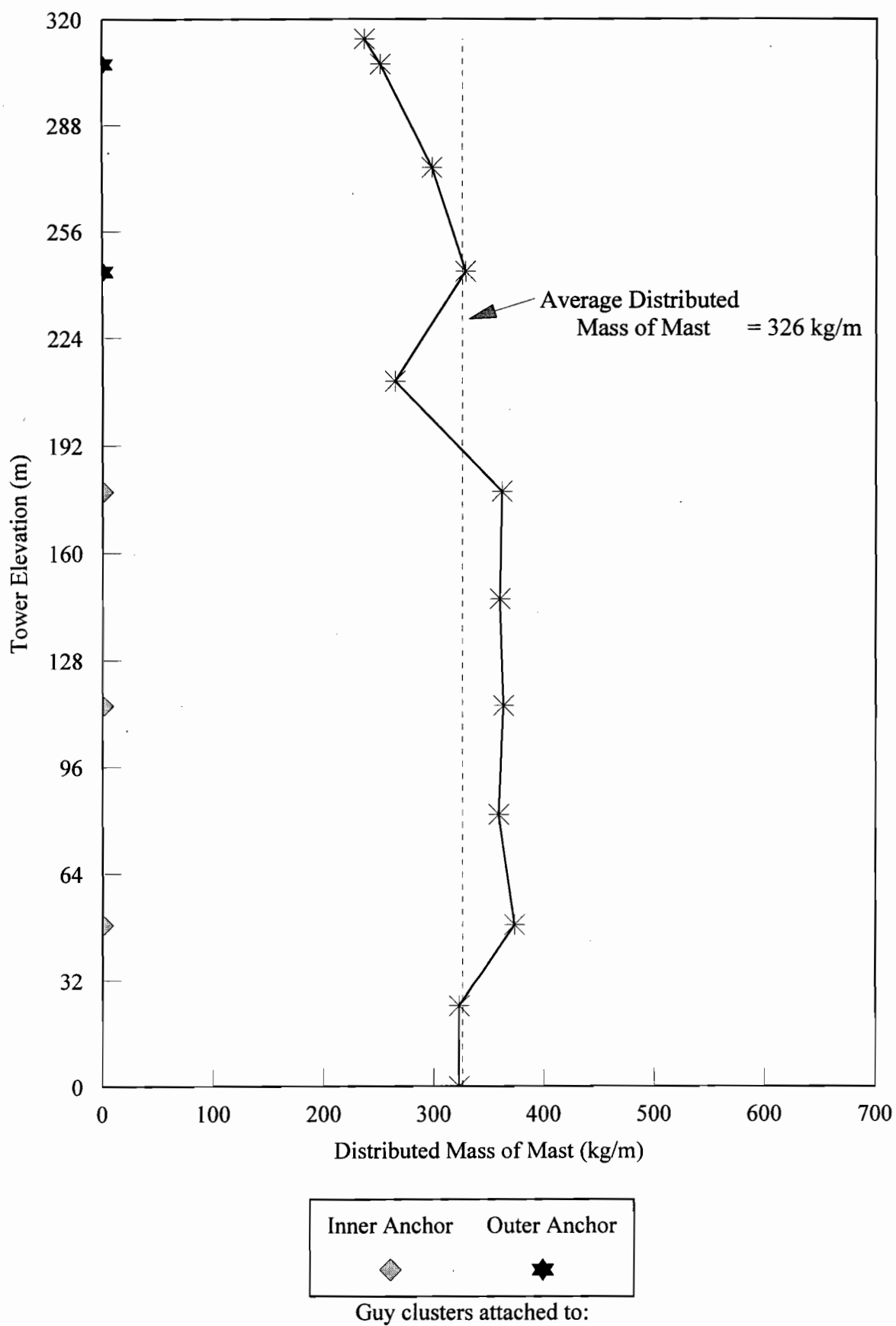
Fig. 5.7. Distributed mass of mast versus tower elevation in 313-m tower

133
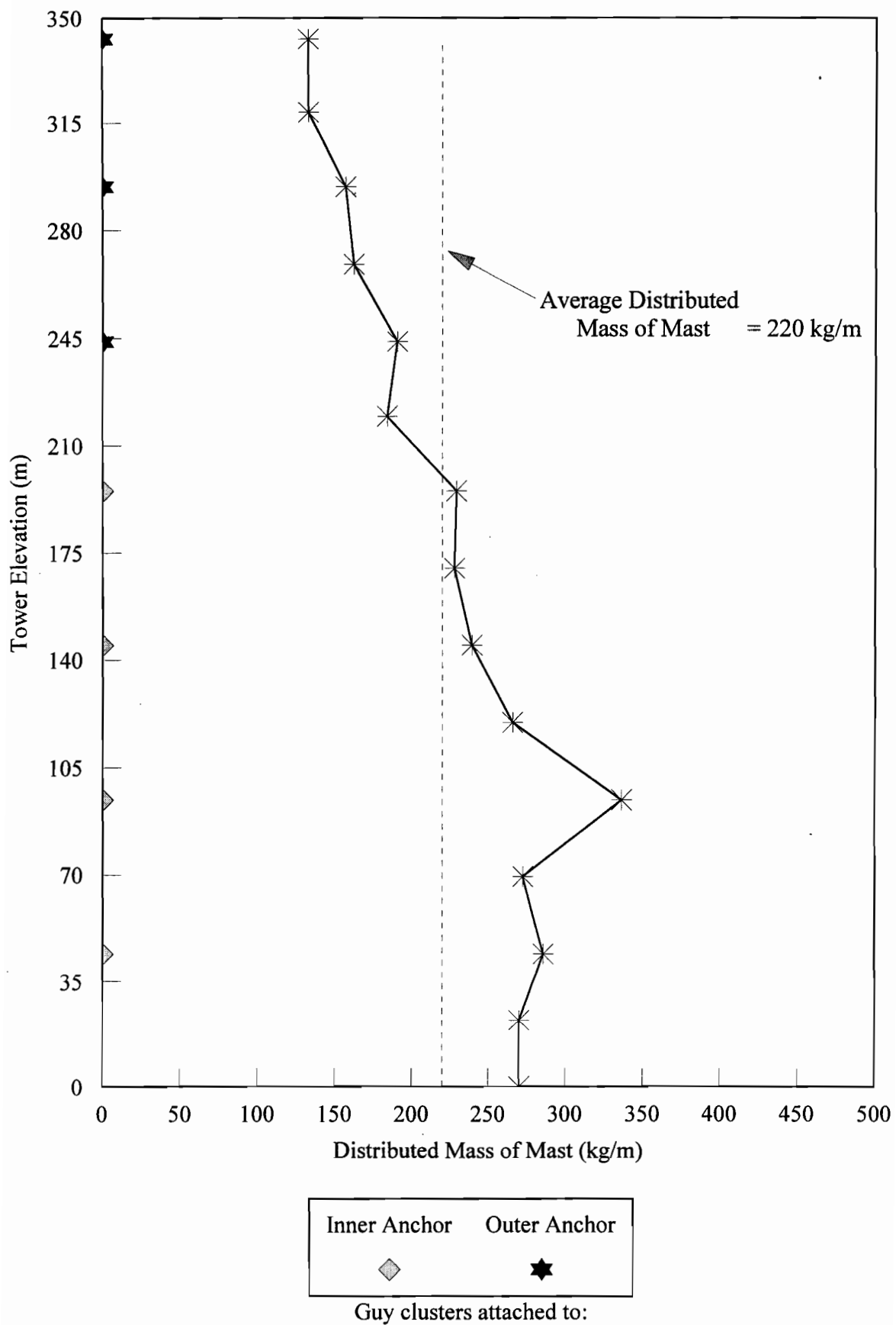
Fig. 5.8. Distributed mass of mast versus tower elevation in 342-m tower

134
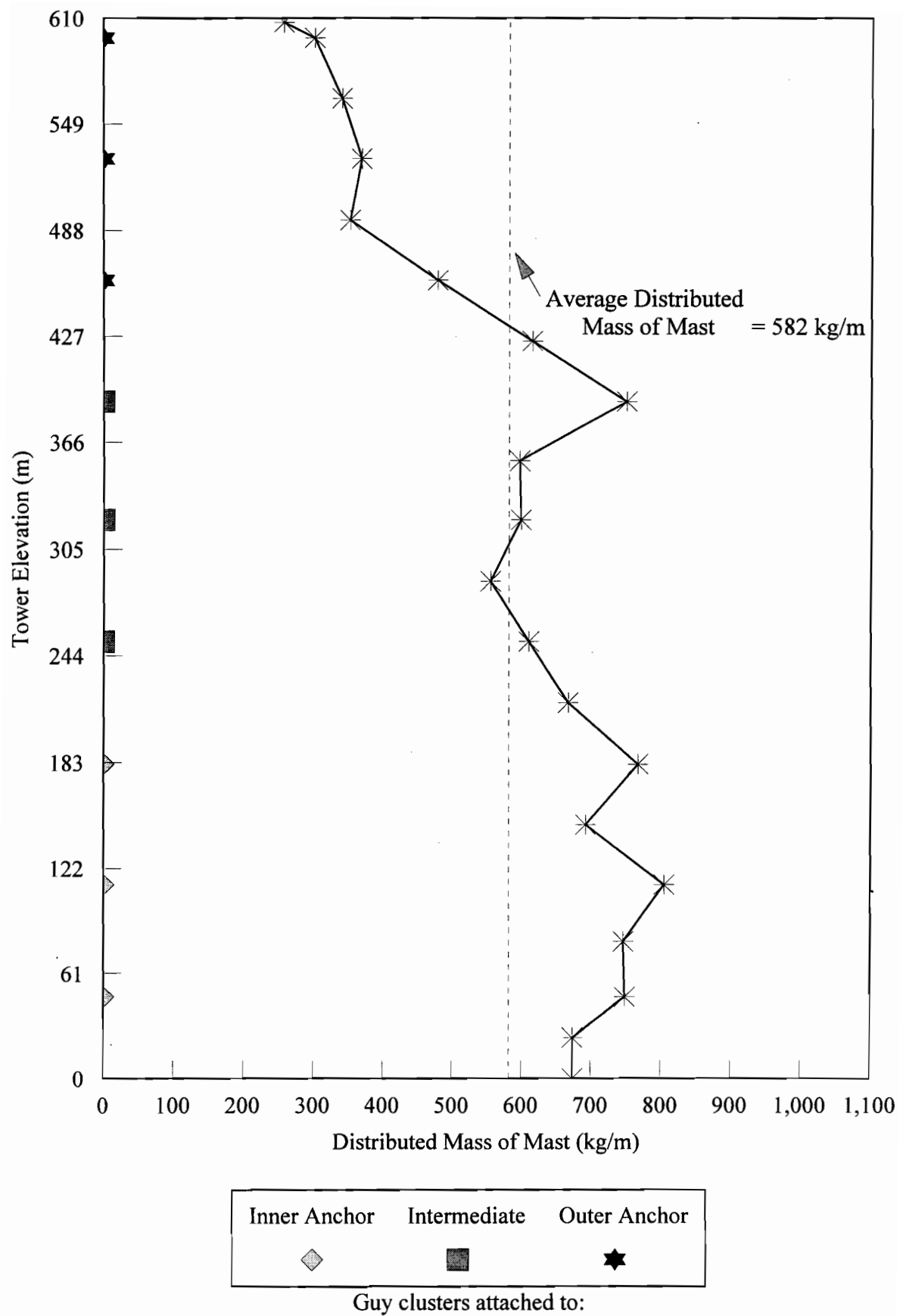
Fig. 5.9. Distributed mass of mast versus tower elevation in 607-m tower

135

5.1.3 Initial Sag of Guy Clusters due to Self Weight and Initial Prestress

The initial sag of guy clusters due to self weight and initial prestress is summarized in Table 5.3 and Figs. 5.10 to 5.15. There are two different parameters in the table and figures. The first one is the initial cable sag in m for each stay level. This is shown in Figs. 5.10 to 5.12. The second parameter represents the percentage of the initial sag of each cluster to the total cable length. This is illustrated in Figs. 5.13 to 5.15. These curves also represent the degree of geometric nonlinearity of the towers. For easier comparison of the results, the 607-m tower is taken out of Figs. 5.10 and 5.11. The 342-m and 313-m towers are taken out of Figs. 5.11 and 5.12, for the same reason, in order to focus the study on the 200-m height. The same is done for Figs. 5.13 to 5.15. As it can be seen in Figs. 5.11 and 5.14, the lower guy cables of the 342-m tower have larger initial sags than those of the other tower with comparable height (313-m tower). One important observation from these results is that the 200-m tower has a significant initial cable sag (with maximum difference about 2 to 2.5%) compared to the other towers of comparable height, especially for the longest guy cables (Figs. 5.12 and 5.15).

The initial tension of each guy cluster is listed in Table 5.4 for all eight towers. It is also expressed as a percentage of the cable ultimate tensile strength. For all cases the initial tension varies from 8% to 12% of ultimate strength. However, it is in the range of 3% to 6% for the 200-m tower. This is consistent with the previous observation that the 200-m tower has relatively slack cables.

5.1.4 Equivalent Lateral Stiffness of Guy Clusters

The lateral stiffness of each guy cluster is summarized in Table 5.5, and it is also illustrated separately for each tower in Figs 5.16 to 5.23. It should be noted that there are two different stiffness values in Table 5.5. The first one is k_0, the lateral stiffness of taut guy clusters (without sag), and it represents the stiffness of a straight rod. Since the cables are prestressed, all the cables in a cluster will contribute to the lateral stiffness, according to

136

Table 5.3. Initial sag (m) of guy clusters due to self weight and initial prestress

Tower Height (m)		Set No.								
		1	2	3	4	5	6	7	8	9
607	Anch	Inner			Intermediate			Outer		
	Sag	1.49	2.12	2.67	10.2	11.4	12.7	24.3	26.4	31.1
	%	1.01	1.18	1.16	2.58	2.57	2.56	3.74	3.77	4.13
342	Acnh	Inner				Outer				
	Sag	2.21	4.20	4.33	4.93	7.66	9.03	9.84		
	%	1.12	1.95	1.78	1.78	2.20	2.34	2.31		
313	Anch	Inner			Outer					
	Sag	1.21	1.79	2.25	7.51	8.61				
	%	0.90	1.06	1.03	2.32	2.31				
213	Anch	Inner			Outer					
	Sag	0.41	0.48	0.60	2.43	2.68	2.94	3.16		
	%	0.53	0.53	0.53	1.18	1.20	1.20	1.18		
200	Anch	Inner		Intermediate			Outer			
	Sag	0.25	0.37	2.08	2.74	3.06	5.47	5.70	8.19	
	%	0.59	0.71	1.83	2.17	2.15	2.88	2.72	3.53	
198	Anch	Inner			Outer					
	Sag	0.58	0.68	0.84	1.97	2.22	2.49			
	%	0.69	0.67	0.67	1.08	1.07	1.06			
152	Anch	Inner					Outer			
	Sag	0.85	0.90	0.92	1.01	1.12	1.76	1.89	2.11	
	%	0.94	0.95	0.89	0.90	0.90	1.13	1.12	1.13	
150	Anch	Inner				Outer				
	Sag	0.40	0.41	0.55	0.64	1.51	1.84	1.82		
	%	0.60	0.57	0.65	0.65	0.99	1.10	0.99		

Anch = Guy clusters attached to Inner, Intermediate or Outer anchor
Sag = Initial sag of guy clusters due to self weight and initial prestress (m)
% = (initial sag/cable length)100
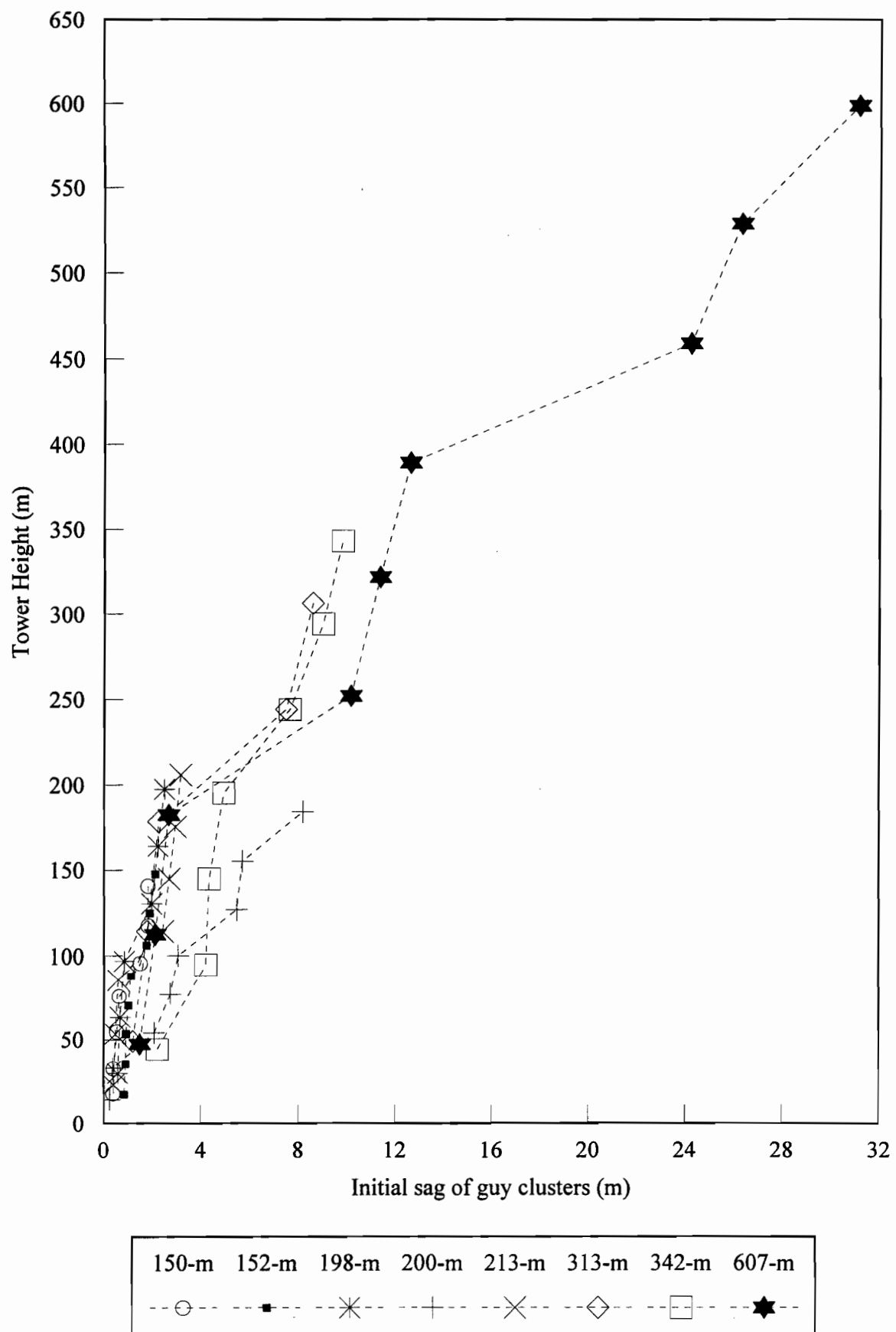
Fig. 5.10. Initial sag of guy clusters due to self weight and initial prestress versus tower elevation
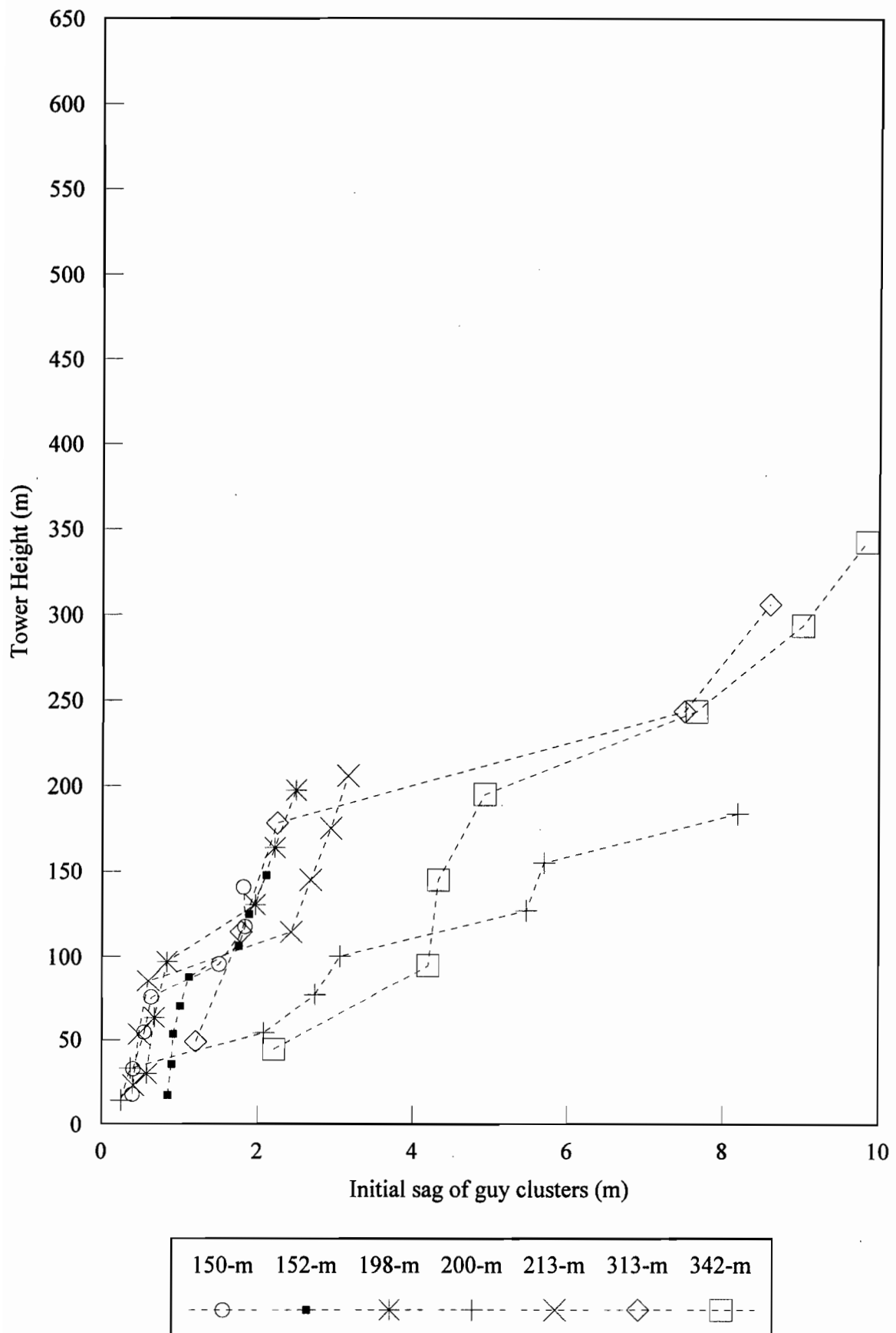
Fig. 5.11. Initial sag of guy clusters due to self weight and initial prestress versus tower elevation
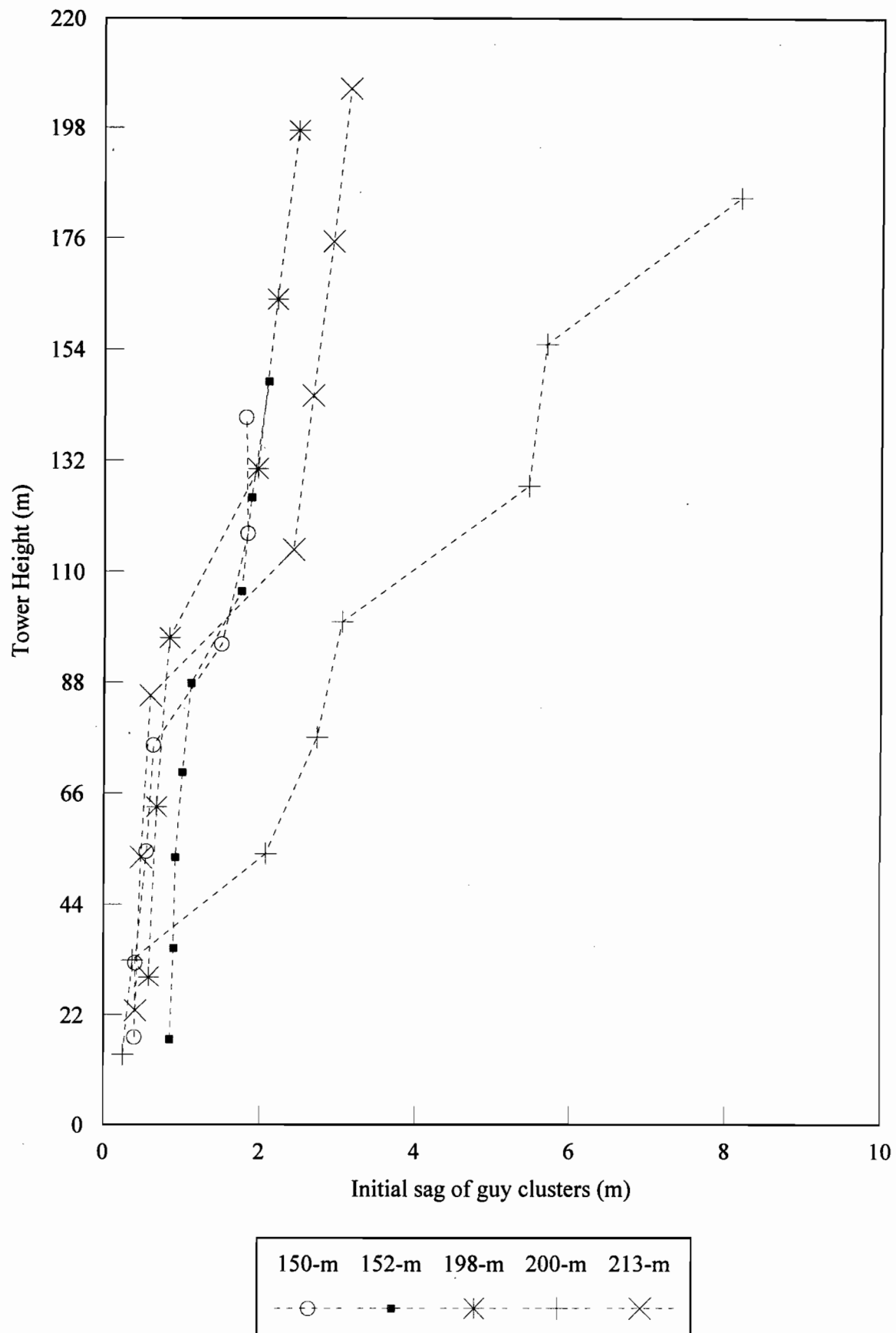
Fig. 5.12. Initial sag of guy clusters due to self weight and initial prestress versus tower elevation

140
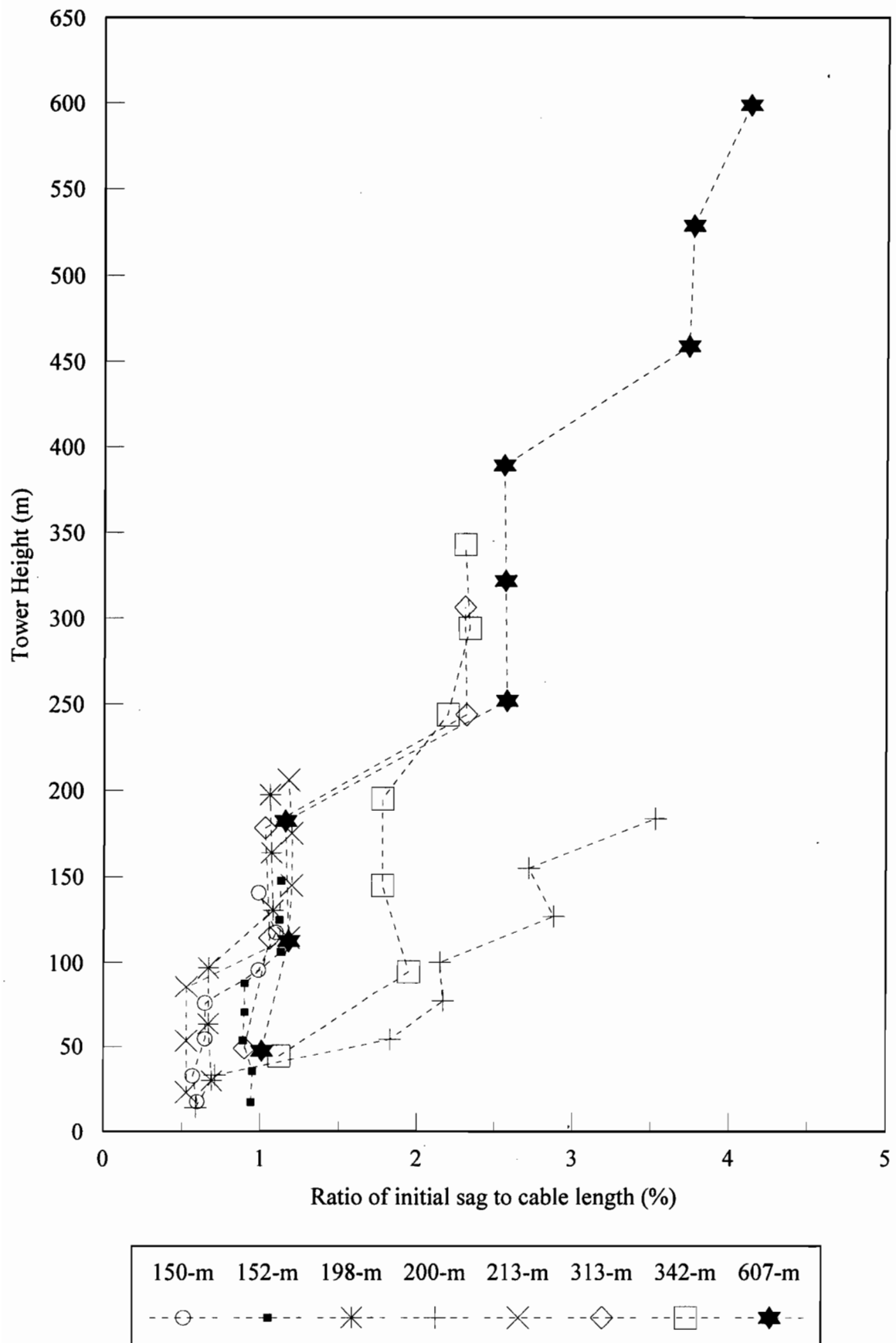
Fig. 5.13. Ratio of initial sag of guy cluster to cable length versus tower elevation

141
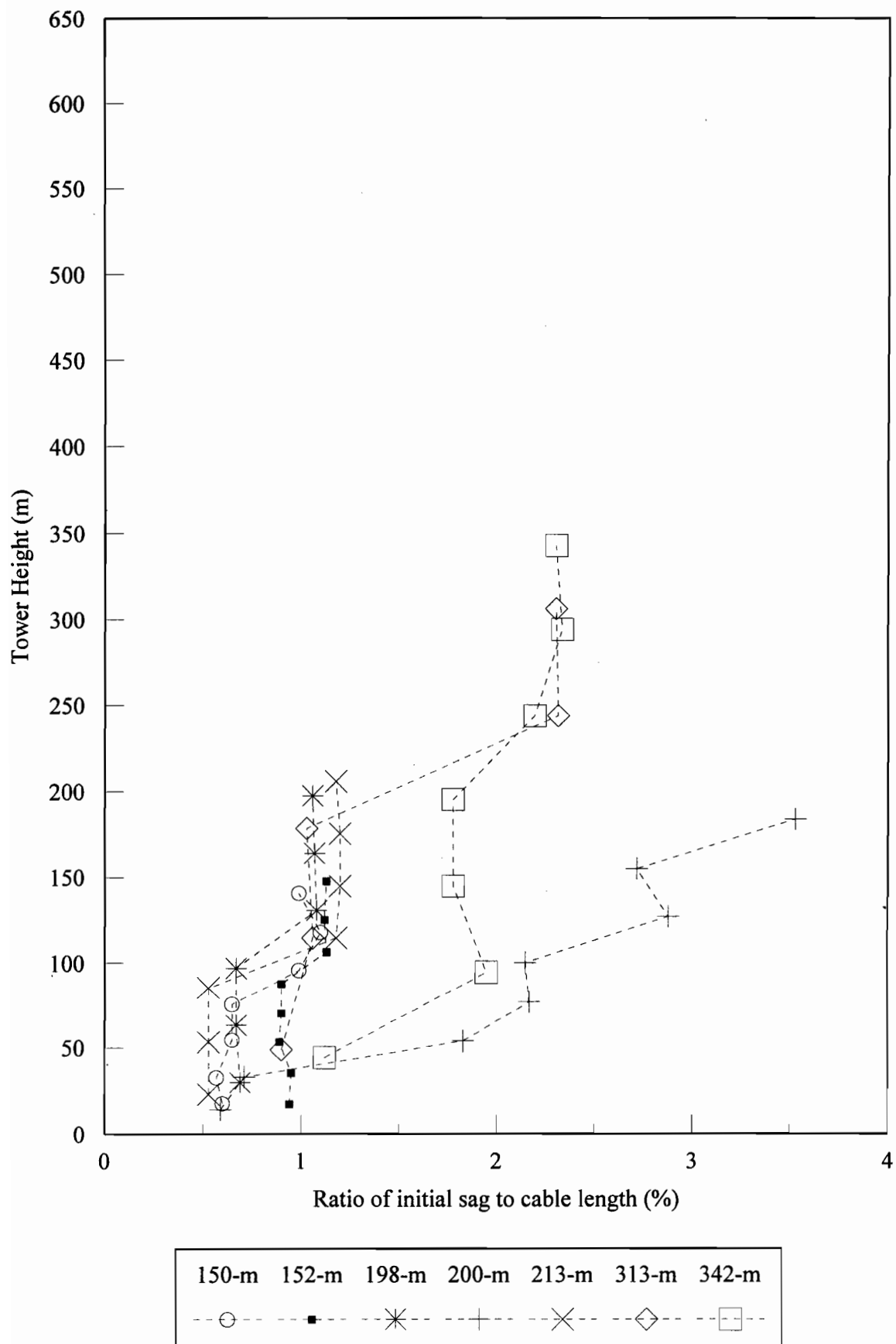
Fig. 5.14. Ratio of initial sag of guy cluster to cable length versus tower elevation

142
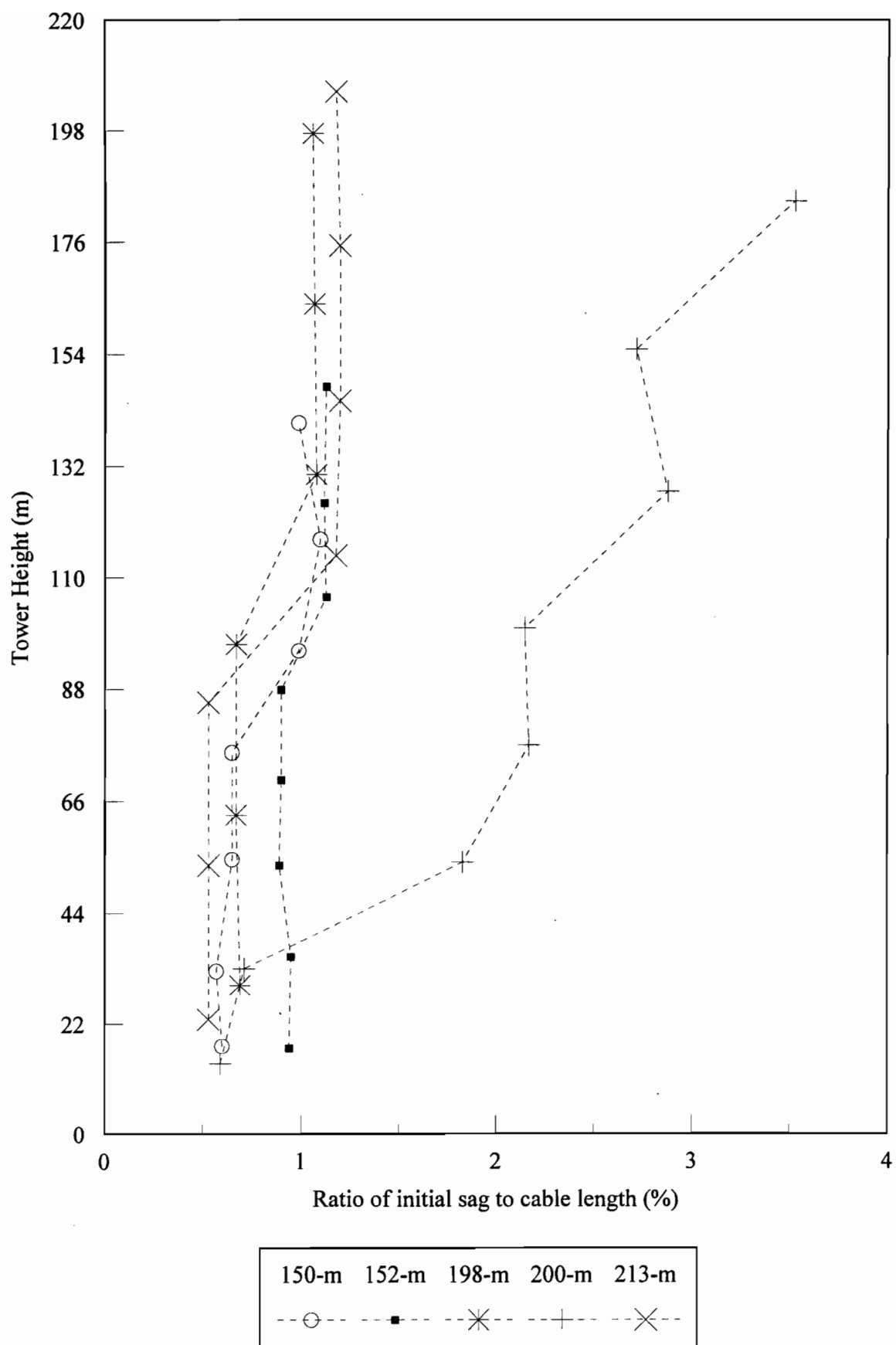
Fig. 5.15. Ratio of initial sag of guy cluster to cable length versus tower elevation

143

Table 5.4. Initial tension of guy clusters

Tower Height (m)		Set No.								
		1	2	3	4	5	6	7	8	9
607	Anch	Inner			Intermediate			Outer		
	I.T.	130	108	108	108	108	108	108	108	97
	%	12	10	10	10	10	10	10	10	9.0
342	Anch	Inner				Outer				
	I.T.	159	91	100	100	103	97	97		
	%	15	8.4	9.3	9.3	9.5	9.0	9.0		
313	Anch	Inner			Outer					
	I.T.	129	108	108	85	86				
	%	12	10	10	7.9	7.9				
213	Anch	Inner			Outer					
	I.T.	129	129	129	129	127	127	129		
	%	12	12	12	12	12	12	12		
200	Anch	Inner		Intermediate			Outer			
	I.T.	62	51	51	43	43	44	47	35	
	%	5.7	4.7	4.7	4.0	4.0	4.1	4.4	3.2	
198	Anch	Inner			Outer					
	I.T.	105	107	107	107	108	108			
	%	9.7	9.9	9.9	9.9	10	10			
152	Anch	Inner					Outer			
	I.T.	87	87	92	92	91	91	91	90	
	%	8.1	8.1	8.5	8.5	8.4	8.4	8.4	8.3	
150	Anch	Inner				Outer				
	I.T.	108	105	106	105	108	108	108		
	%	10	9.7	9.8	9.7	10	10	10		

Anch = Guy clusters attached to Inner, Intermediate or Outer anchor
I.T. = Initial tension of guy clusters (MPa)
% = (Initial Tension/Ultimate Tensile Strength)100
Ultimate Tensile Strength = 1080 MPa

144

$$k_0 = 2AE*Cos^2\alpha/L \tag{5.1}$$

k_0 = lateral stiffness of guy cluster without sag

A = cross sectional area of cable

E = modulus of elasticity

α = angle of cable to horizon

L = length of cable

Equation (5.1) is derived for towers with three or four cables symmetrically arranged in each guy cluster.

The second parameter in Table 5.5 is k, the lateral stiffness of guy clusters accounting for the sag. A comparison of these two parameters indicates the importance of geometric nonlinearity. Since the variation of the effective lateral stiffness of a guy cluster (k) is nonlinear with the amplitude of the horizontal displacement of the anchor point on the tower, the lateral stiffness was evaluated for a range of lateral displacements of the mast from 10% to 100% the maximum displacement observed in seismic analyses. Since there is no significant variation in the measurements (in general, variations are in the range of 10 to 15%), their average value is taken to represent the lateral stiffness of each guy cluster. The percentage values in Table 5.5 represent the ratio of k to k_0.

In the 150-m (Fig. 5.16), 152-m (Fig. 5.17), 198-m (Fig. 5.18), 213-m (Fig. 5.20) and 342-m (Fig. 5.22) towers, it is observed that the equivalent lateral stiffness of the guy clusters generally decreases with the elevation. However, since the guy clusters are designed to control the serviceability of the mast, more stiffness is provided close to the antenna attachment levels than at the intermediate levels. This is not the case for the 200-m and 313-m towers. Also in the 607-m tower, the stiffness of the guy clusters decreases with the elevation for the cables connected to the inner ground anchor point, but it is more or less constant for the two other clusters. In all the towers, the stiffness of the bottom guy clusters is relatively large such that they mimic a fixed support.

Table 5.5. Lateral stiffness of guy clusters (kN/m)

Tower Height (m)		Set No.								
		1	2	3	4	5	6	7	8	9
607	k_0	1886	2006	1166	610	590	664	338	558	290
	k	1054	855	509	79	81	98	23	40	17
	%	56	43	44	13	14	15	7	7	6
	Anch.	Inner			Intermediate			Outer		
342	k_0	482	620	350	348	320	290	218		
	k	386	115 *	72	86	56	44	36		
	%	80	19	21	25	18	15	17		
	Anch.	Inner			Outer					
313	k_0	1026	906	470	810	356				
	k	639	410	216	125	54				
	%	62	45	46	15	15				
	Anch.	Inner			Outer					
213	k_0	810	492	312	278	256	266	266		
	k	517	330	209	126	114	84	117		
	%	64	67	67	45	45	32	44		
	Anch.	Inner			Outer					
200	k_0	804	602	374	348	244	304	226	288	
	k	441	302	49	31	24	17	16	10	
	%	55	50	13	9	10	6	7	3	
	Anch.	Inner		Intermediate			Outer			
198	k_0	1438	1226	650	1096	514	510			
	k	821	747	400	499 *	239	219			
	%	57	61	62	46	46	43			
	Anch.	Inner			Outer					
152	k_0	272	230	490	188	182	156	244	142	
	k	188	117	230 *	94	92	64	97 *	54	
	%	69	51	47	50	51	41	40	38	
	Anch.	Inner				Outer				
150	k_0	988	1264	700	584	560	478	1030		
	k	907	887 *	480	399	284 *	238	406 *		
	%	92	70	69	68	51	50	39		
	Anch.	Inner			Outer					

k_0 = lateral stiffness of guy cluster without sag = $2AE*Cos^2\alpha/L$

k = lateral stiffness of guy cluster

% = $(k/k_0)100$

Anch. = guy clusters attached to Inner, Intermediate or Outer anchor points on the ground

* Outrigger location

146
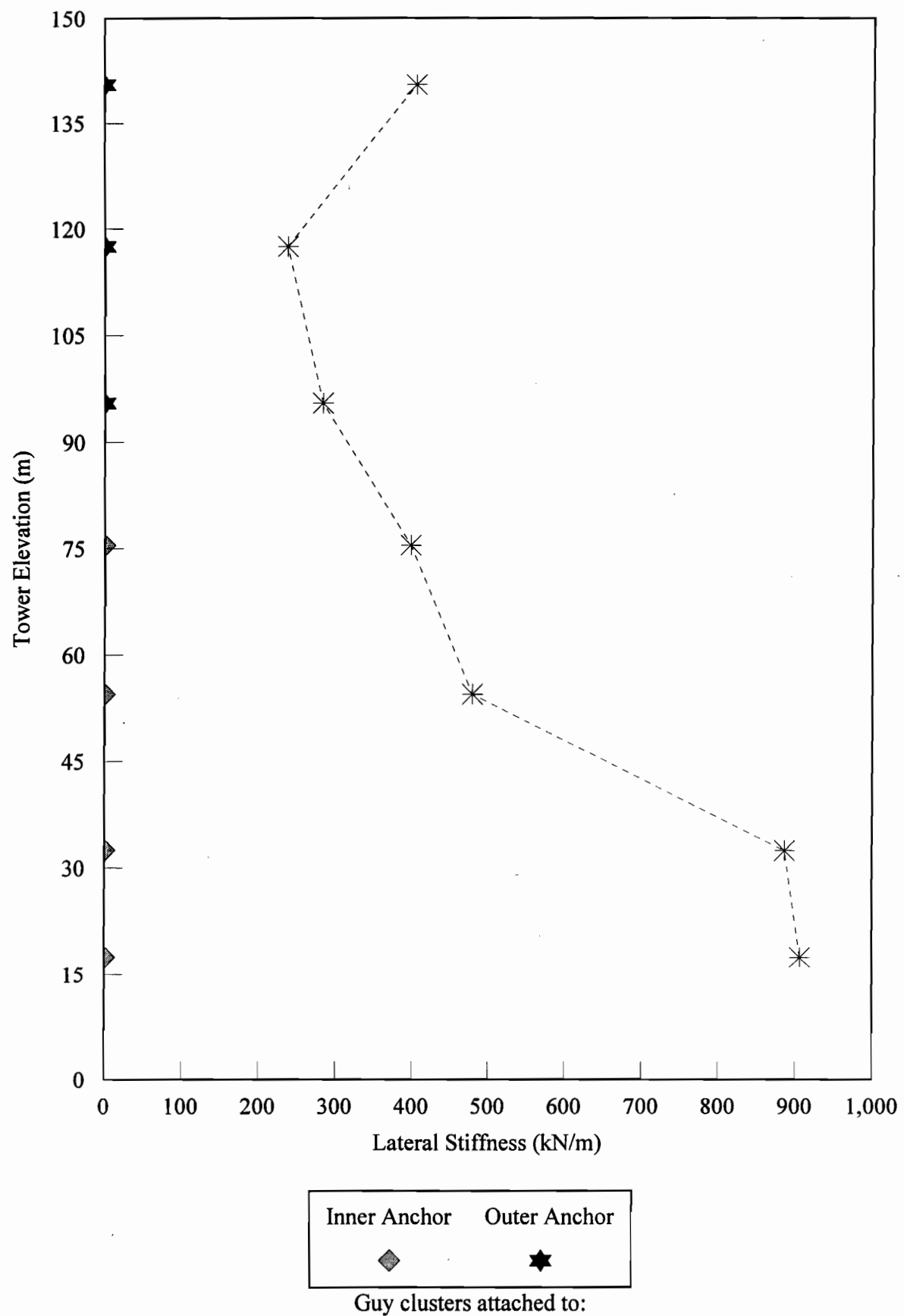
Fig. 5.16. Lateral stiffness of guy clusters versus tower elevation in 150-m tower

147
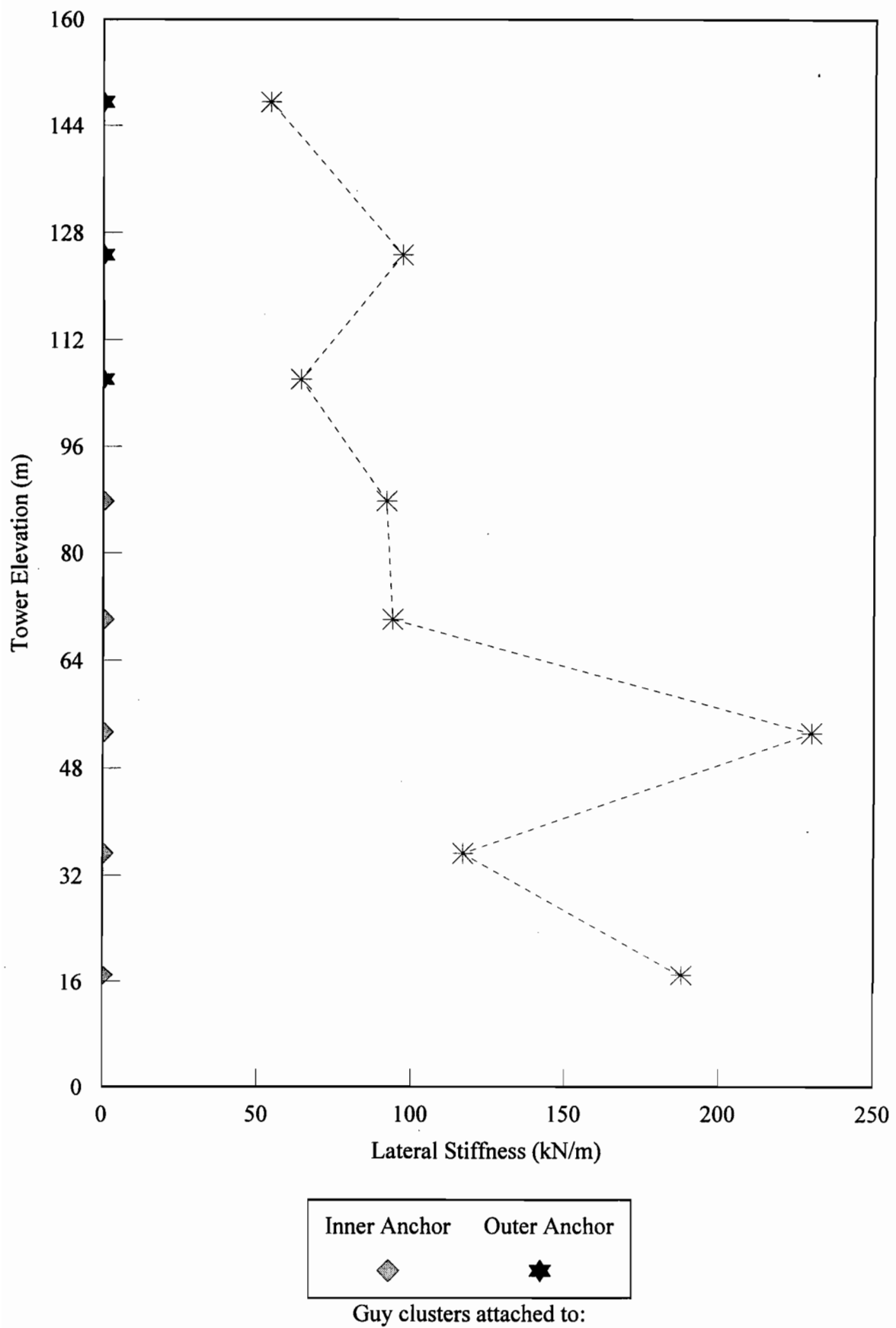
Fig. 5.17. Lateral stiffness of guy clusters versus tower elevation in 152-m tower

148
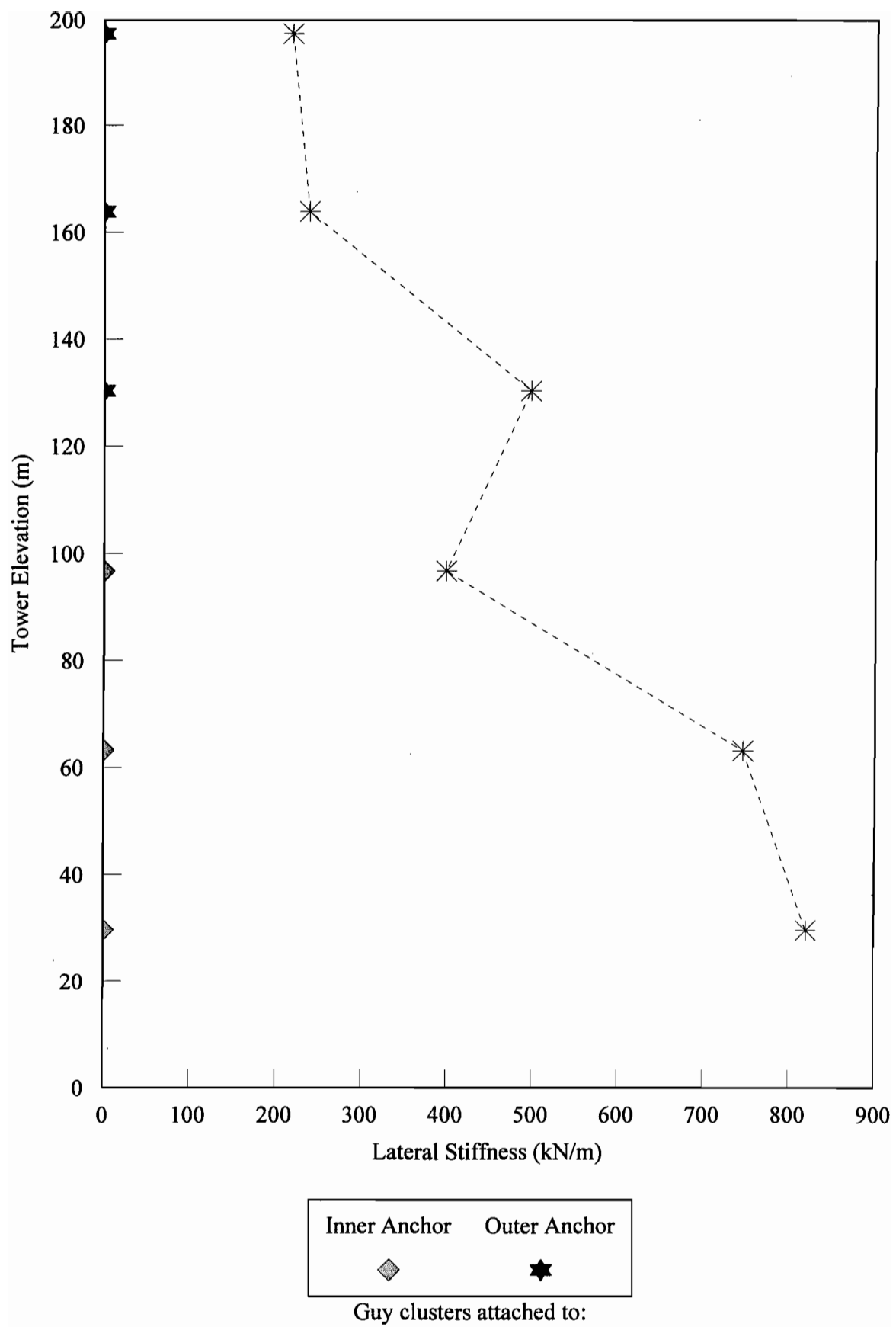
Fig. 5.18. Lateral stiffness of guy clusters versus tower elevation in 198-m tower

149
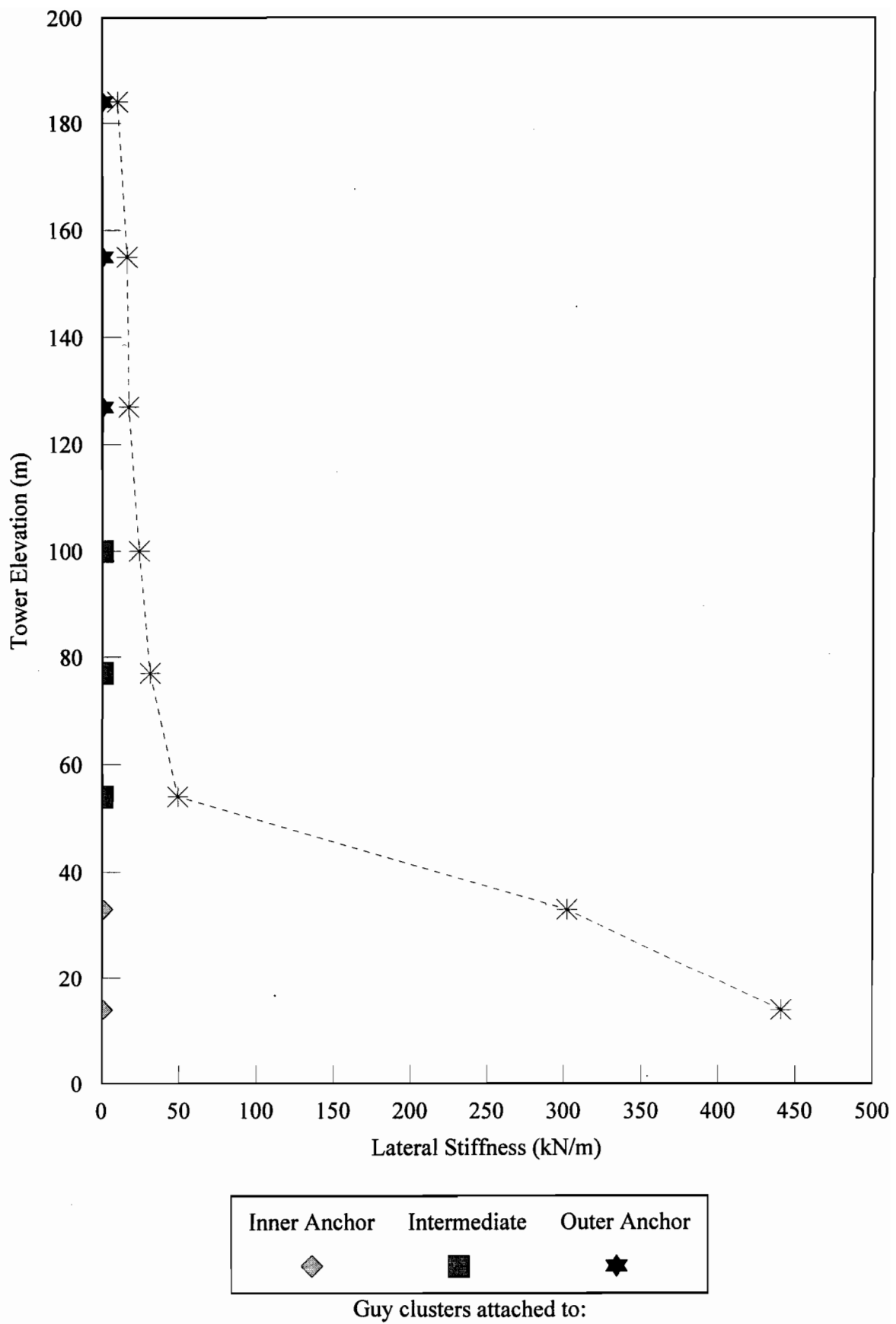
Fig. 5.19. Lateral stiffness of guy clusters versus tower elevation in 200-m tower

150
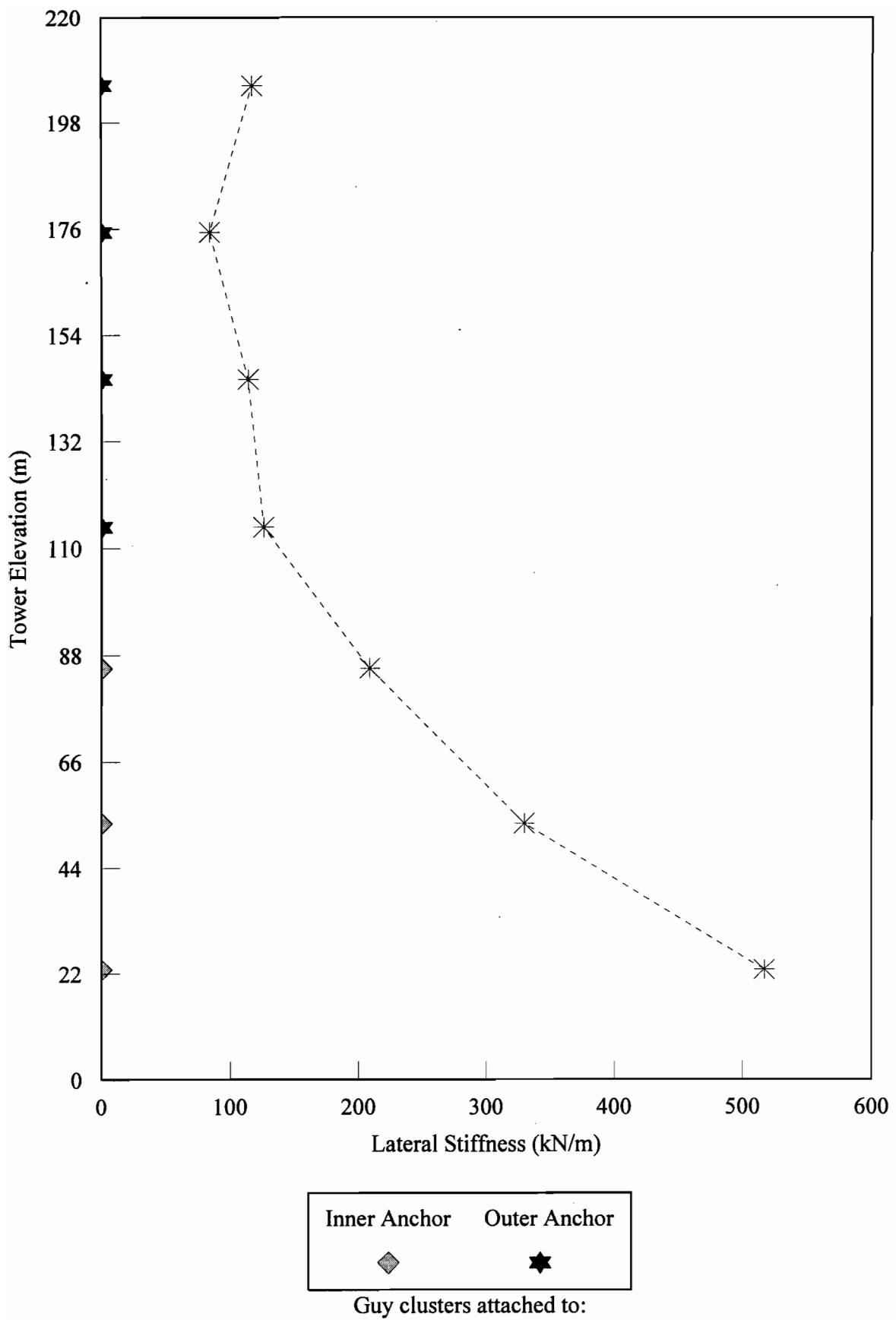
Fig. 5.20. Lateral stiffness of guy clusters versus tower elevation in 213-m tower

151
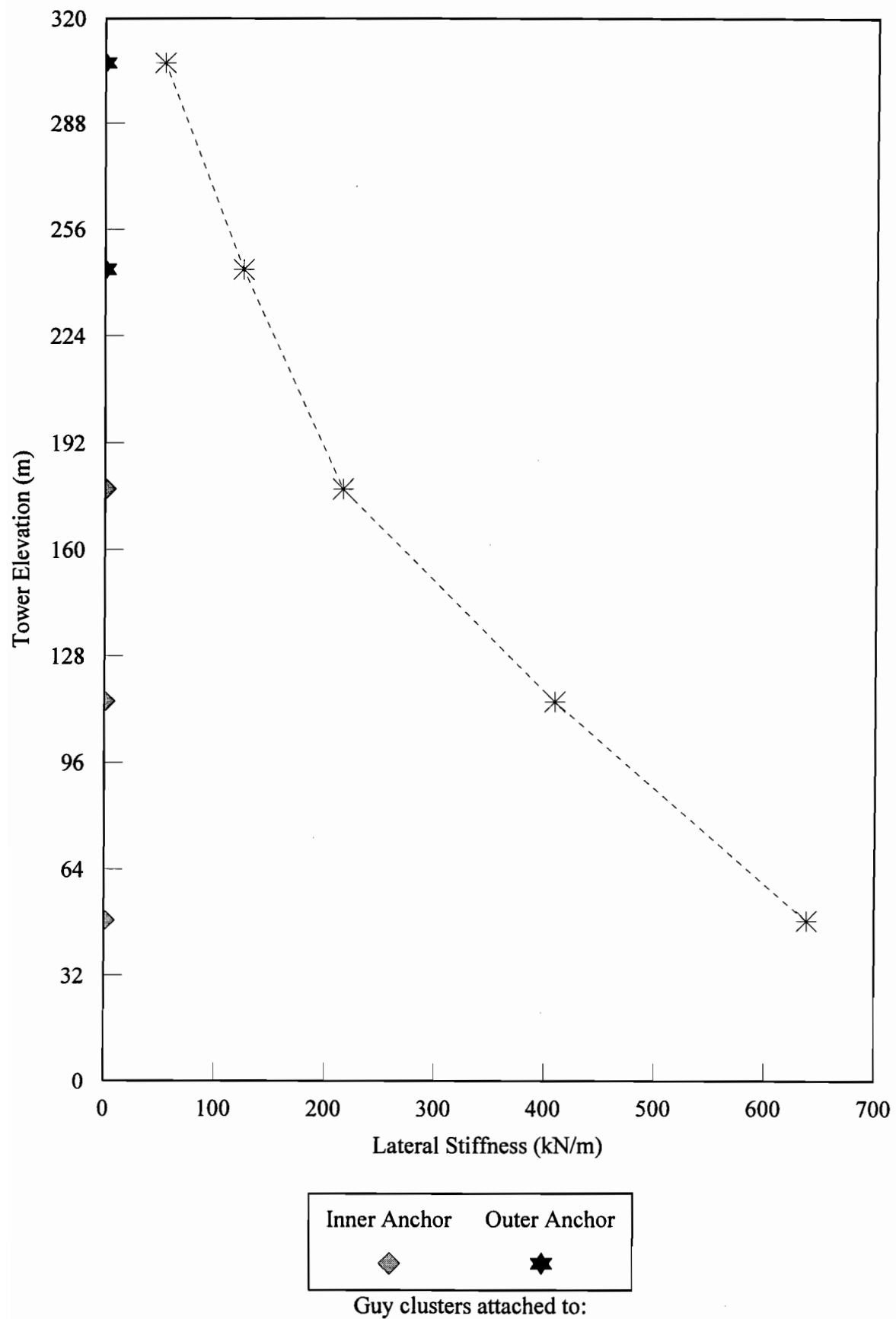
Fig. 5.21. Lateral stiffness of guy clusters versus tower elevation in 313-m tower

152
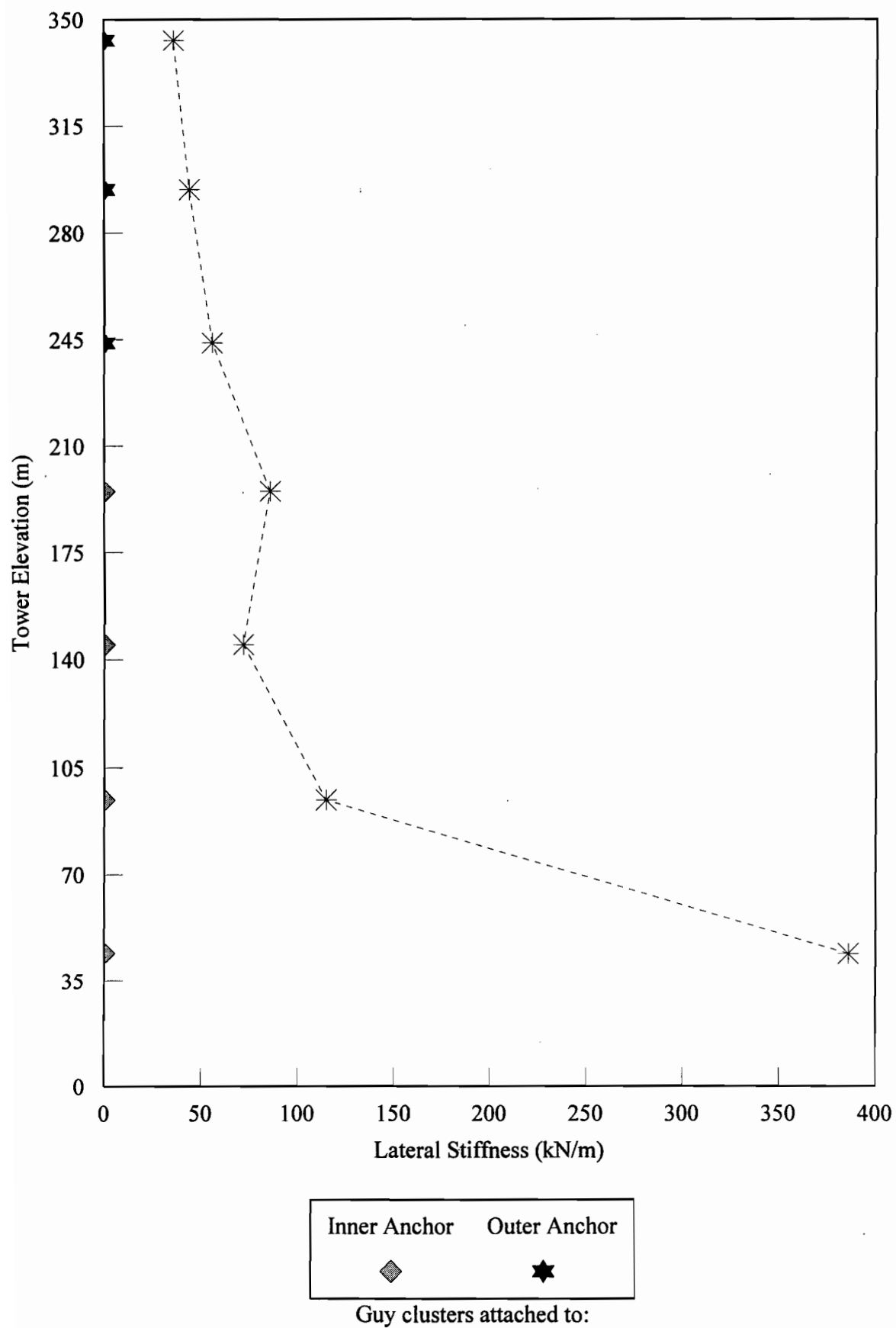
Fig. 5.22. Lateral stiffness of guy clusters versus tower elevation in 342-m tower

153
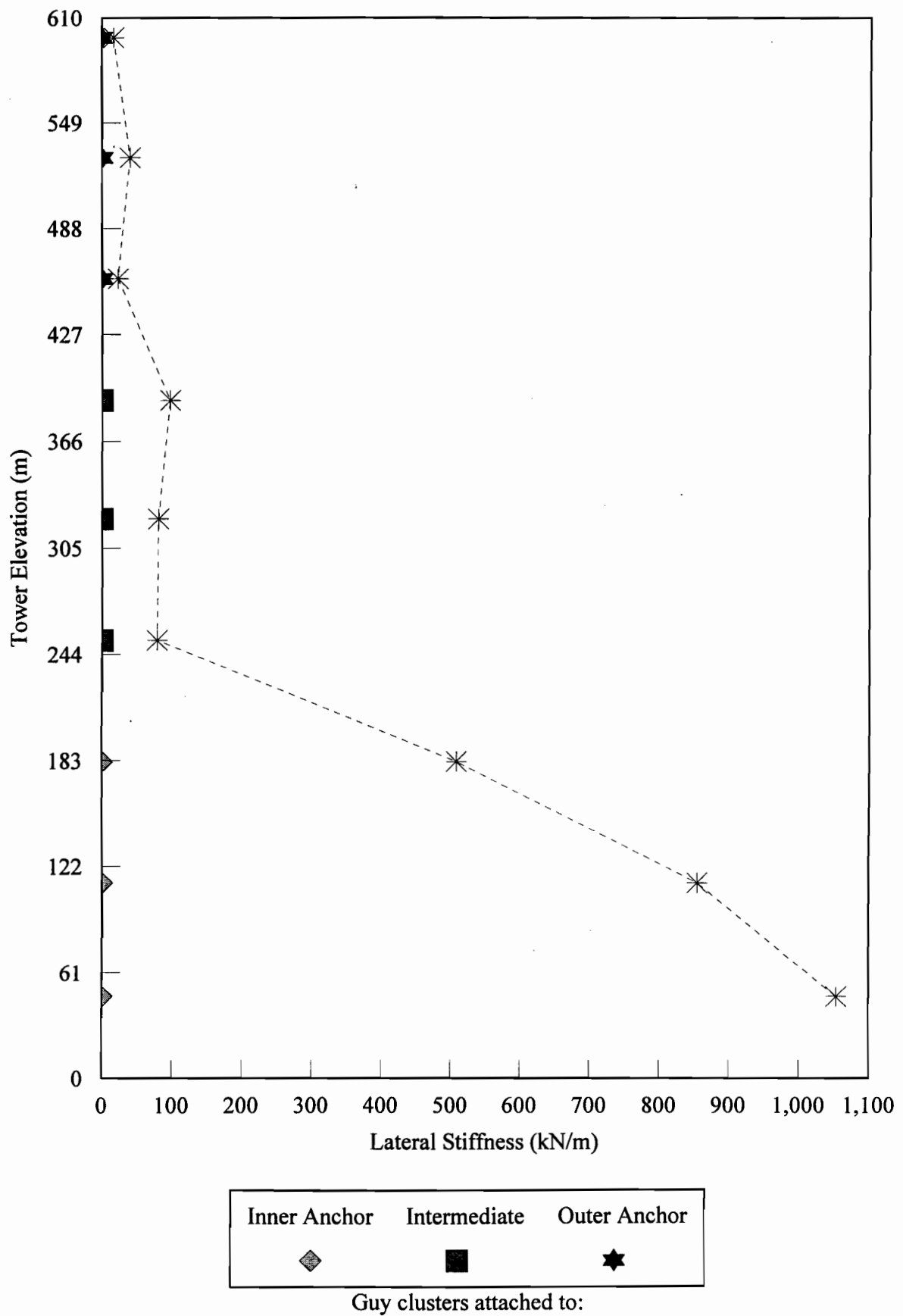
Fig. 5.23. Lateral stiffness of guy clusters versus tower elevation in 607-m tower

154

5.1.5 Sensitive Region

As it was pointed out in Section 4.4, there is a common feature in all eight towers studied. Six of the towers (all except the 200-m and 607-m towers) comprise two groups of cable sets corresponding to the two groups of anchorage points on the ground. For example, for the 213-m tower in Fig. 3.5, cable sets 1, 2, and 3 are connected to the inner anchor points close to the base of the mast, and Sets 4, 5, 6, and 7 are connected to the outer anchor points. This results in a nonuniformity in the trend of the tower lateral stiffness in the transition portion (e.g. between Sets 3 and 4 in the 213-m tower). This nonuniformity tends to force the mast to behave as two independent sections, above and below that transition zone. In terms of the transverse shear, this area becomes a sensitive portion of the tower. For the 200-m and 607-m towers, there are three groups of cables (inner, intermediate and outer anchor points), and as a result one can identify two sensitive regions along the tower. It can also be seen in Table 5.5 that there is a clear discontinuity in the lateral stiffness of each group of guy clusters.

5.1.6 Anticipated Predominant Mode Shape of Mast

The frequency analysis of the towers was discussed in Section 4.1. One important observation obtained was the shape of the lowest flexural mode. It has been found that for most of the towers (150-m, 152-m, 198-m, 213-m and 342-m towers), one of the guy clusters close to the top region is stiffer than the other intermediate ones, as discussed in Section 5.1.4. As a result, the top part of the towers behaves more or less like a pinned support, as it is shown in the mode shapes of Figs. 5.24 to 5.28. Therefore, the lowest flexural mode of the mast is similar to the second lowest mode of a cantilever structure. Clearly, the location of the ground anchorage point cannot alone explain the observed behaviour as the relative lateral stiffness of guy clusters also plays a major role. However, this is not true for the 200-m, 313-m and 607-m towers which have more flexible upper guy clusters. As a result, the first flexural mode of these towers is similar to the lowest mode of a cantilever structure, and the second flexural mode is then similar to the first

155

flexural mode of the other towers. The lowest two mode shapes of these three towers are shown in Figs. 5.29 to 5.34.

5.2 FUNDAMENTAL PARAMETERS OF SEISMIC RESPONSE

5.2.1 Base Shear

Tables 5.6 and 5.7 list the maximum base shears calculated for the eight towers subjected to the three earthquake accelerograms studied. The base shears were obtained by the summation of all horizontal reactions at the ground supports of cables and mast. In both tables, the detailed weights of cables and mast are indicated separately. Table 5.6 presents separately the contributions of the mast and the cables to the base shear. These contributions are also expressed as a percentage of the total weight of the towers. Table 5.7 is similar to Table 5.6, except that the contributions of the mast and the cables are calculated as a percentage of the total base shear instead of the total weight of the tower. All these numerical results are graphed in Figs. 5.35 to 5.38. The total base shears vary in the range of 40% to 80% of the total weights for towers shorter than 213 meters, and in the range of 15% to 30% of the total weights for towers taller than 313 meters. According to Fig. 5.37 the contribution of the mass of the cables to the total base shear is almost constant in the range of 3% to 5% of the total weight of tower. It is interesting to note that although 25% to 30% of the total mass is contributed by the cables in the case of towers shorter than 213 meters, only 5% to 10% of the total base shear is contributed by the cables. For the towers taller than 313 meters the relative contribution of the cables compared to that of the mast increases with height, especially for the El Centro input accelerogram. As it is shown in Fig. 5.38, the 607-m tower has a different response compared to that of the other towers, in which its cables are more excited by the El Centro earthquake.

156
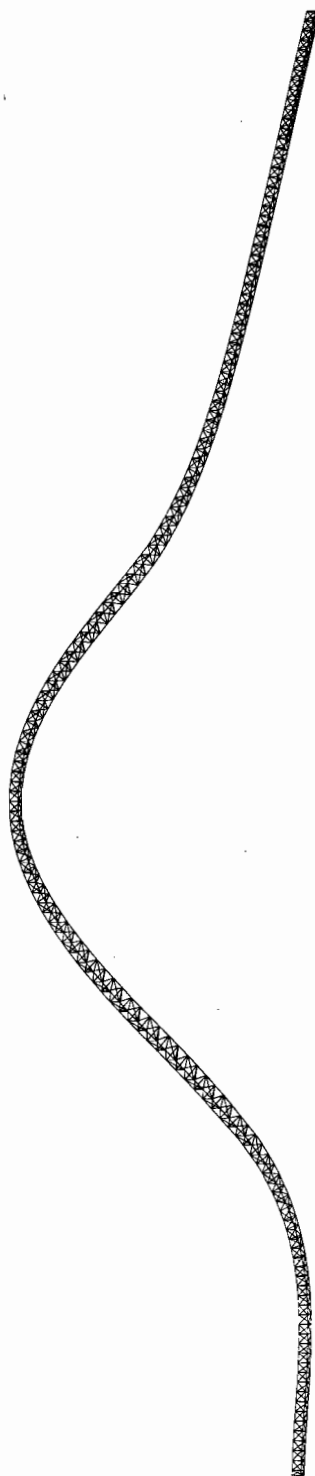
MODE 1

Fig. 5.24. First flexural natural mode shape of mast in the 150-m tower (T = 0.69 s)

MODE 1
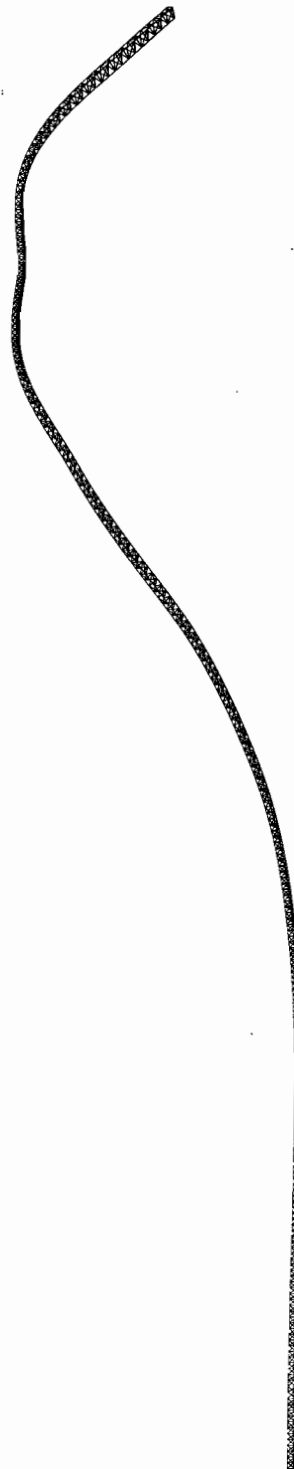
Fig. 5.25. First flexural natural mode shape of mast in the 152-m tower (T = 0.58 s)
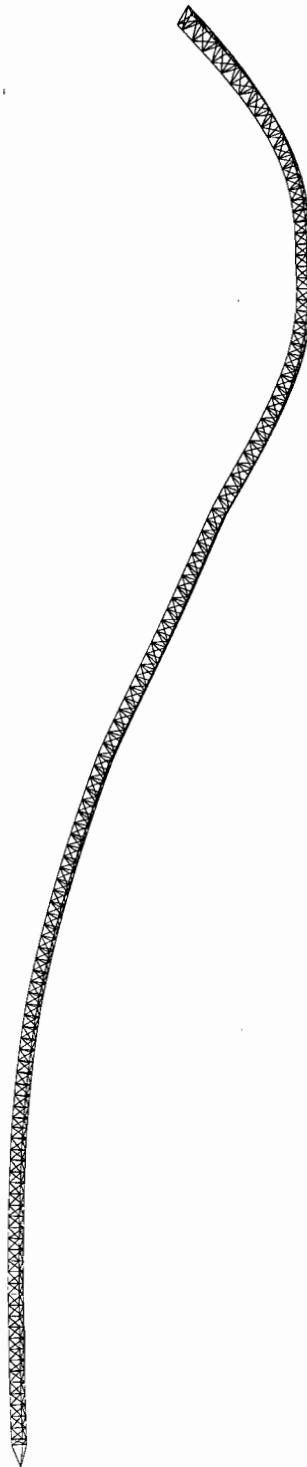
MODE 1

Fig. 5.26. First flexural natural mode shape of mast in the 198-m tower (T = 0.80 s)
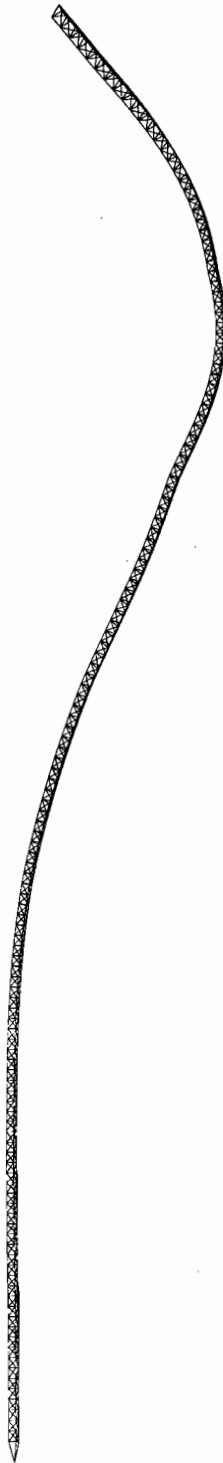
MODE 1

Fig. 5.27. First flexural natural mode shape of mast in the 213-m tower (T = 0.80 s)

MODE 1

Fig. 5.28. First flexural natural mode shape of mast in the 342-m tower (T = 2.10 s)
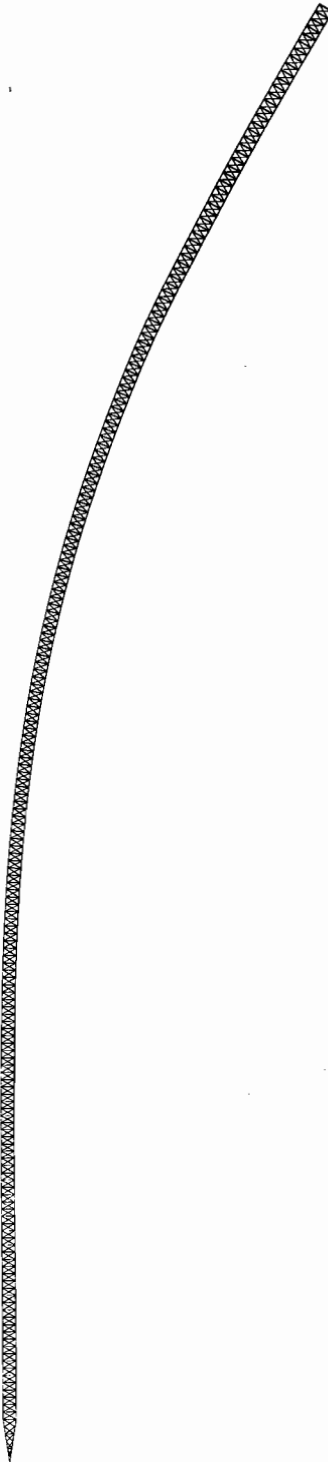
MODE 1

Fig. 5.29. First flexural natural mode shape of mast in the 200-m tower (T = 2.36 s)
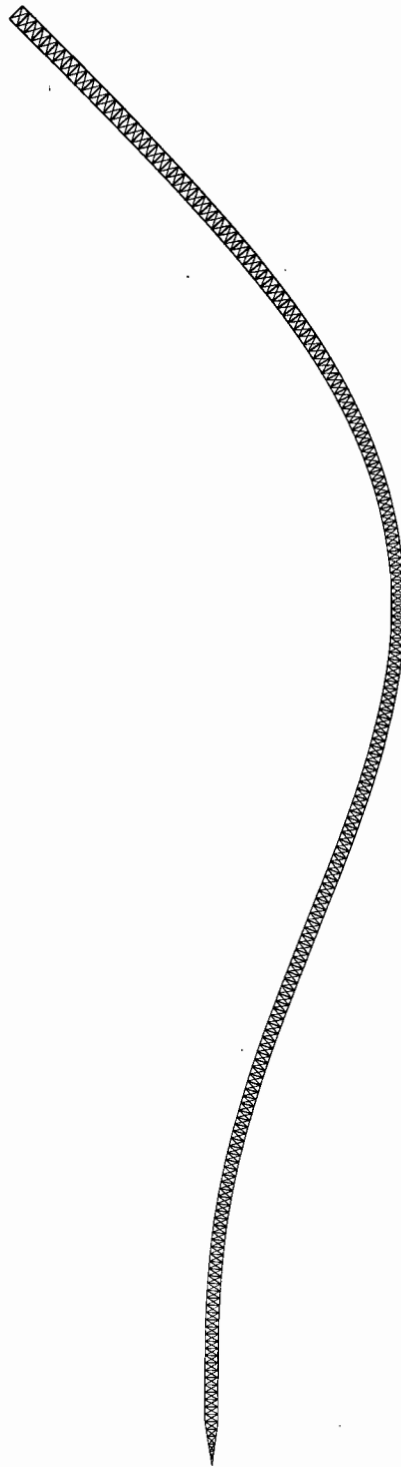
MODE 2

Fig. 5.30. Second flexural natural mode shape of mast in the 200-m tower (T = 1.48 s)

MODE 1
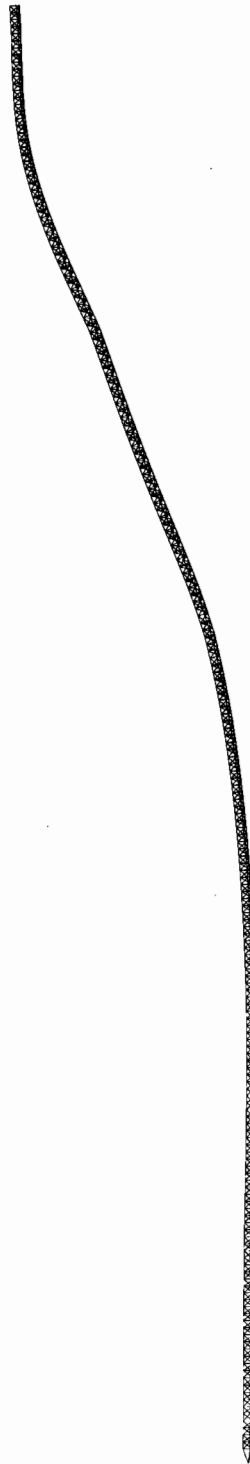
Fig. 5.31. First flexural natural mode shape of mast in the 313-m tower (T = 2.06 s)

MODE 2
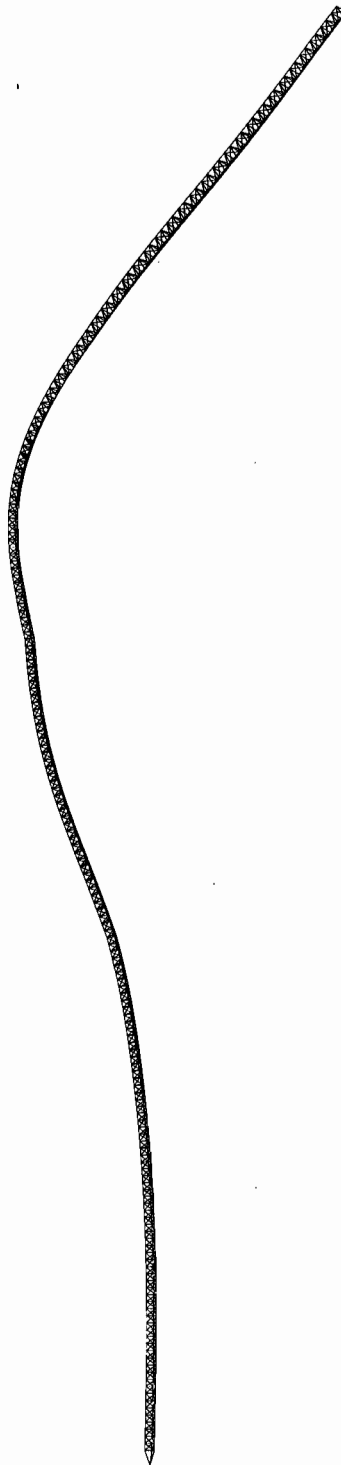
Fig. 5.32. Second flexural natural mode shape of mast in the 313-m tower (T = 1.57 s)

MODE 1

Fig. 5.33. First flexural natural mode shape of mast in the 607-m tower (T = 4.27 s)

Table 5.6. Base shears (B.S.) and detailed weights (W) of towers in kN
(Reference to total weight)

Tower	Weight		%W	El Centro B.S.	%W	Parkfield B.S.	%W	Taft B.S.	%W
607-m	Cable	1595	31	253	5	198	4	172	3
	Mast	3578	69	489	9	812	16	743	14
	Total	5173	100	742	14	1010	20	915	17
342-m	Cable	287	28	44	4	37	3	40	4
	Mast	754	72	214	21	196	19	235	22
	Total	1041	100	258	25	233	22	275	26
313-m	Cable	306	23	44	3	36	3	41	3
	Mast	1033	77	247	19	295	22	339	25
	Total	1339	100	291	22	331	25	380	28
213-m	Cable	91	31	14	5	11	4	15	5
	Mast	205	69	130	44	142	48	161	54
	Total	296	100	144	49	153	52	176	59
200-m	Cable	95	28	15	4	11	3	15	4
	Mast	249	72	146	43	142	41	156	45
	Total	344	100	161	47	153	44	171	49
198-m	Cable	180	25	25	3	22	3	22	3
	Mast	535	75	348	49	274	38	440	62
	Total	715	100	373	52	296	41	462	65
152-m	Cable	36	28	6.7	5	5.4	4	5.2	4
	Mast	91	72	93	74	100	79	75	59
	Total	127	100	100	79	105	83	80	63
150-m	Cable	105	31	16	5	15	4	14	4
	Mast	229	69	217	65	219	66	127	38
	Total	334	100	233	70	234	70	141	42

Table 5.7. Base shears (B.S.) and detailed weights (W) of towers in kN
(Reference to total base shear)

Tower	Weight			Accelerogram					
				El Centro		Parkfield		Taft	
			%W	B.S.	%B.S.	B.S.	%B.S.	B.S.	%B.S.
607-m	Cable	1595	31	253	34	198	20	172	19
	Mast	3578	69	489	66	812	80	743	81
	Total	5173	100	742	100	1010	100	915	100
342-m	Cable	287	28	44	17	37	16	40	15
	Mast	754	72	214	83	196	84	235	85
	Total	1041	100	258	100	233	100	275	100
313-m	Cable	306	23	44	15	36	11	41	11
	Mast	1033	77	247	85	295	89	339	89
	Total	1339	100	291	100	331	100	380	100
213-m	Cable	91	31	14	10	11	7	15	9
	Mast	205	69	130	90	142	93	161	91
	Total	296	100	144	49	153	100	176	100
200-m	Cable	95	28	15	9	11	7	15	9
	Mast	249	72	146	91	142	93	156	91
	Total	344	100	161	100	153	100	171	100
198-m	Cable	180	25	25	7	22	7	22	5
	Mast	535	75	348	93	274	93	440	95
	Total	715	100	373	100	296	100	462	100
152-m	Cable	36	28	6.7	7	5.4	5	5.2	7
	Mast	91	72	93	93	100	95	75	93
	Total	127	100	100	100	105	100	80	100
150-m	Cable	105	31	16	7	15	6	14	10
	Mast	229	69	217	93	219	94	127	90
	Total	334	100	233	100	234	100	141	100
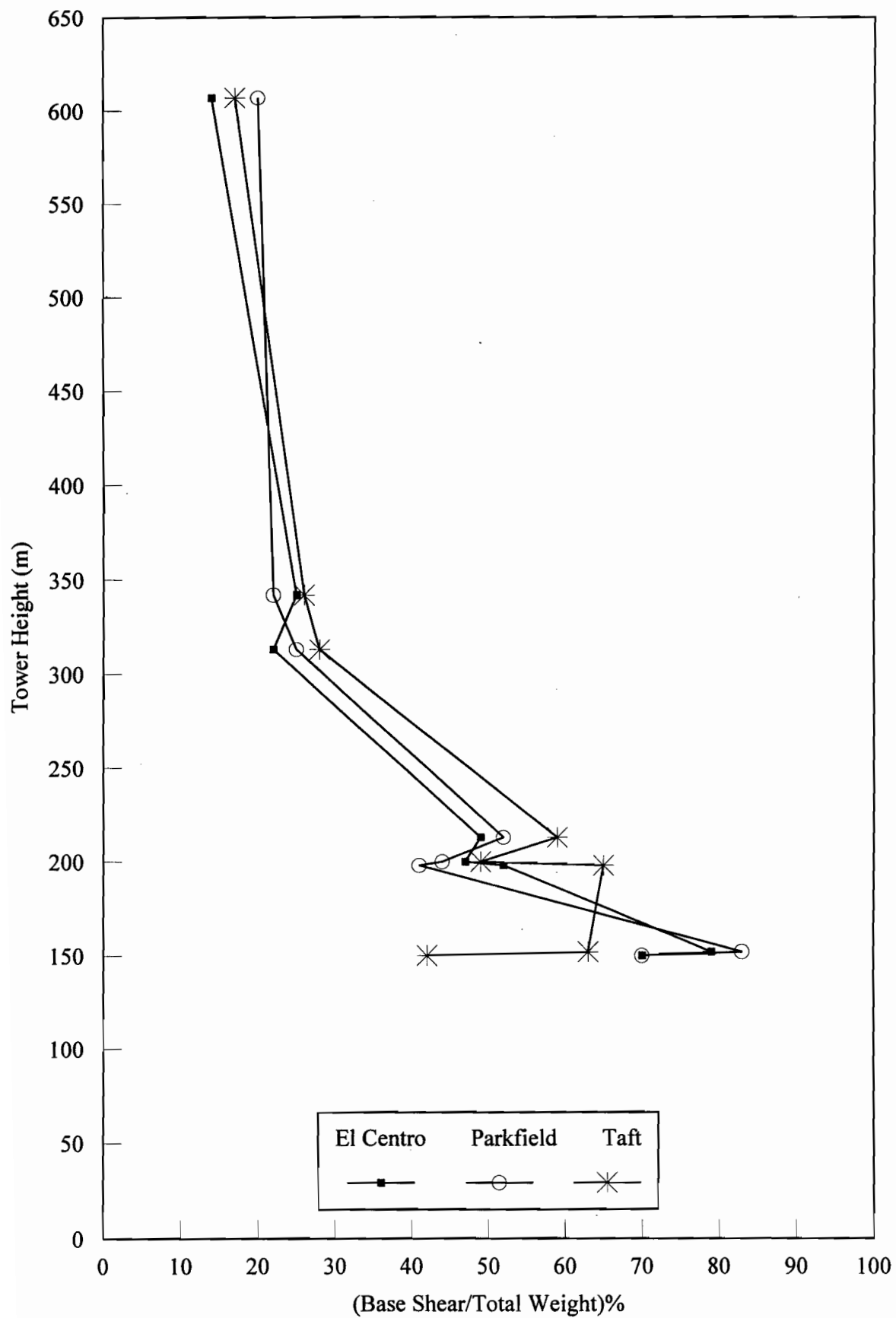
Fig. 5.35. Base shear versus tower height for three base accelerograms

170
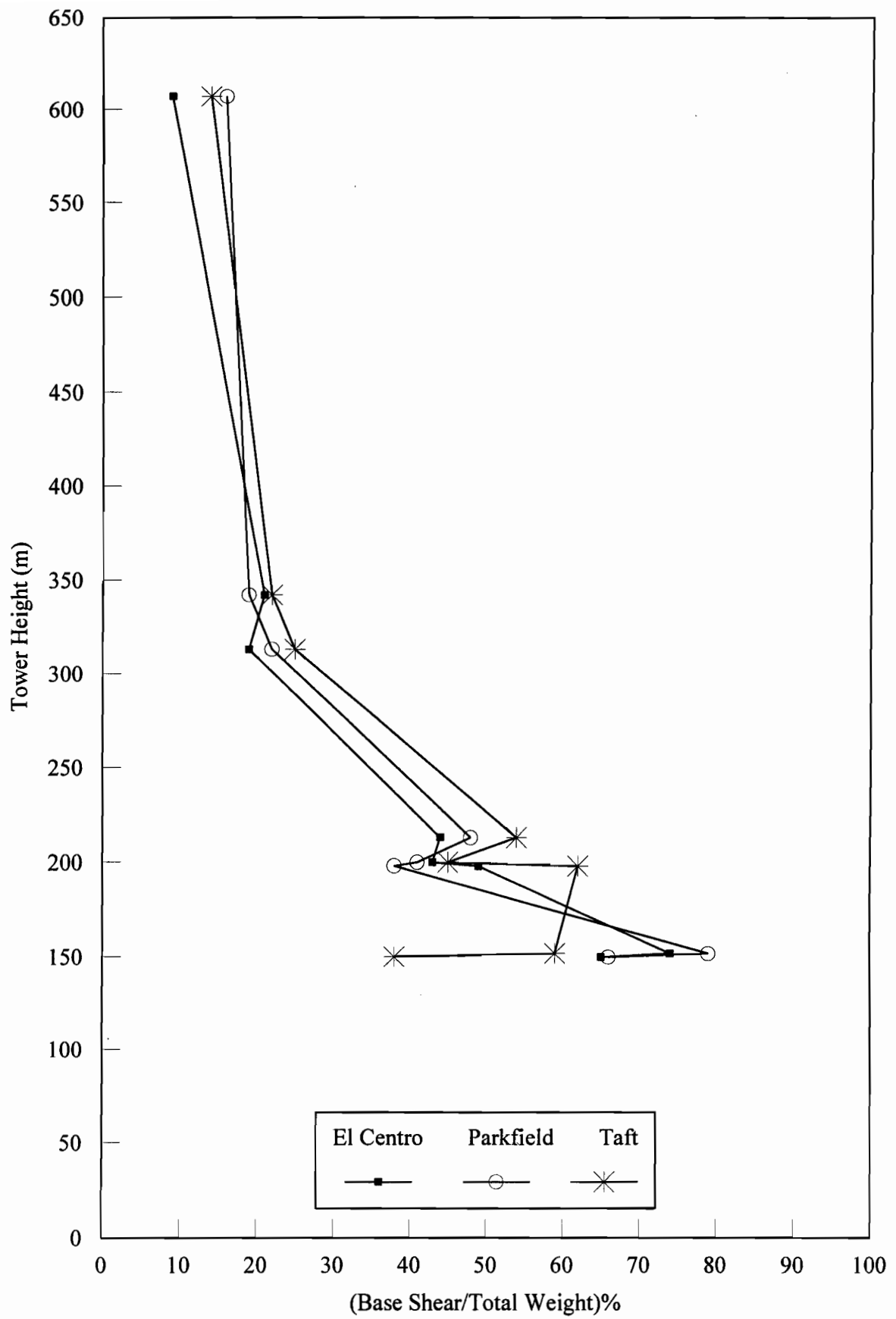
Fig. 5.36. Base shear contributed from mast versus tower height for three base accelerograms

171
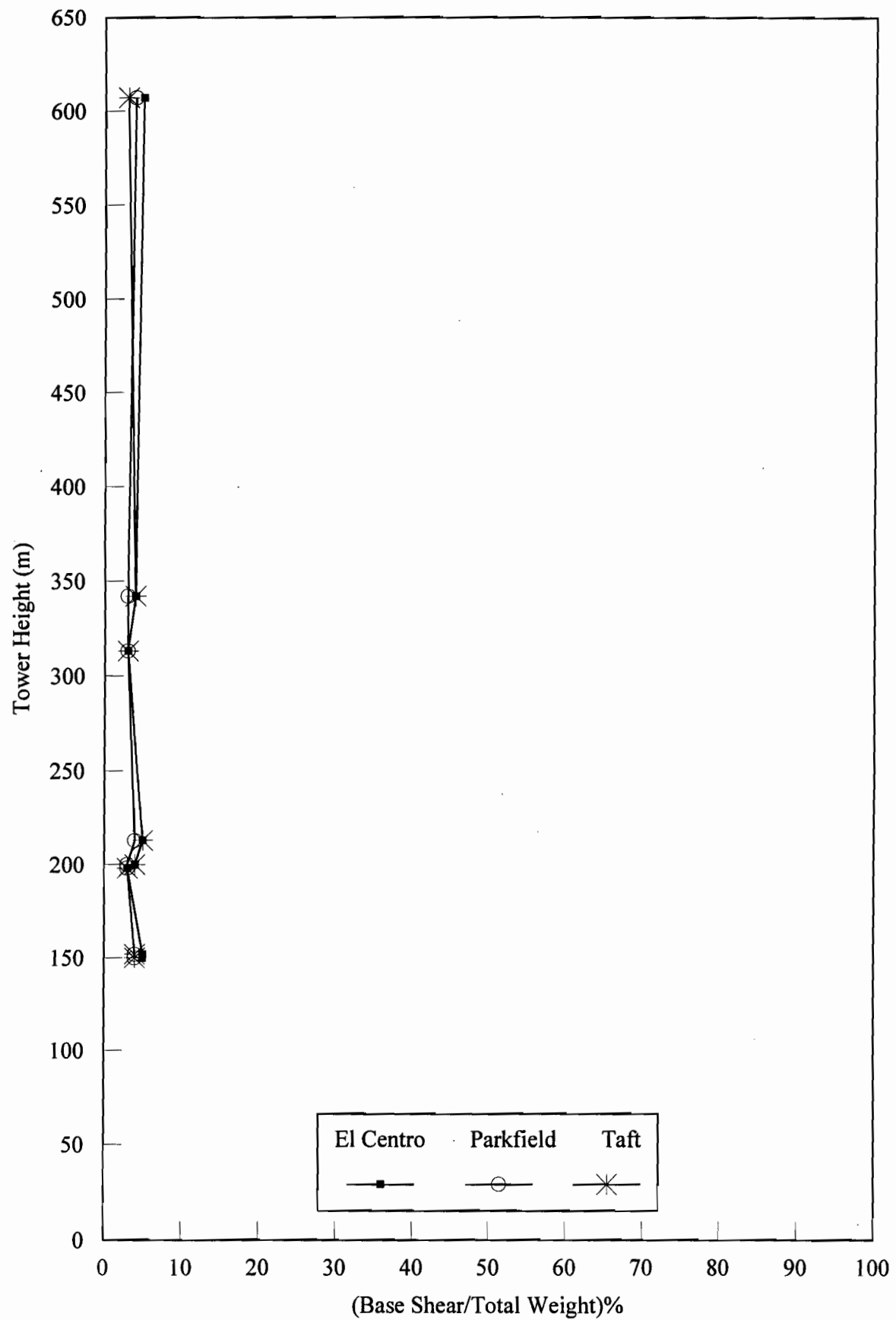
Fig. 5.37. Base shear contributed from cables versus tower height for three base accelerograms
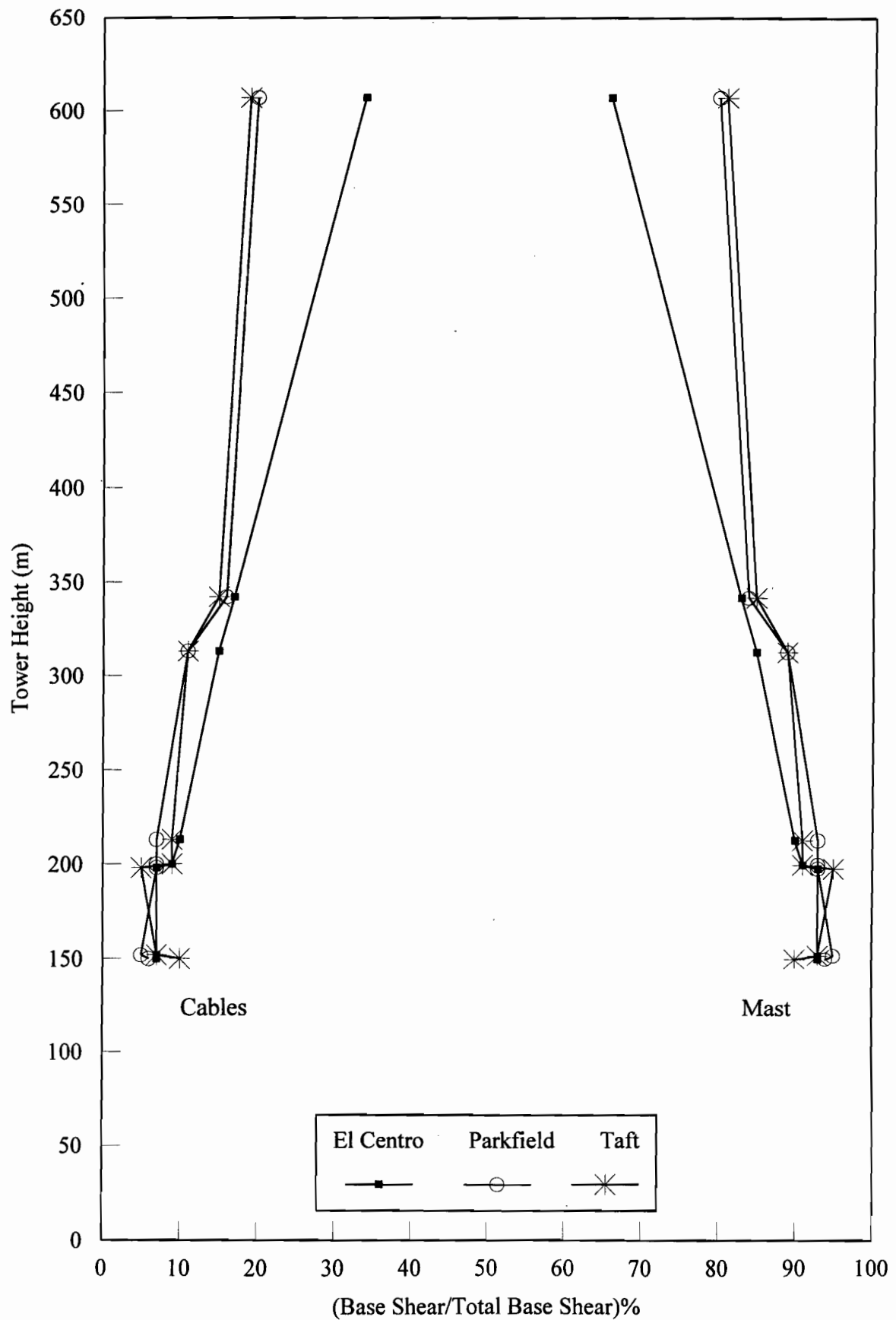
Fig. 5.38. Base shear contributed from mast and cable versus tower height for three base accelerograms

5.2.2 Seismic Component of Mast Base Axial Force

The maximum dynamic component of the axial force at the base of the mast is reported in Table 5.8. It is also expressed as a percentage of the total weight of the tower. Since the axial effects are significantly excited with the vertical component of the earthquake, Table 5.8 is prepared for the case of combined vertical and horizontal accelerograms for the three earthquake motions studied. The results shown in Table 5.8 are illustrated in Figs. 5.39 to 5.41. The horizontal axis of these three figures has the same scale in order to facilitate their comparison. Table 5.8 shows the contributions of the mast and the cables separately, and the dynamic component of the axial compression in the mast at the base is also expressed as a percentage of the total tower weight. The base axial force varies in the range of 44% to 75% of the total weights for the El Centro earthquake, 21% to 43% for Parkfield and 38% to 125% for Taft. As shown in Fig. 5.41, the contribution of the mass of the cables to the total dynamic component of mast base axial force is small, in the range of 4% to 15% of the total weights. Its maximum envelope can be taken as 10% of total weight for all the towers except for the 200-m for which it is 15%. Therefore, the contribution of the cables can be assumed to be constant.

From Fig. 5.39, it can be concluded that regardless of the tower height, the maximum value of the dynamic component of the axial force at the base of the mast is almost constant at about 80% of the total weights, with the exception of the 200-m tower which is much more sensitive.

5.2.3 Seismic Amplification Factor of Cable Tension

Tables 5.9 to 5.16 summarize the maximum dynamic component of cable tension in each guy cluster for all eight towers due to the three earthquake accelerograms studied. These results were calculated for two load cases, horizontal earthquake and combined horizontal and vertical earthquake accelerograms. The dynamic component of cable tension is also expressed as a percentage of the initial cable tension. Tables 5.9 to 5.16 are graphically represented by Figs. 5.42 to 5.57, respectively. It is noted that these

174

Table 5.8. Dynamic component of mast base axial force (B.A.) and detailed weights (W) of towers in kN (Horizontal + Vertical accelerograms)

Tower	Weight			Accelerogram					
				El Centro		Parkfield		Taft	
			%W	B.A.	%W	B.A.	%W	B.A.	%W
607-m	Cable	1595	31	272	5	219	4	436	8
	Mast	3578	69	3619	70	2003	39	1532	30
	Total	5173	100	3891	75	2222	43	1968	38
342-m	Cable	287	28	89	9	48	5	101	10
	Mast	754	72	443	42	304	29	627	60
	Total	1041	100	532	51	352	34	728	70
313-m	Cable	306	23	121	9	69	5	89	7
	Mast	1033	77	752	56	254	19	961	71
	Total	1339	100	873	65	323	24	1050	78
213-m	Cable	91	31	30	10	16	5	18	6
	Mast	205	69	102	34	54	18	176	59
	Total	296	100	132	44	70	23	194	65
200-m	Cable	95	28	44	13	50	15	53	15
	Mast	249	72	170	49	77	22	379	110
	Total	344	100	214	62	127	37	432	125
198-m	Cable	180	25	55	8	26	4	43	6
	Mast	535	75	303	42	194	27	522	73
	Total	715	100	358	50	220	31	565	79
152-m	Cable	36	28	11	9	12	9	13	10
	Mast	91	72	54	42	15	12	86	68
	Total	127	100	65	51	27	21	99	78
150-m	Cable	105	31	41	12	21	6	28	8
	Mast	229	69	161	48	62	19	158	47
	Total	334	100	202	60	83	25	186	55
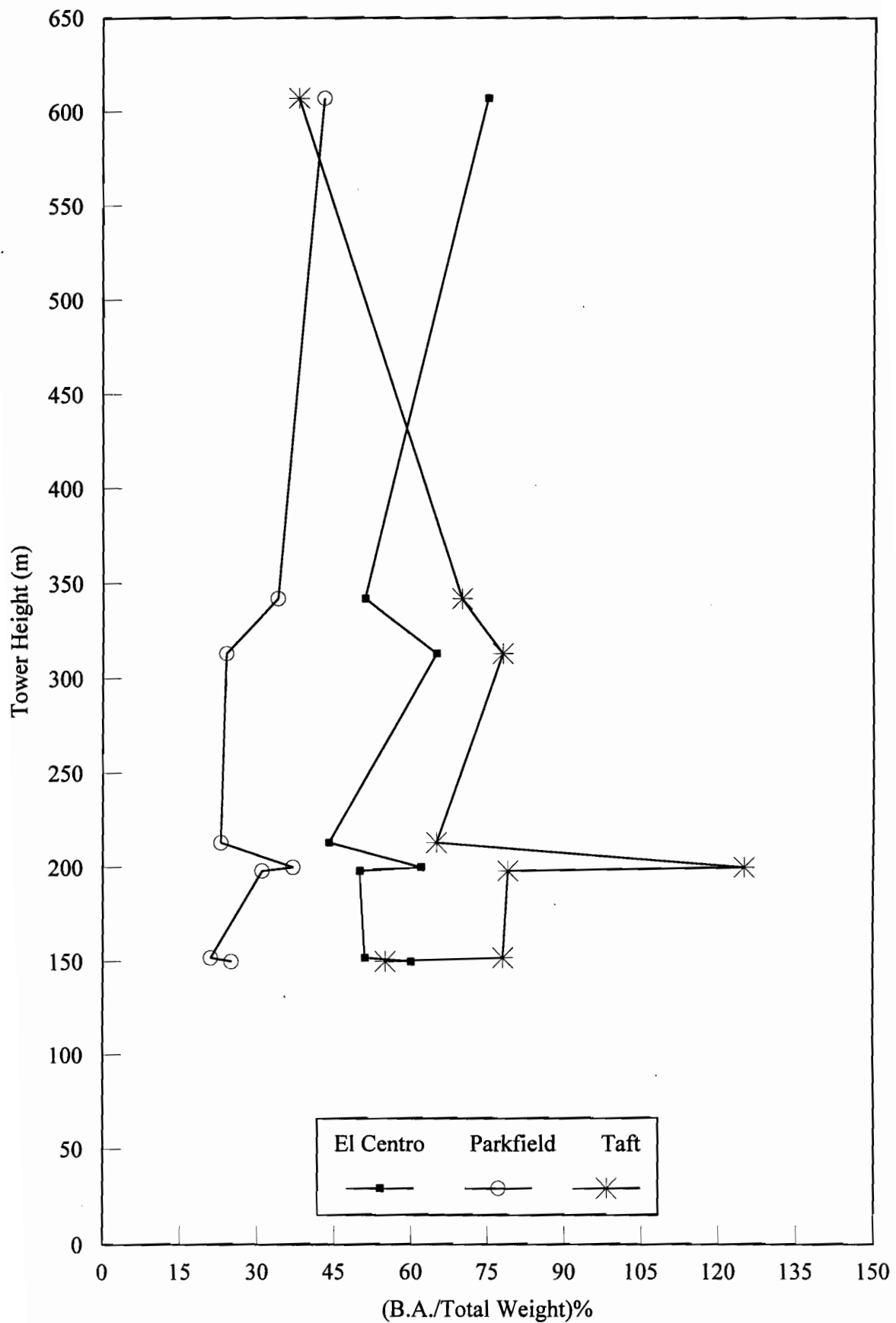
Fig. 5.39. Dynamic component of mast base axial force (B.A.) versus tower height for three base accelerograms (Horizontal + Vertical)

176

Fig. 5.40. Dynamic component of mast base axial force (B.A.) contributed from mast versus tower height for three base accelerograms (Horizontal + Vertical)

177
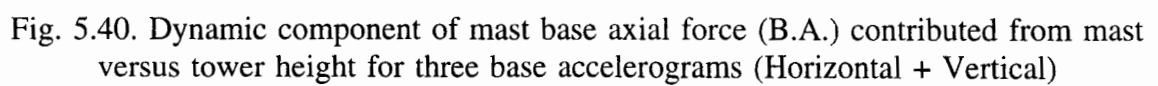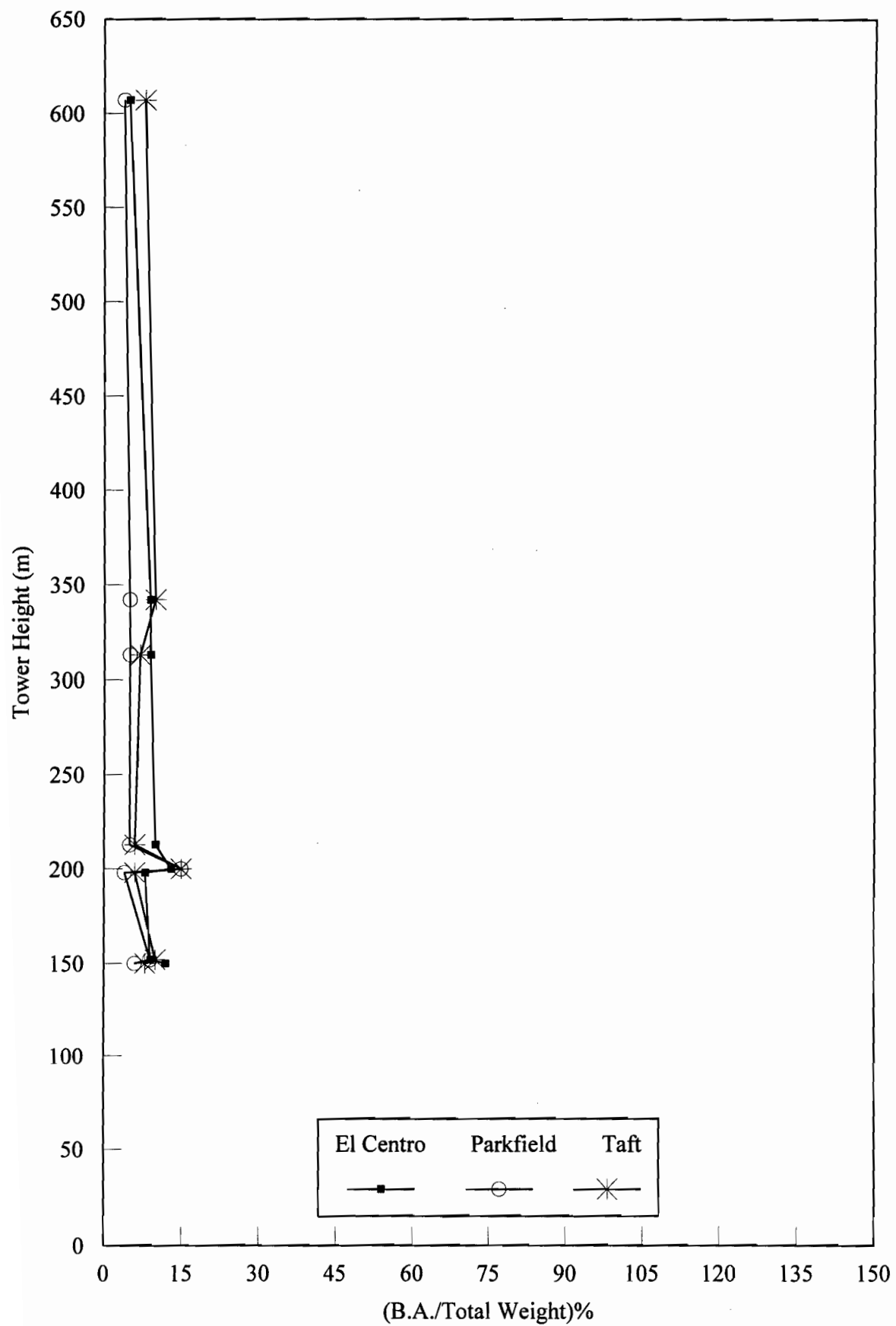
Fig. 5.41. Dynamic component of mast base axial force (B.A.) contributed from cables versus tower height for three base accelerograms (Horizontal + Vertical)

178

figures have the same scale on their horizontal axis. The percentage of the dynamic component of cable tension to the initial tension is defined in these figures by the seismic amplification factor. It is observed that, except for the 200-m tower (Fig. 5.48 and 5.49), all graphs are comparable and vary more or less in the same range of amplification (30% to 150%). The 200-m tower has twice as much amplification compared to the others. This can be explained by considering Table 5.4 which gives the ratio of initial tension to ultimate tensile strength. Since the 200-m tower has relatively slack cables in its initial configuration, its cables are more excited. The same conclusion can also be reached from Table 5.3 which presents values of cable sag. In the 152-m (Figs. 5.44 and 5.45) and 342-m (Figs. 5.54 and 5.55) towers, the second lowest guy stay level has a significant seismic amplification factor compared to the others. This can also be explained by a smaller initial tension with respect to those of the cables of the other levels.

5.2.4 Maximum Shear and Bending Moment of Mast

Tables 5.17 and 5.18 summarize the results obtained for the maximum mast shear and bending moment for the eight towers studied. For ease of comparison, these values have been normalized. Accordingly, in Table 5.17, the maximum mast shear is divided by the maximum base shear of the towers, and the maximum mast bending moment is divided by the product of the panel width and the maximum base shear. Since the bending moment in the mast is in direct relation with the width of the mast (the spacing between the legs), it is reasonable to use the panel width to normalize the moment. Table 5.18 presents the same results·as in Table 5.17, but the maximum base shear is substituted by the total weight of the towers to normalize the maximum mast base shear and bending moment.

Figures 5.58 and 5.59 illustrate the content of Table 5.17, and Figs. 5.60 and 5.61 represent that in Table 5.18. As shown in Figs. 5.58 and 5.59, in the lower range of tower heights (150 to 213 m), the ratio of maximum mast shear to maximum base shear varies from 8% to 12% and the ratio of maximum mast moment to the product of panel width and maximum base shear varies from 57% to 73%. In the upper range of tower heights

179

Table 5.9. Tension of guy cables (kN) in 150-m tower

Anch	Set No.	T_0	Accelerogram (Horizontal only)						Accelerogram (Horizontal + Vertical)					
			El Centro		Parkfield		Taft		El Centro		Parkfield		Taft	
			T_{dyn}	%	T_{dyn}	%	T_{dyn}	%	T_{dyn}	%	T_{dyn}	%	T_{dyn}	%
Outer	7*	76	29	38	26	34	16	21	29	38	22	29	17	22
	6	51	42	81	50	98	25	48	44	86	48	93	28	55
	5*	23	21	90	24	105	12	50	22	93	23	100	13	57
Inner	4	43	33	76	31	72	21	47	33	76	30	70	21	49
	3	31	22	71	25	78	23	74	23	73	25	80	23	73
	2*	17	9.6	56	9.8	57	11	62	8.9	51	9.2	54	11	66
	1	22	4.9	23	5.6	26	5.8	27	6.2	29	4.8	22	6.3	29

T_0 = Cable tension due to self weight and initial prestress (kN)

T_{dyn} = Dynamic component of cable tension (i.e. T_{total} - T_0)

% = $(T_{dyn}/T_0)100$

Anch = guy clusters attached to Inner, Intermediate or Outer anchor points on the ground

* Outrigger location

Table 5.10. Tension of guy cables (kN) in 152-m tower

Anch	Set No.	T_0	Accelerogram (Horizontal only)						Accelerogram (Horizontal + Vertical)					
			El Centro		Parkfield		Taft		El Centro		Parkfield		Taft	
			T_{dyn}	%	T_{dyn}	%	T_{dyn}	%	T_{dyn}	%	T_{dyn}	%	T_{dyn}	%
Outer	8	20	7.7	38	7.5	37	4.9	24	8.0	39	6.2	30	4.8	24
	7*	13	9.1	71	9.5	73	4.9	38	9.2	71	8.6	67	5.9	46
	6	13	15	120	14	108	6.9	54	15	119	12	96	7.9	62
Inner	5	12	12	97	12	98	6.4	52	12	95	12	94	6.3	51
	4	9.4	7.6	81	7.7	82	6.0	64	7.2	76	7.4	79	6.1	64
	3*	9.4	8.0	85	8.2	87	9.2	99	8.0	86	7.9	85	9.2	99
	2	6.3	11	177	12	188	12	195	11	178	11.6	184	12	194
	1	6.3	6.3	100	6.3	99	6.0	95	6.1	96	6.3	99	6.4	101

T_0 = Cable tension due to self weight and initial prestress (kN)
T_{dyn} = Dynamic component of cable tension (i.e. T_{total} - T_0)
% = $(T_{dyn}/T_0)100$
Anch = guy clusters attached to Inner, Intermediate or Outer anchor points on the ground
* Outrigger location

Table 5.11. Tension of guy cables (kN) in 198-m tower

Anch	Set No.	T_0	Accelerogram (Horizontal only)						Accelerogram (Horizontal + Vertical)					
			El Centro		Parkfield		Taft		El Centro		Parkfield		Taft	
			T_{dyn}	%	T_{dyn}	%	T_{dyn}	%	T_{dyn}	%	T_{dyn}	%	T_{dyn}	%
Outer	6	140	56	40	56	40	62	44	55	39	61	43	60	43
	5	96	71	74	59	62	92	96	71	74	63	66	100	104
	4*	68	59	87	59	87	86	127	61	91	62	91	82	121
Inner	3	65	61	93	74	113	79	121	61	94	75	115	79	121
	2	64	84	131	83	130	75	117	88	137	83	129	76	118
	1	41	57	137	57	138	42	101	57	138	59	142	39	94

T_0 = Cable tension due to self weight and initial prestress (kN)

T_{dyn} = Dynamic component of cable tension (i.e. T_{total} - T_0)

% = $(T_{dyn}/T_0)100$

Anch = guy clusters attached to Inner, Intermediate or Outer anchor points on the ground

* Outrigger location

Table 5.12. Tension of guy cables (kN) in 200-m tower

Anch	Set No.	T_0	Accelerogram (Horizontal only)						Accelerogram (Horizontal + Vertical)					
			El Centro		Parkfield		Taft		El Centro		Parkfield		Taft	
			T_{dyn}	%	T_{dyn}	%	T_{dyn}	%	T_{dyn}	%	T_{dyn}	%	T_{dyn}	%
Outer	8	25	25	101	36	146	42	171	25	102	47	191	38	155
	7	17	26	150	19	110	34	199	24	143	35	203	22	127
	6	16	25	161	24	154	42	267	31	195	45	289	25	159
Inter.	5	9.8	21	210	16	168	26	260	20	202	27	274	17	177
	4	9.4	19	201	16	167	24	259	22	238	25	267	17	179
	3	7.8	14	176	9.9	126	14	184	14	178	14	182	9.2	118
Inner	2	7.9	13	171	14	172	13	171	14	174	13	170	14	175
	1	6.7	6.2	92	7.7	115	8.6	128	6.7	100	8.7	129	7.5	113

T_0 = Cable tension due to self weight and initial prestress (kN)

T_{dyn} = Dynamic component of cable tension (i.e. T_{total} - T_0)

% = $(T_{dyn}/T_0)100$

Anch = guy clusters attached to Inner, Intermediate or Outer anchor points on the ground

* Outrigger location

Table 5.13. Tension of guy cables (kN) in 213-m tower

Anch	Set No.	T_0	Accelerogram (Horizontal only)						Accelerogram (Horizontal + Vertical)					
			El Centro		Parkfield		Taft		El Centro		Parkfield		Taft	
			T_{dyn}	%	T_{dyn}	%	T_{dyn}	%	T_{dyn}	%	T_{dyn}	%	T_{dyn}	%
Outer	7	74	17	23	21	29	22	30	22	30	19	26	24	32
	6	55	21	37	21	38	31	56	25	45	22	39	39	70
	5	41	24	58	34	83	36	90	22	55	36	89	40	98
	4	34	21	62	29	84	29	85	20	58	28	82	30	88
Inner	3	32	29	90	38	117	28	85	31	95	41	125	28	86
	2	26	29	110	30	113	24	91	29	111	30	114	23	87
	1	26	20	78	17	65	15	58	20	78	17	65	15	57

T_0 = Cable tension due to self weight and initial prestress (kN)
T_{dyn} = Dynamic component of cable tension (i.e. $T_{total} - T_0$)
% = $(T_{dyn}/T_0)100$
Anch = guy clusters attached to Inner, Intermediate or Outer anchor points on the ground
* Outrigger location

Table 5.14. Tension of guy cables (kN) in 313-m tower

Anch	Set No.	T_0	Accelerogram (Horizontal only)						Accelerogram (Horizontal + Vertical)					
			El Centro		Parkfield		Taft		El Centro		Parkfield		Taft	
			T_{dyn}	%	T_{dyn}	%	T_{dyn}	%	T_{dyn}	%	T_{dyn}	%	T_{dyn}	%
Outer	5	122	58	48	60	49	59	48	55	45	62	51	57	47
	4	174	86	49	83	48	108	62	77	44	79	46	134	77
Inner	3	107	53	50	89	83	83	78	60	56	93	87	92	86
	2	93	77	83	71	77	100	108	77	83	77	83	98	106
	1	59	55	93	47	80	51	86	57	96	50	83	55	92

T_0 = Cable tension due to self weight and initial prestress (kN)

T_{dyn} = Dynamic component of cable tension (i.e. $T_{total} - T_0$)

% = $(T_{dyn}/T_0)100$

Anch = guy clusters attached to Inner, Intermediate or Outer anchor points on the ground

* Outrigger location

Table 5.15. Tension of guy cables (kN) in 342-m tower

Anch	Set No.	T_0	Accelerogram (Horizontal only)						Accelerogram (Horizontal + Vertical)					
			El Centro		Parkfield		Taft		El Centro		Parkfield		Taft	
			T_{dyn}	%	T_{dyn}	%	T_{dyn}	%	T_{dyn}	%	T_{dyn}	%	T_{dyn}	%
Outer	7	96	32	33	15	16	21	22	32	34	16	17	23	24
	6	93	38	41	37	40	39	42	36	39	40	43	42	45
	5	77	49	64	51	66	54	70	60	78	54	70	54	71
Inner	4	65	52	80	48	74	57	87	49	75	50	77	57	88
	3	43	36	84	34	78	36	84	36	84	35	83	35	82
	2*	24	35	148	19	80	23	96	36	151	20	86	25	104
	1	47	25	54	15	33	18	39	27	58	17	35	19	40

T_0 = Cable tension due to self weight and initial prestress (kN)
T_{dyn} = Dynamic component of cable tension (i.e. T_{total} - T_0)
% = (T_{dyn}/T_0)100
Anch = guy clusters attached to Inner, Intermediate or Outer anchor points on the ground
* Outrigger location

Table 5.16. Tension of guy cables (kN) in 607-m tower

Anch	Set No.	T_0	Accelerogram (Horizontal only)						Accelerogram (Horizontal + Vertical)					
			El Centro		Parkfield		Taft		El Centro		Parkfield		Taft	
			T_{dyn}	%	T_{dyn}	%	T_{dyn}	%	T_{dyn}	%	T_{dyn}	%	T_{dyn}	%
Outer	9	232	57	25	60	27	48	21	100	45	63	28	101	45
	8	372	87	23	123	33	98	26	127	34	119	32	112	30
	7	175	66	38	84	48	57	32	89	51	80	46	62	35
Inter.	6	329	147	45	144	44	113	34	210	64	154	47	111	34
	5	203	96	47	124	61	85	42	121	59	132	65	91	45
	4	144	79	55	119	82	92	64	93	65	130	90	97	67
Inner	3	245	131	53	168	68	168	68	145	59	181	73	178	72
	2	195	168	86	152	78	187	96	179	92	151	78	199	102
	1	116	106	91	83	71	96	82	110	94	81	70	101	87

T_0 = Cable tension due to self weight and initial prestress (kN)
T_{dyn} = Dynamic component of cable tension (i.e. T_{total} - T_0)
% = $(T_{dyn}/T_0)100$
Anch = guy clusters attached to Inner, Intermediate or Outer anchor points on the ground
* Outrigger location

187
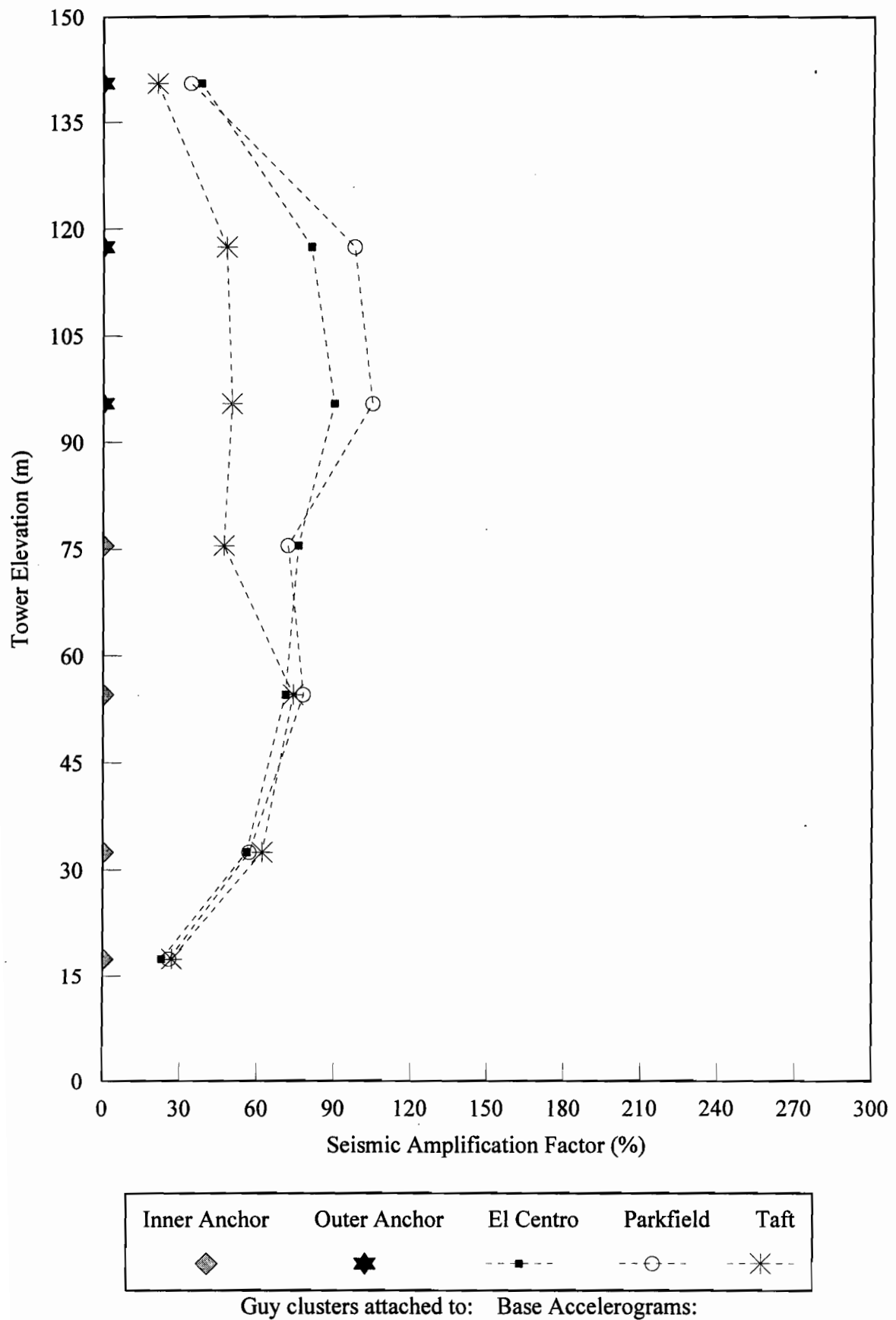
Fig. 5.42. Seismic amplification factor of cable tension in 150-m tower to three base accelerograms
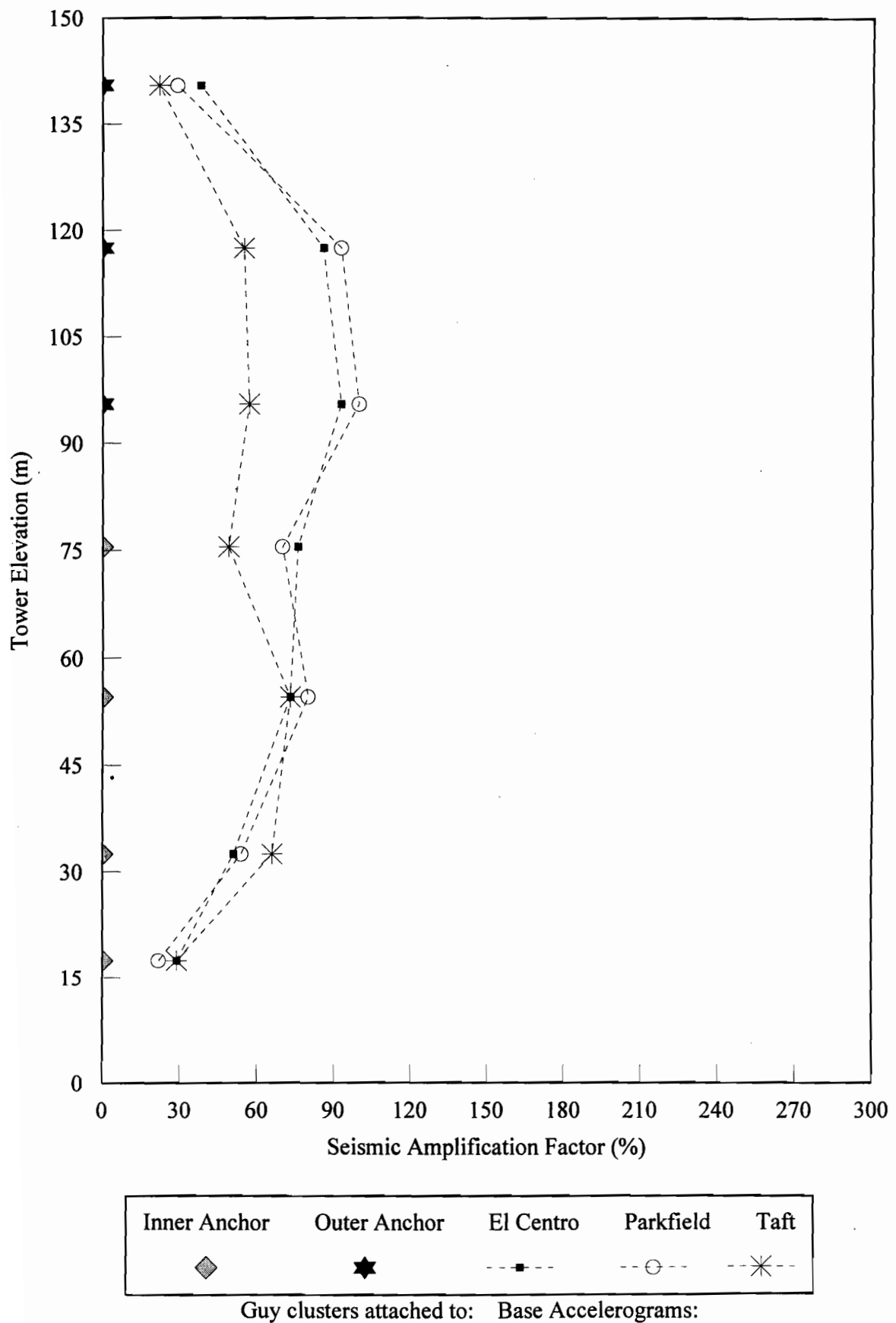
Fig. 5.43. Seismic amplification factor of cable tension in 150-m tower to three base accelerograms (Horizontal + Vertical)
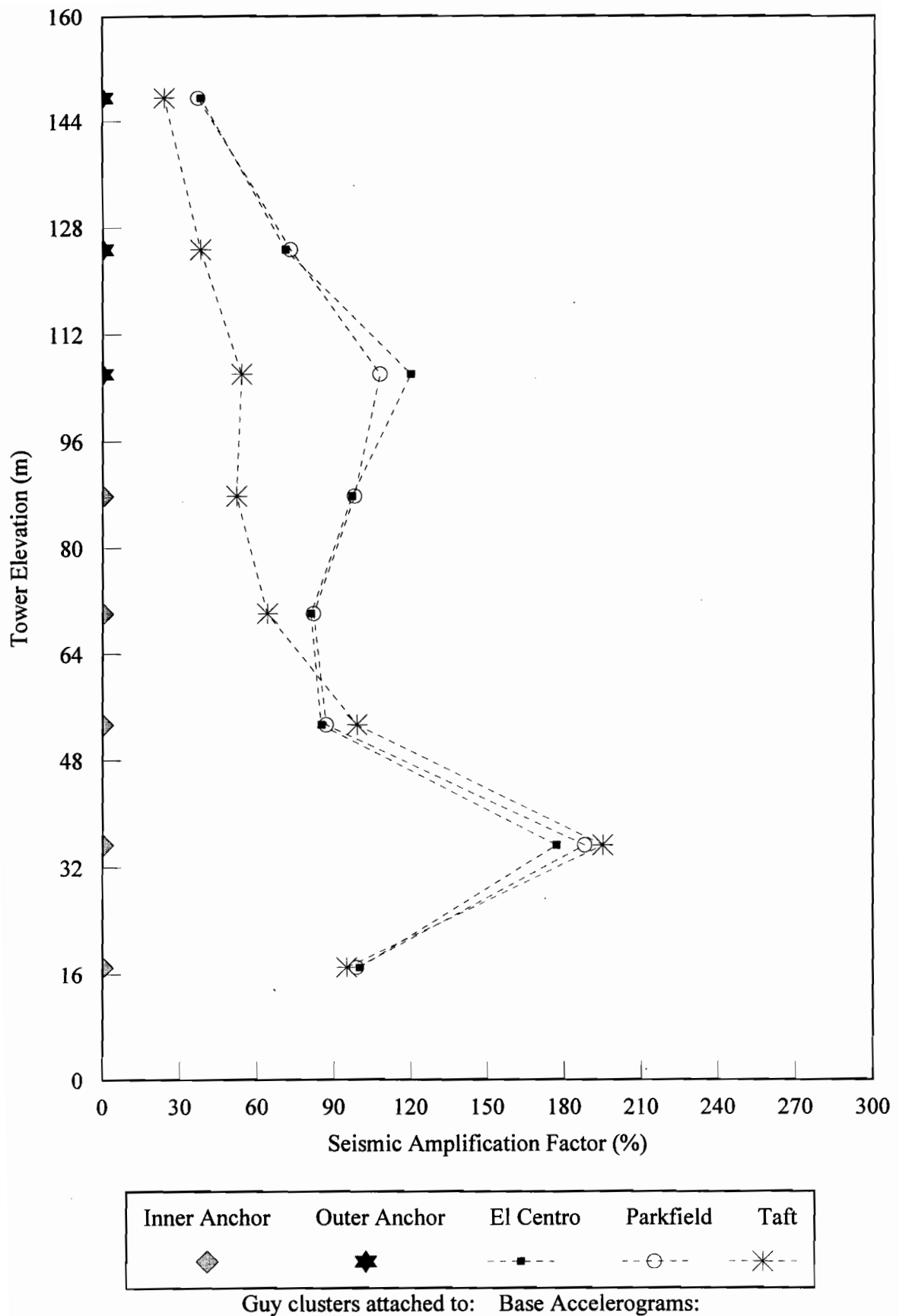
Fig. 5.44. Seismic amplification factor of cable tension in 152-m tower to three base accelerograms

190
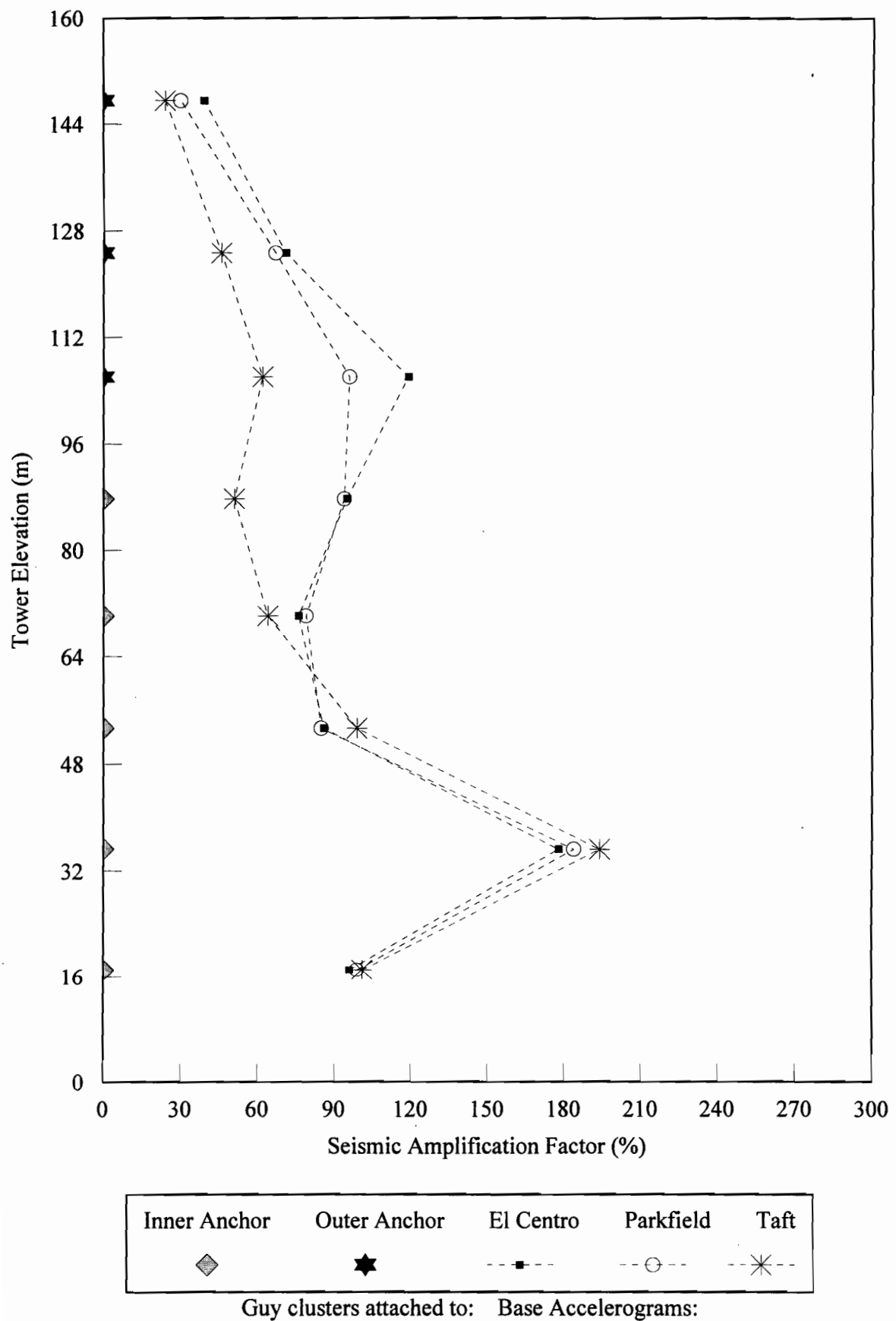
Fig. 5.45. Seismic amplification factor of cable tension in 152-m tower to three base
accelerograms (Horizontal + Vertical)
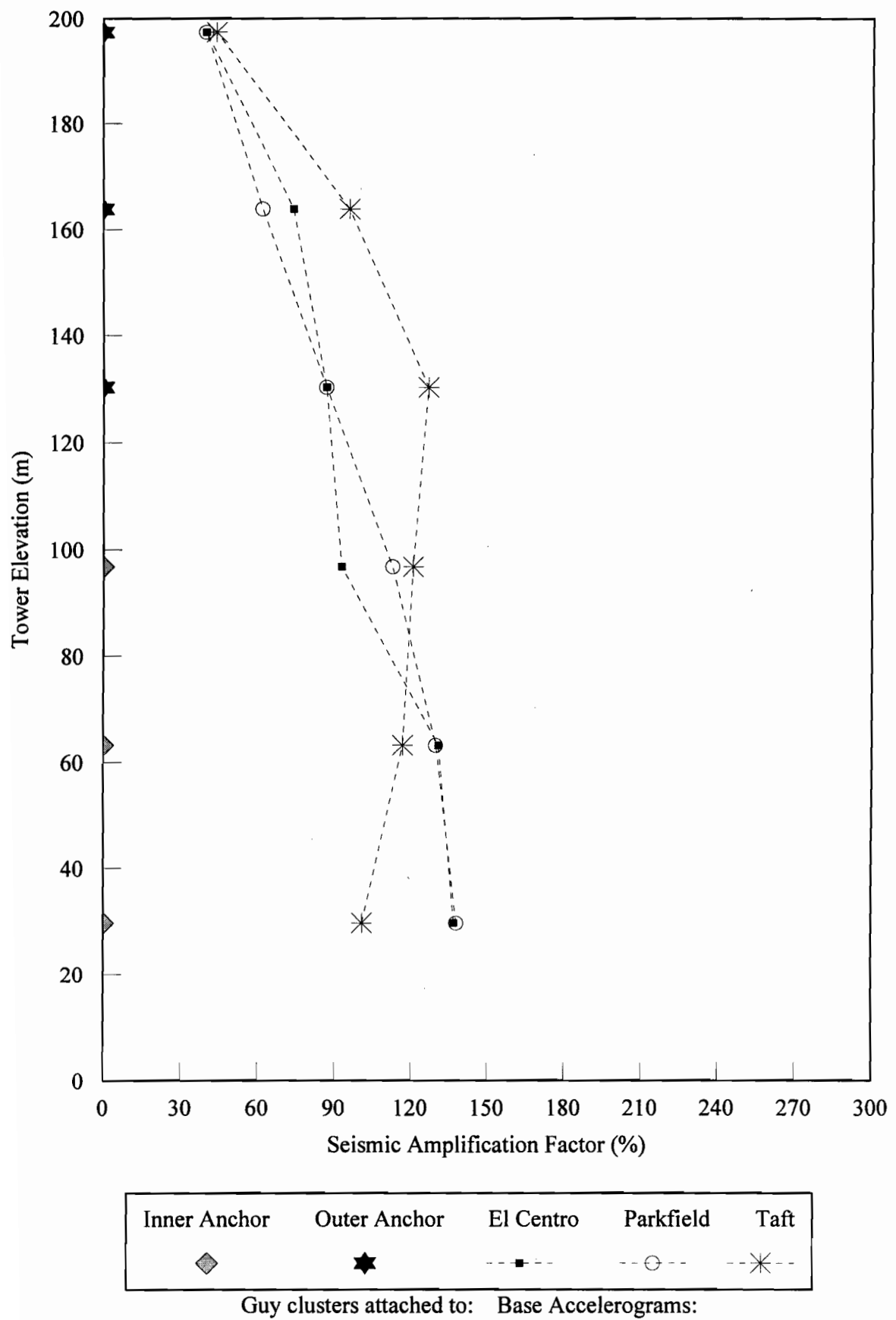
Fig. 5.46. Seismic amplification factor of cable tension in 198-m tower to three base accelerograms
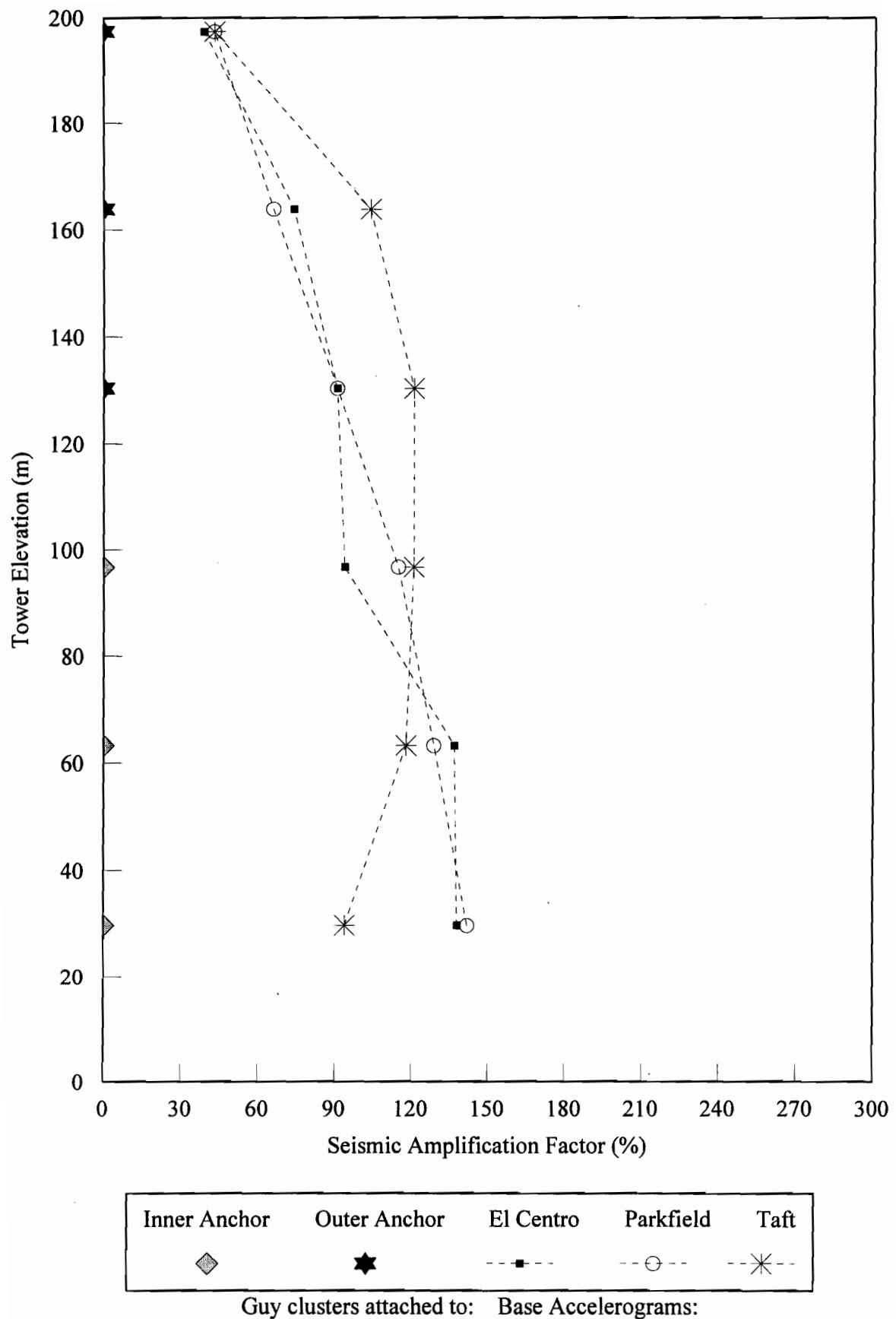
Fig. 5.47. Seismic amplification factor of cable tension in 198-m tower to three base accelerograms (Horizontal + Vertical)

193
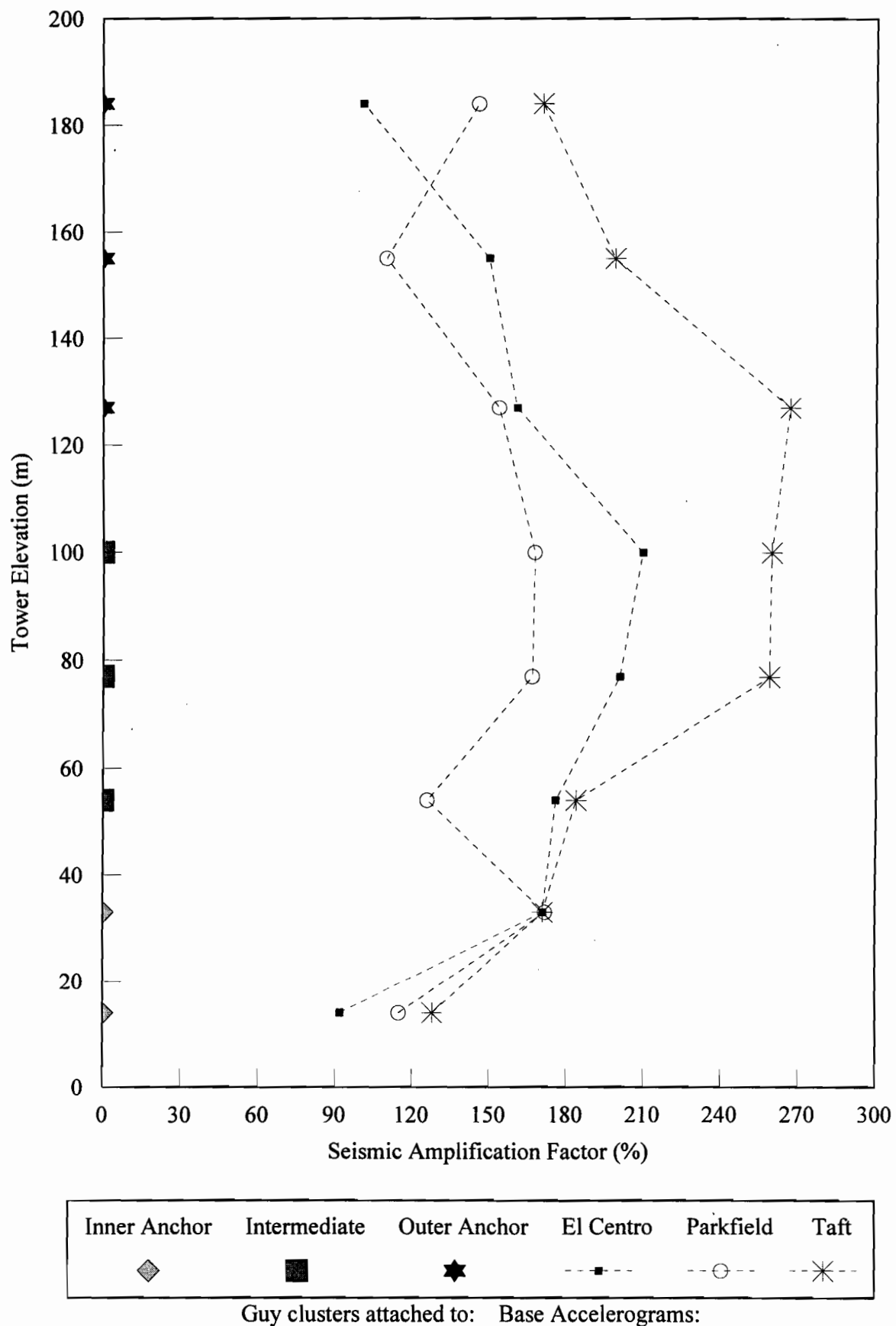
Fig. 5.48. Seismic amplification factor of cable tension in 200-m tower to three base accelerograms
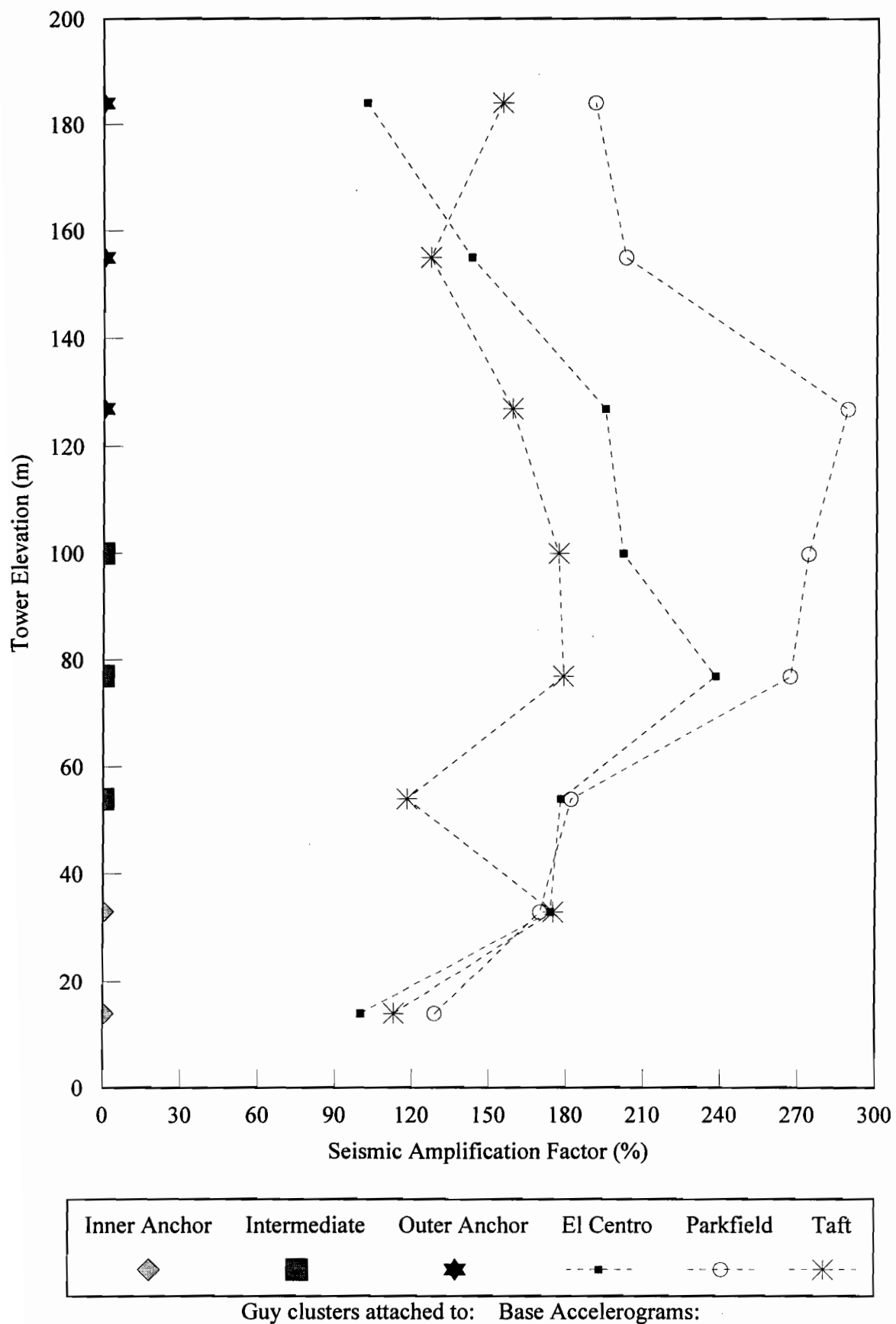
Fig. 5.49. Seismic amplification factor of cable tension in 200-m tower to three base accelerograms (Horizontal + Vertical)

195
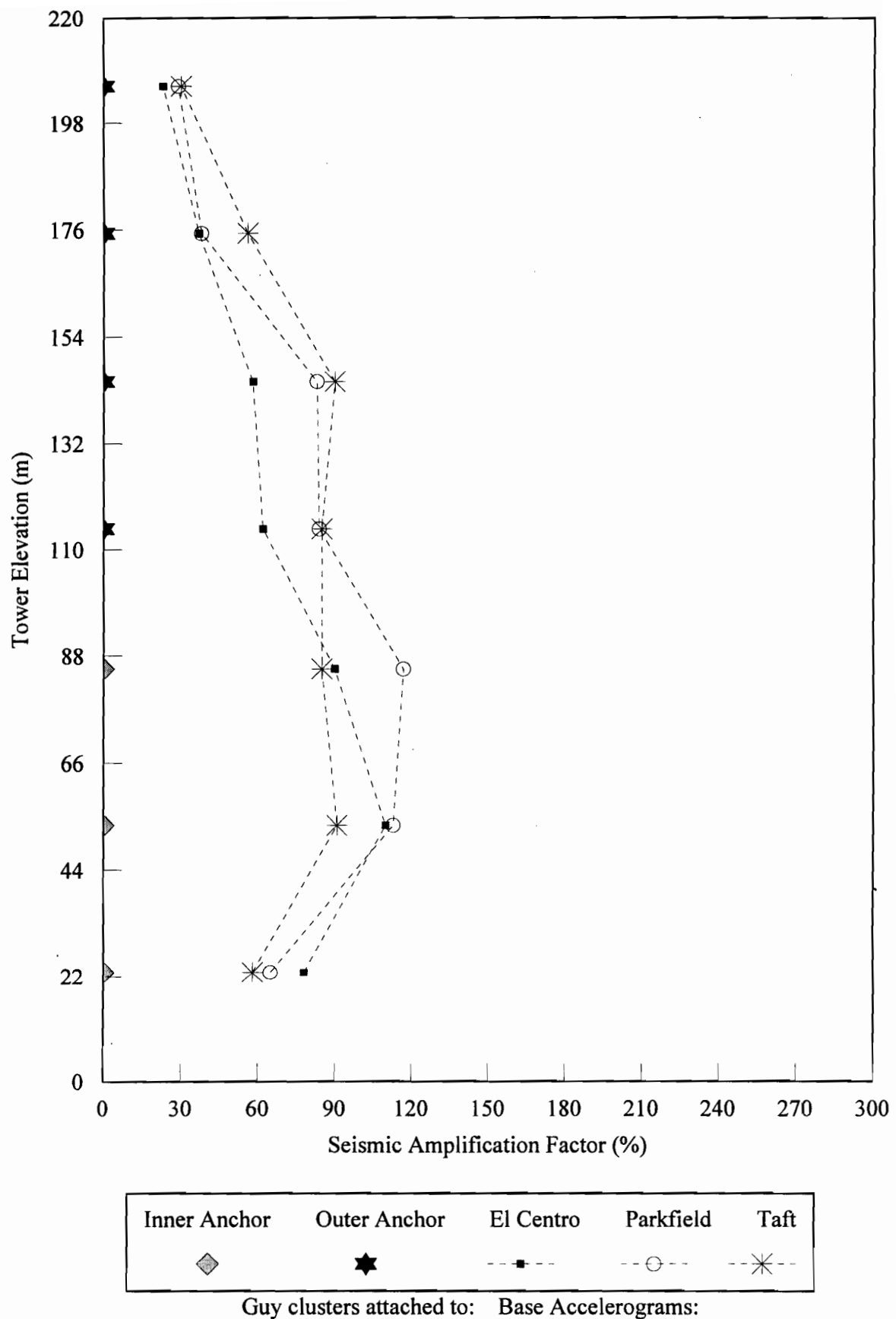
Fig. 5.50. Seismic amplification factor of cable tension in 213-m tower to three base accelerograms

196
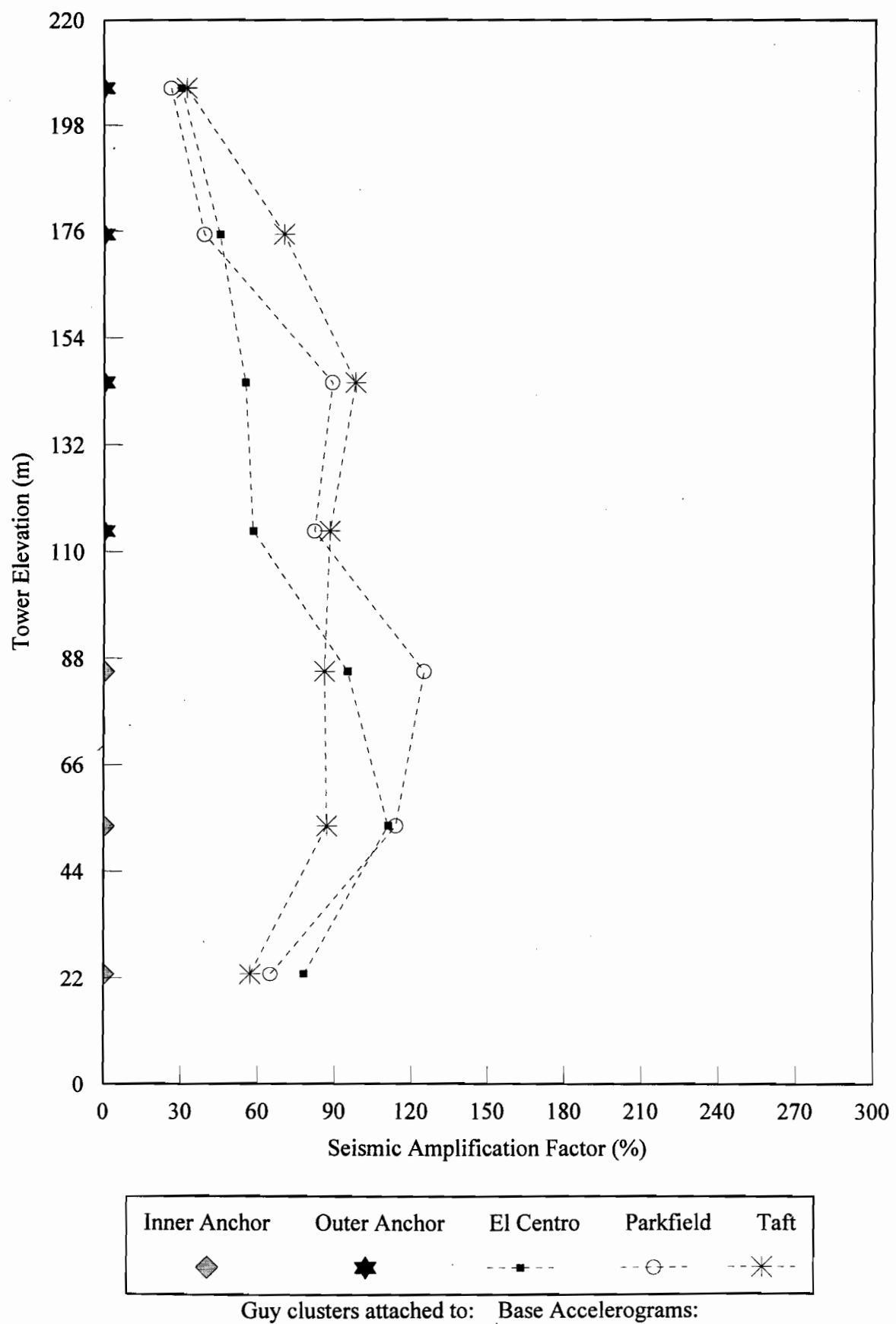
Fig. 5.51. Seismic amplification factor of cable tension in 213-m tower to three base accelerograms (Horizontal + Vertical)
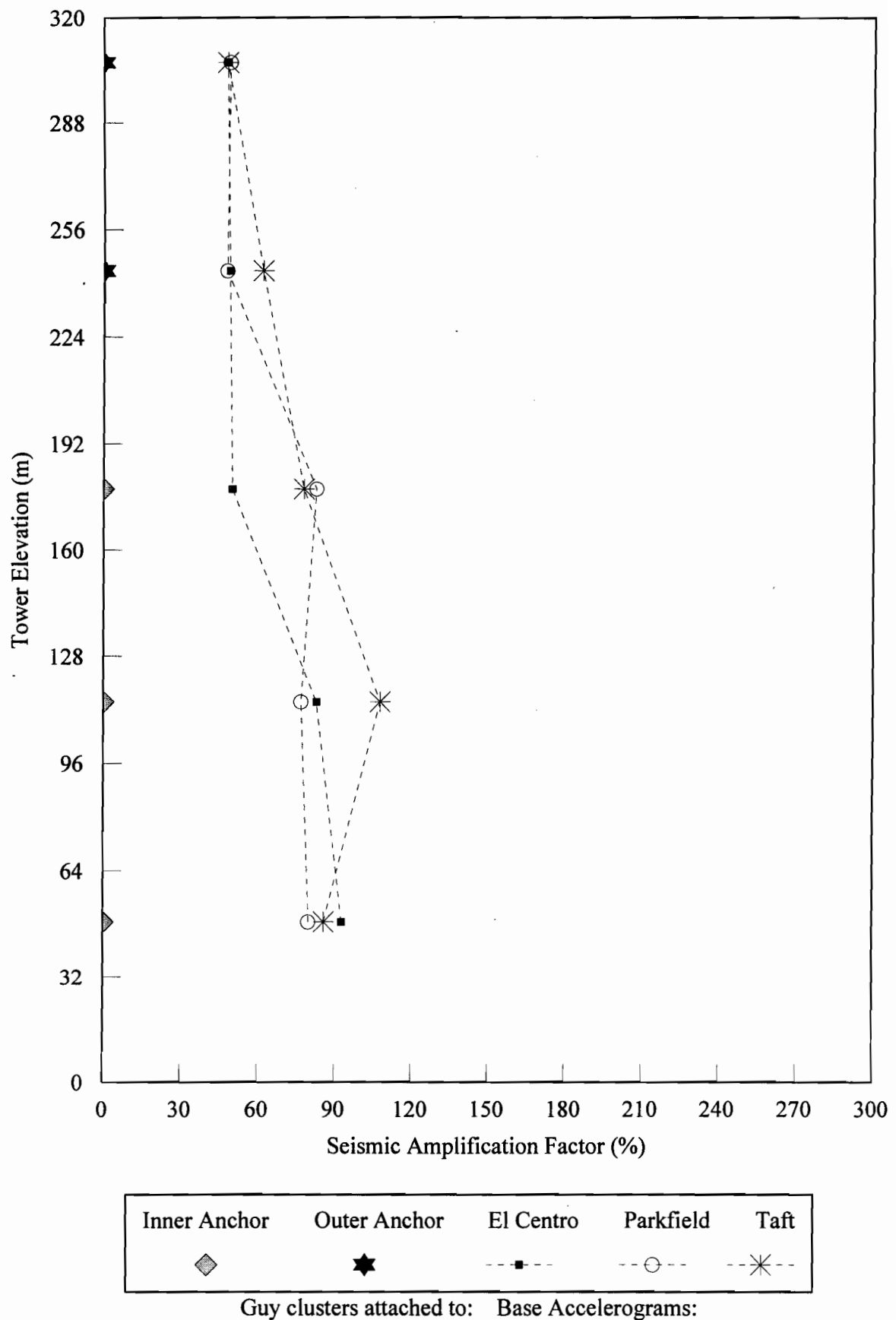
Fig. 5.52. Seismic amplification factor of cable tension in 313-m tower to three base accelerograms

198
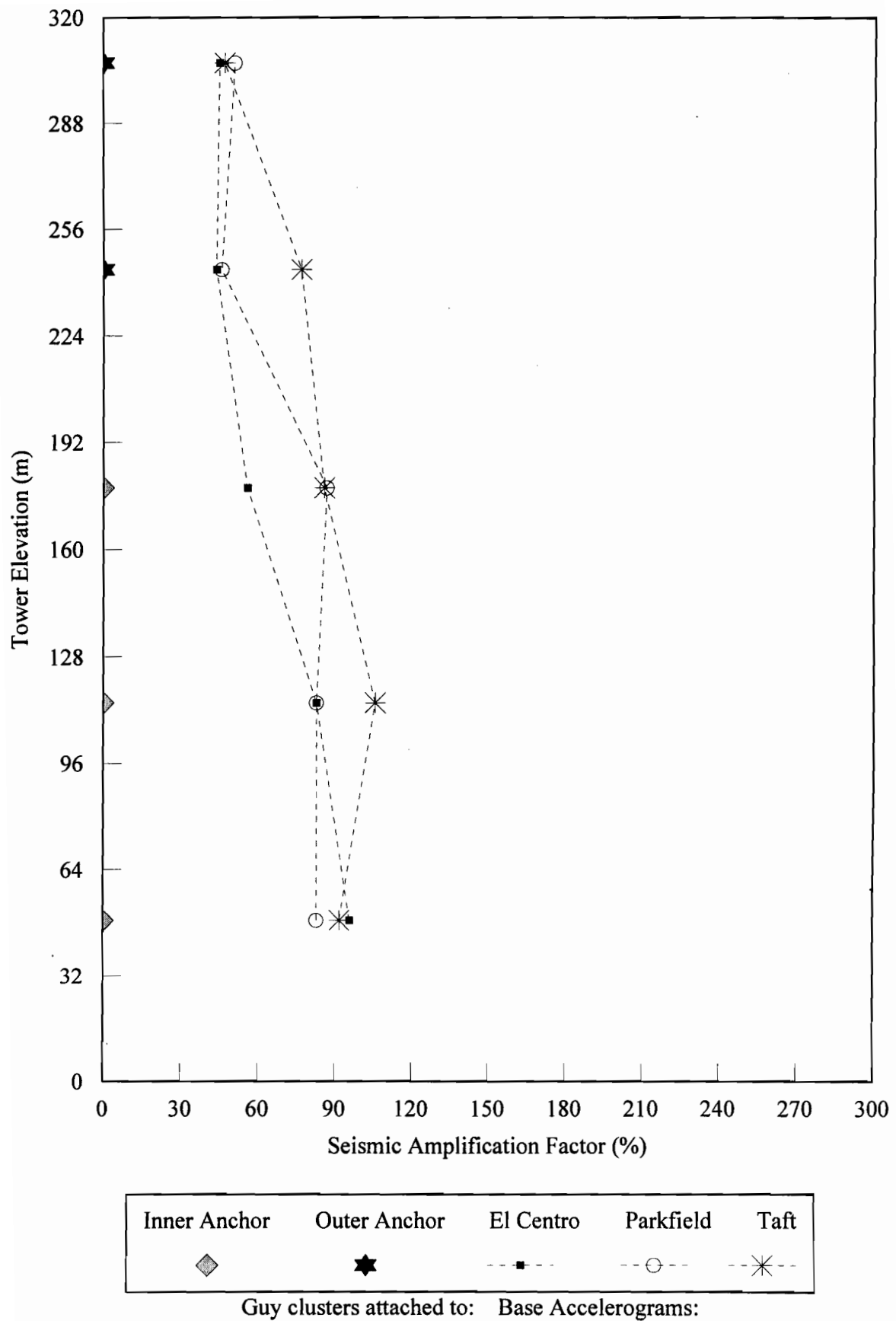
Fig. 5.53. Seismic amplification factor of cable tension in 313-m tower to three base accelerograms (Horizontal + Vertical)
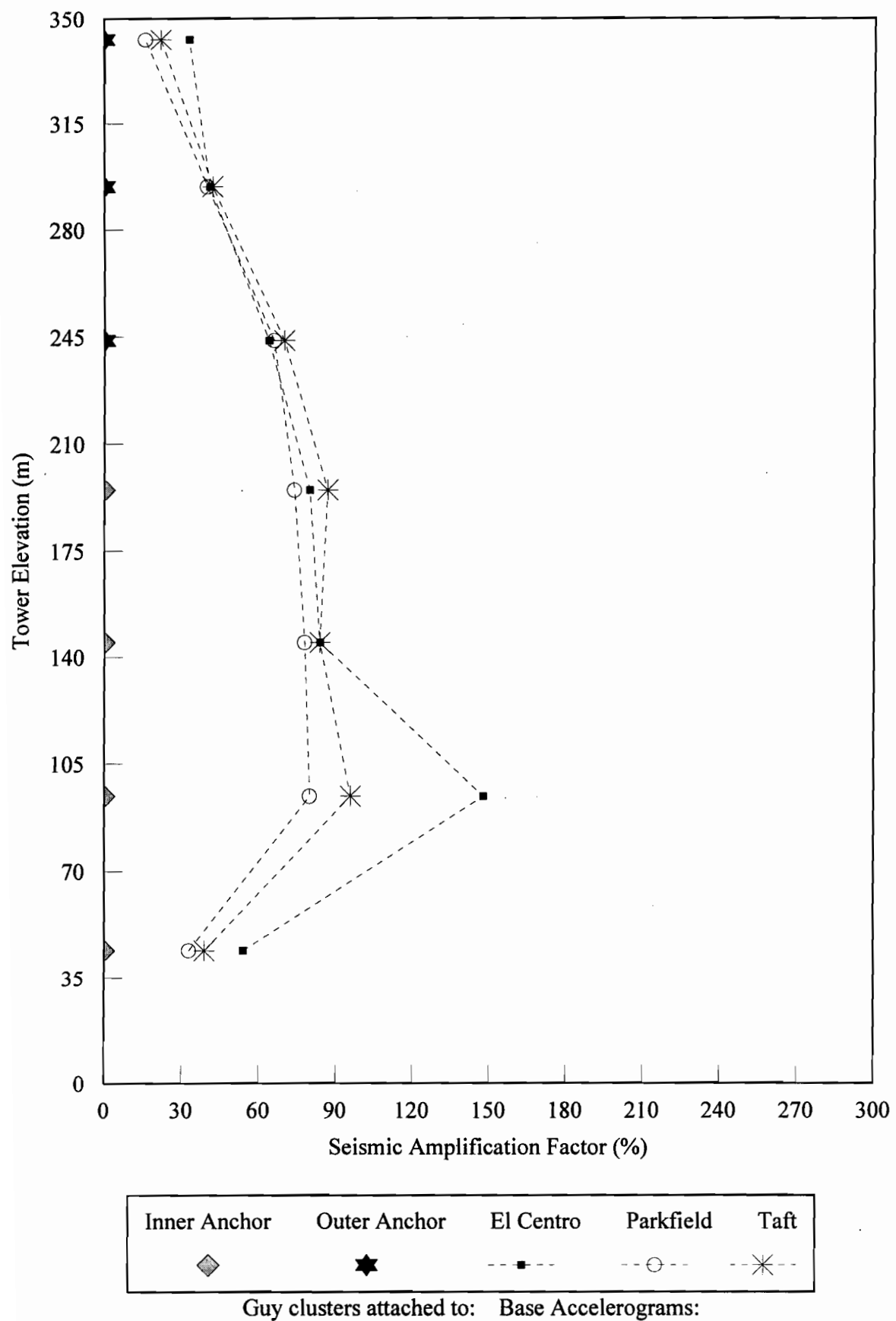
Fig. 5.54. Seismic amplification factor of cable tension in 342-m tower to three base accelerograms

200
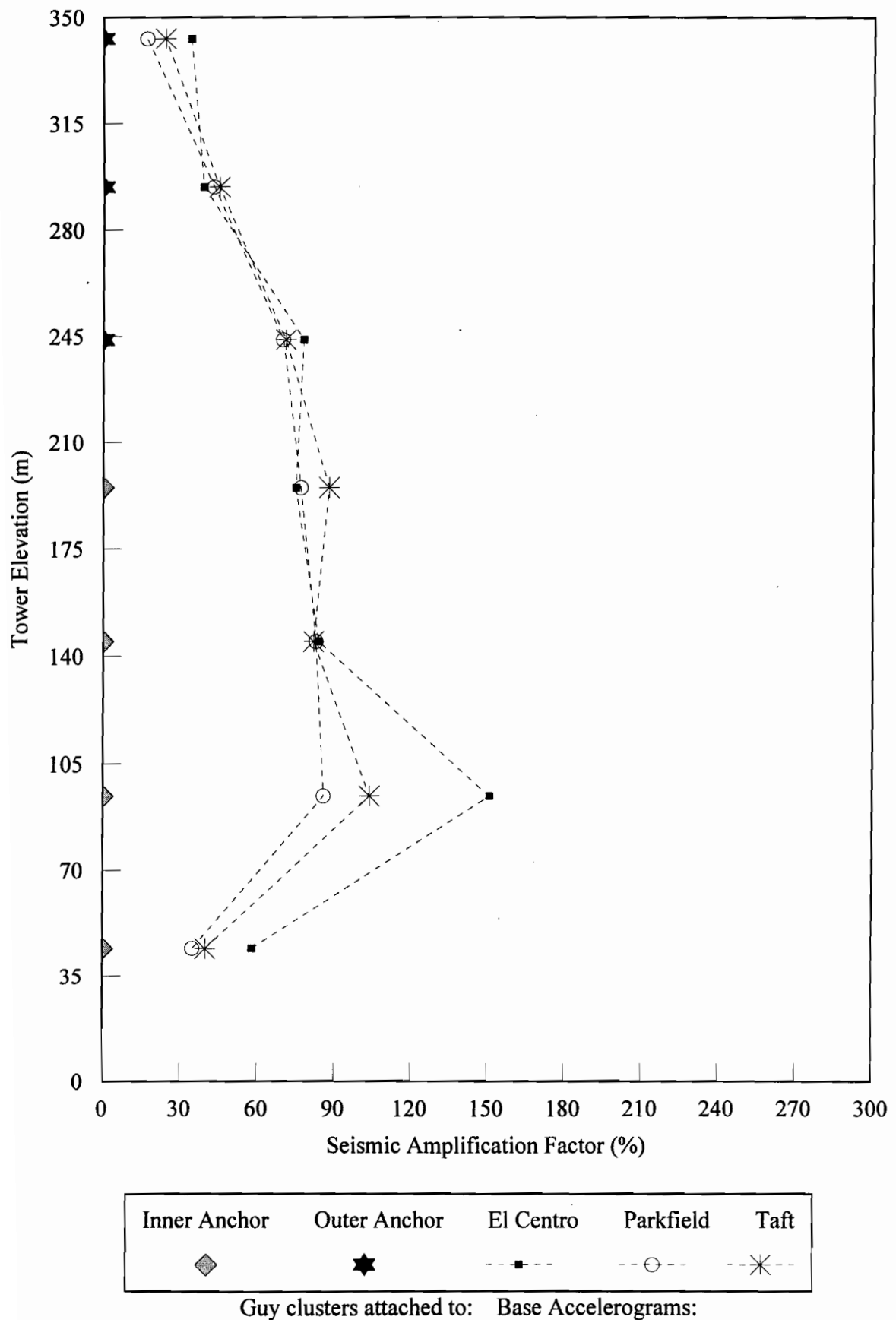
Fig. 5.55. Seismic amplification factor of cable tension in 342-m tower to three base accelerograms (Horizontal + Vertical)
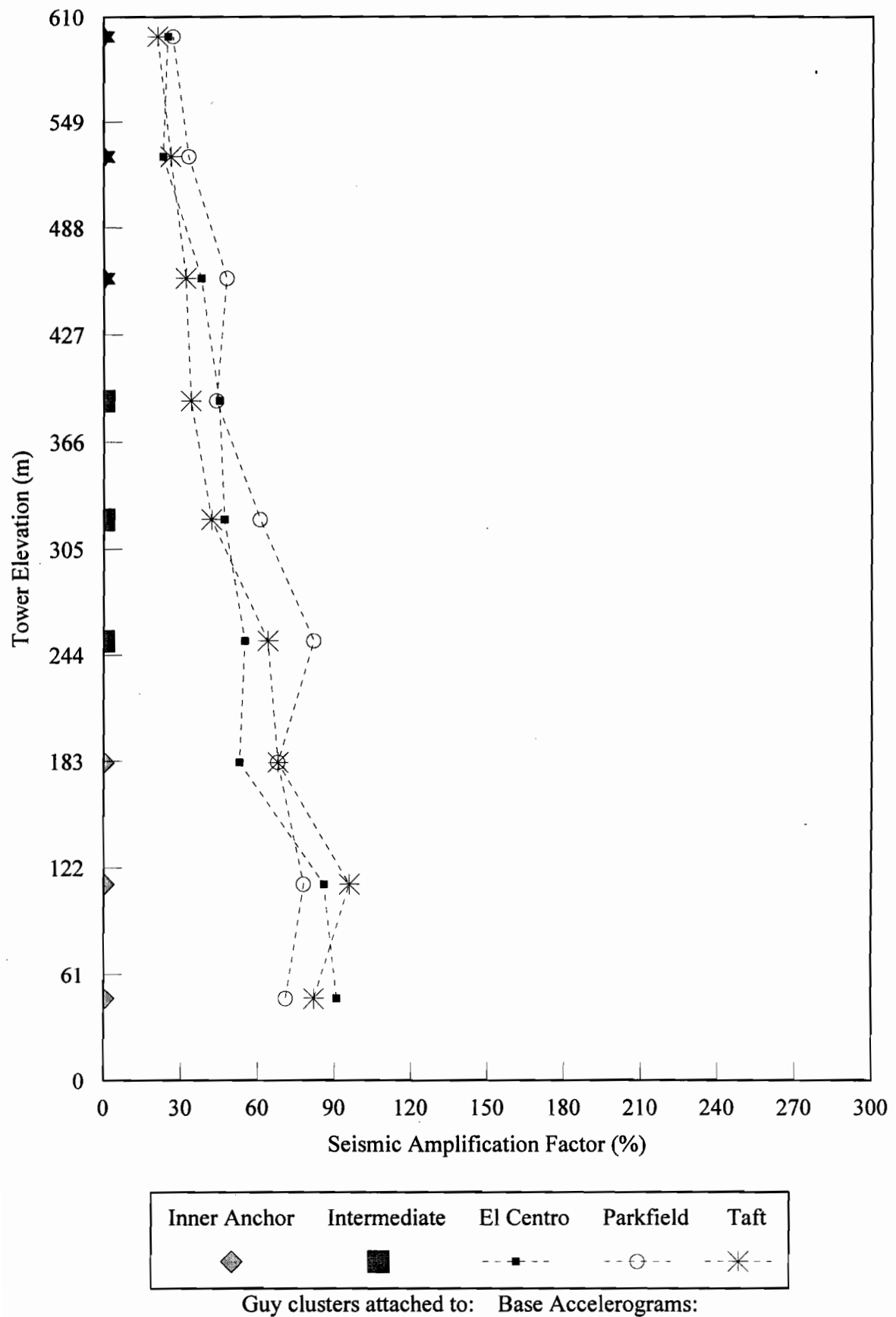
Fig. 5.56. Seismic amplification factor of cable tension in 607-m tower to three base accelerograms

202
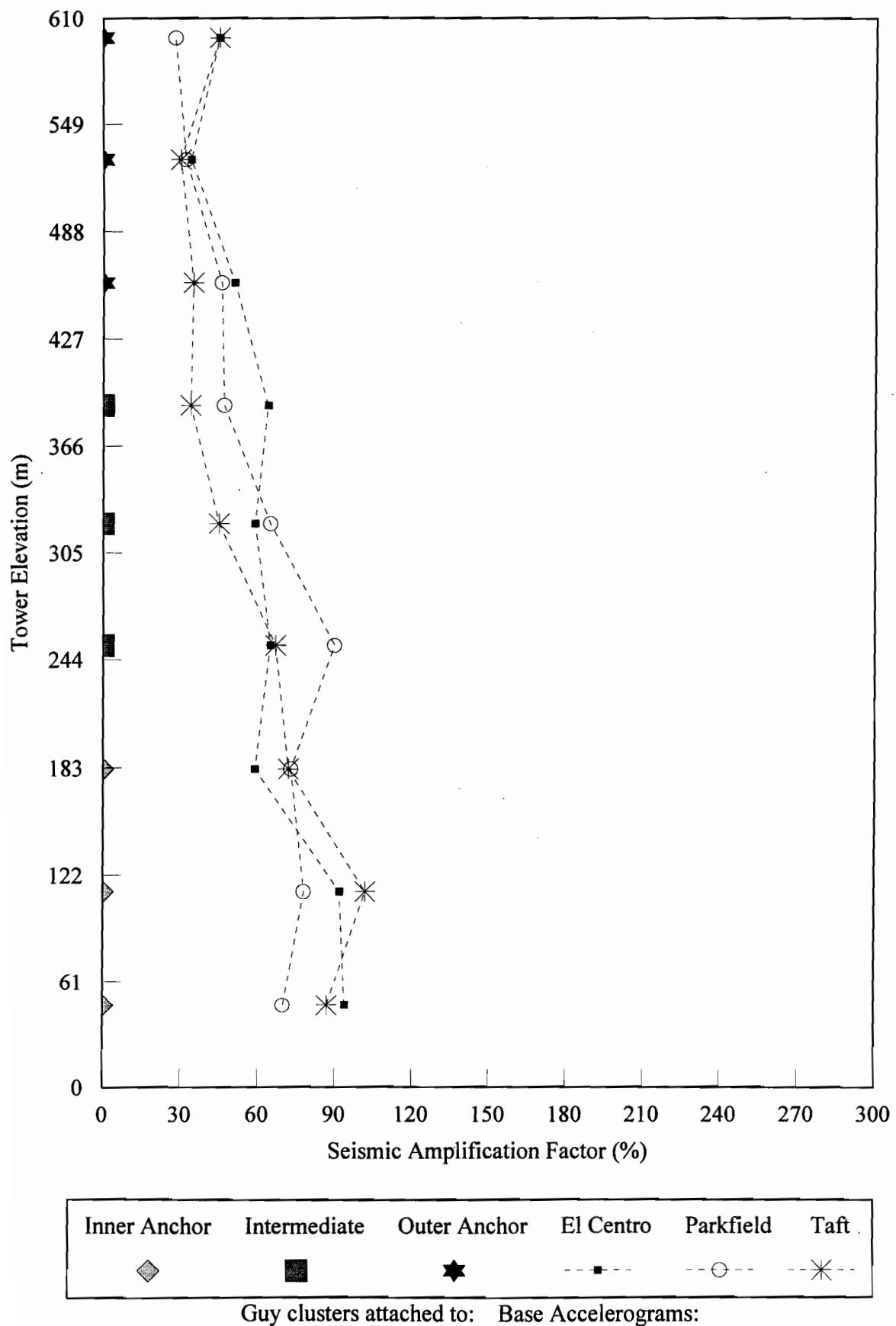
Fig. 5.57. Seismic amplification factor of cable tension in 607-m tower to three base
accelerograms (Horizontal + Vertical)

203

(313 to 607 m), the response is slightly higher, with the mast shear in the range of 13% to 17% and the corresponding bending moment in the range of 73% to 123%. As illustrated in Figs. 5.60 and 5.61, where the results are expressed in terms of tower weight, the ratios vary from 6% to 7% for the shear in the lower towers and from 36% to 48% for the bending moments. For the taller towers (313 to 607 m), the corresponding shear is in the range of 2.5% to 5% and the bending moment parameter varies from 14% to 35%.

5.3 SIMPLIFIED MODELS PROPOSED FOR SEISMIC BEHAVIOUR

5.3.1 Maximum Base Shear

Since one of the most important response indicators for design purposes is the total base shear of the structure due to earthquake loading, the maximum base shear of the towers for the three earthquake responses is investigated more precisely. Figure 5.62 summarizes the percentage ratio of maximum base shear to the total weight of the towers versus the tower height. A curve fit is suggested on the figure to predict the maximum base shear for different heights of towers in the range of 150 to 607 meters. The curve obtained has the following formulation:

$$B.S. = 28300 \ H^{-1.17}$$ (5.2)

where B.S. is the maximum base shear as a percentage of total weight of tower and H is the tower height in meters. This formula is proposed for a quick evaluation of the maximum base shear of guyed towers due to an earthquake which is comparable to the sensitivity level of the Victoria region in Canada (Peak Horizontal Ground Acceleration = 0.34g and Peak Horizontal Ground Velocity = 0.29 m/s).

204

Table 5.17. Maximum mast shear and bending moment of the towers (% of base shear)

Tower Height (m)	Max Mast Shear ---------------------- % Max Base Shear	Max Mast Moment --- % Panel Width * Max Base Shear
607	13	73
342	14	95
313	17	123
213	11	71
200	12	73
198	10	61
152	8.0	58
150	9.8	57

Table 5.18. Maximum mast shear and bending moment of the towers (% of total weight)

Tower Height (m)	Max Mast Shear ---------------------- % Total Weight	Max Mast Moment --- % Panel Width * Total Weight
607	2.5	14
342	3.7	25
313	4.7	35
213	6.3	42
200	5.8	36
198	6.7	39
152	6.6	48
150	6.8	40
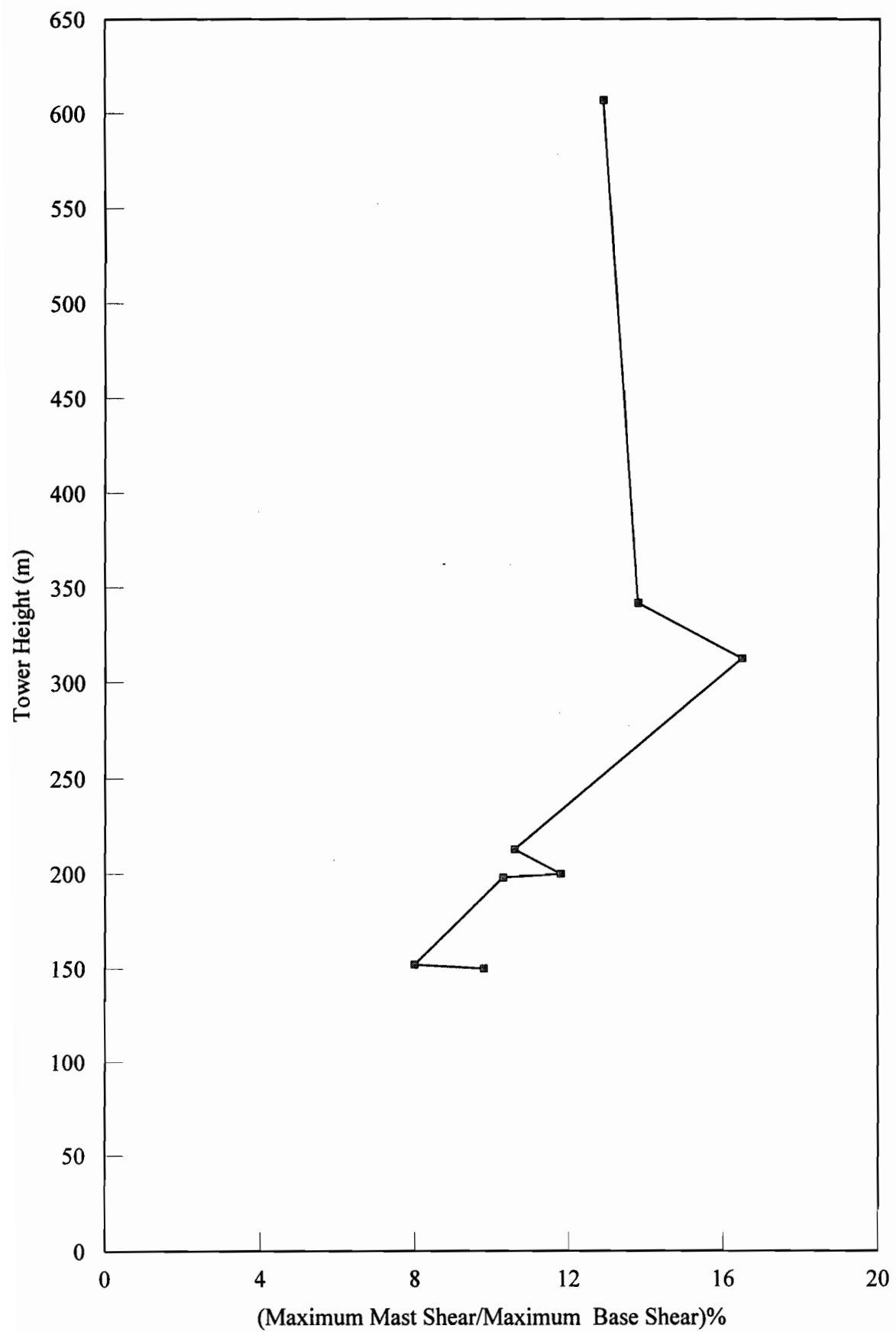
Fig. 5.58. Maximum mast shear of the towers (% of maximum base shear)
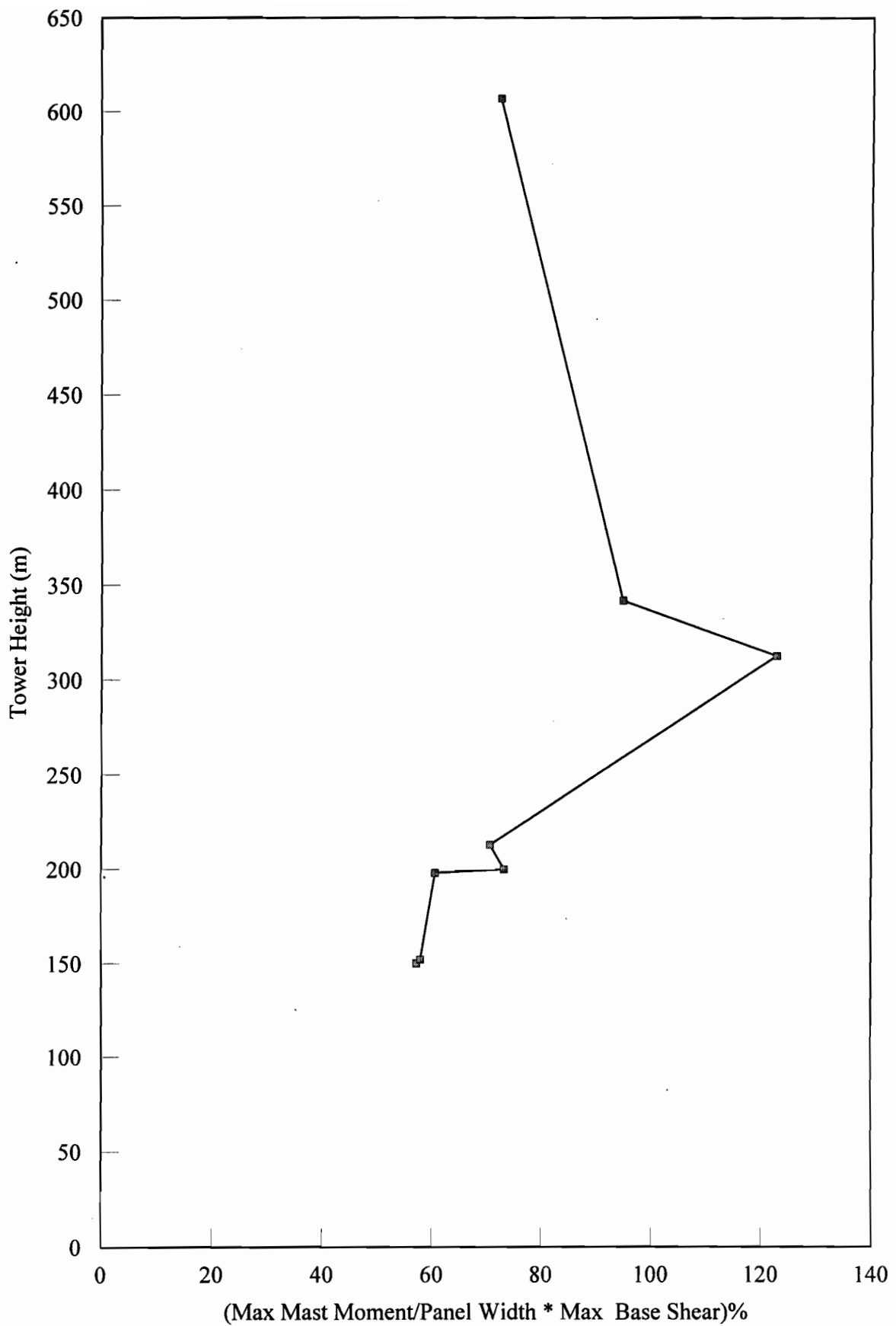
Fig. 5.59. Maximum mast bending moment of the towers (% of panel width * maximum base shear)
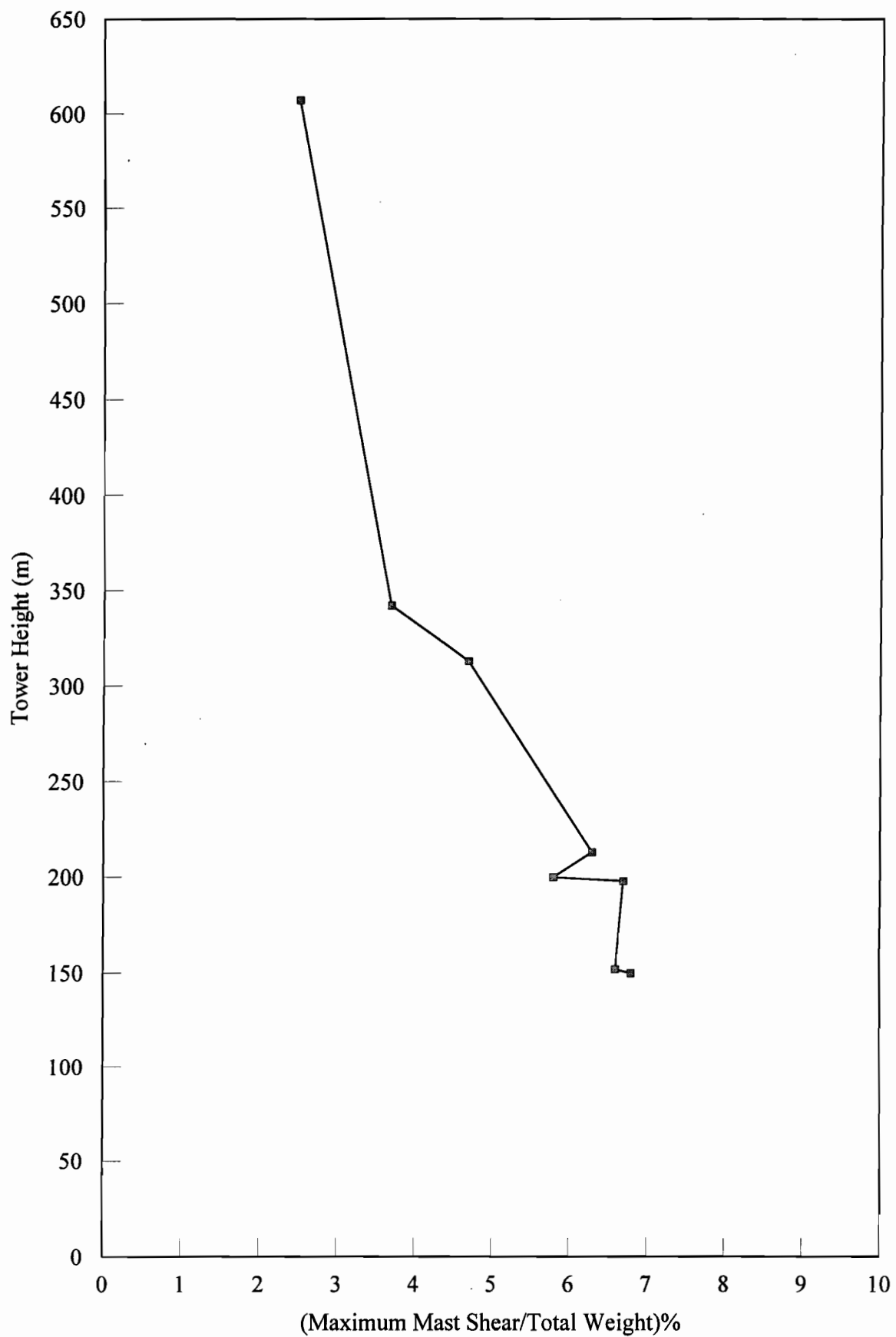
Fig. 5.60. Maximum mast shear of the towers (% of total weight)
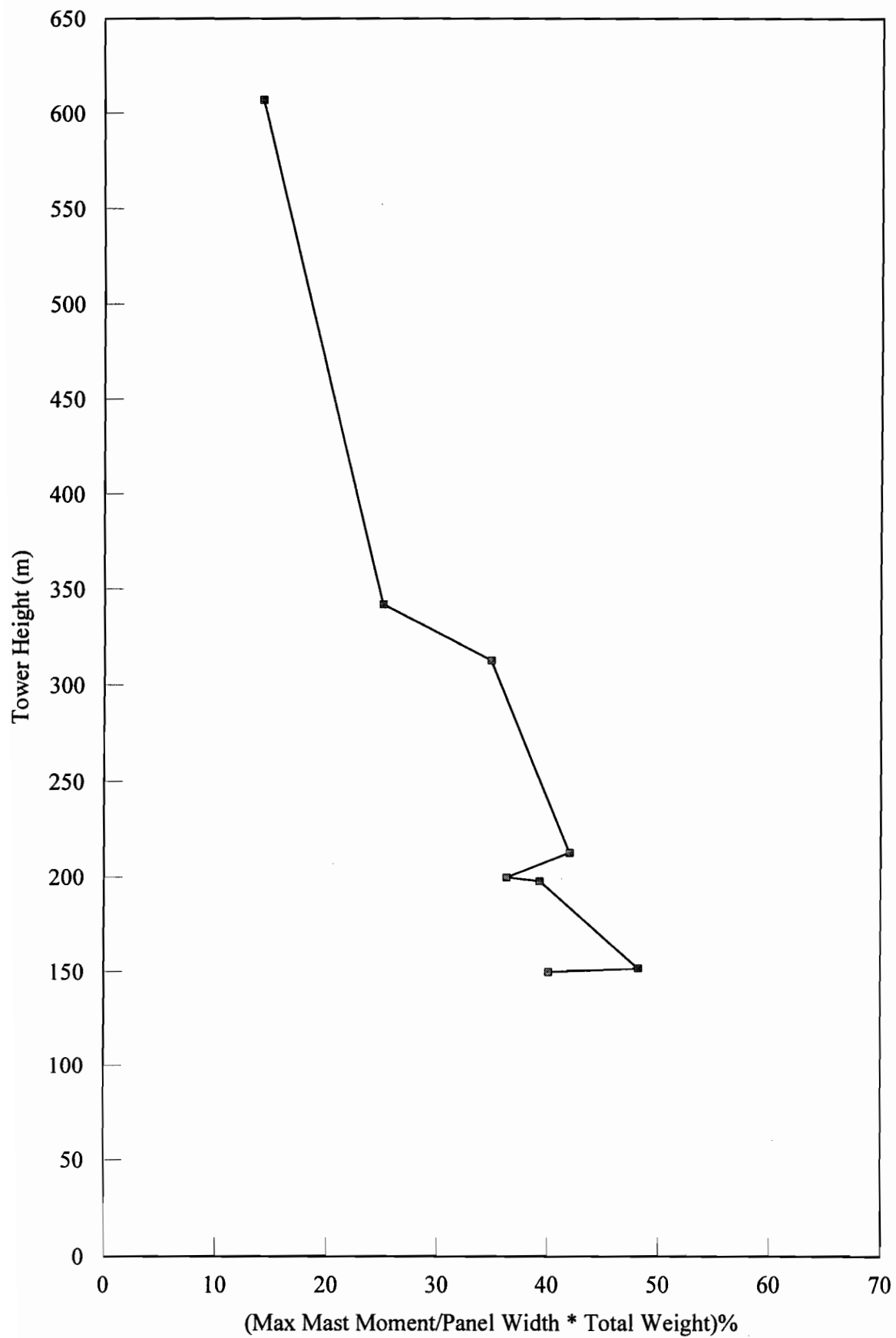
Fig. 5.61. Maximum mast bending moment of the towers (% of panel width * total weight)
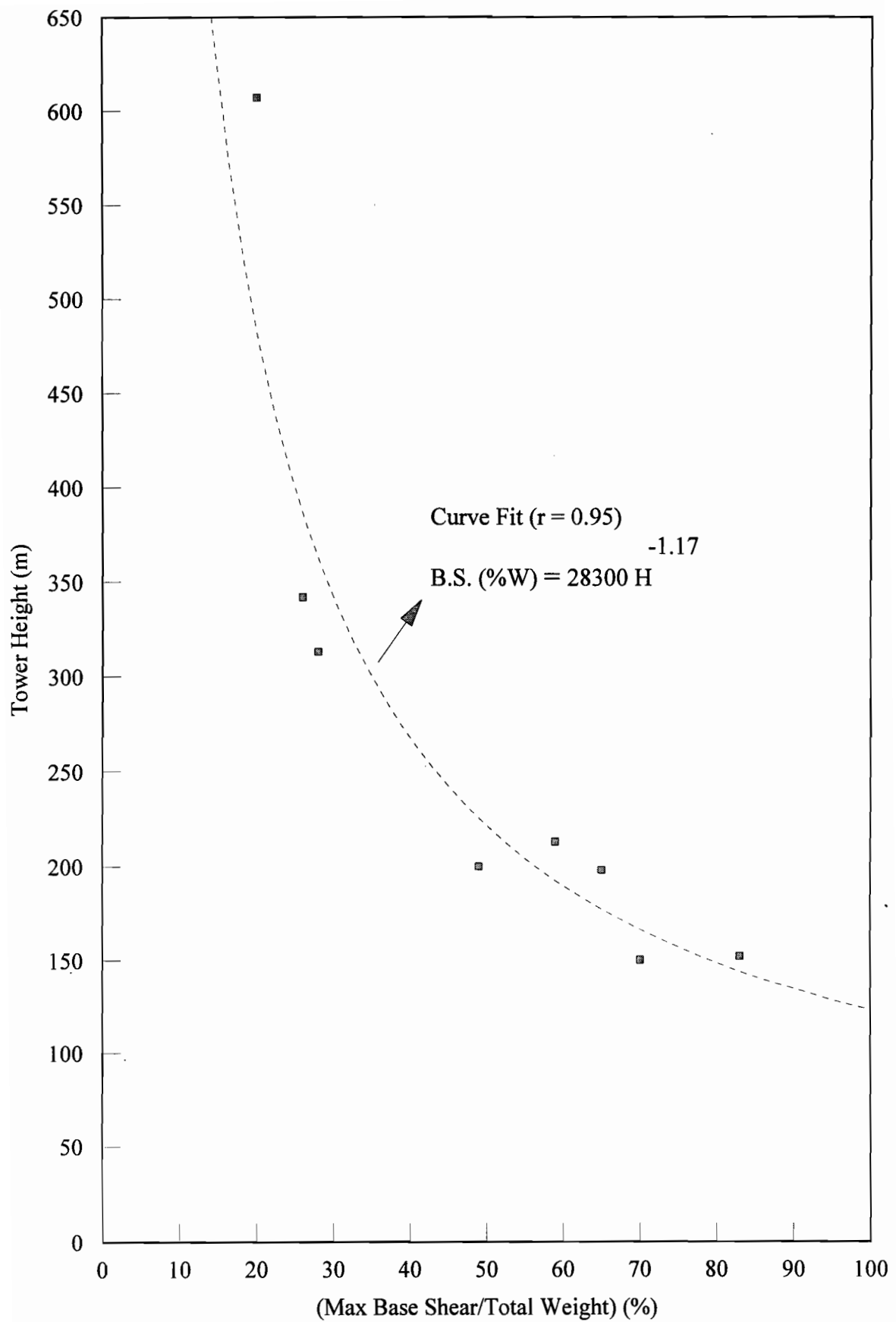
Fig. 5.62. Curve fit for maximum tower base shear versus tower height

5.3.2 Distribution of Earthquake Forces with Tower Elevation

A concept of simplified model will be developed for the distribution of earthquake forces along the tower height. In this regard, three fundamental aspects should be considered in order to propose a valid model. These aspects are as follows:

1) Predominant mode shape of mast (Figs. 5.24 to 5.33)

2) Distribution of mass of mast (Figs. 5.2 to 5.9)

3) Sensitive region between the different guy cluster groups.

As discussed in sections 5.2.1 and 5.2.2, the contribution of the mass of the cables to the total base shear and to the seismic component of the mast axial force at the base is almost constant and is small compared to that of the mast. Therefore, only the inertia of the mast has a major effect on the earthquake forces. As a result, the mass distribution of the mast is a significant factor. The predominant mode shape of the mast can represent the horizontal acceleration profile along the tower height. The presence of sensitive regions (i.e. transition zones between stay levels of different trends of lateral stiffness) can also affect the overall seismic behaviour.

Figures 5.63 to 5.70 illustrate the distribution of the horizontal earthquake forces induced along the tower elevations for all eight towers due to the three accelerograms. The earthquake forces are expressed as a percentage of the total base shear. It is noted that the scale of the abscissae is identical in the eight graphs for easier comparison. In general, the predominant mode shape of the mast, which can explain the distribution of earthquake forces along the towers, is the lowest flexural mode of the mast which is close to the first flexural mode of a simply-supported beam on flexible supports. As discussed in Section 5.1.6, this mode shape is the lowest flexural mode for the 150-m, 152-m, 198-m, 213-m and 342-m towers, and the second lowest mode for the 200-m, 313-m and 607-m towers.

The second aspect which should be used to explain the distribution of the earthquake forces is the mass distribution in the mast. For example in Fig. 5.63 for the 150-m tower, the graph of earthquake forces at the top of the tower does not follow the predominant mode shape, because at that location there is a concentrated mass (presence

211

of an outrigger) which increases the earthquake force. There is also an outrigger at the lowest third level of the 152-m tower, which explains the large earthquake force at that location in Fig. 5.64. Also, it is useful to employ the concept of the sensitive region in addition to the two other concepts in describing the nonuniform behaviour around cable Sets 4 and 5. Using the same procedure the response of all the other cases can be explained.

The above-mentioned simplified model (predominant mode shape and mass distribution) is similar to that used in building codes for seismic forces. In general, the response of a lightly damped system follows the fundamental mode shape. The main difference between guyed towers and common buildings is the shape of the predominant mode, which is close to that of cantilever beams for tall buildings, while for guyed towers it is closer to that of simply-supported beams on flexible supports. The other difference is the concept of sensitive region for guyed towers for which no reference has been made in building codes.

It is noted that the earthquake forces along the mast are an envelope of maximum amplitudes, and therefore their summation is not equal to the total base shear. The maximum earthquake force along the mast for most of the towers is in the range of 23% to 33% of the total base shear. This value is 13% of the total base shear for the 200-m tower and 42% for the 198-m tower. As a result, the total base shear of a guyed tower can be calculated approximately using equation (5.2), and the distribution of earthquake forces along the tower could be figured out by using the three concepts explained above.

Recall that in the absence of better guidelines, the IASS (IASS, 1981) suggested to use the seismic design provision of usual buildings for the earthquake effects of guyed towers. The distribution of base shear along the tower based on usual building codes would therefore be according to the lowest flexural mode of a cantilever structure. This is not reconcilable with the results of this study.
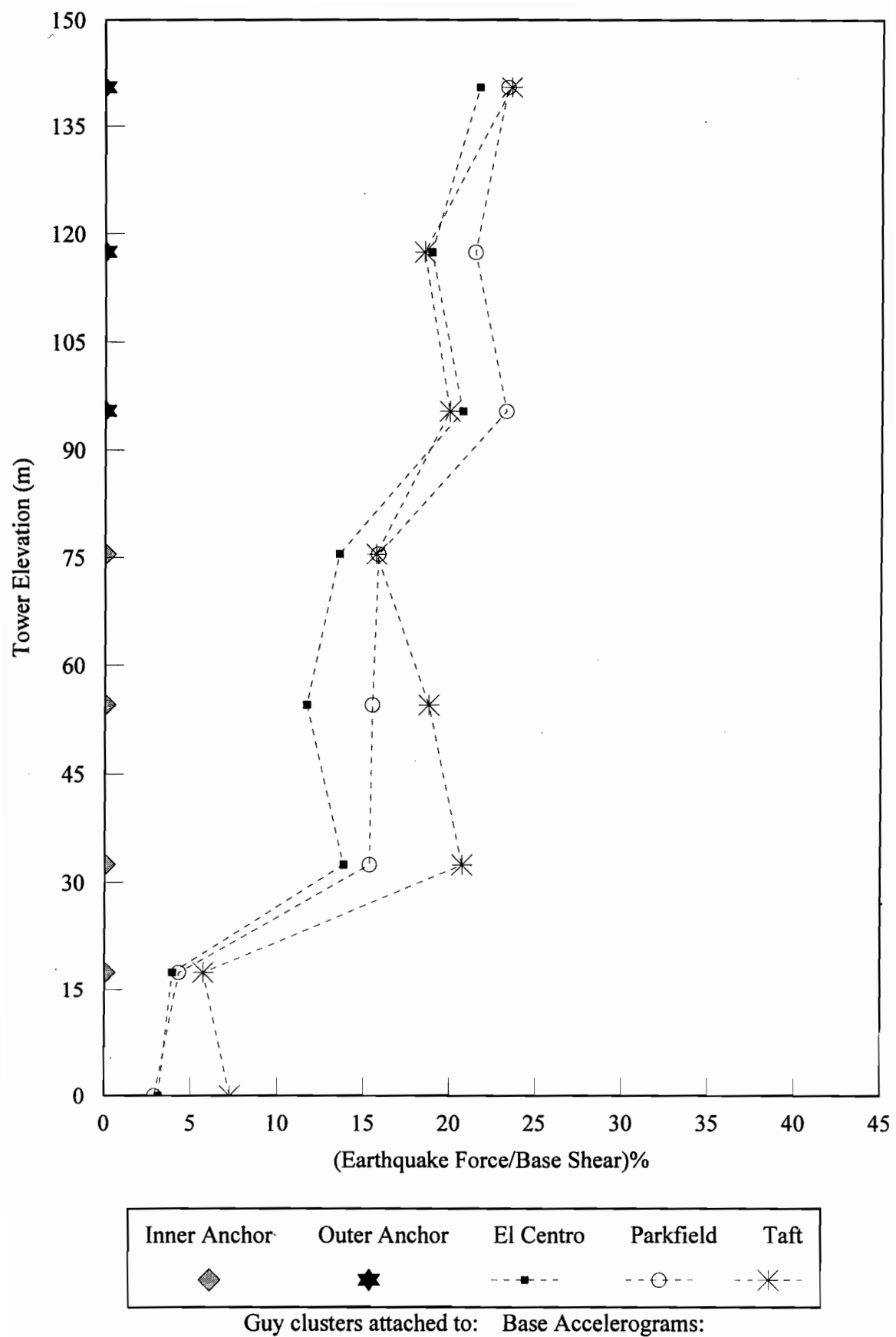
Fig. 5.63. Distribution of earthquake forces along height in 150-m tower

213
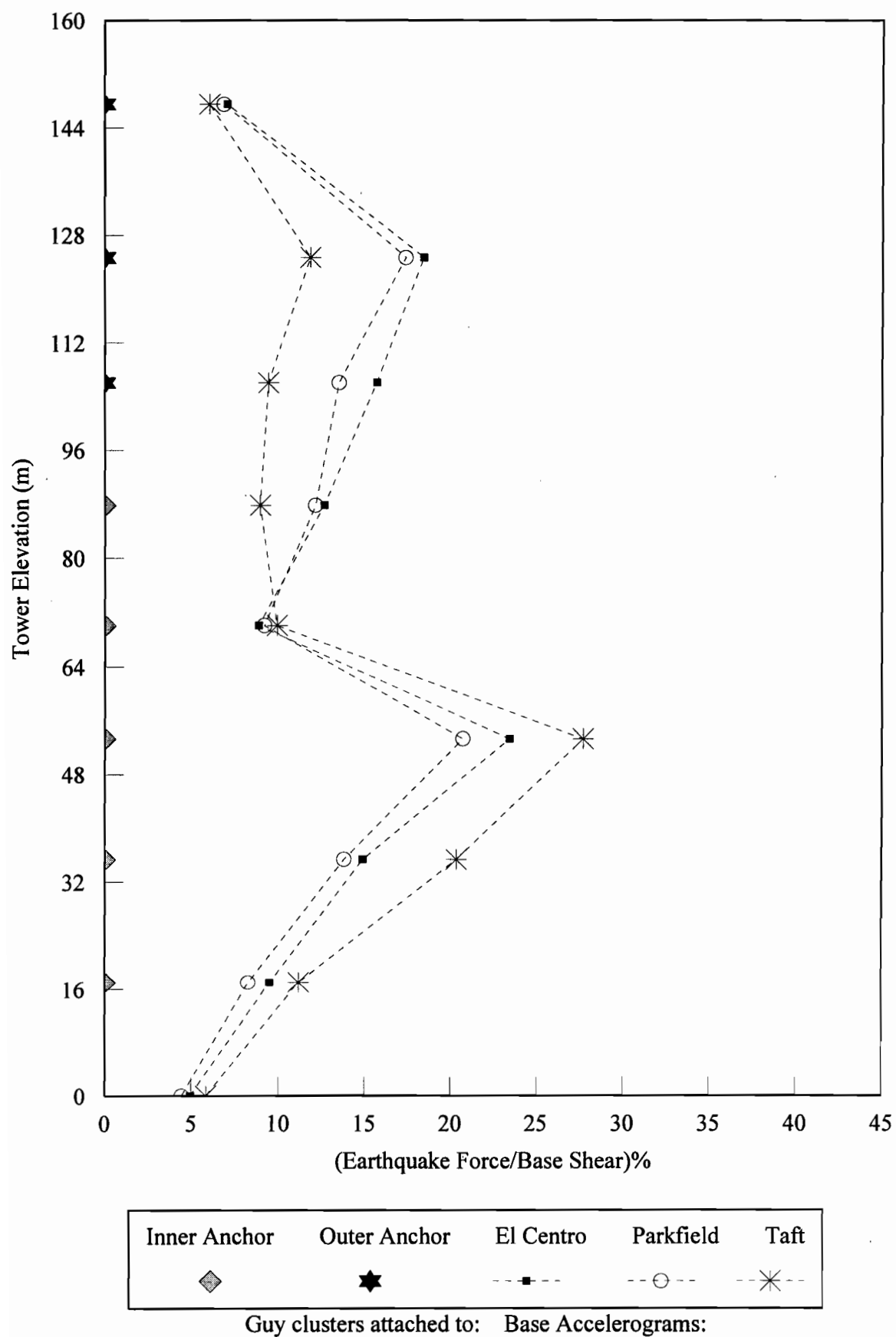
Fig. 5.64. Distribution of earthquake forces along height in 152-m tower

214
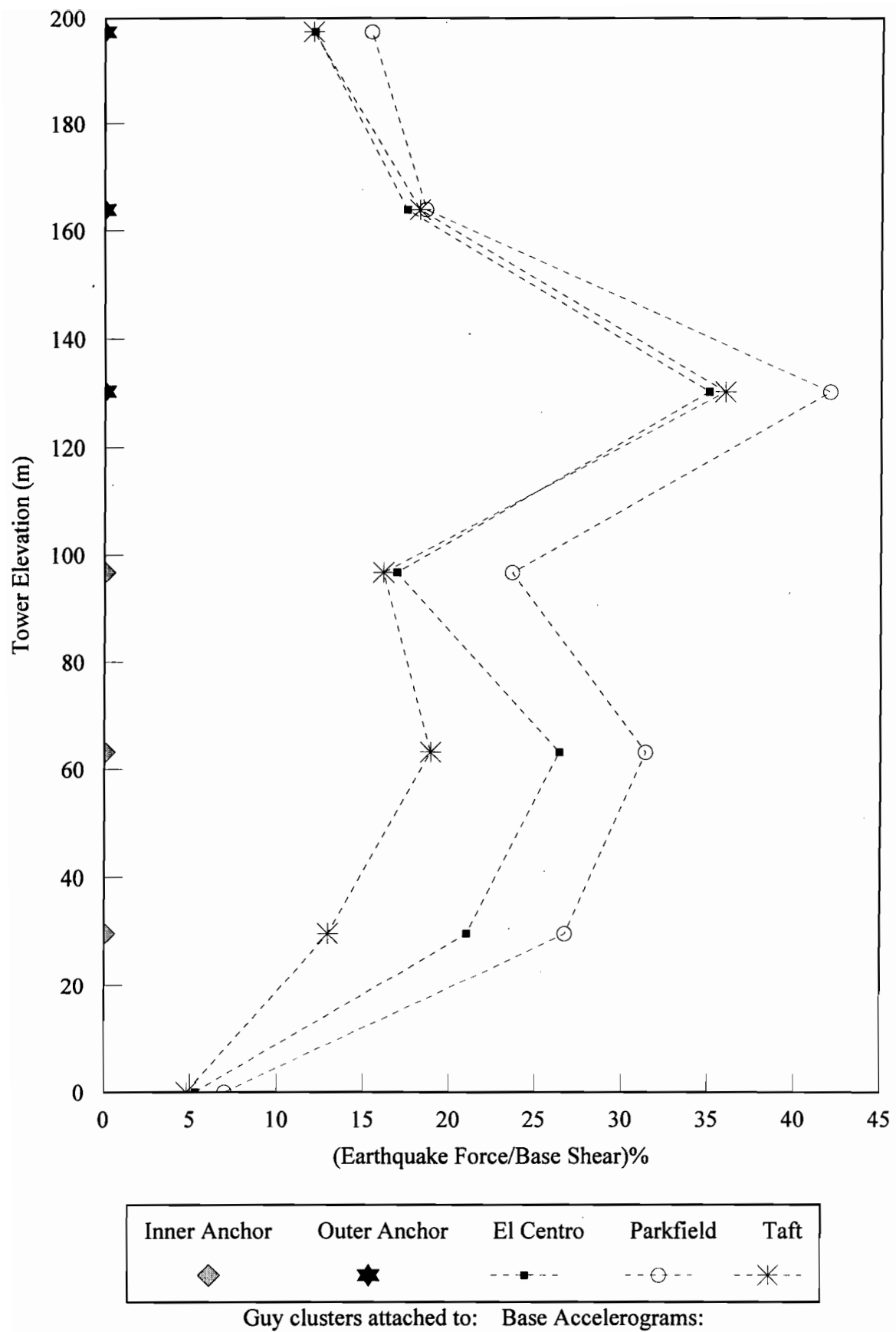
Fig. 5.65. Distribution of earthquake forces along height in 198-m tower

215
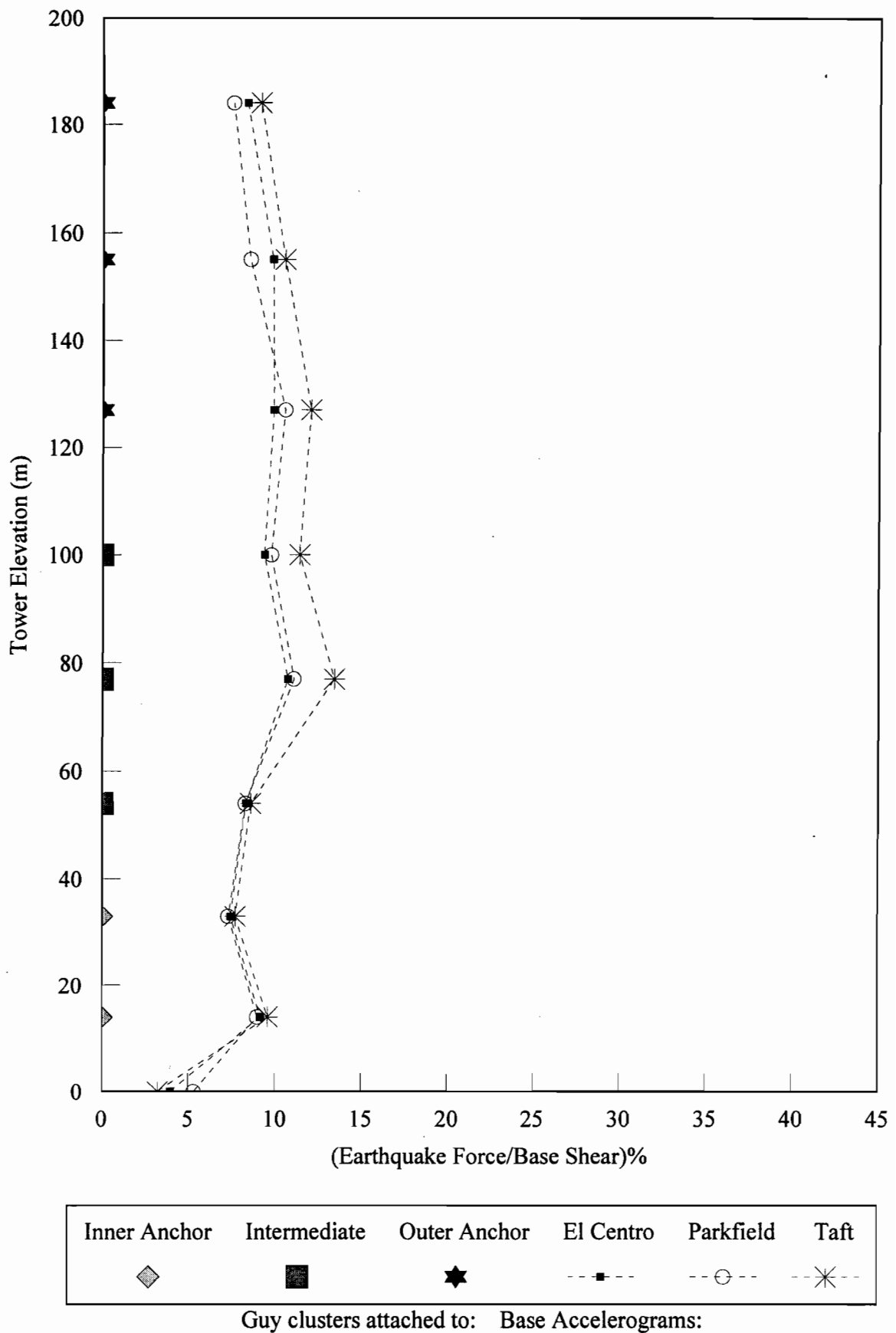
Fig. 5.66. Distribution of earthquake forces along height in 200-m tower

216
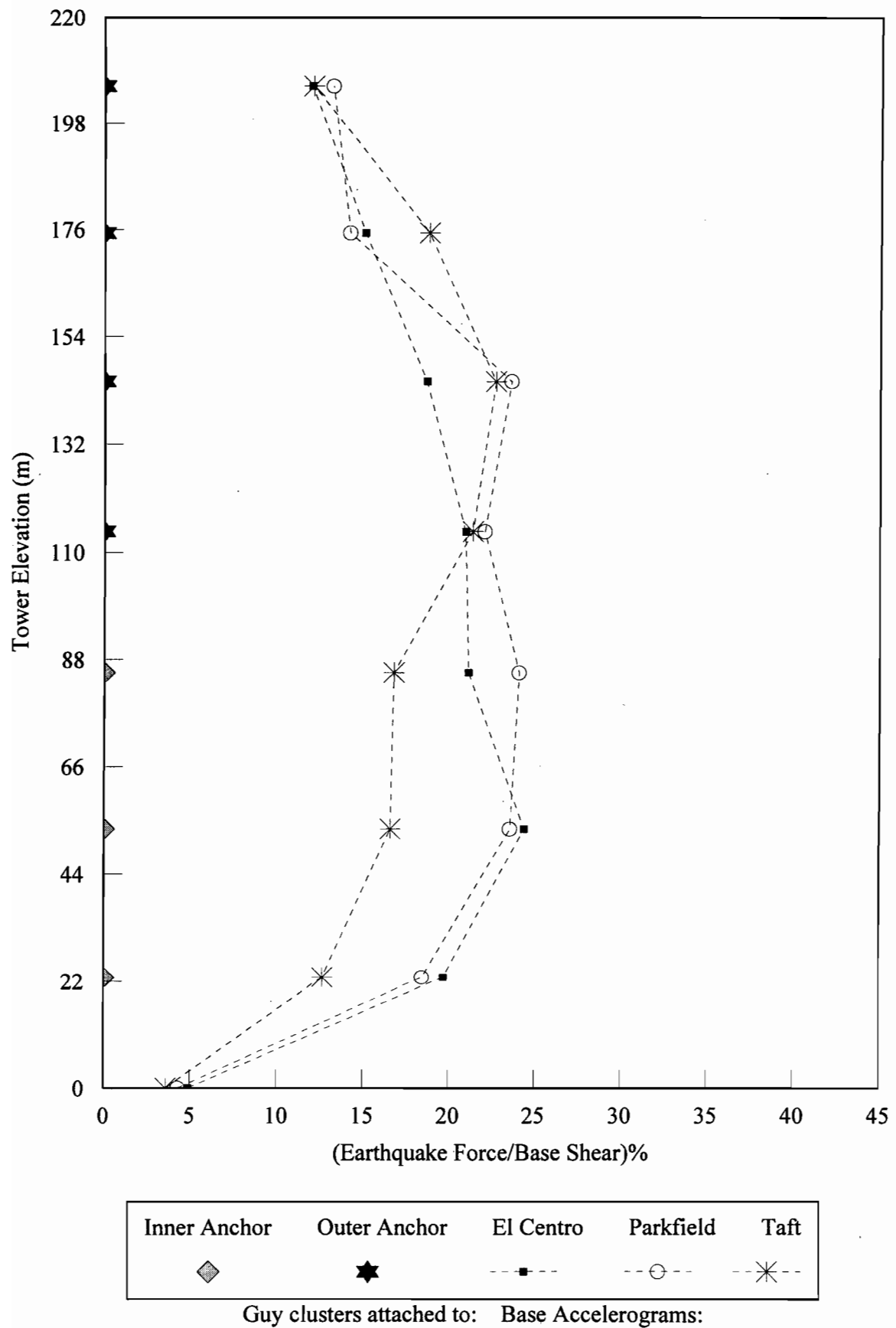
Fig. 5.67. Distribution of earthquake forces along height in 213-m tower
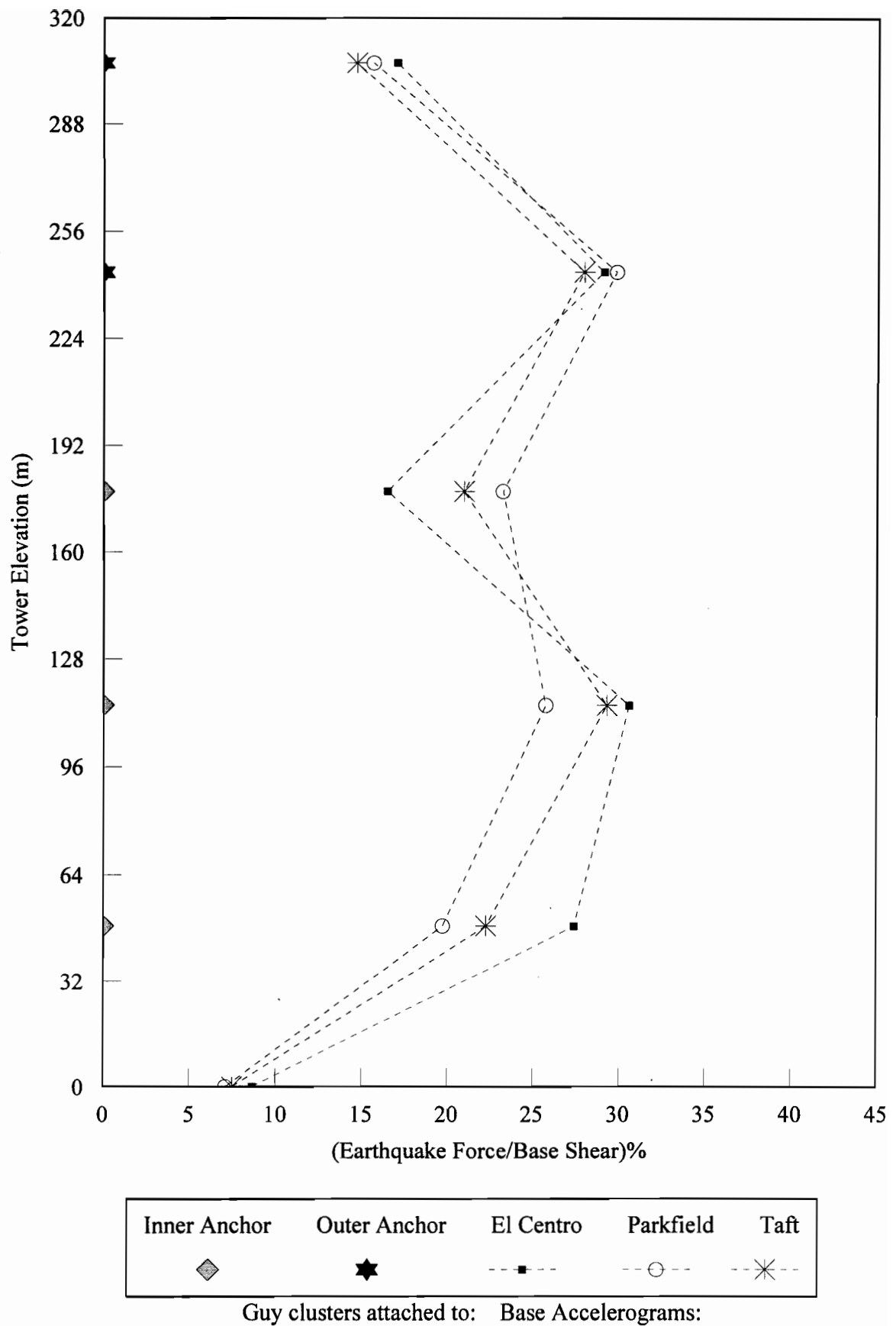
Fig. 5.68. Distribution of earthquake forces along height in 313-m tower

218
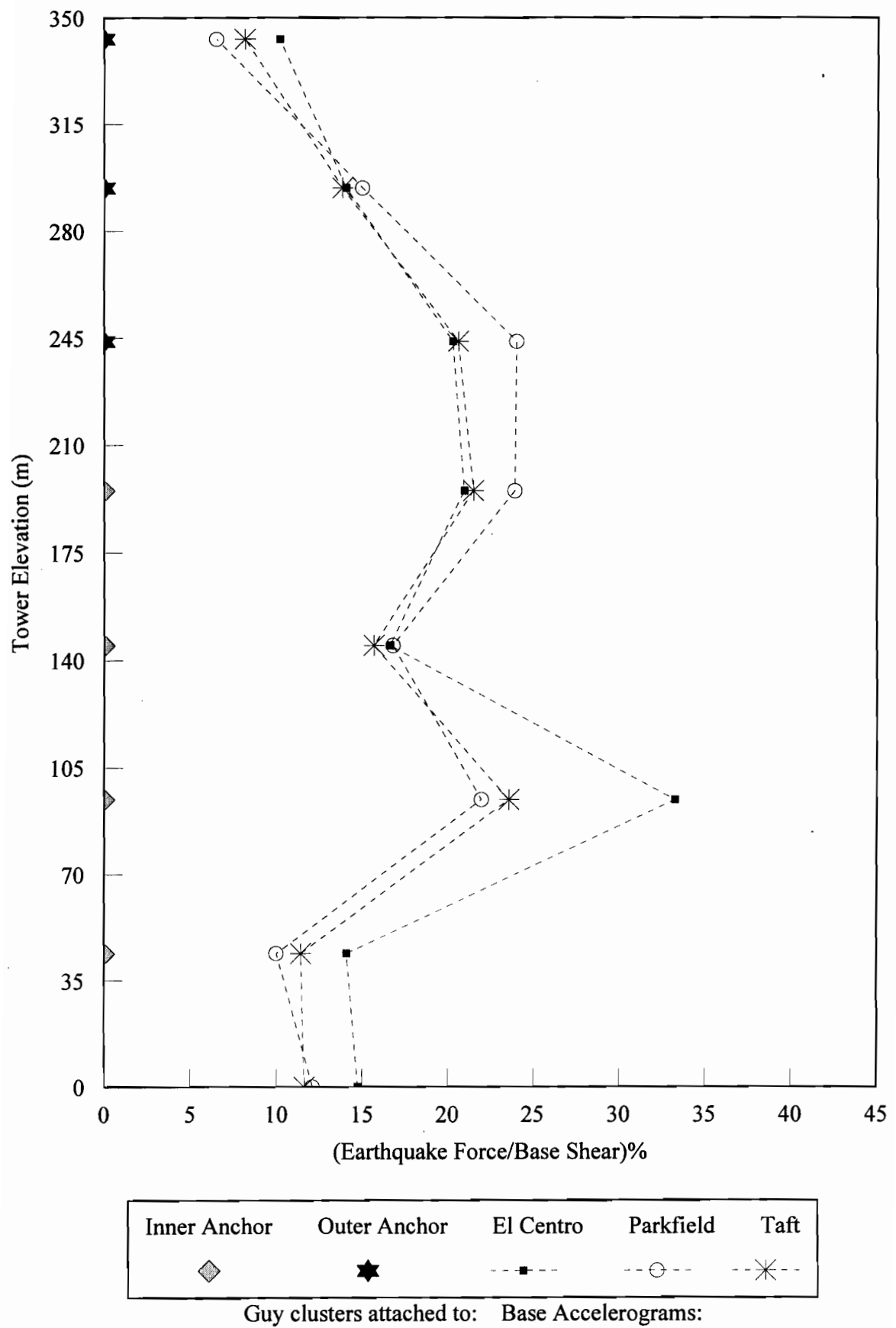
Fig. 5.69. Distribution of earthquake forces along height in 342-m tower

219
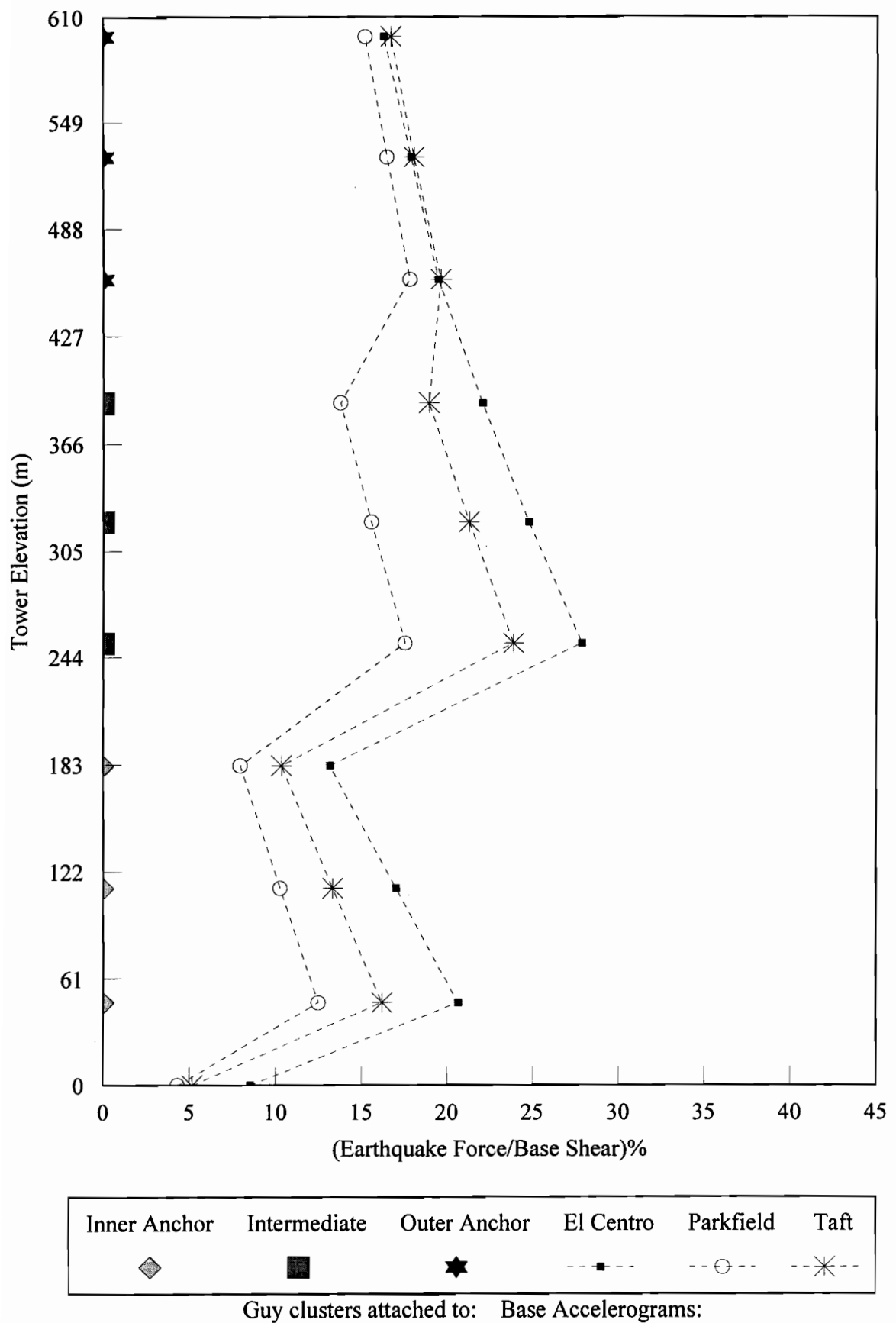
Fig. 5.70. Distribution of earthquake forces along height in 607-m tower

5.3.3 Distribution of Maximum Dynamic Component of Mast Axial Forces with Tower Elevation

The distribution of the maximum dynamic component of the axial forces in the mast along the height for all eight towers is summarized in Fig. 5.71. The response to combined horizontal and vertical earthquake motions is considered here. In this graph the horizontal axis represents the ratio of the maximum dynamic component of the mast axial forces to the maximum dynamic component of mast base axial force. This ratio is expressed as a percentage. The vertical axis shows the ratio of the sectional elevation of mast to the total tower height. It can be seen in Fig. 5.71 that the results of all the towers are relatively close to each other and form a narrow band. They can be appropriately (and conservatively) represented by a parabolic curve fit (darker line in Fig. 5.71). The parabola has the following equation:

$$(P_{dyn}/\text{Max B.A.}) = 100 - 95 \ (h/H)^2 \tag{5.3}$$

where $(P_{dyn}/\text{Max B.A.})$ is the percentage ratio of the maximum dynamic component of axial force in the mast at a section of given elevation (h) to the maximum dynamic component of the axial force at the base of the mast. It is noted that H is the total height of the tower.

As discussed in Section 5.2.2, the maximum dynamic component of the axial force at the base of the mast is almost constant at about 80% of the total weight of the towers (except for the 200-m tower).

$$(P_{dyn}/\text{Max B.A.}) = 100 - 95\,(h\,/\,H)^{2}$$
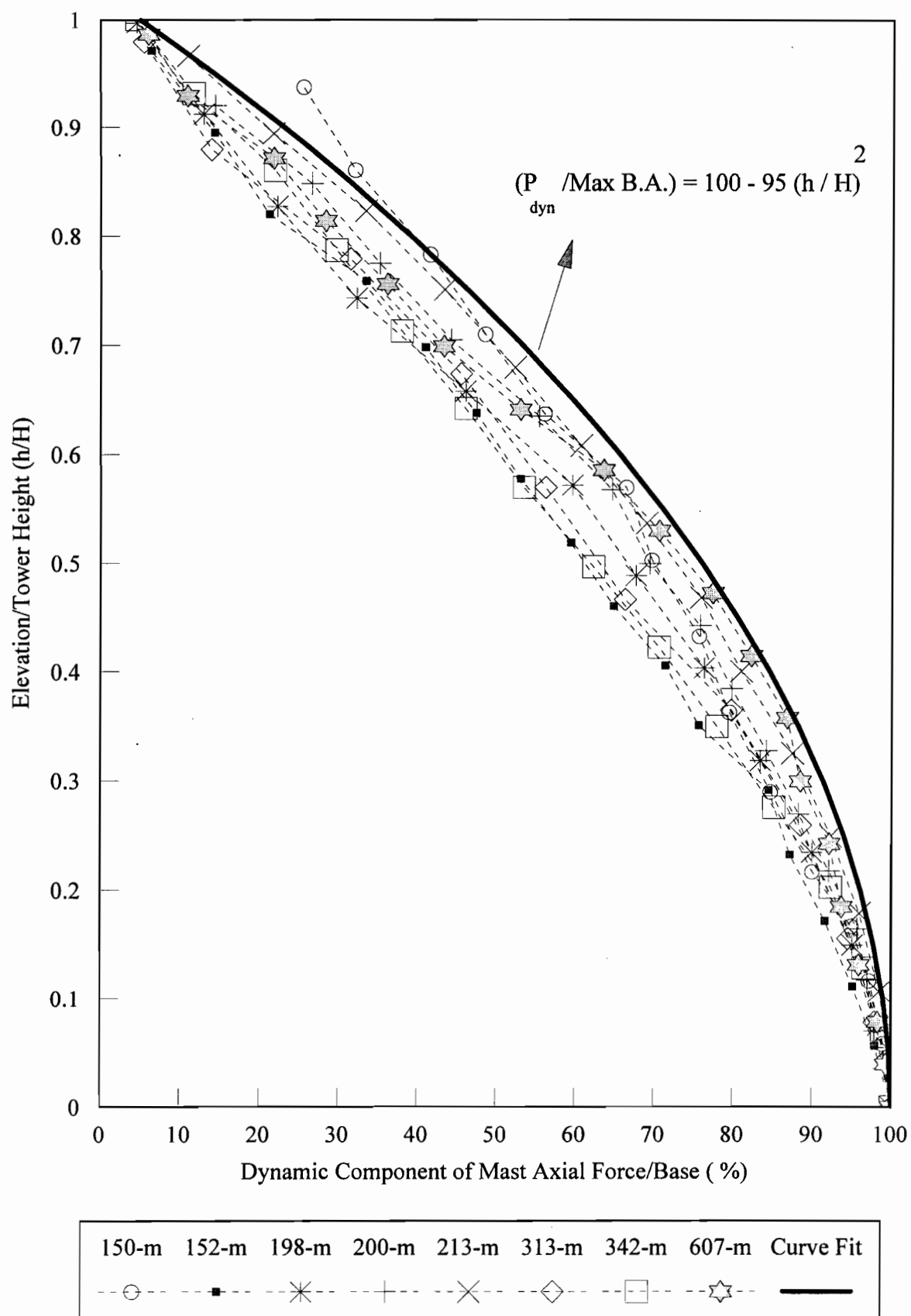
Fig. 5.71. Distribution of maximum dynamic component of mast axial forces along height (Horizontal + Vertical)

5.4 SEISMIC SENSITIVITY INDICATORS

Some seismic sensitivity indicators can now be proposed which may be used by tower designers to assess whether a particular tower is sensitive to the earthquake effects, and if so, whether a detailed nonlinear modelling study is necessary. The followings are the important aspects of tower behaviour for seismic sensitivity:

1) Total base shear
2) Dynamic component of mast axial force
3) Seismic amplification factor of cable tension.

As shown in Fig. 5.35, guyed towers shorter than 250 meters exhibit a relatively large base shear in the range of 40% to 80% of their total weight. Therefore, from the viewpoint of total base shear, this range of guyed towers may be sensitive to seismic effects. Since the amount of the total base shear can be predicted (for the seismicity level studied here), a detailed modelling study may not be necessary. As shown in Fig. 5.38, the contribution of the mass of the cables and the mast to the base shear is unpredictable for the 607-m tower, and therefore a detailed study may be necessary to assess the response of towers of 400 meters and taller.

As illustrated in Fig. 5.39, the maximum dynamic component of the axial force at the base of the mast for all the towers is about 80% of their total weight, with the exception of the 200-m tower. From the point of view of strength and stability of the mast, these guyed towers may be sensitive to earthquake effects. However, the behaviour of the 200-m tower is unpredictable, mainly because it has a relatively small initial cable tension compared to that of the other towers. This fact can also be explained from Table 5.3 in which the 200-m tower has a relatively large initial cable sag. Therefore, guyed towers with relatively small initial cable tensions (i.e. much less than 10% of their ultimate tensile strength) may be very sensitive to seismic effects in the axial direction. For these towers, a detailed modelling study would be necessary.

Also, as shown in Figs. 5.48 and 5.49 and explained in section 5.2.3, the 200-m tower has a significant seismic amplification factor of cable tension compared to that of the other towers. This also confirms the necessity of a detailed modelling study for this

tower.

Comparing Figs. 5.48 and 5.49, it can be concluded that the cables are more excited by the Taft accelerogram than the other two in the case of horizontal earthquake motion. However, when combined vertical and horizontal earthquake motions are studied, the Parkfield accelerogram governs the cable response. For this combined load case, as shown in Fig. 5.39, the axial effects in the mast of the 200-m tower are largest with the Taft accelerogram. Comparing Figs. 5.39 and 5.49, this time the Taft accelerogram governs for the vertical behaviour of mast, while the Parkfield earthquake governs for the vertical oscillation of the cables. In conclusion, the behaviour of the 200-m tower is not predictable and only a detailed modelling study can provide insight to the response.

It was mentioned in Section 2.3 that Moossavi Nejad (1996) had recently reported the seismic response of a 327-m tower. From the results of his paper, the initial tension of the guy cables was found to be relatively small, around 3.5% of the ultimate tensile strength. The maximum dynamic component of the base mast axial force of the tower was calculated and found to be around 100% of the total weight of the tower. This conclusion is confirming the proposed idea of this thesis regarding the sensitivity of guyed towers with relatively small initial cable tension (i.e. inferior to 10% of the ultimate tensile strength) to vertical seismic load. It should be recalled that the maximum intensity of the vertical accelerations used in this thesis is 75% of 0.34g (Peak Horizontal Ground Acceleration of Victoria). When comparing this value (0.26g) to the 0.2g used by Moossavi Nejad, it is seen that his result for the ratio of the maximum dynamic component of mast base axial force to the total weight of tower (100%) is comparable to the corresponding result of this thesis for the 200-m tower (125%). Also, from the results of Moossavi Nejad, the seismic amplification factor of the cable tension was found to be in the range of 55% to 250% which is comparable with that is obtained in this thesis for the 200-m tower (i.e. 90% to 290%). It is worth mentioning that in Moossavi Nejad's work the maximum axial force at the base of the mast due to the earthquake load was found to be much larger than the corresponding result of the static wind load analysis. However, the maximum tensions in the guy cables due to the earthquake load were smaller (but comparable) than those of the static wind load analysis.

224

According to the Canadian Standard CAN/CSA-S37-94 for structural design of antenna-supporting structures, the initial cable tension (at the anchorage points) is normally 10% of the ultimate tensile strength. However, it may vary from 8% to 15%. Because of the temperature variations and some other practical reasons, there may be a significant difference between the design value of the initial tensions and their actual field value. As a result, guyed towers with initial cable tensions of much less than 10% of the cable ultimate tensile strength (say 5%) may exist in reality. A recent study reported by Wahba et al. (Wahba et al., 1996) is addressing the issue of the variability of the initial guy tension. They have investigated the effect of changing the initial cable tension on the design of guyed towers under wind load. Variations from 5% to 20% of the ultimate tensile strength of the cables have been studied. They have found some important effects from the variation of initial tension in the guys on the design of guyed towers under wind load.

CHAPTER 6

CONCLUSIONS

6.1 SUMMARY OF MAIN CONCLUSIONS

This chapter summarizes the findings of this thesis. It should be recalled that all the results are obtained for the seismicity level of the Victoria region in Canada with PGA = 0.34g and PGV = 0.29 m/s. The horizontal accelerograms with 75% of their amplitude are used for the vertical earthquake. The height of the guyed towers studied in this research varied in the range of 150 to 607 m. Since these guyed towers exist and are typical of other towers, some of the observations can be generalized. However, whenever a reference is made to the magnitude of a response indicator, it should be kept in mind that it corresponds to the specific seismicity level considered. Since the seismic zone selected is one of the most severe ones in Canada, these results can be interpreted as upper bounds for applications in Canada.

6.1.1 Seismic Sensitivity Indicators

The followings are some seismic sensitivity indicators which may be used by tower designers to assess whether a particular tower is sensitive to earthquake effects, and if so, whether a detailed nonlinear modelling study is necessary.

226

1)   When seismic vertical effects are considered, guyed towers with slack cables, i.e. with small initial cable tension (less than 5% of the ultimate tensile strength), are very sensitive to the combination of vertical and horizontal earthquake motions. Since their behaviour is unpredictable, a detailed nonlinear modelling study is recommended.

2)   For guyed towers with usual initial cable tension (i.e. around 10% of their ultimate tensile strength), the maximum dynamic component of the axial force at the base of the mast due to combined vertical and horizontal earthquake motions, is about 80% of their total weight. From the point of view of the strength and stability of the mast, these guyed towers may be sensitive to seismic vertical effects. Their behaviour is predictable, and a detailed nonlinear modelling study would not be necessary.

3)   When the total base shear is considered, guyed towers shorter than 250 m have a relatively large base shear in the range of 40% to 80% of their total weight. Therefore, this range of towers may be considered to be sensitive to the seismic effects. Since the magnitude of base shear can be predicted, a detailed nonlinear modelling study would not be necessary.

4)   The relative contributions of mass of the cables and the mast to the base shear is unpredictable for guyed towers taller than 400 m. This may be due to the small number of towers modelled in that range. Therefore, until more knowledge is available, a detailed nonlinear modelling study is recommended for towers higher than 400 m.

6.1.2 Simplified Models Proposed for Seismic Behaviour

Three simplified models are proposed in the thesis for predicting the seismic behaviour of tall guyed towers in the 150 - 600 m range. These are:

227

1)   The following equation is proposed to evaluate the maximum base shear:

$$\text{B.S.} = 28300\ H^{-1.17} \qquad (5.2)$$

where B.S. is the maximum base shear as a percentage of total weight of tower and H is the tower height in meters.

2)   A simplified model for the distribution of earthquake forces along the height of the towers has been presented. This model is based on the following three concepts:

a) Predominant mode shape of the mast;

b) Mass distribution of the mast along the height;

c) Transition region between two guy cluster groups.

The distribution of earthquake forces along the mast is proportional to the product of the distributed mass of the mast and its predominant mode shape. Also discontinuities in behaviour are expected in the transition region between guy cable clusters of different trends of lateral stiffness.

The predominant mode shape is the lowest flexural mode of the mast which is close to the lowest flexural mode of a simply-supported beam on flexible supports. Usually guyed towers have a uniform mass distribution along their mast, except for the presence of outriggers which locally increase the mass.

The maximum earthquake force (lateral force) along the mast for most of the towers studied is in the range of 23% to 33% of the total base shear.

3)   A simplified model in the form of an equation is proposed for the distribution of the maximum dynamic component of the axial force in the mast along the height of the tower due to combined vertical and horizontal

228

earthquake motions:

$$(P_{dyn}/\text{Max B.A.}) = 100 - 95 \ (h/H)^2 \qquad\qquad (5.3)$$

where $(P_{dyn}/\text{Max B.A.})$ is the percentage of the ratio of the maximum dynamic component of axial force in the mast along the height to the maximum dynamic component of the axial force of the mast at the base; h is the sectional elevation along the mast, and H is the total tower height.

6.1.3 Estimate of Maximum Dynamic Component of Mast Base Axial Force

For guyed towers with usual initial cable tension (i.e. around 10% of the ultimate tensile strength), the maximum dynamic component of mast base axial force due to combined vertical and horizontal earthquake motions, is almost constant at about 80% of their total weight.

6.1.4 Sensitive Region

There is a sensitive region along the guyed towers in the transition zone between guy clusters anchored to the ground at different points. This area connects two portions of the tower with different trends of lateral stiffness, which causes nonuniformity in most aspects of the tower seismic behaviour. Also, with the exception of the dynamic component of the axial force in the mast and the rotation (tilt) of the mast, the maximum amplitude of the response indicators occurs in the vicinity of a transition region.

6.1.5 Serviceability Considerations

The usual serviceability requirements (normally the maximum rotation of the mast at specific antenna locations) are met in all the towers studied in this research.

229

6.1.6 General Observations

1) The contribution of the mass of the cables to the total base shear is almost constant in the range of 3% to 5% of the total weight of tower.

2) Generally, the maximum values of the mast shear occur at stay levels and the minimum ones occur at midspan between two stay levels, and vice versa for the mast bending moment.

3) The predominant mode shape observed is not similar to the one suggested by IASS (IASS, 1981), which is according to the lowest flexural mode profile of a cantilever structure (based on usual building codes).

For guyed towers with usual initial cable tension (i.e. around 10% of their ultimate tensile strength):

4) The lowest flexural natural period of the towers can be predicted by the following equation:

$$T = 0.0083 \ H - 0.74 \qquad\qquad (4.1)$$

where T is the lowest flexural natural period in seconds and H is the total height of the tower in meters.

5) The maximum contribution of the mass of the cables to the dynamic component of the axial force at the base of the mast due to combined vertical and horizontal earthquake motions is 10% of the total weight of the tower.

6) The maximum amplification factor of cable tension is in the range of

100% to 130%. These percentage values are with respect to the initial cable tension.

7) Except for the dynamic component of mast axial force, there is no significant difference between the results from a dynamic analysis with only the horizontal earthquake and those from the combined horizontal and vertical earthquake motions.

For guyed towers of total height in the range of 150 to 213 m:

8) For the towers with usual initial cable tension (i.e. around 10% of their ultimate tensile strength), more lateral stiffness is provided close to the top antenna attachment points than at the intermediate levels. This makes the tower behave like a simply-supported beam on flexible supports. In that case, the lowest flexural mode of the mast is similar to the second lowest mode of a cantilever beam.

9) Most of the base shear is contributed by the mass of the mast, which is more than proportional to its weight compared to cable weight. The average contribution of the mast to the total weight of guyed towers is 72%, which leaves an average of 28% for the contribution of the cables, for the towers studied.

10) The ratio of maximum mast shear to the total weight varies from 6% to 7% and the ratio of maximum mast moment to the product of panel width and total weight varies from 36% to 48%.

For guyed towers of total height in the range of 313 to 607 m:

11) The ratio of maximum mast shear to the total weight varies from 2.5% to

5%, and the ratio of maximum mast moment to the product of panel width and total weight varies from 14% to 35%.

6.2 RECOMMENDATIONS FOR FUTURE WORK

Many interesting conclusions have been derived from this thesis, and some of them may lack generality due to the specific parameters considered. It is recommended to investigate the following aspects of the problem in order to increase the applicability of some of the findings of this study.

1)   Consider different levels of seismicity other than that of the Victoria region.

2)   Add the effect of antennas and accessories (e.g. ladder, transmision lines, lights for aircraft warning, etc.) to the models. This will also create torsional effects which have not been addressed so far.

3)   Model more real guyed towers (especially above 400 m).

4)   Simulate the effect of more earthquake accelerograms.

5)   Experiment with the modelling of damping.

STATEMENT OF ORIGINALITY

This research program has been conducted in order to study the seismic sensitivity of tall guyed telecommunication towers, and to provide an improved understanding of the seismic behaviour of these structures. Eight existing guyed towers of heights varying from 150 m to 607 m have been analyzed in detailed using nonlinear dynamic finite element models. Three different classical earthquakes (El Centro, Parkfield and Taft) have been used with the seismicity level of the Victoria region which is among the zones in the highest seismic risk in Canada. In addition to the horizontal excitation, the combined vertical and horizontal earthquake motions have been investigated. The followings summarize the original contributions of this thesis to the engineering knowledge in this field:

1)   Proposing simple seismic sensitivity indicators which may be used by tower designers to assess whether a particular tower is sensitive to earthquake effects, and if so, whether a detailed nonlinear modelling study is necessary;

2)   Developing a simplified model in the form of an equation for predicting the maximum base shear;

3)   Finding an estimate of the maximum dynamic component of the axial force at the base of the mast due to the combined vertical and horizontal earthquake motions;

4)   Presenting a simplified model in the form of a conceptual approach for the distribution of earthquake lateral forces along the tower height;

5)   Suggesting a simplified model in the form of an equation for the distribution of the maximum dynamic component of the axial forces in the mast along the tower height due to the combined vertical and horizontal earthquake motions;

6)   Introducing some guidelines to evaluate the seismic amplification factor of the cable tension , and the maximum shear and bending moment in the mast.

BIBLIOGRAPHY

ADINA R&D, Inc. (1992), "ADINA (Automatic Dynamic Incremental Nonlinear Analysis) Theory and Modelling Guide", Report ARD 92-8, Watertown, MA.

ADINA R&D, Inc. (1992), "ADINA-IN for ADINA Users Manual", Report ARD 92-4, Watertown, MA.

ADINA R&D, Inc. (1992), "ADINA-PLOT Users Manual", Report ARD 92-7, Watertown, MA.

ADINA R&D, Inc. (1992), "ADINA Verification Manual - Nonlinear Problems", Report ARD 92-10, Watertown, MA.

Amiri, G. G. (1995), "Seismic Response of Guyed Telecommunication Towers - Literature Review", Structural Engineering Report, No. 95-1, Department of Civil Engineering and Applied Mechanics, McGill University, Montreal, 25 p.

Amiri, G. G., and McClure, G. (1996), "Simplified Model For Seismic Behaviour of Tall Guyed Telecommunication Towers", Proceedings of the Canadian Society for Civil Engineering, First Structural Specialty Conference, Edmonton, Alberta, May 29 to June 1, Vol. IIb, 823-834.

Amiri, G. G., and McClure, G. (1996), "Seismic Response of Tall Guyed Telecommunication Towers", Proceedings of the Eleventh World Conference on Earthquake Engineering, Acapulco, Mexico, June 23-28, Paper #1882, 8 p.

Amiri, G. G., and McClure, G. (1996), "Distribution of Earthquake Forces Along Tall Guyed Telecommunication Towers", Proceedings of the Conference on Civil Engineering

by Iranian Students in Canada, Montreal, Quebec, July 19-20, 243-250.

Amiri, G. G., and McClure, G. (1997), "Detailed Nonlinear Seismic Analysis of a 150-m Guyed Telecommunication Tower", Structural Engineering Report, No. 97-1, Department of Civil Engineering and Applied Mechanics, McGill University, Montreal.

Amiri, G. G., and McClure, G. (1997), "Detailed Nonlinear Seismic Analysis of a 152-m Guyed Telecommunication Tower", Structural Engineering Report, No. 97-2, Department of Civil Engineering and Applied Mechanics, McGill University, Montreal.

Amiri, G. G., and McClure, G. (1997), "Detailed Nonlinear Seismic Analysis of a 198-m Guyed Telecommunication Tower", Structural Engineering Report, No. 97-3, Department of Civil Engineering and Applied Mechanics, McGill University, Montreal.

Amiri, G. G., and McClure, G. (1997), "Detailed Nonlinear Seismic Analysis of a 200-m Guyed Telecommunication Tower", Structural Engineering Report, No. 97-4, Department of Civil Engineering and Applied Mechanics, McGill University, Montreal.

Amiri, G. G., and McClure, G. (1997), "Detailed Nonlinear Seismic Analysis of a 213-m Guyed Telecommunication Tower", Structural Engineering Report, No. 97-5, Department of Civil Engineering and Applied Mechanics, McGill University, Montreal.

Amiri, G. G., and McClure, G. (1997), "Detailed Nonlinear Seismic Analysis of a 313-m Guyed Telecommunication Tower", Structural Engineering Report, No. 97-6, Department of Civil Engineering and Applied Mechanics, McGill University, Montreal.

Amiri, G. G., and McClure, G. (1997), "Detailed Nonlinear Seismic Analysis of a 342-m Guyed Telecommunication Tower", Structural Engineering Report, No. 97-7, Department of Civil Engineering and Applied Mechanics, McGill University, Montreal.

Amiri, G. G., and McClure, G. (1997), "Detailed Nonlinear Seismic Analysis of a 607-m Guyed Telecommunication Tower", Structural Engineering Report, No. 97-8, Department of Civil Engineering and Applied Mechanics, McGill University, Montreal.

Argyris, J., and Mlejnek, H. P. (1991), "Dynamics of Structures", Texts on Computational Mechanics, Vol. V, North-Holland, New York, 505-510.

AS3995(Int)-1991 Interim Australian Standard (1991), "Design of Steel Lattice Towers and Masts", Standard Australia, Standard House, 80 Arthur St., North Sydney NSW, Australia.

Augusti, G., Borri, C., and Gusella, V. (1990), "Simulation of Wind Loading and Response of Geometrically Non-linear Structures with Particular Reference to Large Antennas", Structural Safety, Vol. 8, No., 161-179.

Augusti, G., Borri, C., Marradi, L., and Spinelli, P. (1986), "On the Time-Domain Analysis of Wind Response of Structures", Journal of Wind Engineering & Industrial Aerodynamics, Vol. 23, No. 1-3, 449-463.

Bathe, K. J. (1995), "Finite Element Procedures in Engineering Analysis", Prentice-Hall, Englewood Cliffs, NJ.

Ben Kahla, N. (1993), "Static and Dynamic Analysis of Guyed Towers", Ph.D. Thesis, University of Wisconsin - Madison, 176 p.

Ben Kahla, N. (1994), "Dynamic Analysis of Guyed Towers", Engineering Structures, 16(4):293-301.

Ben Kahla, N. (1995), "Equivalent Beam-Column Analysis of Guyed Towers", Computers & Structures, 55(4): 631-645.

Buchholdt, H. A., Moossavinejad, S., and Iannuzzi, A. (1986), "Non-linear Dynamic Analysis of Guyed Masts Subjected to Wind and Guy Ruptures", Proceedings of the Institution of Civil Engineers (London), Vol. 81, Pt. 2, 353-359.

Canadian Association for Earthquake Engineering (CAEE/ACGS) (1995), "The Hyogo-Ken Nanbu (Kobe) Earthquake of 17 January 1995", Preliminary Reconnaissance Report", Vancouver, 257 p.

Chajes, A., and Chen, W.-S. (1979), "Stability of Guyed Towers", Journal of the Structural Division, ASCE, Vol. 105, No. 1, 163-174.

Chajes, A., and Ling, D. (1981), "Post Buckling Analysis of Guyed Towers", Journal of the Structural Division, ASCE 107, 2313-2323.

Clough, R. W., and Penzien, J. (1993), "Dynamics of Structures", McGraw-Hill, New York, 738 p.

Cohen, E., and Perrin, H. (1957), "Design of Multi-Level Guyed Towers: Wind Loading", Journal of the Structural Division, ASCE, Vol. 83, No. ST5, Article 1355.

Cohen, Edward, and Perrin, H. (1957), "Design of Multi-Level Guyed Towers: Structural Analysis", Journal of the Structural Division, ASCE, Vol. 83, No. ST5, Article 1356.

CSA (Canadian Standards Association) CAN/CSA-S37-94 (1994), "Antennas, Towers and Antenna-Supporting Structures", A National Standard of Canada, CSA, Rexdale, Ontario.

Davenport, A. G., and Steels, G. (1965), "Dynamic Behavior of Massive Guy Cables", Journal of the Structural Division, ASCE, 91, ST2, 43-70.

Dean, D. L. (1961), "Static and Dynamic Analysis of Guy Cables", Journal of the

Structural Division, ASCE, 87(1), 1-21.

Dussault, S. (1991), "Nonlinear Seismic Analysis Using Vector Superposition Methods",
M. Eng. Thesis, Department of Civil Engineering and Applied Mechanics, McGill
University, 78 p.

Ekhande, S. G., and Madugula, M. K. S. (1988), "Geometric Non-linear Analysis of
Three-Dimensional Guyed Towers", Computers & Structures, Vol. 29, No. 5, 801-806.

Fiesenheiser, E. (1957), "How to Approach the Design of Tall Guyed Towers", Consulting
Engineering, March.

Gantes, C., Khoury, R., Connor, J., and Pouangare, C. (1993), "Modelling, Loading, and
Preliminary Design Considerations for Tall Guyed Towers", Computers & Structures,
49(5):797-805.

Gerstoft, P., and Davenport, A. G. (1986), "Simplified Method for Dynamic Analysis of
A Guyed Mast", Journal of Wind Engineering & Industrial Aerodynamics, Vol. 23, No.
1-3, 487-499.

Goldberg, J. E., and Gaunt, J. T. (1973), "Stability of Guyed Towers", Journal of the
Structural Division, ASCE, Vol. 99, No. ST4, 741-756.

Goldberg, J. E., and Meyers, V. J. (1965), "A Study of Guyed Towers", Journal of the
Structural Division, ASCE, Vol. 91, No. ST4, 57-76.

Guevara, E. I. (1993), "Nonlinear Seismic Analysis of Antenna-Supporting Structures",
M. Eng. Project Report, Department of Civil Engineering and Applied Mechanics, McGill
University, 84 p.

Guevara, E., and McClure, G. (1993), "Nonlinear Seismic Response of Antenna-Supporting Structures", <u>Computers & Structures</u>, Vol. 47, No. 4-5, 711-724.

Huey, S. (1994), "Tallest Guyed Tower - 2 Are Taller", <u>Civil Engineering</u>, ASCE, 64(6):40.

Hull, F. H. (1962), "Stability Analysis of Multilevel Guyed Towers", <u>Journal of the Structural Division</u>, ASCE 88, 61-80.

Huston, R. L., and Kamman, J. W. (1982), "Validation of Finite Segment Cable Models", <u>Computers & Structures</u>, 15, 653-660.

IASS (International Association for Shell and Spatial Structures), Working Group No. 4 (1981), "<u>Recommendations for Guyed Masts</u>", IASS, Madrid, 107 p.

Irvine, H. M. (1981), "<u>Cable Structures</u>", MIT Press, Cambridge, MA, 135-139 and 148-150.

Issa, R. R. A., and Avent, R. R. (1991), "Microcomputer Analysis of Guyed Towers as Lattices", <u>Journal of Structural Engineering</u>, ASCE, Vol. 117, 1238-1256, Related Material: Discussion, Vol. 118:1983-1984, Jul. 1992.

Jayaraman, H. B., and Knudson, W. C. (1981), "A Curved Element for the Analysis of Cable Structures", <u>Computers & Structures</u>, Vol. 14, No. 3-4, 325-333.

Karna, T. (1984), "<u>Dynamic and Aeroelastic Action of Guy Cables</u>", Ph.D. Thesis, Technical Research Center of Finland, Publications 18, Helsinki University of Technology, Finland, 91 p.

Kennedy, J. S., Wilson, D. J., Adams, P. F., and Perlynn, M. (1980), "Effect of Guy

Cable Constraint on Structural Damping of Open Lattice Antenna Towers", <u>Canadian Journal of Civil Engineering</u>, Vol. 7, No. 4, 614-620.

Leonard, J. W. (1988), "<u>Tension Structures: Behavior and Analysis</u>", McGraw-Hill, 25-34.

Lin, N. (1993), "<u>Dynamic Response of Guyed Antenna Towers Due to Ice Shedding</u>", M. Eng. Project Report, Department of Civil Engineering and Applied Mechanics, McGill University, 70 p.

Magued, M. H., Bruneau, M., and Dryburgh, R. B. (1989), "Evolution of Design Standards and Recorded Failures of Guyed Towers in Canada", <u>Canadian Journal of Civil Engineering</u>, Vol. 16, No. 5, 725-732.

McCaffrey, R., and Hartman, A. J. (1972), "Dynamics of Guyed Towers", <u>Journal of the Structural Division</u>, ASCE, 98(ST6), 1309-1323.

McClure, G. (1984), "<u>Geometric Nonlinearities in Guyed Towers</u>", M.Sc. Thesis, Massachusetts Institute of Technology, Department of Civil Engineering, 183p.

McClure, G., and Guevara, E. I. (1994), "Seismic Behaviour of Tall Guyed Telecommunication Towers", <u>Proceedings of the IASS-ASCE International Symposium 1994 on Spatial, Lattice and Tension Structures</u>, Atlanta, Georgia, 259-268.

McClure, G., Guevara, E. I., and Lin, N. (1993), "Dynamic Analysis of Antenna-Supporting Structures", <u>Proceedings of the Canadian Society for Civil Engineering Annual Conference</u>, Fredericton, N.B., June 8-11, Vol. II, 335-344.

McClure, G., and Lin, N. (1994), "Transient Response of Guyed Telecommunication Towers Subjected to Cable Ice-Shedding", <u>Proceedings of the IASS-ASCE International</u>

Symposium 1994 on Spatial, Lattice and Tension Structures, Atlanta, Georgia, 801-809.

Moossavi Nejad, S. E. (1996), "Dynamic Response of Guyed Masts to Strong Motion Earthquake", Proceedings of the Eleventh World Conference on Earthquake Engineering, Acapulco, Mexico, June 23-28, Paper #289, 8 p.

Nakamoto, R. T., and Chiu, N. L. (1985), "Investigation of Wind Effects on Tall Guyed Tower", Journal of Structural Engineering, ASCE, Vol. 111, 2320-2332.

National Research Council of Canada (1995), "National Building Code of Canada 1995", 11th Edn. Ottawa.

Odley, E. G. (1966), "Analysis of High Guyed Towers", Journal of the Structural Division, ASCE, No. ST1, 169-197.

Peil, U., Nolle, H., and Wang, Z. H. (1993), "Dynamic Behaviour of Guys", Meeting of the IASS-Working Group No. 4 "Mast and Towers", Prague, 10 p.

Poskitt, T. J., and Livesley, R. K. (1963), "Structural Analysis of Guyed Masts", Proceedings of the Institution of Civil Engineers, London, Vol. 24, 373-386.

Raman, N. V., Surya Kumar, G. V., and Sreedhara Rao, V. V. (1988), "Large Displacement Analysis of Guyed Towers", Computers & Structures, Vol. 28, No. 1, 93-104.

Reichelt, K. L., Brown, D. M., and Melin, J. W. (1971), "Tower: Design System for Guyed Towers", Journal of the Structural Division, ASCE, Vol. 97, No. ST1, 237-251.

Rosenthal, F., and Skop, R. A. (1980), "Guyed Towers Under Arbitrary Loads", Journal of the Structural Division, ASCE, Vol. 106, No. 3, 679-692.

241

Rosenthal, F., and Skop, R. A. (1982), "Method for Analysis of Guyed Towers", Journal of the Structural Division, ASCE, Vol. 108, No. ST3, 543-558.

Sachs, P. (1972), "Wind Forces in Engineering", Pergamon Press, New York, 251-252.

Schiff, S. D. (1988), "Seismic Design Studies of Low-Rise Steel Frames", Ph.D. Thesis, Department of Civil Engineering, University of Illinois at Urbana-Champaign, 221 p.

Schrefler, B. A., Odorizzi, S., and Wood, R. D. (1983), "A Total Lagrangian Geometrically Nonlinear Analysis of Combined Beam and Cable Structures", Computers & Structures, 17, 115-127.

Shears, M., and Clough, R. W. (1968), "Static and Dynamic Behaviour of Guyed Masts", Report No. 68.6, Department of Civil Engineering, University of California, Berkeley, CA, 167 p.

Sticka, D. (1994), "Tallest Guyed Tower - Guess Again", Civil Engineering, ASCE, 64(9): Page 30.

Wahba, Y. M. F., Madugula, M. K. S., and Monforton, G. R. (1992), "Limit States Design of Antenna Towers", Final Report Submitted to the CSA Technical Committee S37 on Antenna Towers, Department of Civil and Environmental Engineering, University of Windsor Ontario, 176 p.

Wahba, Y. M. F., Madugula, M. K. S., and Monforton, G. R. (1996), "Effect of Guy Initial Tension on Design of Guyed Antenna Towers", Canadian Journal of Civil Engineering, Vol. 23, 457-463.

Williamson, R. A., and Margolin, M. N. (1966a), "Discussion - A Study of Guyed Towers", Journal of the Structural Division, ASCE, No. ST2, 419-426.

Williamson, R. A., and Margolin, M. N. (1966b), "Discussion - Analysis of High Guyed Towers", <u>Journal of the Structural Division</u>, ASCE, No. ST5, 354-356.

Yu, A.-T. (1952), "Vibration Damping of Stranded Cable", <u>Proceedings of the Society of Experimental Stress Analysis</u>, Vol. 9, No. 2, 141-158.